MIT-2249-1
(MITNE-44)

RATE OF EXCHANGE OF DEUTERIUM BETWEEN WATER AND DISSOLVED HYDROGEN IN PRESENCE OF DIETHYLAMINE

TAKANOBU ISHIDA
AND
MANSON BENEDICT

FEBRUARY 1964

DEPARTMENT OF NUCLEAR ENGINEERING
MASSACHUSETTS INSTITUTE OF TECHNOLOGY
CAMBRIDGE, MASSACHUSETTS, 02139

FOR THE
U. S. ATOMIC ENERGY COMMISSION
UNDER CONTRACT AT(30-1)-2249

DISTRIBUTION

This report is being distributed under the category, "Isotope Separation," TID 4500. Additional copies may be obtained from USAEC Division of Technical Information Extension (DTIE), P. O. Box 62, Oak Ridge, Tennessee.

Previous reports on this project:

NYO-2346
NYO-2347 (MITNE-2)
NYO-2348

LEGAL NOTICE

MIT-2249-1
(MITNE-44)

RATE OF EXCHANGE OF DEUTERIUM BETWEEN WATER AND DISSOLVED HYDROGEN IN PRESENCE OF DIETHYLAMINE

Takanobu Ishida
Manson Benedict

Department of Nuclear Engineering
Massachusetts Institute of Technology
Cambridge 39, Massachusetts

M.I.T. DSR No. 8069

Contract AT(30-1)-2249
U. S. Atomic Energy Commission

Issued February 1964

ACKNOWLEDGMENTS

The contents of this report have been submitted by Takanobu Ishida to the Nuclear Engineering Department of Massachusetts Institute of Technology in partial fulfilment of the requirements for the degree of Doctor of Philosophy.

The authors acknowledge with gratitude the assistance rendered by Dr. Jean-Marie Rayroux in the design and construction of the equipment and by Messrs. Achilles Adamantiades, Sang Kyong, Robert Barthelemy, Kenneth Congdon and Douglas Webster in carrying out the experimental measurements. Without the dedicated participation of these men it would not have been possible to complete this investigation.

TABLE OF CONTENTS

Page

Page

LIST OF TABLES

LIST OF FIGURES

I. ABSTRACT

The object of this research was to measure the rate of exchange of deuterium between water and dissolved hydrogen in the presence of diethylamine (DEA) as a homogeneous liquid-phase catalyst. Alkali hydroxides such as KOH are known to catalyze this reaction but are corosive to steel equipment. It was hoped that less corosive DEA, with the highest dissociation constant of any volatile base, would have sufficient catalytic activity to serve in a practical dual temperature exchange process for heavy water production.

The reaction rate was measured in a batch system consisting of a one-liter high-pressure autoclave, equipped with a magnetically driven stirrer and surrounded by a constant-temperature oil bath. The experimental procedure consisted in charging the autoclave with about 500 ml of a degassed dilute solution of DEA in water containing about 25 atom percent deuterium of accurately known isotopic content. Hydrogen gas of natural isotopic content was charged to a measured pressure of about 80 atmospheres. The reaction rate was determined by comparing the thermal conductivity of gas samples taken at known times with samples of known deuterium content.

Experiments were made at temperatures of 100, 150 and 200°C, and at DEA concentrations between 0.78 and 1.83 normal. The reaction rate was found to be proportional to the partial pressure of hydrogen and to increase with

increasing temperature and amine concentration. The reaction rate varies as the 1.07 power of the amine concentration at 100°C, the 1.46 power at 150°, and the 1.58 power at 200°C. The average activation energy of the reaction is 8.0, 7.5, 6.9 and 6.1 Kcal per gram mole at total DEA concentrations of 2.0, 1.6, 1.2 and 0.8 normal, respectively.

A set of reaction mechanisms has been proposed to explain the observed results.

At 100°C and under a hydrogen pressure of 200 atmospheres, transfer of deuterium from hydrogen to water in the liquid phase reaction

$$HD + H_2O \longrightarrow H_2 + HDO$$

will proceed at a rate of 0.5 gram atoms D transferred per hour per liter of 1.64 N DEA solution. This is about one third of the rate of the same exchange reaction at this temperature and pressure when catalyzed by 1 N KOH solution in place of DEA. As the rate with KOH is too slow to serve as the basis for an economic process for heavy water production, it is concluded that DEA does not have sufficient catalytic activity to serve as a practical catalyst in a dual-temperature exchange process.

Tetra-alkylammonium hydroxides and soluble salts of the transition elements are suggested as substances to be investigated for possibly greater activity as homogeneous catalysts.

II. INTRODUCTION

In many respects, heavy water is the best moderator known for nuclear reactors. Yet, at the price of $24.50 per pound for which heavy water is produced by the U.S. Atomic Energy Commission, nuclear power reactors moderated by heavy water have not been able to compete economically in the United States with reactors moderated by light water. If a process for making heavy water at substantially lower cost could be devised, heavy water reactors would become more attractive economically and the cost of nuclear power would be reduced.

In the heavy water plants of the U.S. AEC primary concentration is effected by the dual temperature exchange process employing the reaction

$$H_2S + HDO \rightleftharpoons HDS + H_2O \qquad (1)$$

The equilibrium constant for this reaction, defined as

$$K^{(s)} = \frac{[HDS]\ [H_2O]}{[H_2S]\ [HDO]} \qquad (2)$$

increases with increasing temperature. By combining two countercurrent exchange towers as shown in Fig. 1, one at a low temperature (e.g. 30°C) and the other at a higher temperature (e.g. 130°C), deuterium concentrates in the

water leaving the cold tower and in the hydrogen sulfide leaving the hot tower, because the lower equilibrium constant $K_c^{(s)}$ in the cold tower favors the conversion of H_2O to HDO and the higher equilibrium constant $K_h^{(s)}$ in the hot tower favors the conversion of H_2S to HDS. Feed water of natural deuterium abundance is brought in at the top of the cold tower and is enriched in deuterium by exchange with enriched hydrogen sulfide entering the bottom of the cold tower. A portion of the enriched water leaving the cold tower is removed as product, and the remainder, entering the hot tower is stripped of deuterium by exchange with the depleted hydrogen sulfide entering the bottom of the hot tower. The stripped water leaves the plant as depleted product. The hydrogen sulfide recycles through the plant and need not be fed except to charge the plant initially.

The hydrogen-sulfide exchange reaction (1) has the practical advantage that it proceeds rapidly and without catalysis. It has two disadvantages, however:

i) Aqueous solutions of hydrogen sulfide are corrosive and parts of the plant handling them must be built of expensive stainless steel.

ii) The ratio $K_h^{(s)}/K_c^{(s)}$ is rather close to unity, about 1.30 for 130° and 30°C, so that the separability of the process is not great, and a large plant with high heat consumption is needed for a given output.

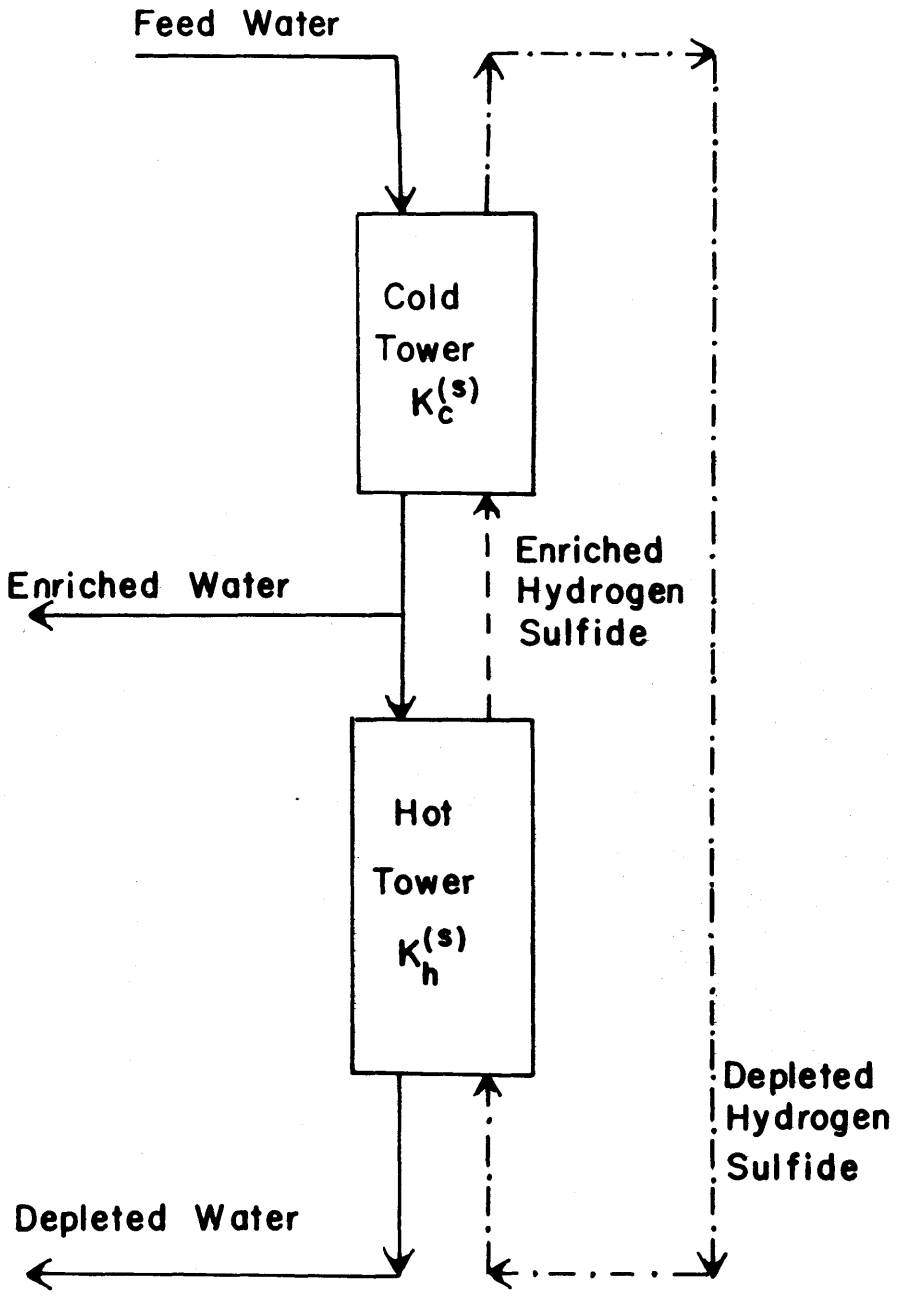

Fig. 1 Dual Temperature Hydrogen Sulfide-Water Exchange Process $K_c^{(s)} < K_h^{(s)}$

At the first Geneva Conference, Benedict (1) pointed out that the reaction between hydrogen gas and water

$$H_2 + HDO \rightleftharpoons HD + H_2O \qquad (3)$$

would be less disadvantageous in these respects, because solutions of hydrogen in water are relatively non-corrosive, and the ratio of equilibrium constants over a given temperature span is higher than with hydrogen sulfide and water. For example, the equilibrium constant K, defined as

$$K = \frac{[HD][H_2O]}{[H_2][HDO]} \qquad (4)$$

is 1.47 times greater at 150 °C than at 50 °C. This would permit use of a smaller plant and less heat with hydrogen gas circulated in the flowsheet of Fig. 1 than with hydrogen sulfide.

However, the reaction (3) between hydrogen and water does not proceed without catalysis. It was pointed out (1), therefore, that one of the most useful steps toward reducing the cost of heavy water would be to find a cheap, effective catalyst for the deuterium exchange reaction between water and dissolved hydrogen, preferably a catalyst which dissolved readily in the liquid phase and could be separated readily from the product water streams.

As explained below, it was anticipated that diethylamine would be one of the most practical and effective catalysts for this reaction. The purpose of the experimental research described in this thesis has been to measure the rate of the deuterium exchange reaction between water and dissolved hydrogen in the presence of diethylamine.

The history of experience with other catalysts tried for this reaction and the reasoning which led to choice of diethylamine for this work will be described briefly.

During World War II a stationary bed of solid catalyst whose active ingredient was platinum or nickel was found not be be effective (2) because i) molecular diffusion of dissolved hydrogen to and from the active surface of the solid catalyst through water-layer was rate-controlling and slow and ii) the surface of these solid catalysts was very susceptible to poisoning.

Two approaches for solving this problem seemed to be promising. One was to use dispersed or colloidal catalyst, and the other was to use homogeneous or soluble catalyst. The former has advantages over the stationary bed method in the increased specific surface area of catalyst and in the substantial homogeneity of active centers of catalysis in the solution, which minimize effect of molecular diffusion. It was found that colloidal platinum and palladium have very high specific activities (A-1), (A-2), (A-3), (A-4). It was also found, however, that they are very susceptible to

catalyst poisons. Furthermore, recovery of the colloidal catalysts from product water stream seems to present a problem. It has been suggested (3), (A-2) that water, instead of hydrogen, be circulated in the closed cycle of a stage of the duel-temperature process. Such a process, however, would give up one of the greatest advantages of the process in which hydrogen is circulated in closed cycle, the independence of the plant from a hydrogen-producing industry for feed.

The other method, that of utilizing a homogeneous catalyst, is expected to have much less difficulty than the fixed heterogeneous catalyst with slow reactant diffusion and no problem of aging or poisoning. By proper choice of catalyst economic recovery by either ion-exchange or distillation should be possible.

The only homogeneous catalyst that has been investigated for the purpose of utilizing it in heavy water production with reaction (3) is caustic alkali KOH or NaOH (A-4), (A-22), (A-23). It has been found that the exchange rate of deuterium is proportional to the partial pressure of hydrogen and to the concentration of hydroxyl ion in the temperature range of 80 to 200 ^{o}C. The rate constant of reaction

$$D_2 + H_2O \longrightarrow HD + HDO \qquad (5)$$

was found (A-22) to be 0.344 gram-atom deuterium per liter per minute per (gmole/liter)^2 at 100 ^{o}C. This would, for instance,

correspond to an exchange rate of 0.15 gram-atom of deuterium exchanged per liter of water per hour under a partial pressure of hydrogen gas of 10 atmospheres and with a concentration of hydroxyl ion of one normal. Experimental average value of the activation energy of above reaction was reported to be about 25 kcal in a temperature range of 80 to 110 °C. To explain these experimental facts, following mechanism has been suggested in these papers:

$$D_2 + OH^- \longrightarrow D^- + HDO \qquad (6)$$

$$D^- + H_2O \longrightarrow HD + OH^- \qquad (7)$$

in which the reaction (6) is stated to be rate-controlling. A theoretical value of the enthalpy change of a reaction

$$H_2 + OH^- \longrightarrow H^- + H_2O \qquad (8)$$

which is different from the reaction (6) only in the isotopic species, calculated from thermodynamic data given in Latimer's "Oxidation Potentials" (A-24), is 20 ± 4 kcal at 25 °C, the uncertainty of four kilocalories arising from uncertainty in the solvation energy of H^- in water. Neglecting an isotopic effect, this would set a lower limit of the activation energy of the exchange reaction (5) through the stated mechanism.

Although the rate of reaction (5) observed in the presence of concentrated KOH is high enough to be of some practical interest, corrosion by concentrated alkali at the temperatures

of 150 ^{o}C or higher needed for the hot tower is so severe (A-4) that stainless steel would be needed for this process also, thus removing the major hoped-for advantage over the hydrogen sulfide exchange process.

It has been found (A-22, A-23) that acids do not significantly catalyze the exchange reaction (5).

An exchange of deuterium between D_2 and H_2O induced by gamma radiation has been observed. It seems that the rate of exchange is too small to be practical, and the simultaneous decomposition of water into H_2 and H_2O_2 presents a serious practical problem in operating the process.

Catalysis activated by OH^- or nuclear radiations are discussed in more detail in APPENDIX Section A.

To reduce the corrosion associated with a caustic alkali, in the present work it was proposed that an organic amine be investigated as a catalyst. A literature survey showed that amines are much less corrosive than caustic alkali. Aqueous solutions of a soluble organic amine were expected to have a catalytic activity on the exchange reaction due both to hydroxyl ion generated through hydrolysis of the amine and to the undissociated amine itself.

From the survey of physical properties of organic amines described in APPENDIX Section A, it was concluded that diethylamine was the most promising substance in this class of materials, for the following reasons:

i) It is the strongest base; i.e., it has the highest dissociation constant into substituted ammonium ion and hydroxyl ion.

ii) Diethylamine does not react with hydrogen under pressure or with water.

iii) Diethylamine is thermally stable at temperatures even higher than would be needed in a dual-temperature process.

iv) Diethylamine has a boiling point sufficiently lower than water to permit it to be readily distilled from product water without excessive consumption of heat.

v) At the same time, its vapor pressure is low enough so that a high concentration of diethylamine can be obtained in the liquid phase, without having too high a partial pressure in the vapor.

vi) Diethylamine and water are miscible in all proportions below 143.5°C. Although the solubility of diethylamine in water is somewhat limited at higher temperatures, decreasing to about 2.5 N diethylamine in water at 200 °C, this concentration would be high enough if diethylamine had a reasonably high catalytic activity.

The main steps of a dual-temperature hydrogen-water exchange process catalyzed by diethylamine (DEA) are illustrated in Fig. 2. The two DEA strippers are used to prevent loss of DEA in product water. The DEA-water exchanger

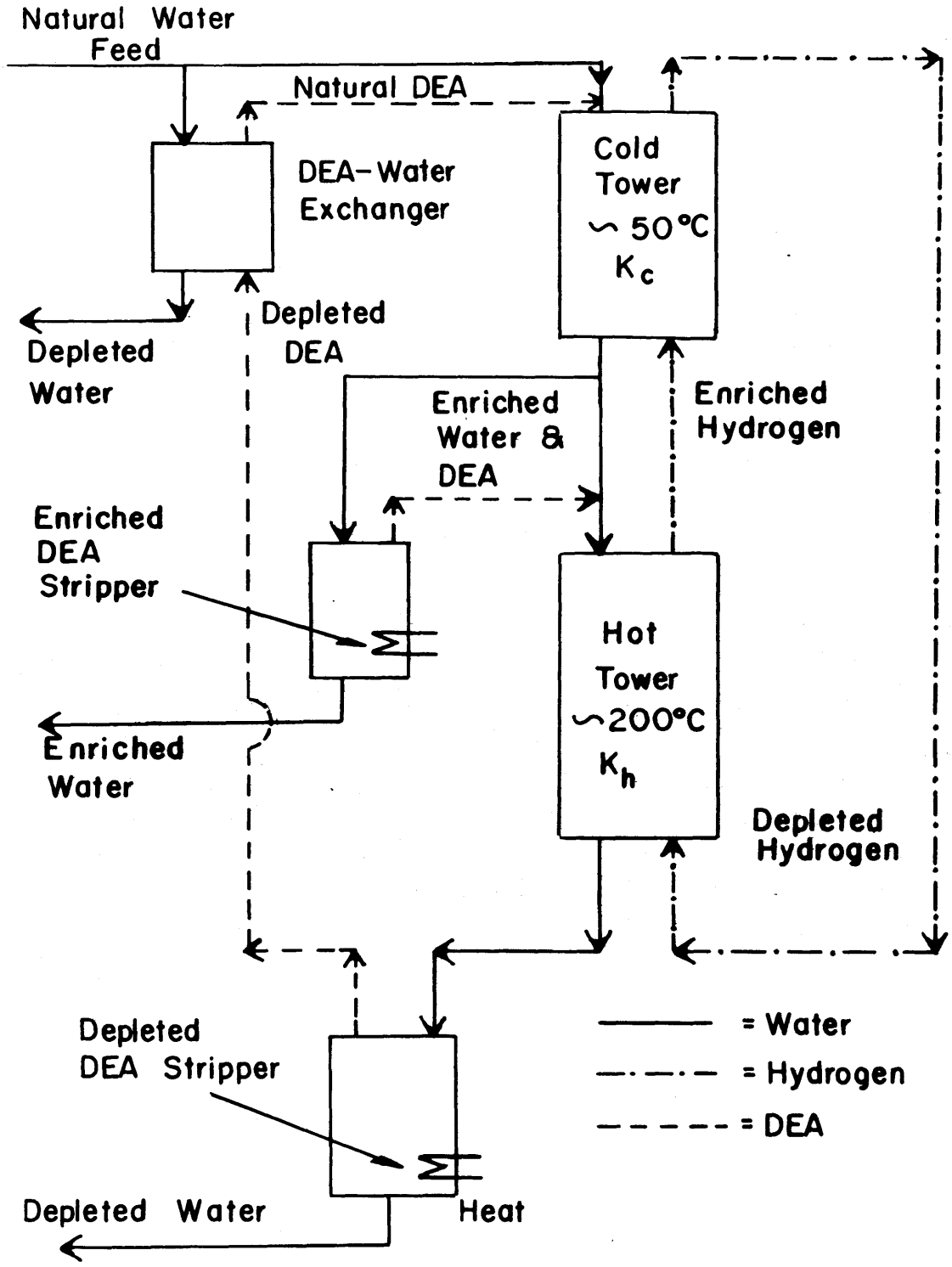

Fig. 2 Dual Temperature Hydrogen-Water Exchange Process Catalyzed by Diethyl Amine (DEA)

$K_c < K_h$

is required because deuterium is exchanged between water and DEA in the reaction

$$(C_2H_5)_2ND + H_2O \rightleftharpoons (C_2H_5)_2NH + HDO \qquad (9)$$

The exchange reaction investigated was reaction (3) because this, rather than reaction (5), is the principal reaction occurring during deuterium exchange in water of low deuterium enrichment, the case of greatest importance in a practical process.

Thus, it was proposed in the present work

i) To measure the rate of reaction (3) in the presence of diethylamine at various concentrations and at temperatures up to 200 °C.

ii) To obtain numerical values of the specific rate constant for reaction (3) as a function of the temperature and the concentration of diethylamine.

iii) Using these results, to propose a mechanism for the catalytic effect of diethylamine from the dependence of the observed reaction rate on the concentration of diethylamine and of the reactants.

III. PROCEDURE

1. Principle of Experiments

The reaction vessel used for these experiments was a high-pressure, stainless steel autoclave of one liter internal volume, provided with a magnetically driven reciprocating stirrer and transfer lines and valves connecting with charging, discharging and sampling-and-analysis systems. The autoclave was maintained at constant temperature by a thermostatted oil bath. A measured amount of a deuterium-enriched aqueous solution of diethylamine of known chemical and isotopic content was charged to the reaction vessel and brought to reaction temperature. Hydrogen gas of natural isotopic content was charged to the reaction vessel, and a zero-point gas sample was taken to serve as a bench mark against which composition changes could be measured. The reaction was started by turning on the stirrer. The mass of hydrogen in the system was inferred from the measured pressure. Samples of the gas phase were taken at measured time intervals and were analyzed for deuterium content by condensing out water and diethylamine in a liquid-nitrogen trap and comparing the thermal conductivity of the uncondensed hydrogen with the thermal conductivity of synthetic mixtures of hydrogen and deuterium of known deuterium content. The specific reaction rate constant was inferred from the rate of change of detuerium content of hydrogen and the known quantities of hydrogen, partially deuterated water and diethylamine present in the reaction system.

Some exchange of deuterium from water to hydrogen gas took place at a slow but measurable rate in the absence of diethylamine catalyst. This was attributed to heterogeneous catalysis on the stainless steel walls of the autoclave, as has been observed by Bigelow (A-5) at higher temperatures. To make possible a correction for this extraneous reaction occurring in the absence of diethylamine, a series of blank runs with hydrogen and water, but without diethylamine, were made at each temperature at which catalyzed runs were carried out.

A preliminary series of runs at different stirring rates was carried out at 200°C and 1.5-normal diethylamine, at which the highest measured reaction rates occurred, to find a stirring rate sufficiently rapid to ensure that the reaction rate measured was representative of the homogeneous liquid-phase reaction of interest and was not hindered by a finite rate of mass transfer between gas and liquid phases. As the reaction rate observed in this series increased with an increase in stirring rate from 1.5 to 6 strokes per second, but remained constant on further increase from 6 to 8 strokes per second, it was concluded that at the 8 strokes per second used in all subsequent runs the reaction rate was not hindered by finite rate of mass transfer, and that no correction for this effect was necessary.

In Subsection 2 the apparatus and experimental procedure will be described in more detail. In Subsection 3 the procedur for obtaining the specific reaction rate constant from observed data will be described.

2. Experimental Procedure

a) Autoclave

The autoclave used was a product of Autoclave Engineers, Inc., Erie, Pennsylvania. It was constructed of type 316 stainless steel and was designed for a maximum working pressure of 5,000 pounds per square inch. The highest pressure used in the present work was about 1,500 pounds per square inch. The total internal volume of the reaction system, V^o, which is equal to that of the autoclave plus tubing connected to the autoclave up to confining valves, was measured and found to be 1,001 milliliters. The autoclave was equipped with a reciprocating agitator actuated by two solenoids. This provided agitation without a stuffing box and prevented leakage from the autoclave. Its design is described in more detail in Section C of the APPENDIX.

b) Constant-Temperature Bath

The constant-temperature oil bath was constructed after a design of Collins (B-1) and is described in detail in Section B of the APPENDIX. The bath fluid used was General Electric's Dimethyl-Silicone-Fluid SF-96-Grade No. 50. It was heated by two separate electric heating systems, one of them, wound on the outside of the vessel holding the oil and called the external heater, was kept on throughout a period of operation. The other one, immersed in the bath fluid and called the internal heater, was turned on or off as needed to control the temperature. It was actuated by a temperature-controlling unit which sensed the bath-temperature by means of a thermistor

detector and amplified the signal through an alternating-current bridge, amplifier and control relay. The bath was insulated with about 8 inches of packed asbestos powder both radially and longitudinally. With this bath the temperature could be maintained within 0.05°C of a desired temperature. The temperatures of the bath fluid and the contents of the autoclave were measured by an iron-constantan thermocouple and a copper-constantan thermocouple, respectively, and voltages from each thermocouple were read with a precision potentiometer.

c) Preparing Amine Solution

Diethylamine of analytical-reagent grade was distilled three times within one month before its use. Portions of the distillate between temperatures 55 and 57 °C were used. Diethylamine is known not to form an azeotrope with water.

Water of known deuterium content was prepared by mixing a weighed amount of heavy water containing 99.95 atom percent deuterium with a weighed amount of natural water chemically purified by distillation and ion-exchange. Atom fraction deuterium of the mixture is denoted by a symbol j. Water of two different deuterium concentrations was used to make up aqueous amine solutions, depending on the amine concentration in the solution to be prepared: water of $j = 0.2285$ was used for blank runs and a diethylamine solution whose nominal amine concentration was 1 N, and water of $j = 0.2667$ was used to prepare a solution whose nominal amine concentration was 2 N.

Roughly known volumes of diethylamine and partially enriched water thus prepared were mixed to make up a solution of

approximately 1 N or 2 N amine concentration, which was eventually used for a catalyzed run.

If any air remained in the solution charged to the autoclave, it would invalidate analysis of gaseous samples by means of the thermal conductivity method. So, the amine solution thus prepared was subjected to a degassing process. Degassing was achieved by evacuating a flask in which the amine solution was placed. Equipment used for this purpose is described in Section D of the APPENDIX and step-by-step procedures are described in Section G of the APPENDIX.

Because more amine than water is extracted from the solution during degassing, the actual amine concentration of a nominal 1 N solution was reduced to around 0.8 N and that of a nominal 2 N solution was reduced to around 1.5 N. The amine concentration of a degassed solution, N, was determined by titration with a standard hydrochloric acid solution using alcoholic solution of Bromthymol-blue as an indicator. From results of a series of density measurements experiments, density, ρ grams/ml, of the degassed amine solution could be obtained from

$$\rho = - 0.01637\ N + 1.0188 \qquad (10)$$

for a solution in which heavy water of j = 0.2285 was used, and

$$\rho = - 0.01767\ N + 1.0149 \qquad (11)$$

for a solution in which heavy water of j = 0.2667 was used. The separate experiments which led to the relations (10) and (11) are described in Section H of the APPENDIX. With knowledge of N and ρ, atom fraction deuterium in the total exchangeable atoms of hydrogen isotopes in the solution, f_d, could be

computed by

$$f_d = \frac{0.2285}{1 + \frac{N}{0.1084\ (1000\rho - 73.14N)}} \qquad (12)$$

for a solution in which heavy water of j = 0.2285 was used, and

$$f_d = \frac{0.2667}{1 + \frac{N}{0.1080\ (1000\rho - 73.14N)}} \qquad (13)$$

for a solution in which heavy water of j = 0.2667 was used.

d) Charging Amine Solution

The degassed solution was transferred by hydrogen pressure to an evacuated steel vessel with an internal volume of about 500 ml. The design of this liquid-charging vessel is described in Section C of the APPENDIX. The total weight of the vessel plus the solution was determined.

The autoclave, in the constant temperature bath at a reaction temperature, was evacuated. The liquid-charging vessel was attached to the autoclave through two high-pressure lines connected with the autoclave. The liquid content of the charging vessel was drained by gravity into the autoclave through one of the connecting lines cooled by water while pressure of the vapors in the autoclave was equalized with that in the charging vessel by means of the other line. The liquid-charging system and the liquid-charging procedures are described in detail in the APPENDIX, Sections C and G, respectively.

After the liquid was charged into the autoclave, confining

valves on the liquid-charging system and autoclave were closed, and the charging vessel was detached from the autoclave and weighed. Difference in the total weights of the vessel before and after charging represents the weight of amine solution charged to the reaction system, G grams.

Temperatures of the autoclave and the charged amine solution were brought back to a desired reaction temperature before charging hydrogen gas.

e) Charging Hydrogen Gas

Commercial hydrogen of "prepurified"-grade, whose chemical purity was guaranteed to be better than 99.95%, was used. The chemical purity was checked for each tank of hydrogen used by means of a gas-combustion method. The system and procedures used for the chemical gas analysis are described in the APPENDIX, Sections D and G, respectively.

Purchased hydrogen is supplied at pressures around 2,500 pounds per square inch, while the hydrogen pressure used in the reaction system in the present work was around 1,000 pounds per square inch. It was, therefore, not necessary to use a compressor for charging the hydrogen gas. The commercial hydrogen was first brought into a steel vessel, called hydrogen-charging vessel, to as high a pressure as possible with the existing pressure of the commercial tank. A valve which connects the hydrogen-charging vessel with the autoclave was cracked for a short time period to admit hydrogen into the autoclave. Difference in pressures in the charging vessel and the autoclave, measured by two Bourdon gauges each connected

with one of the vessels, was kept above 100 pounds per square inch during gas admission. This was to prevent backflow of vapors of the amine and water from the autoclave into the charging vessel.

The final total pressure in the autoclave, $P_{(0)}$, was read on a standard Bourdon gauge and recorded. This pressure was later used to compute the amount of hydrogen gas charged. The system and precedures used for charging hydrogen gas are described in detail in the APPENDIX, Sections C and G, respectively.

f) Sampling

A gaseous sample was taken immediately after the charging of hydrogen gas. This sample was called zero-point sample because the result of the thermal conductivity analysis of this sample was later used to correct analytical results of all the subsequent samples for any presence of chemical impurities in the reaction system. Residual pressure in the autoclave after taking the zero-point sample was measured by the standard Bourdon gauge and recorded as $P_{(1)}$.

The reciprocating agitator of the autoclave was started, and the time was recorded. This is the time zero of the run.

Subsequent samples were taken at desired time intervals. Samples were numbered 1, 2, 3, etc., in sequence of sampling. The time of each sampling and the residual pressure in the autoclave after each sampling were recorded. The sampling times and the residual pressures are denoted by t_1, t_2, t_3, etc., and $p_{(2)}$, $p_{(3)}$, $p_{(4)}$, etc. In subsequent treatment of the observed data, each run was divided into partial runs,

each partial run consisting of the interval between two consecutive samplings during which no materials were withdrawn from the reacting system. Thus, partial run number n occurs between times t_{n-1} and t_n, at constant pressure $p_{(n)}$; gas composition changes from that of sample n-1 to that of sample n. Section J of the APPENDIX describes the nomenclature in more detail.

Sampling was carried out by admitting the gaseous sample from the autoclave, through a series of high-pressure valves, to a liquid-nitrogen trap. Water, diethylamine and any other condensable constituents of the sample were condensed in the trap, and only hydrogen, and some contaminating air if present, would pass through the trap. The purified sample was pumped into one of ten storage bottles without material loss by means of a manual Töpler pump. The high pressure portion of the sampling system is described in Section C of the APPENDIX, the purification and storage systems are described in the APPENDIX, Section D-3, and the procedures are described in the APPENDIX, Section G.

g) Analyzing Samples

Analysis of the chemically purified hydrogen samples for deuterium content was performed by means of a thermal conductivity method. The thermal conductivity cell used was the "PRETZEL" type manufactured by Gow-Mac Instrument Company, Madison, New Jersey. It had two passages in a block of stainless steel; one passage was filled with the gas sample to be analyzed, and the other was filled with hydrogen gas of

natural enrichment which was used as reference gas. Each passage had two vertical wells, in each of which a tungsten filament was mounted. Each of the four filaments was connected electrically into one of the four arms of a Wheatstone bridge, with the two filaments in the sample gas in one pair of opposite arms and the two filaments in the reference gas in the other pair of opposite arms. Design and construction of the system and the operating procedures used for the thermal conductivity analysis are described in Sections D-3 and G of the APPENDIX.

The direct information obtained from the thermal conductivity analysis was the output voltage from the bridge. The bridge output was a smooth function of the deuterium content of a gas sample, provided other operating conditions of the bridge such as composition of the reference gas, total current of the bridge, ambient temperature of the cell block, and pressures and flow rates of the reference and sample gases were kept unvaried. The operating conditions used in the present work were as follows:

Reference gas:	H_2(natural enrichment) at 50 mmHg
Total bridge current:	190 milliamperes
Ambient temperature:	50°C
Pressure of sample gas:	50 mmHg
Flow rates:	Zero

Calibration curves for these conditions, which relate the bridge output to the deuterium content in the gas sample, were constructed by measuring the outputs for standard hydrogen gases

of known deuterium content, placed in the sample passage. These standard gas mixtures were prepared by mixing measured amounts of H_2 and D_2 and then isotopically equilibrating the mixture by catalyzing the equilibrium reaction

$$H_2 + D_2 \rightleftharpoons 2HD \qquad (14)$$

with a nickel wire at 600°C. The equipment used for preparing the standard gases is described in Section D-3 of the APPENDIX. The calibration curves obtained were as follows:

$$r' \equiv \frac{f_d'}{1 + f_d'} = 0.02175\ E \qquad (15)$$

for a lower recorder sensitivity, called sensitivity setting "1", and

$$r' \equiv \frac{f_d'}{1 + f_d'} = 0.01225\ E \qquad (16)$$

for a higher recorder sensitivity, called sensitivity setting "2", where r' and f_d' are, respectively, the deuterium/hydrogen atom ratio and atom fraction of deuterium in the sample gas, and E is the bridge output in millivolts. The method of calibration and effects of deviations in operating conditions are discussed in Section E of the APPENDIX.

3. Computational Procedure

The quantities observed experimentally are the masses of water and diethylamine charged to each run, the atom fraction deuterium in this liquid mixture, the gas-phase pressures during

each partial run, and the atom fraction deuterium in the M gas samples taken at times t_1, t_2, ..., t_M. The reaction rate in each run is to be expressed as the specific rate constant k_1 for the reaction

$$H_2 + HDO \longrightarrow HD + H_2O$$

and/or k_2 for the reaction

$$HD + H_2O \longrightarrow H_2 + HDO$$

occurring in the liquid phase, expressed as gram atoms of deuterium transferred per milliliter per hour per unit molar concentrations of HDO and dissolved H_2 in the liquid phase each expressed in grammoles per milliliter. In order to obtain k_1 and/or k_2 from observed quantities, it is necessary 1) to calculate the equilibrium distribution of all reacting species (H_2, HD, H_2O, $(C_2H_5)_2NH$ and $(C_2H_5)_2ND$) between the liquid and vapor phases present in the reacting system of known total volume and then 2) to interpret the observed changes in isotopic content in terms of the specific rate constant for the above reaction. These two types of calculation, of phase equilibria and the specific rate constant, will

be described separately in the following subsections.

As pointed out in the INTRODUCTION, the system water-diethylamine has a critical mixing temperature at 143.5°C, and the solubility of diethylamine in water decreases as the temperature increases beyond the critical temperature (see Fig. A-1 in Section A of the APPENDIX). This would indicate that the system is not ideal. Activity coefficients of water and deithylamine in the saturated aqueous solution of DEA were obtained by applying the Van Laar equation with each other at a given temperature. Results are

Temperature	Activity Coefficient	
(°C)	Water	Diethylamine
155	1.035	7.32
150	1.038	6.70
147	1.046	5.90
145	1.065	4.44

Extrapolation of these results to the temperature of 200°C shows that the activity coefficients of water and diethylamine would be very close to unity and around 8.5,

respectively, in the saturated solution at 200°C. Because of lack of activity coefficient-data for diethylamine in the dilute aqueous solutions used in the present work, however, it was decided to treat the experimental data assuming that the water and diethylamine formed ideal solutions. Although the actual non-ideality will affect the discussion of the final results in terms of molal concentrations of DEA, the assumption of ideality does not introduce any appreciable error in the phase-equilibrium calculation or in the rate calculation. This is because the total pressures were high and the mole fractions of DEA were very low (~5%). In particular, the calculated partial pressure of hydrogen in the vapor phase would not be affected significantly by using an activity coefficient for diethylamine greater than unity, because the partial pressure of DEA would still be very low compared with the total pressure. Also, the calculated concentration of DEA in the liquid phase at equilibrium would not be changed significantly by using a higher activity coefficient for DEA because very little of the DEA is transferred to the vapor in any case.

a) Phase Equilibrium Calculations

The experimental data available for the phase equilibrium calculations were the total volume and the temperature of the

reaction system (V^{o}ml and $T^{o}K$), the total amount of the amine solution charged (G grams), the amine concentration in the charged solution (N normal), the density of the charged solution (ρ grams/ml) and the residual total pressures of the reaction system after each sampling ($p_{(1)}$, $p_{(2)}$, etc.) and the total pressure before taking the zero-point sample ($p_{(0)}$).

Total masses of water and the amine charged, W_1 grams and W_2 grams, respectively, were first computed by

$$W_1 = G\ (1 - 0.07314\frac{N}{\rho}) \qquad (17)$$

and

$$W_2 = G - W_1 \qquad (18)$$

Computation of the equilibrium amounts of water and diethylamine in two phases before starting a run, m_1 grams, m_1' grams, m_2 grams and m_2' grams, in which subscripts 1 and 2 are denoted for water and diethylamine, respectively, was performed with assumptions that specific properties are all identical for various isotopic species of water, that the liquid solution of diethylamine in water is an ideal solution at temperatures above $100^{o}C$, that partial pressures of water and diethylamine over the liquid phase follow Rauolt's law, that Gibbs-Dalton's law holds for the partial pressures in the vapor phase, and that Henry's law can be used for solubility of hydrogen gas in the liquid phase. Applicability of these ideal laws are discussed in Section L-2 of the APPENDIX. Thermodynamic data necessary for the phase equilibrium calculations

such as the specific volumes of liquid water and liquid amine (v_{f1} and v_{f2}), the specific volumes of vapors of water and the amine (v_{g1} and v_{g2}), the vapor pressures of water and the amine (π_1 and π_2) and the Henry's law constant were obtained by procedures described in Section H of the APPENDIX.

The masses of water m_1 and m_1' in liquid and vapor phases, respectively, the masses of diethylamine m_2 and m_2' in these phases and the volumes V and V' of liquid and vapor, respectively, were obtained by trial-and-error solution of the following equations by the procedures described in Section I of the APPENDIX.

Mass balance for water: $$W_1 = m_1 + m_1' \quad (19)$$

Mass balance for DEA : $$W_2 = m_2 + m_2' \quad (20)$$

Volume of liquid : $$V = m_1 v_{f1} + m_2 v_{f2} \quad (21)$$

Volume of vapor : $$V' = m_1' v_{g1} \quad (22)$$

$$V' = m_2' v_{g2} \quad (23)$$

Total volume : $$V^o = V + V' \quad (24)$$

The partial volumes of water and DEA in the liquid phase, v_{f1} and v_{f2}, were assumed to be equal to the specific volumes of the corresponding pure substance at its vapor pressure at the temperature of interest. The specific volume of water in the vapor phase, v_{g1}, was assumed to be equal to the specific volume of saturated steam at the temperature of interest, v_{g1}^s, an assumption justified by the fact that the mole fraction of water in the vapor phase is nearly unity.

The specific volume of DEA in the vapor phase, v_{g2}, was evaluated from

$$v_{g2} = \frac{RT}{M_2 \pi_2 x_2} + \beta_2 \tag{25}$$

where M_2 is the molecular weight of DEA, R is the gas constant 82.07 ml.atm./gm-mole·°K, β_2 is the first virial coefficient for DEA in ml/gram, π_2 is the vapor pressure of DEA and x_2 is the mole fraction of DEA in the liquid:

$$x_2 = \frac{\frac{m_2}{M_2}}{\frac{m_1}{M_1} + \frac{m_2}{M_2}} \tag{26}$$

It is the dependence of v_{g2} on m_1 and m_2 that makes trial-and-error solution of these equations necessary.

The gram moles of hydrogen $n'_{o,0}$ in the vapor phase before taking the zero-point sample is

$$n'_{o,0} = \frac{p_{o,0} V'}{RT} \tag{27}$$

where the partial pressure of hydrogen at this time $p_{o,0}$ is

$$p_{o,0} = p_{(0)} - (\pi_1 x_1 + \pi_2 x_2) \tag{28}$$

The gram moles of hydrogen in the liquid phase at this time $n_{o,0}$ was obtained from the Henry's law constant for hydrogen c, in mm Hg/mole fraction:

$$\frac{n_{o,0}}{n_{o,0} + n_{1,0} + n_{2,0}} \simeq \frac{n_{o,0}}{n_{1,0} + n_{2,0}} \simeq \frac{760\, p_{o,0}}{c} \tag{29}$$

where $n_{1,o}$ and $n_{2,o}$ are the gram moles of water and DEA in the liquid phase, obtained from m_1 and m_2 by

$$n_{i,o} = \frac{m_i}{M_i} \tag{30}$$

Using these results, the fractions of hydrogen and water that are in the liquid phase, λ_o and λ_1, respectively, and those that are in the vapor phase, λ_o' and λ_1', were computed as follows:

$$\lambda_o = 760\ (n_{1,o} + n_{2,o})\ \frac{RT}{cV'} \tag{31}$$

$$\lambda_1 = \frac{m_1}{W_1} \tag{32}$$

$$\lambda_o' = 1 - \lambda_o \tag{33}$$

$$\lambda_1' = 1 - \lambda_1 \tag{34}$$

From phase equilibrium calculations made after successive gas samples were taken, it was found that the amounts of water and diethylamine removed with the samples were so small that the mass of each substance present and its distribution between liquid and vapor phases could be assumed to remain constant during each run at the values found before the zero-point sample was taken. This point is illustrated in Section K-1 of the APPENDIX. Only the amounts of hydrogen gas in the system, therefore, remained to be re-evaluated for each partial run, and V', m_1, m_2, m_1' and m_2' obtained for the system before taking the zero-point sample were assumed to remain unchanged throughout the run and to be applied for all partial runs in

in the run. Consequently, λ_o and λ_1 also remain constant throughout the run. The amounts of hydrogen gas present during partial run n were obtained by

$$p_{o,n} = p_{(n)} - (\pi_1 x_1 + \pi_2 x_2) \tag{35}$$

and

$$n'_{o,n} = \frac{p_{o,n} V'}{RT} \tag{36}$$

p(n) is the total pressure during the n-th partial run. x_1 and x_2 used in Eqn. (35) are the same ones obtained for the system before taking the zero-point sample.

b) Rate Calculations

As the results of the phase equilibrium calculations, the gram moles of water in the liquid and vapor phases ($n_{1,o}$ and $n'_{1,o}$), the gram moles of diethylamine in the liquid and vapor phases ($n_{2,o}$ and $n'_{2,o}$) before taking the zero-point sample, and the gram moles of hydrogen present before taking the zero-point sample ($n'_{o,o}$) and those remaining in the system after taking sample number n-1 ($n'_{o,n}$; n=1,2,...) have been calculated.

Because appreciable amounts of hydrogen gas were withdrawn via gaseous samples, solution of the differential rate equation could not be applied to an entire run. Instead, each run was divided into partial runs as described previously, the amounts of individual isotopic species present in the system at the beginning of each partial run were re-evaluated for the state of the system at that time, and a solution of

a rate equation was applied to each partial run using the re-evaluated amounts of the reactants as the initial conditions of the solution. In the following, the material balance calculations for the evaluation of the initial conditions for each partial run will be discussed first, a differential rate equation and its general solution for the present reaction will be presented next, and finally application of the solution of the rate equation to the partial runs and, subsequently, to the entire run will be described.

i) Material Balance Calculations

Total amounts of the isotopic species present in both phases before taking the zero-point sample were computed as follows:

H_2^* : $A_0 = n'_{o,0}$ (37)

HDO : $B_0 = 2(\eta - f_d)(n_{1,0} + n'_{1,0})$ (38)

HD : $C_0 = 0$ (39)

H_2O : $D_0 = (1 - \eta)(n_{1,0} + n'_{1,0})$ (40)

$(C_2H_5)_2NH$: $E_0 = (1 - f_d)(n_{2,0} + n'_{2,0})$ (41)

$(C_2H_5)_2ND$: $G_0 = f_d(n_{2,0} + n'_{2,0})$ (42)

---

*Strictly speaking, this equation should be

$$A_0 = n'_{o,0}/(1 - \lambda_o)$$

but λ_o is small (0.02 to 0.03), and the factor $(1 - \lambda_o)$ has been replaced by unity.

where f_d is obtained from Eqn. (12) or (13), and η is a solution of the quadratic solution

$$(4 - K_w)\eta^2 + [K_w - 2 f_d(4 - K_w)]\eta + 2 f_d(2 f_d - K_w) = 0 \tag{43}$$

in which K_w is the equilibrium constant of the reaction

$$H_2O + D_2O \rightleftharpoons 2HDO \tag{44}$$

whose values were obtained as described in Section H of the APPENDIX.

The fraction of exchangeable deuterium present in water, F, was then computed from

$$F = \frac{2(B_0 + D_0)}{(E_0 + G_0) + 2(B_0 + D_0)} \tag{45}$$

It was assumed to remain constant throughout the run, as the fraction of the charge of water and diethylamine removed via gas phase samples was very small.

Total amounts of H_2 and HD, A_n and C_n, present in the system at the beginning of a partial run, Run No. n, that is, right after the sample No. (n-1) was taken, were obtained from $n'_{o,n}$, the total amounts of all isotopic species of hydrogen gas present in the system at the beginning of the partial run, and $f'_{d,(n-1)}$, the atom fraction deuterium in hydrogen gas at the beginning of the partial run obtained as a result of the thermal conductivity analysis of the sample No. (n-1), as follows

$$H_2: \quad A_n = n'_{o,n}\left[1 - f'_{d,(n-1)}\right]^2 \tag{46}$$

$$\text{HD} : \quad C_n = 2 n'_{o,n} \left[1 - f'_{d,(n-1)}\right] f'_{d,(n-1)} \tag{47}$$

These equations were derived by assuming that the equilibrium constant of the reaction (14) had the value 4.0. Gram atoms of deuterium transferred ΔX_n from water to hydrogen gas during time period Δt_n, the period of the partial run No. n, was obtained from $n'_{o,n}$, $f'_{d,(n-1)}$ and $f'_{d,n}$, the last one being the atom fraction deuterium in hydrogen gas at the end of the partial run obtained as a result of the thermal conductivity analysis of the sample No. n, as follows:

$$\Delta X_n \simeq 2 n'_{o,n} \left[f'_{d,n} - f'_{d,(n-1)}\right] \tag{48}$$

This is an approximate formula since it neglects the presence of small amounts of D_2. Total amounts of HDO and H_2O, B_n and D_n, present at the beginning of the partial run No. n were obtained from B_{n-1} and D_{n-1}, the amounts present at the beginning of the preceding partial run, and ΔX_{n-1}, the amount of deuterium transferred from water to hydrogen gas during the preceding partial run, as follows:

$$\text{HDO} : \quad B_n = B_{n-1} - F\Delta X_{n-1} \tag{49}$$

$$H_2O : \quad D_n = D_{n-1} + F\Delta X_{n-1} \tag{50}$$

ii) Rate Equation and Its Solution

The deuterium transfer reaction of interest was the one occurring in the liquid phase

$$H_2 + \text{HDO} \underset{k_2}{\overset{k_1}{\rightleftharpoons}} \text{HD} + H_2O \tag{3}$$

where the specific rate constants for the forward reaction k_1 and the reverse reaction k_2 may be assumed related to the equilibrium constant K defined by Eqn. (4) through

$$k_1 = K\, k_2 \tag{51}$$

At the same time, a small amount of deuterium is transferred in a similar reaction occurring in the vapor phase, with specific rate constants k_1' and k_2', related by a similar equation

$$k_1' = K\, k_2' \tag{52}$$

On the assumption that the rate of transfer of deuterium in each phase is proportional to the concentration of reacting species and total volume of each phase, the differential equation for the number of gram atoms of deuterium X transferred from water to hydrogen in time t may be expressed as

$$\frac{dX}{dt} = \left[\frac{\lambda_o \lambda_1 k_2}{V} + \frac{\lambda_o' \lambda_1' k_2'}{V'}\right] K(A - X)(B - FX) - (C + X)(D + FX) \tag{53}$$

where A, B, C and D are the number of gram moles of the reactants present at time zero, and k_2 and k_2' are the specific rate constants of the backward reaction of Eqn. (3) in the liquid and vapor phases, respectively, each expressed as gram-atoms deuterium transferred/hour·ml.$(\text{gmole/ml})^2$. Obtaining values of k_2 for various reaction conditions was the primary objective of the present work.

In deriving this equation, the vapor phase reactions were treated as a volume reaction rather than a surface reaction which it actually is. This was primarily because the area of the internal surface of the stainless steel wall which is primarily exposed to the vapor phase, although mostly wetted by a thin layer of water, was not known to any precision. It was secondarily to keep a symmetrical form for the rate equation.

The solution of Eqn. (53) is

$$\frac{1}{\beta - \alpha} \ln \frac{\beta\ (X - \alpha)}{\alpha\ (X - \beta)} = \frac{\langle k_2 \rangle}{V^o} F\ (1 - K)\ t \tag{54}$$

where

$$\alpha = \frac{-\delta_1 - \sqrt{\delta_1^2 - \delta_2}}{2F\ (1 - K)} \tag{55}$$

$$\beta = \frac{-\delta_1 + \sqrt{\delta_1^2 - \delta_2}}{2F\ (1 - K)} \tag{56}$$

$$\delta_1 = K\ (AF + B) + (CF + D) \tag{57}$$

$$\delta_2 = -\ 4F\ (1 - K)\ (KAB - CD) \tag{58}$$

and

$$\frac{\langle k_2 \rangle}{V^o} \equiv \lambda_0\lambda_1 \frac{k_2}{V} + \lambda'_0\lambda'_1 \frac{k'_2}{V'} \tag{59}$$

β has the physical significance of the number of gramatoms of deuterium which could be transferred to HD by the time equilibrium was reached and the net reaction rate dX/dt became zero.

The derivation of the rate equation and its solution are presented in detail in Section J of the APPENDIX.

.iii) Application of Solution of Rate Equation

The solution (54) was applied to each partial run as follows. Eqn. (54) for the n-th partial run could be expressed as

$$\frac{1}{\beta_n - \alpha_n} \ln \frac{\beta_n(\Delta X_n - \alpha_n)}{\alpha_n(\Delta X_n - \beta_n)} = \frac{\langle k_2 \rangle}{V^o} F\ (1 - K)\Delta t_n \tag{60}$$

The left side of Eqn. (60), equated to ΔL_n by definition

$$\Delta L_n \equiv \frac{1}{\beta_n - \alpha_n} \ln \frac{\beta_n(\Delta X_n - \alpha_n)}{\alpha_n(\Delta X_n - \beta_n)} \tag{61}$$

was calculated from A_n, B_n, C_n, and D_n by using equations identical with Eqns. (55) to (58) except that each symbol in those equations, except F and K, is accompanied by a subscript n. ΔL_n was computed for every partial run of a run, which may be called a complete run to distinguish it from the partial runs that constitute it, and, then, a quantity L_n defined by

$$L_n = \sum_{i=1}^{n} \Delta L_i \tag{62}$$

was computed for every value of n. These values of L_n were plotted against t_n, the total time elapsed between the start of the complete run and the end of the n-th partial run, the time at which the sample No. n was taken. A probable experimental error $P(L_n)$ associated with each L_n was computed by propagating estimated experimental errors in individual measurements by the standard manner, and a weight w_n, defined by

$$w_n \equiv \frac{P^2(L_1)}{P^2(L_n)} \tag{63}$$

was assigned to each L_n. Equations used for the error calculations are presented in Section J of the APPENDIX. This procedure makes L_n of the larger n less and less important very rapidly. A slope S of a best straight line drawn through the origin and among the plotted points was determined by the standard least-squares method. A mean probable experimental error in L_n predicted from the estimated experimental errors in the individual L_n's, obtained from

$$\text{Predicted:} \qquad \overline{P(L)} = \sqrt{\frac{\sum_{}^{M} w_n P^2(L_n)}{(M-1)\sum_{}^{M} w_n}} \tag{64}$$

was compared with a mean observed error in L_n obtained from the deviations of individual L_n's from the best straight line, obtained from

$$\text{Observed:} \qquad P(\overline{L}) = 0.675 \sqrt{\frac{\sum_{}^{M} w_n (L_n - St_n)^2}{(M-1)\sum_{}^{M} w_n}} \tag{65}$$

The observed probable error $P(\overline{L})$ would be smaller than or of the same order of magnitude as the predicted probable error $\overline{P(L)}$ if the assumption that the rate was proportional to the hydrogen pressure and water concentration were valid.

The slope S of the plot of L_n vs t, thus obtained, was used to compute the overall rate constant $\langle k_2 \rangle$ by

$$\langle k_2 \rangle = \frac{SV^o}{F\ (1 - K)} \tag{66}$$

Finally, the liquid phase rate constant k_2 was calculated from the overall rate constant $\langle k_2 \rangle$ and the k_2', obtained from a blank run performed at the same temperature by

$$k_2 = \frac{V^o - V'}{\lambda_o \lambda_1} \left[\frac{\langle k_2 \rangle}{V^o} - \frac{(1 - \lambda_o)\ (1 - \lambda_1)\ k_2'}{V'} \right] \tag{67}$$

These procedures for the application of the solution of the rate equation are explained in detail in Section J of the APPENDIX and the computational procedures are illustrated by the sample calculations in Section K of the APPENDIX.

IV. RESULTS

Table I presents results of the measurement of the liquid-phase specific rate constant k_2 for eleven runs catalyzed by diethylamine. The constant k_2 expresses the rate at which deuterium is transferred from HD to H_2O in the reaction

$$HD + H_2O \longrightarrow HDO + H_2$$

It is expressed in units of gram atoms of deuterium transferred per milliliter of liquid per hour, per unit concentrations of HD and H_2O expressed as gram moles per milliliter.

The error assigned to each value of k_2 is an observed probable error obtained from the mean deviation* of a plot of L vs. t from the straight line predicted by Eqn. (65) for a reaction of first order in reactant concentrations. The procedure for evaluating the error in k_2 is described in Section J of the APPENDIX.

The principal experimental variables characterizing each run are listed: the temperature, the stirring rate in strokes per second, and the concentration of diethylamine expressed as normality in gram moles per liter. The concentration of hydroxyl ion from hydrolysis of diethylamine

$$(C_2H_5)_2NH + H_2O \rightleftharpoons (C_2H_5)_2NH_2 + OH^-$$

---

*This is the quantity $P(\overline{L})$ described in Section III.3.

Table I

Summary of Results of Catalyzed Runs

Run No.	Temp. (°C)	Stir. Rate (s/s)	Amine Conc. (N)	OH^- Conc. (N)	Liq. Phase Rate Const., k_2 $\frac{\text{g-atom D}}{\text{hr.ml.(gmole/ml)}^2}$	
					Cerrai's Experimental K's	Kirschenbaum's Theoretical K's
16	200	8	1.60	0.0142	755 ± 40	834 ± 40
26	200	8	1.55	0.0140	869 ± 27	928 ± 26
15	200	6	1.78	0.0150	1030 ± 39	1121 ± 41
27	200	6	1.50	0.0138	796 ± 19	843 ± 21
17	200	1.5	1.67	0.0145	483 ± 11	520 ± 13
21	200	6	0.84	0.0103	291 ± 4	324 ± 6
29	150	8	1.80	0.0360	443 ± 5	460 ± 6
28	150	8	0.84	0.0177	143 ± 2	147 ± 2
24	150	8	0.78	0.0171	136 ± 2	140 ± 2
19	100	8	1.83	0.0396	111 ± 2	119 ± 2
25	100	8	0.76	0.0256	49 ± 2	51 ± 2

with dissociation constants K_a listed below is also given.

Temperature, °C	K_a
100	8.6×10^{-4}
150	3.75×10^{-4}
200	1.27×10^{-4}

The source of these values of K_a is described in Section L of the APPENDIX.

Two sets of values of the rate constant have been computed, the left column for values of the equilibrium constant K for the liquid-phase reaction

$$H_2 + HDO \rightleftharpoons HD + H_2O \qquad (3)$$

measured experimentally by Cerrai et al (H-11) and the right column for values of K quoted by Kirschenbaum (H-8) from theoretical calculations based on spectroscopic data. The two sets of values of K are given in Table II.

Table II

Two Sets of Equilibrium Constant K

for the Liquid Phase Reaction

$H_2 + HDO \rightleftharpoons HD + H_2O$

	K	
Temperature, °C	Cerrai's Experimental	Kirschenbaum's Theoretical
100	0.382	0.370
150	0.446	0.433
200	0.501	0.478

More information on the sources of these equilibrium constants is given in Section H of the APPENDIX. Rate constants evaluated with Kirschenbaum's equilibrium data are from 4 to 5% lower than with Cerrai's. None of the current experiments were run close enough to equilibrium to provide an independent estimate of the equilibrium constants, and the rate data are represented equally well by an equation based on either set, as may be seen from the fact that the percentage probable errors are about the same for both sets.

Reference to the first five runs listed, at 200°C and amine concentrations between 1.50 and 1.78 N show that an increase in stirring rate from 6 to 8 strokes per second does not increase k_2, but a decrease from 6 to 1.5 strokes per second causes a very substantial decrease in k_2. This is used to justify acceptance of all runs at stirring rates of 6 or 8 strokes per second as providing a measurement of k_2 unretarded by finite rate of transfer between phases.

Table III is a similar tabulation of six blank runs made without diethylamine. The specific rate constant k_2' tabulated here represents the number of gram atoms of deuterium transferred from HD to H_2O per milliliter of gas phase volume per hour per unit concentrations of HD and H_2O in the gas phase expressed as gram moles per milliliter.

To give an idea of how well the integrated rate equation (54) fits the experimental data, Figs. 3 to 19 provide plots of the extent of reaction represented by the quantity L in $(\text{gmole})^{-1}$ against time, for each run. Each

Table III

Summary of Results of Blank Runs

Run No.	Temp. (°C)	Stir. Rate (s/s)	Vapor Phase Rate Const., k_2' $\frac{\text{g-atom D}}{\text{hr.ml.(gmole/ml)}^2}$	
			Cerrai's Experimental K's	Kirschenbaum's Theoretical K's
12	200	8	35.5 ± 0.6	39.0 ± 0.6
10	200	6	34.8 ± 0.7	38.9 ± 0.7
11	200	1.5	40.6 ± 0.4	44.7 ± 0.4
Average for 200°C			38.2 ± 0.5	42.2 ± 0.6
9	150	8	58.7 ± 0.8	62.0 ± 0.8
Average for 150°C			58.7 ± 0.8	62.0 ± 0.8
13	100	8	164.4 ± 1.0	173.2 ± 1.1
14	100	8	163.1 ± 1.1	171.3 ± 1.2
Average for 100°C			168.8 ± 1.0	172.3 ± 1.1

point represents k_2 evaluated with Kirschenbaum's equilibrium constant. The limits of error assigned to each point are those predicted from estimates of the errors in measuring each of the quantities going into L. The straight line drawn through the origin in each Figure has been fitted by the method of least squares with weights inversely proportional to the square of the error predicted for each point. In most runs the straight line passes each value of L within the predicted limit of error. This is evidence that the order of reaction assumed in deriving Eqn. (53) is correct. The slope of each line is the quantity S in $(\text{gmole}\cdot\text{hour})^{-1}$ and is used in evaluating the overall rate constant $\langle k_2 \rangle$.

To illustrate how equally well the integrated rate equation (54) fits the experimental data worked up with Cerrai's experimental equilibrium constant, Figs. 12, 13 and 14 also provide the similar plots of L obtained by using the Cerrai's values against time: Figs. 12, 14 and 13 are examples of runs at 100, 150 and 200°C, respectively.

Detailed data for each run are given in Section M of the APPENDIX.

Fig. 3 Results of Run 9 (150°C, 8 s/s , Blank)

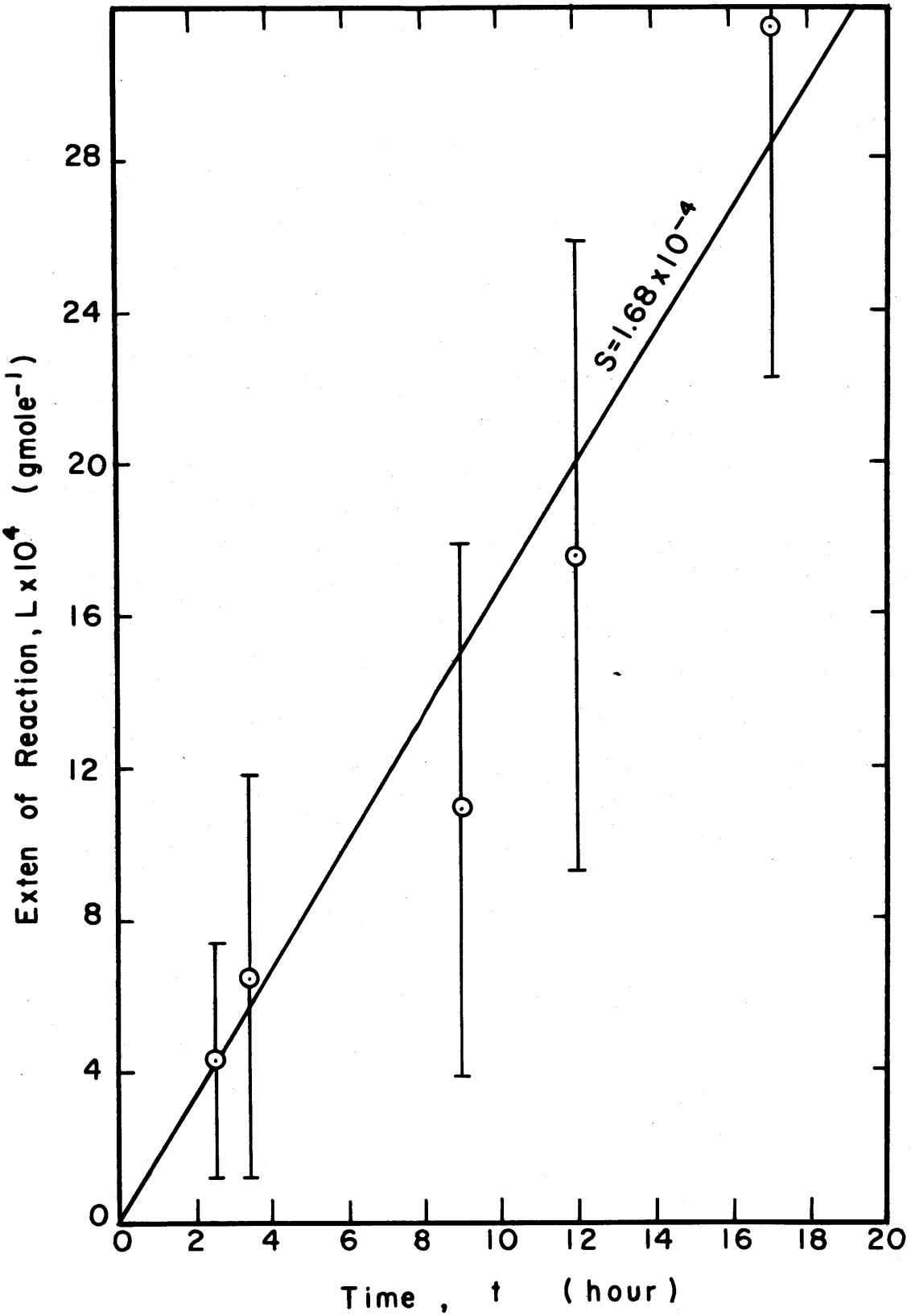

Fig.4 Results of Run 10 (200°C, 6 s/s, Blank)

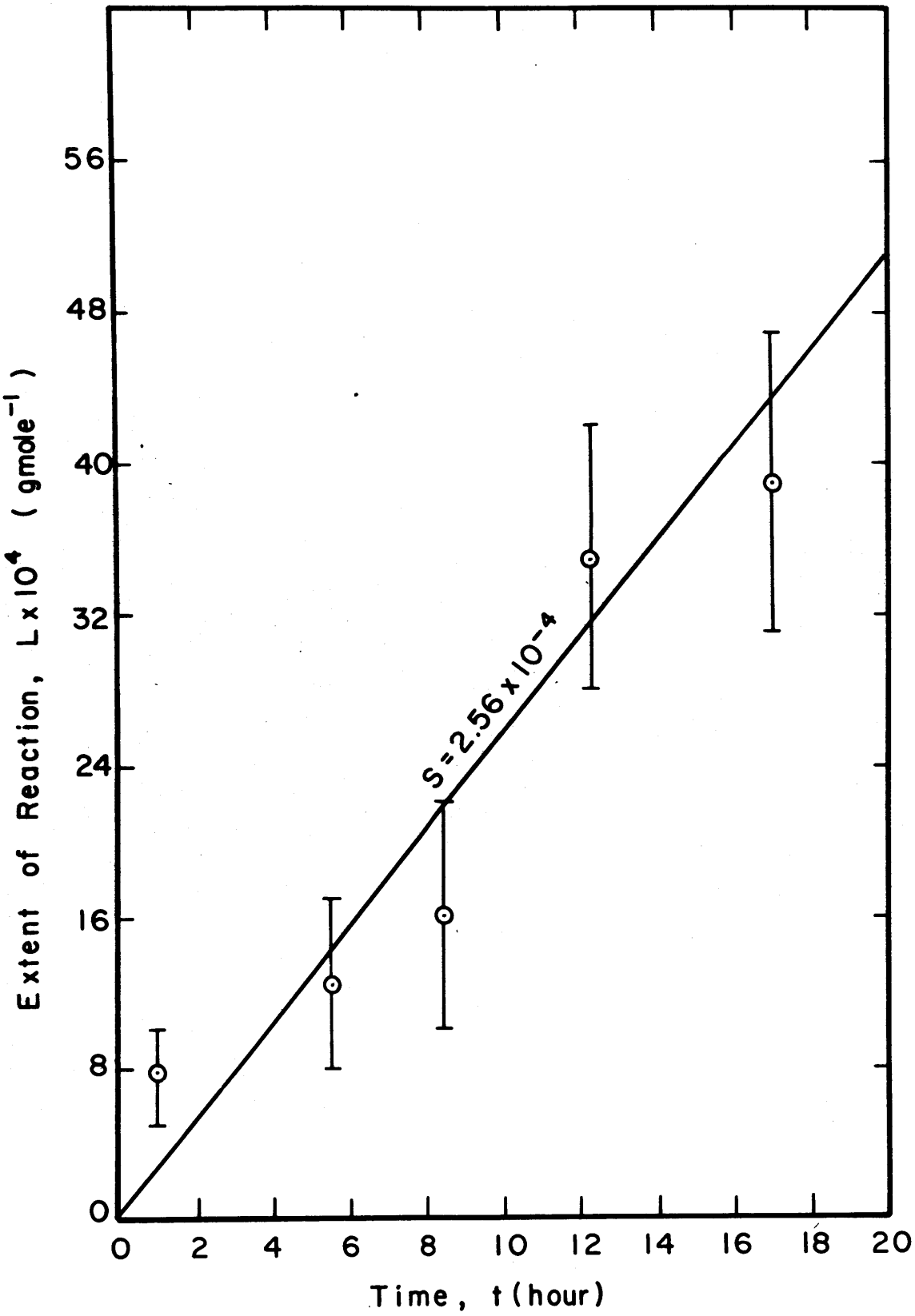

Fig. 5 Results of Run II (200°C, 1.5 s/s, Blank)

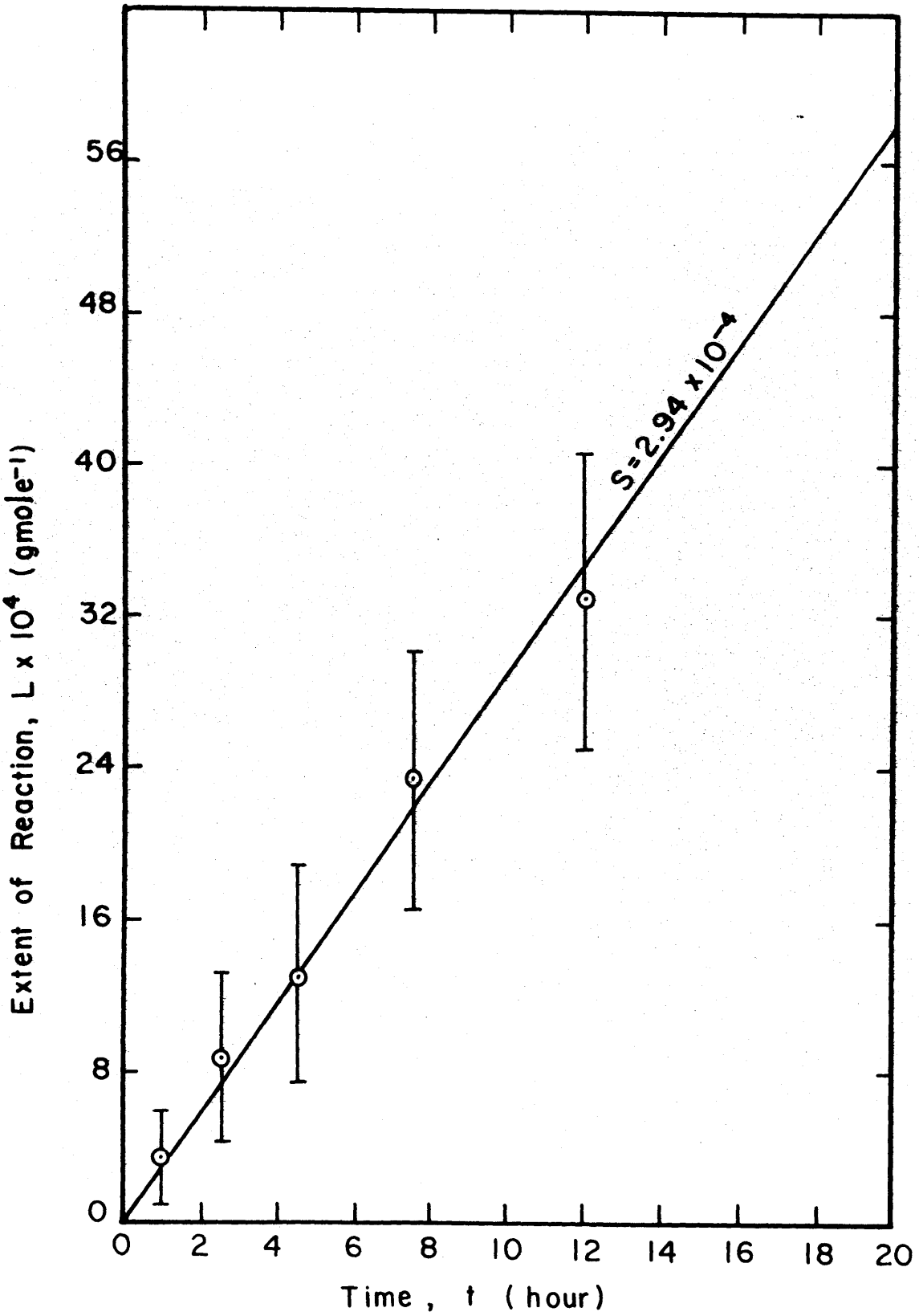

Fig. 6 Results of Run 12 (200°C, 8 s/s,Blank)

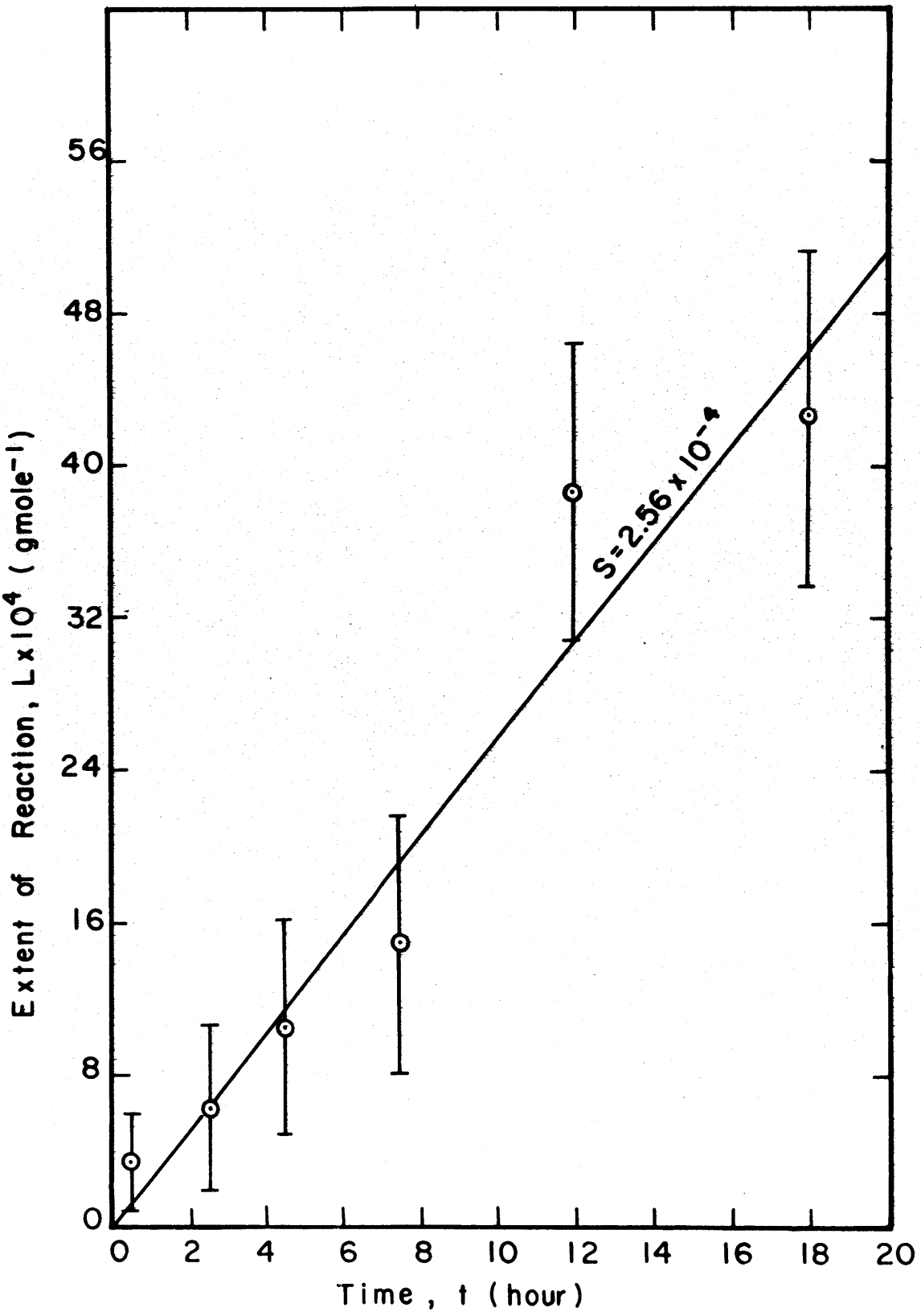

Fig. 7 Results of Run 13 (100°C, 8 s/s, Blank)

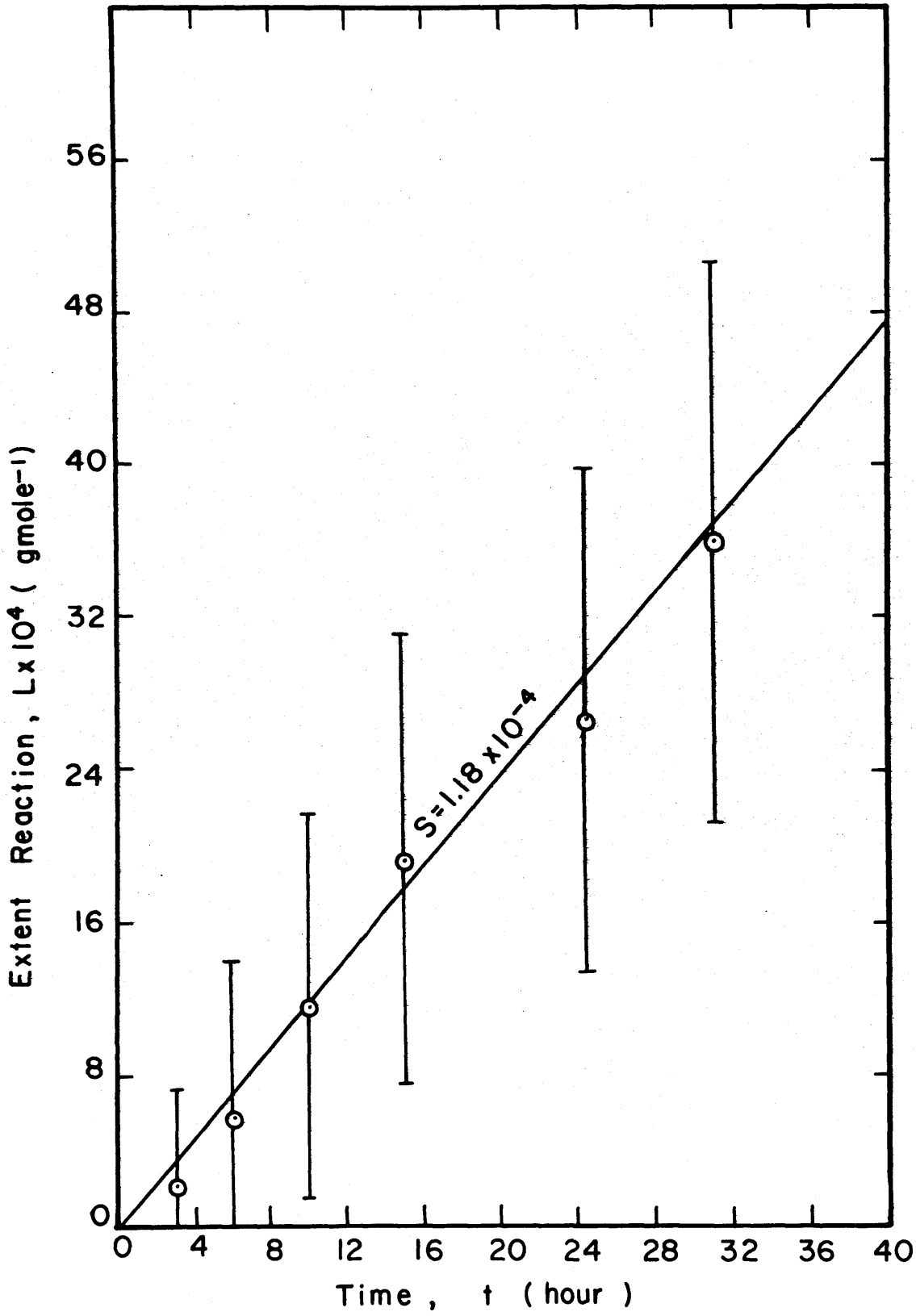

Fig. 8 Results of Run 14 (100°C, 8 s/s, Blank)

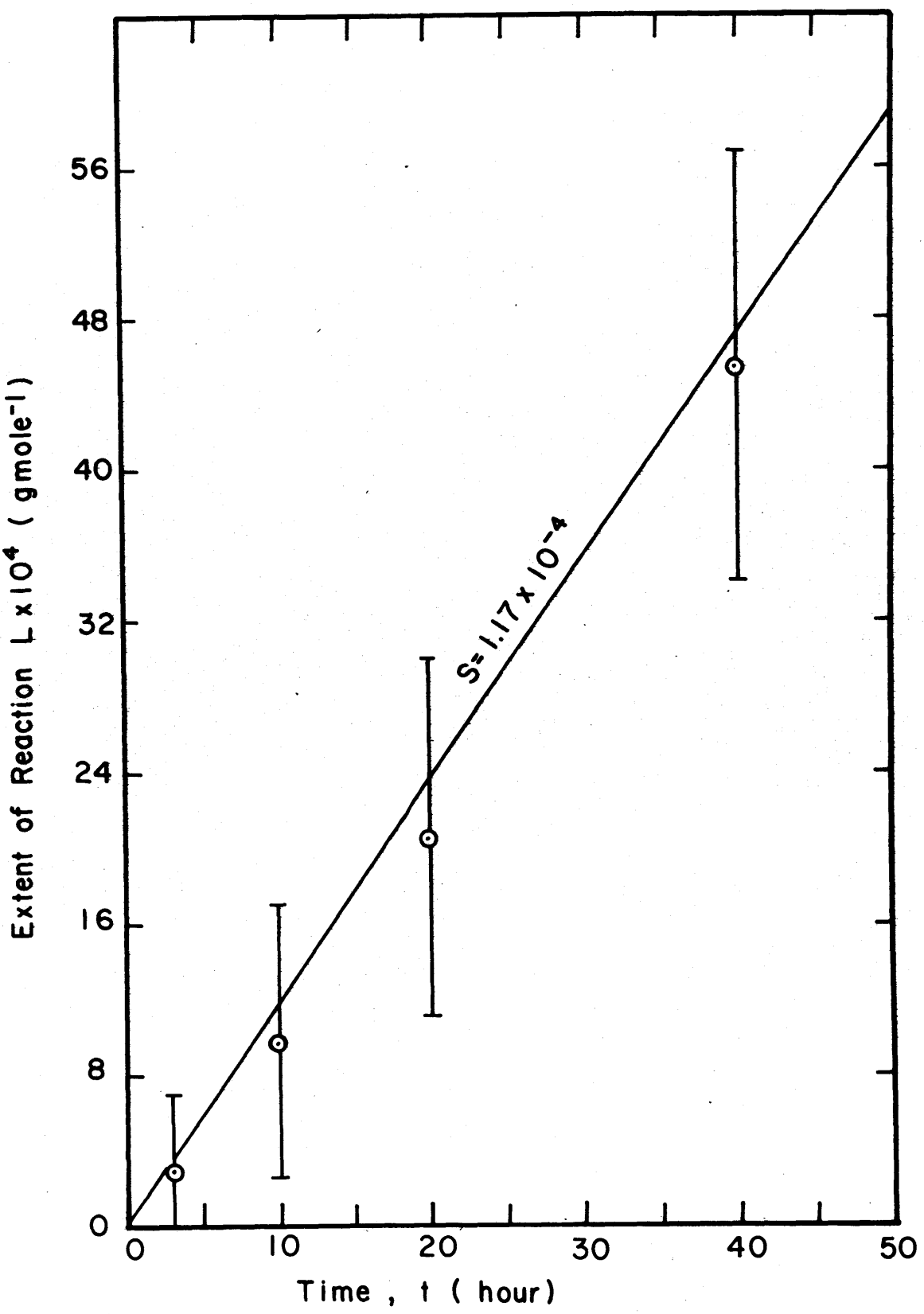

Fig. 9 Results of Run 15 (200°C, 6 s/s, 1.78 N)

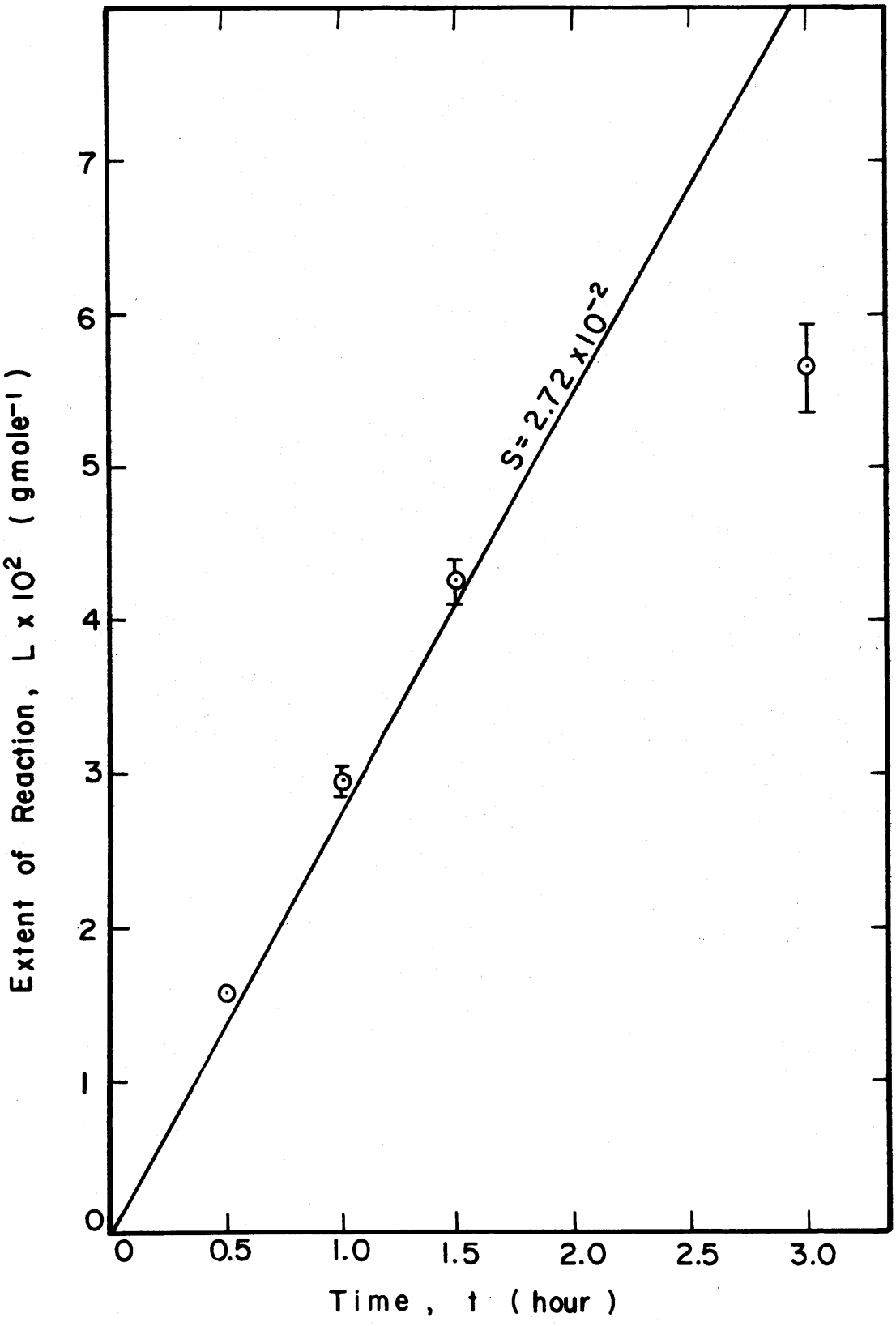

Fig. 10 Results of Run 16 (200°C, 8 s/s, 1.60 N)

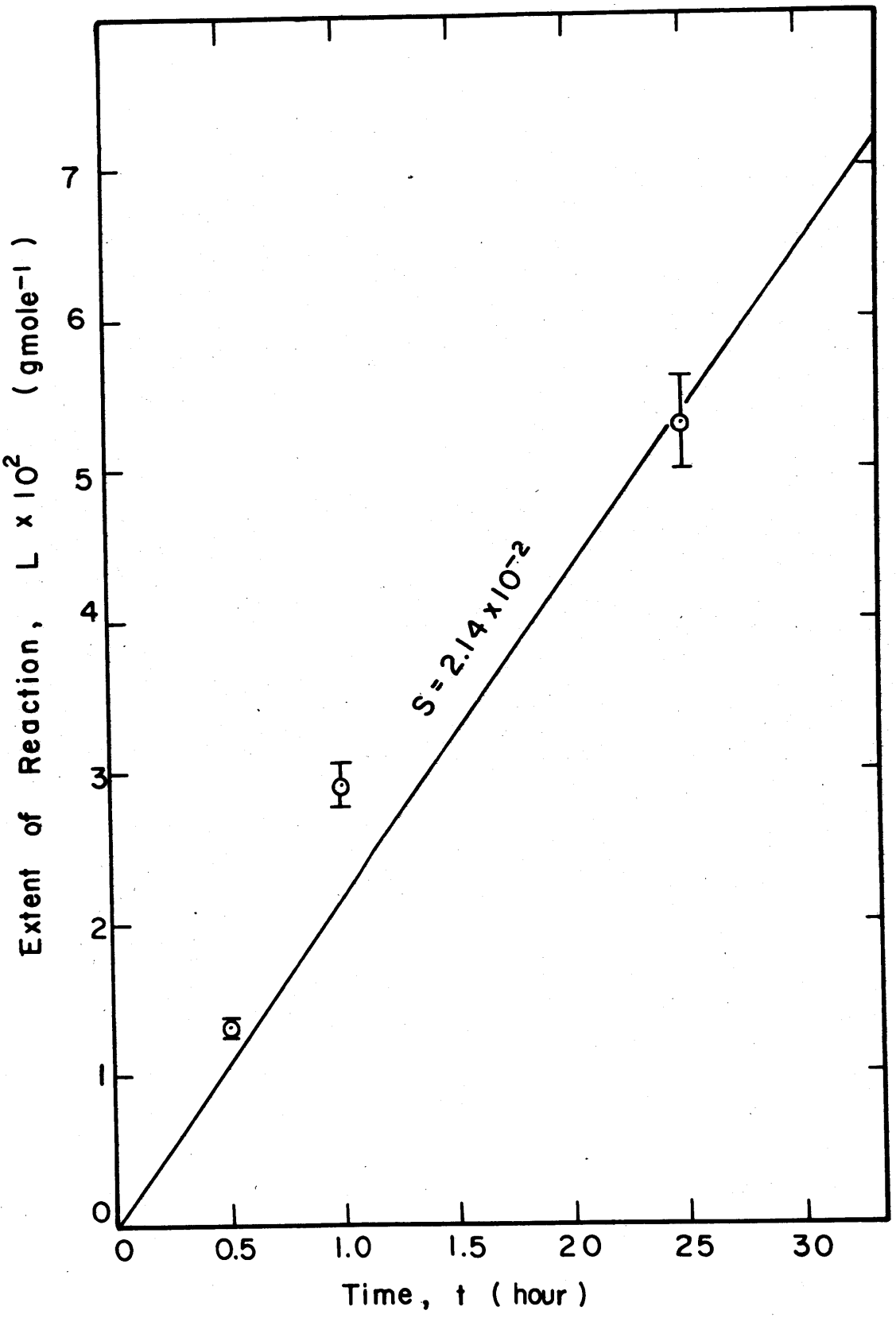

Fig. 11 Results of Run 17 (200°C, 8 s/s , 1.67N)

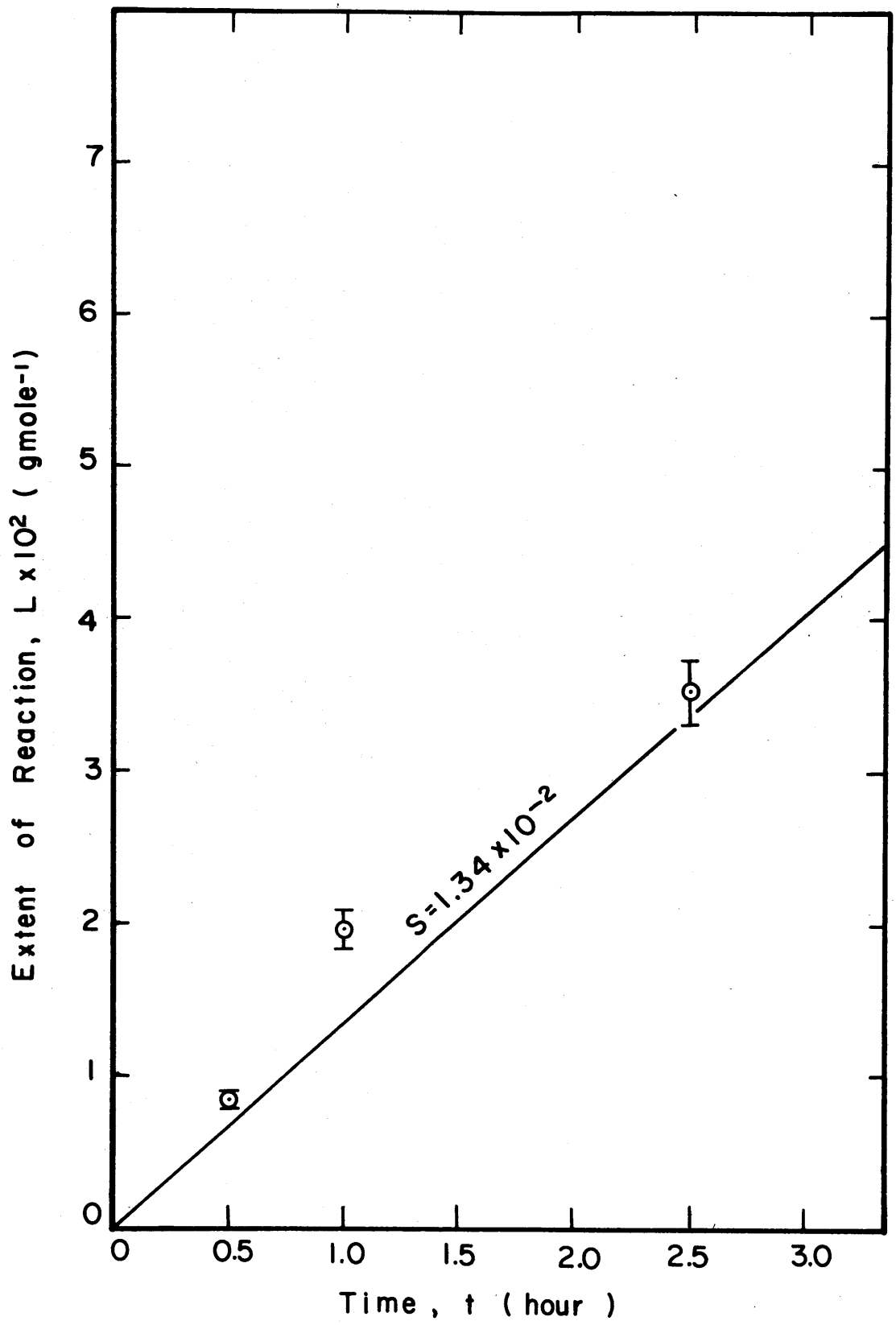

Fig. 12 Results of Run 19 (100°C, 8 s/s, 1.83N)

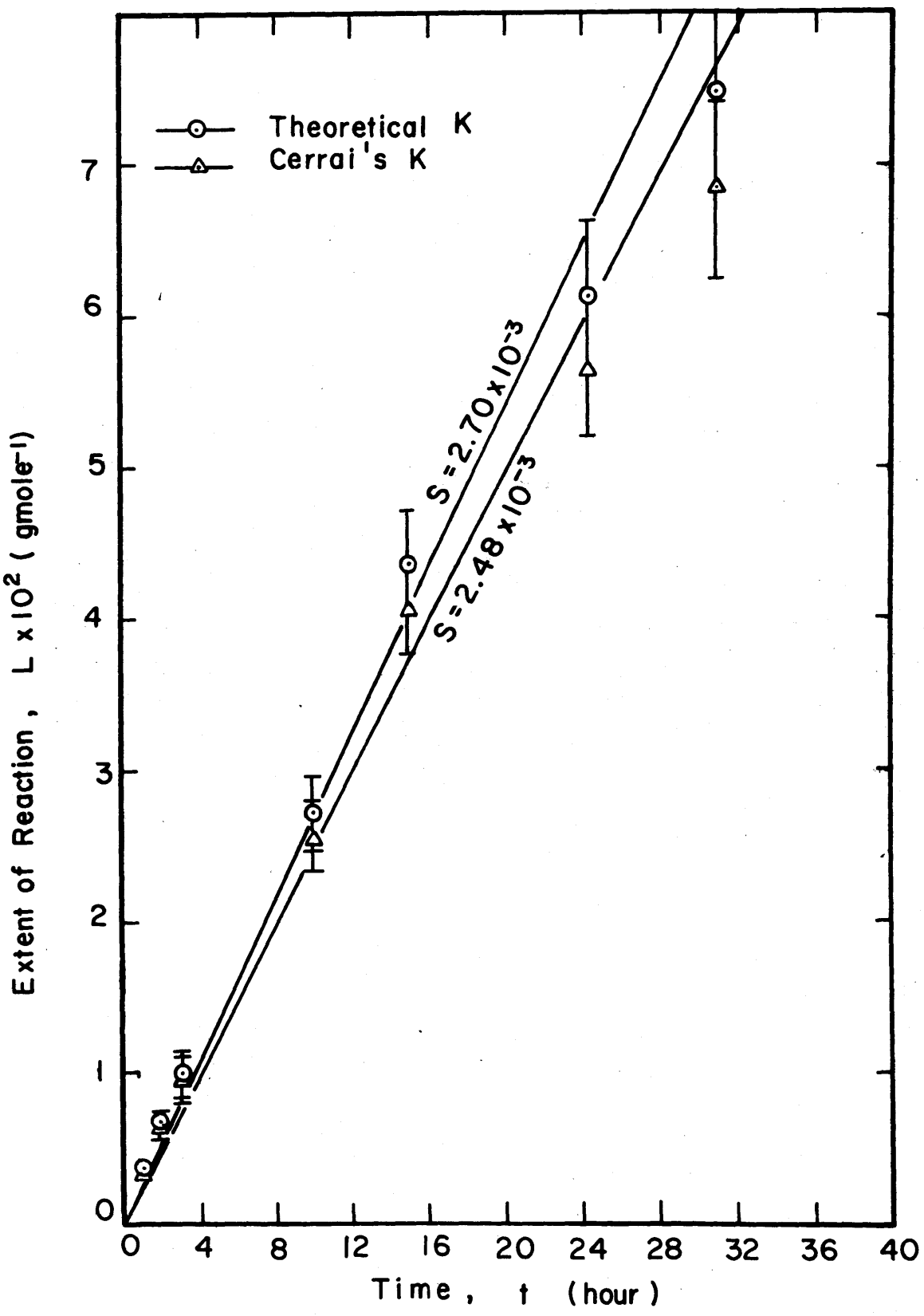

Fig. 13 Results of Run 21 (200°C, 6 s/s, 0.84 N)

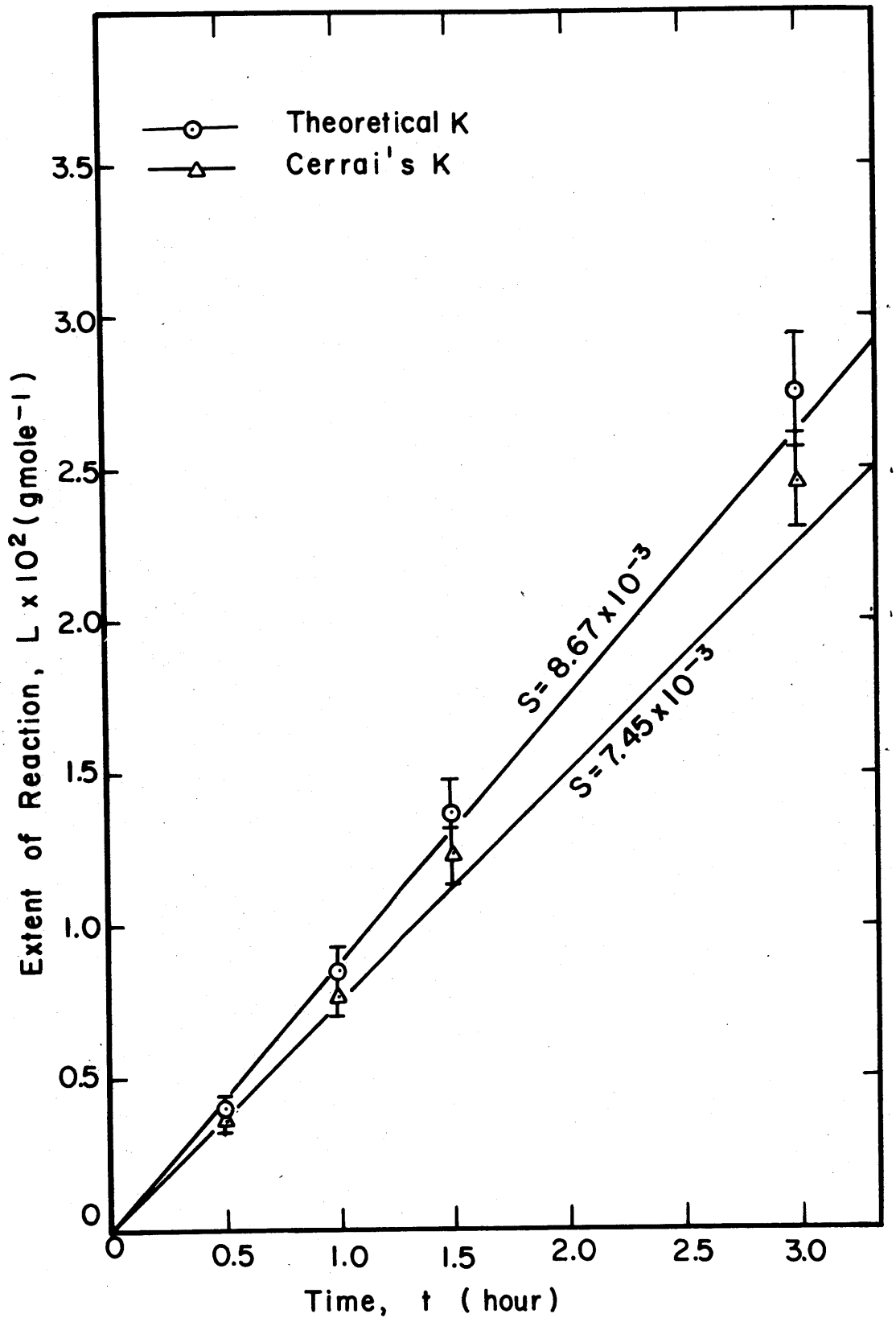

Fig 14 Results of Run 24 (150°C, 8 s/s, 0.78N)

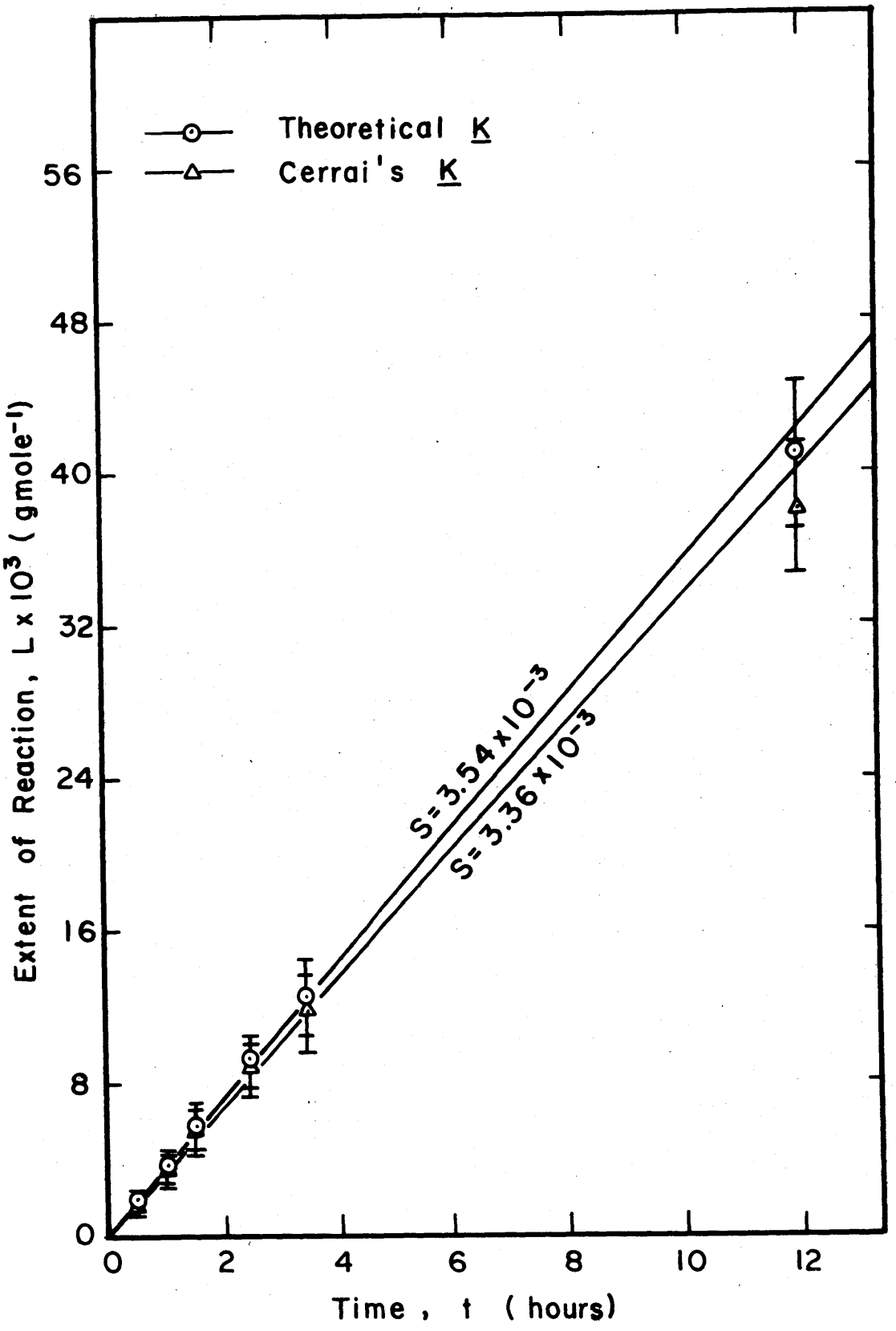

Fig. 15 Results of Run 25 (100°C, 8 s/s, 0.76N)

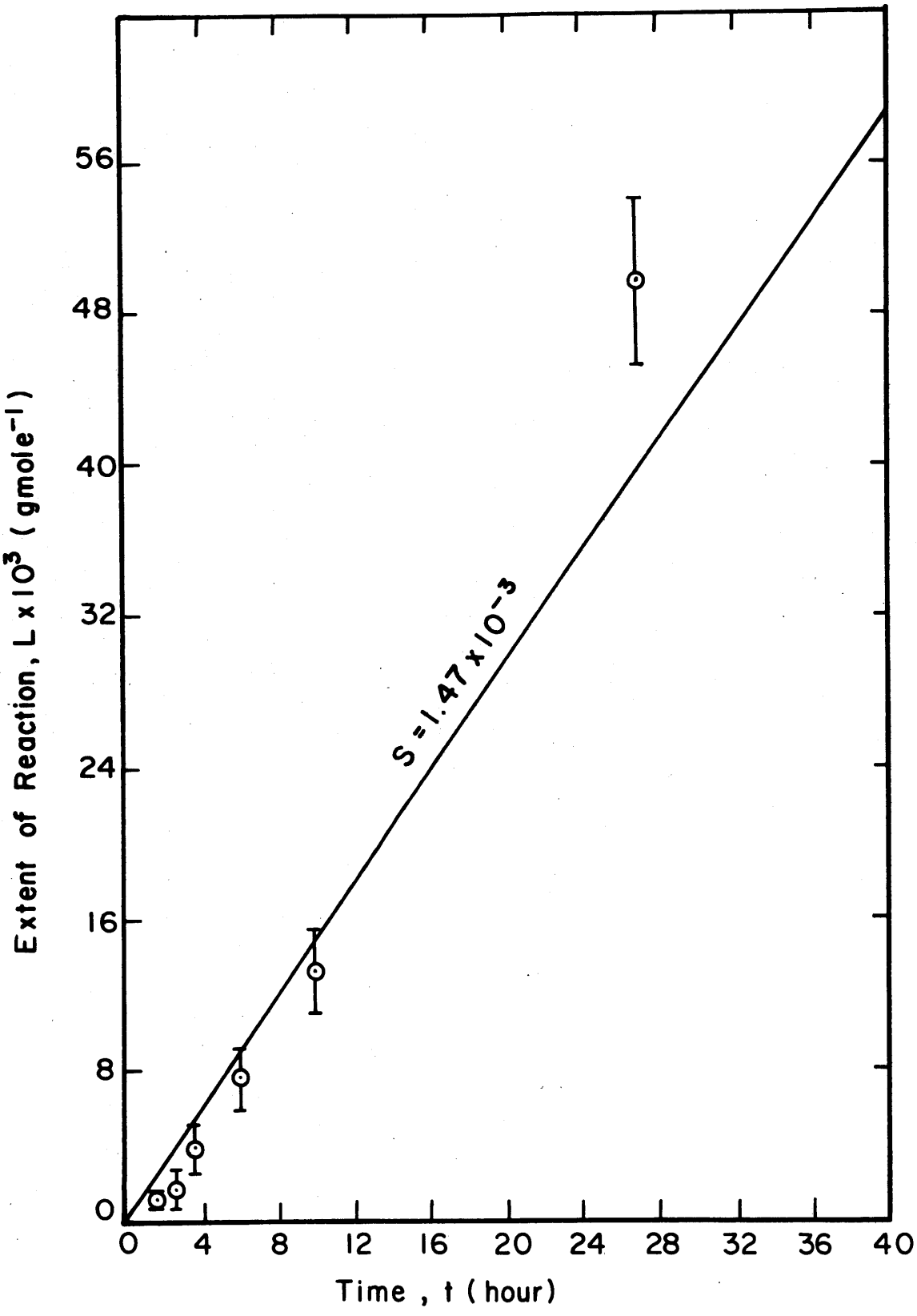

Fig. 16 Results of Run 26 (200 °C, 8 s/s, 1.55 N)

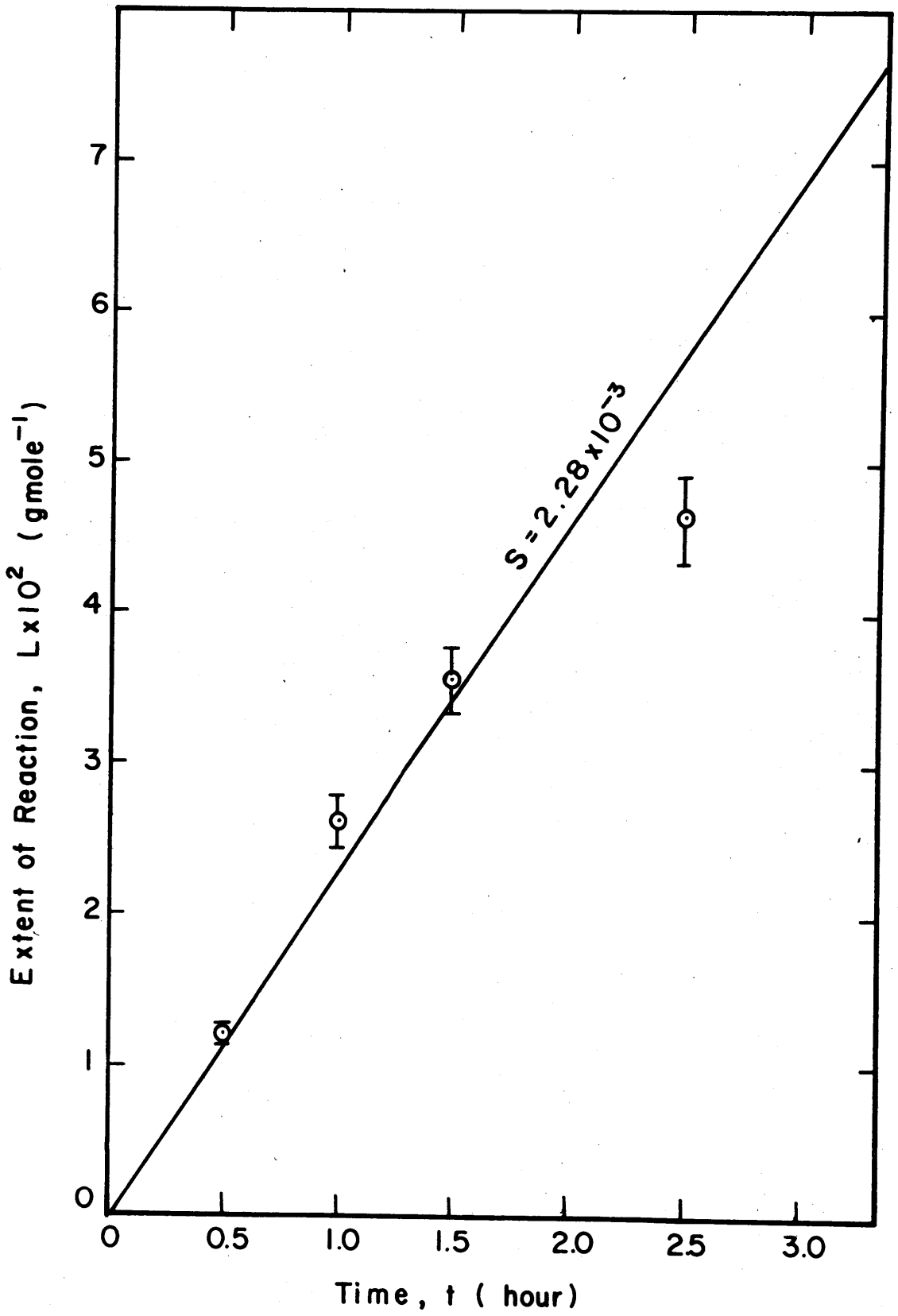

Fig 17 Results of Run 27 (200°C, 6 s/s, 1.50 N)

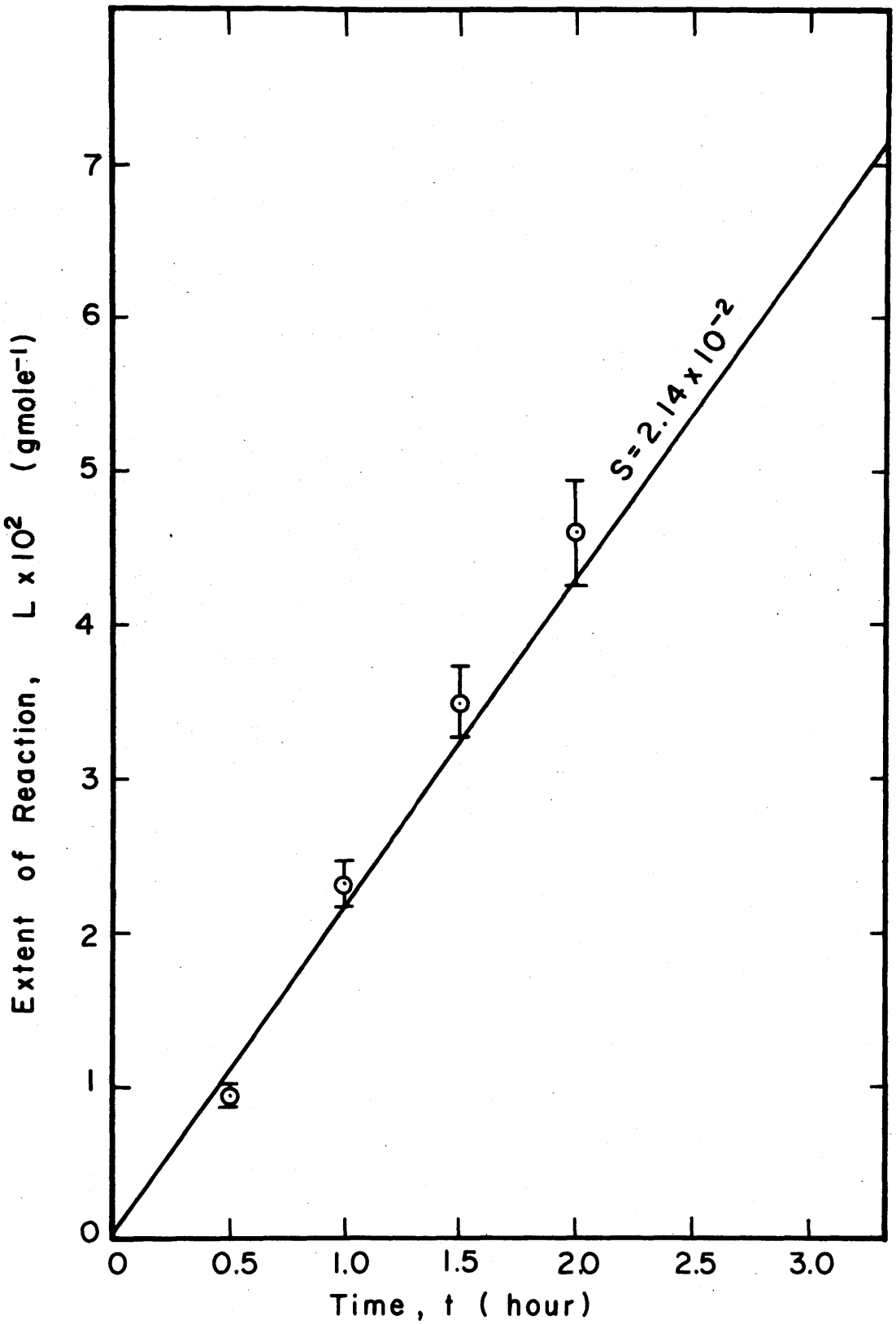

Fig. 18 Results of Run 28 (150°C , 8 s/s , 0.84N)

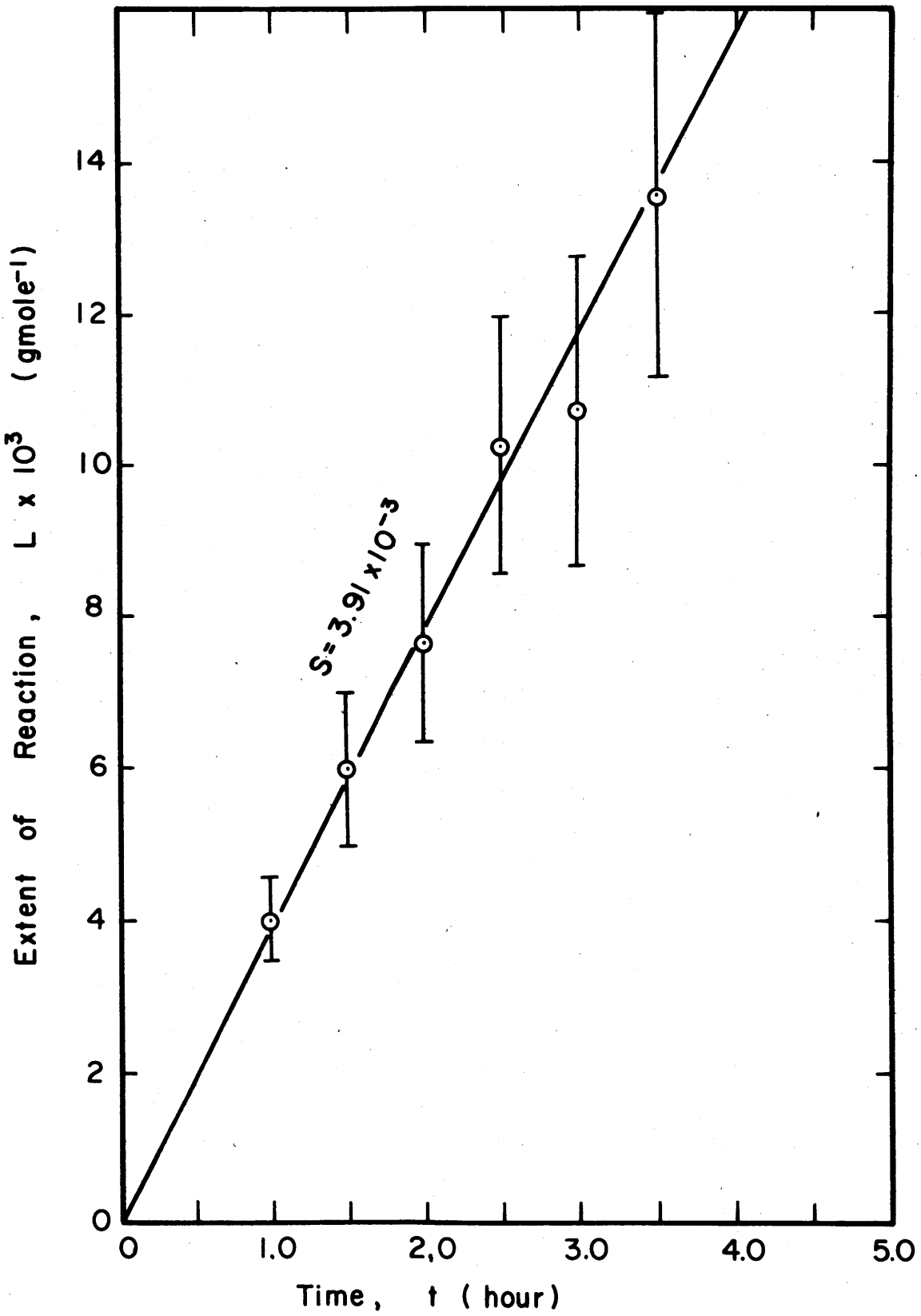

Fig 19 Results of Run 29 (150°C, 8 s/s, 1.80 N)

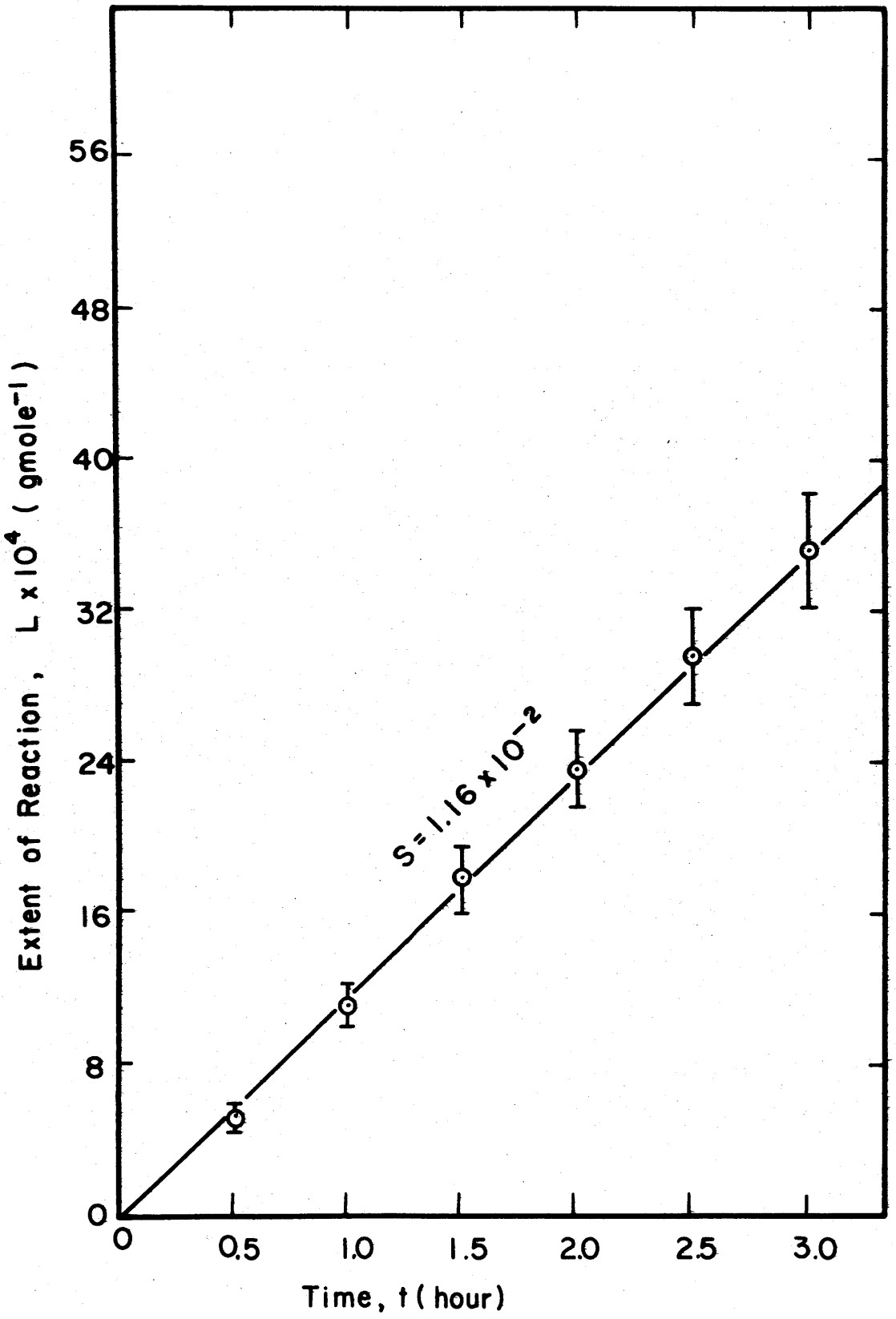

V. DISCUSSION OF RESULTS

In this Chapter, the results of this research will be discussed under four headings. Section 1 discusses the reliability of the experimental results presented in Chapter IV and the validity of the assumed first-order dependence of the reaction rates on the concentrations of HDO and H_2O and dissolved H_2 and HD. Section 2 discusses the dependence of the specific rate constant k_2 on amine concentration and temperature. Section 3 takes up possible mechanisms for the catalytic effect of diethylamine on the exchange reaction. Section 4 compares the rate of deuterium exchange in the presence of diethylamine with the rate for other catalysts reported by other investigators, in order to draw conclusions regarding the practical utility of diethylamine as a catalyst in a heavy water production process.

In view of the observation in Chapter IV, that the experimental data can be interpreted equally well by either set of equilibrium constants K, the theoretical values or Cerrai's experimental ones, the following discussions will, unless stated otherwise, be based on the results obtained with the theoretical equilibrium constants only.

1. Reliability of the Results

As shown in Figs. 3 to 19 in preceding Chapter, a straight line drawn through the origin in each run passes most of the values of L within the predicted limit of error.

L was defined in Eqn. (54), which was drived under the assumption of a first order dependence of the exchange rate on concentrations HDO and H_2O and dissolved H_2 and HD, at least on the hydrogen-rich side of equilibrium. The fact that the points lie close to the line partially confirms the assumption.

To show the point numerically, the mean observed probable error $P(\overline{L})$ of each of the catalyzed runs obtained from the deviations of individual L's from the best straight line is compared in Table IV with the mean predicted probable error $\overline{P(L)}$ obtained from estimates of the errors in measuring each of the quantities going into L. Two sets of values of $P(\overline{L})$ and $\overline{P(L)}$ are given for each run: one is for the values of the equilibrium constant K obtained from Kirschenbaum, and the other for the values of K obtained from Cerrai's experimental data. It is seen that, except for most of the runs at 200°C, the observed probable error $P(\overline{L})$ is smaller than or comparable in magnitude with the predicted probable error $\overline{P(L)}$ for both sets of K's. Only in some of the runs at 200°C in which the reaction system was brought closer to exchange equilibrium than in other runs is $P(\overline{L})$ considerably larger than $\overline{P(L)}$. This is due to wide deviations of L_n from the best straight line obtained in points late in the run when the system has come close to exchange equilibrium. A slight accidental error in measurement of the thermal conductivity bridge-output would

Table IV

Comparison of Observed Error $P(\overline{L})$ with Predicted Error $\overline{P(L)}$

Run No.	Temp. (°C)	Cerrai's Experimental K's		Kirschenbaum's Theoretical K's	
		Observed, $P(\overline{L})$ ($gmole^{-1}$)	Predicted, $\overline{P(L)}$ ($gmole^{-1}$)	Observed, $P(\overline{L})$ ($gmole^{-1}$)	Predicted, $\overline{P(L)}$ ($gmole^{-1}$)
16	200	2.11×10^{-3}	5.66×10^{-4}	1.96×10^{-3}	6.35×10^{-4}
26	200	9.56×10^{-4}	5.65×10^{-4}	9.85×10^{-4}	6.36×10^{-4}
15	200	1.53×10^{-3}	3.84×10^{-4}	1.55×10^{-3}	4.33×10^{-4}
27	200	4.88×10^{-4}	4.89×10^{-4}	5.80×10^{-4}	5.43×10^{-4}
17	200	1.16×10^{-3}	4.64×10^{-4}	1.30×10^{-3}	5.17×10^{-4}
21	200	1.22×10^{-4}	3.29×10^{-4}	2.82×10^{-4}	3.65×10^{-4}
29	150	1.09×10^{-4}	4.74×10^{-4}	1.26×10^{-4}	5.03×10^{-4}
28	150	7.81×10^{-5}	4.37×10^{-4}	8.14×10^{-5}	4.63×10^{-4}
24	150	8.05×10^{-5}	4.11×10^{-4}	8.25×10^{-5}	4.20×10^{-4}
19	100	4.66×10^{-4}	5.64×10^{-4}	4.43×10^{-4}	6.01×10^{-4}
25	100	4.47×10^{-4}	5.08×10^{-4}	4.85×10^{-4}	5.35×10^{-4}

cause a large error in the measured L_n, but such an accidental error is not included in the predicted probable error $P(L_n)$ or, consequently, in $\overline{P(L)}$. An accidental error, especially the one which would make L_n too small, was likely to happen because a steady value of the thermal conductivity bridge-output was obtained by approaching it only from the lower side when the output was close to 10 millivolts, which is the maximum range of the recorder used in the present work. Such an error did not so much affect values of the average slope of the straight line obtained by the least squares method because the probable error $P(L_n)$ for points close to equilibrium are very large compared with that on the points obtained from earlier partial runs so that those points were given very small weights compared with the earlier points.

Since the species whose concentrations changed principally in each run and from run to another were H_2 and HD, the fact that a plot of L vs t yielded a straight line primarily confirms the fact that the reaction rate has first-order dependence on the concentrations of these two species. During some of the runs, such as Runs 15, 17, 21, and 25, the amount of hydrogen in the reacting system was reduced down to 30 to 50% of its amount initially charged (see Tables in APPENDIX Section M). Run 26 (200°C, 8 s/s, 1.55 N) was carried out with an initial hydrogen charge about one half of the charge used for other runs performed under otherwise similar operating condition, and the specific rate constant checked other runs

at higher initial hydrogen content. As the concentrations of HDO and H_2O varied little from time to time or from run to run, no significant confirmation of a first-order dependence on their concentrations was obtained.

Results on specific rate constant k_2' of the vapor phase reaction, as tabulated in Table III, indicate that k_2' decreases with increasing temperature. This apparently anomalous effect is due to the fact that k_2' has been expressed as the gram atoms of D exchanged per unit volume per unit time per unit concentrations of H_2O and HD, as would be appropriate for a homogeneous gas-phase reaction. This was done in order to treat the blank runs in a manner consistent with the catalyzed runs. The reaction actually occurring in the blank runs, however, is probably a heterogeneous reaction taking place on metal walls completely wetted with liquid water, at a rate independent of the concentration of water in the gas phase. To provide a more readily interpretable specific rate constant for the blank runs, the values of k_2' have been converted in Table V into a specific rate constant k_2^s based on metal surface, with the units of gram atoms D transferred per hour per square centimeter of autoclave surface per atmospheric hydrogen partial pressure. The relation between k_2' and k_2^s is

$$k_2^s = \frac{k_2' V' \pi_1}{a (RT)^2} \qquad (68)$$

where V' is the vapor phase volume, approximately 500 ml,

a is the metal surface of the autoclave, approximately 400 cm^2, π_1 is the vapor pressure of water in atmospheres (Table H-1) at absolute temperature $T^{\circ}K$, and R is the gas constant 82.06 ml·atm/gram-mole·$^{\circ}K$.

Table V.

Specific Rate Constants for Blank Runs

Temperature ($^{\circ}C$)	Homogeneous k_2'	Heterogeneous k_2^s
100	172.3±1.1	$(2.12\pm0.02)\times10^{-7}$
150	62.0±0.8	$(2.81\pm0.04)\times10^{-7}$
200	44.7±0.4	$(5.70\pm0.06)\times10^{-7}$

k_2^s increases with increasing temperature in the normal manner.

In correcting the catalyzed runs to obtain the liquid-phase rate constant, it is really immaterial how the results of the blank runs are expressed, because the blank and catalyzed runs were made at the same temperature and with the same vapor-phase volume and same amount of metal surface.

2. Dependence of Rate Constant on Amine Concentration and Temperature

Figures 20, 21 and 22 are plots on log-log paper of the specific rate constant k_2 from the last column of Table I (evaluated with theoretical equilibrium constants) against diethylamine normality N. The average order of the exchange

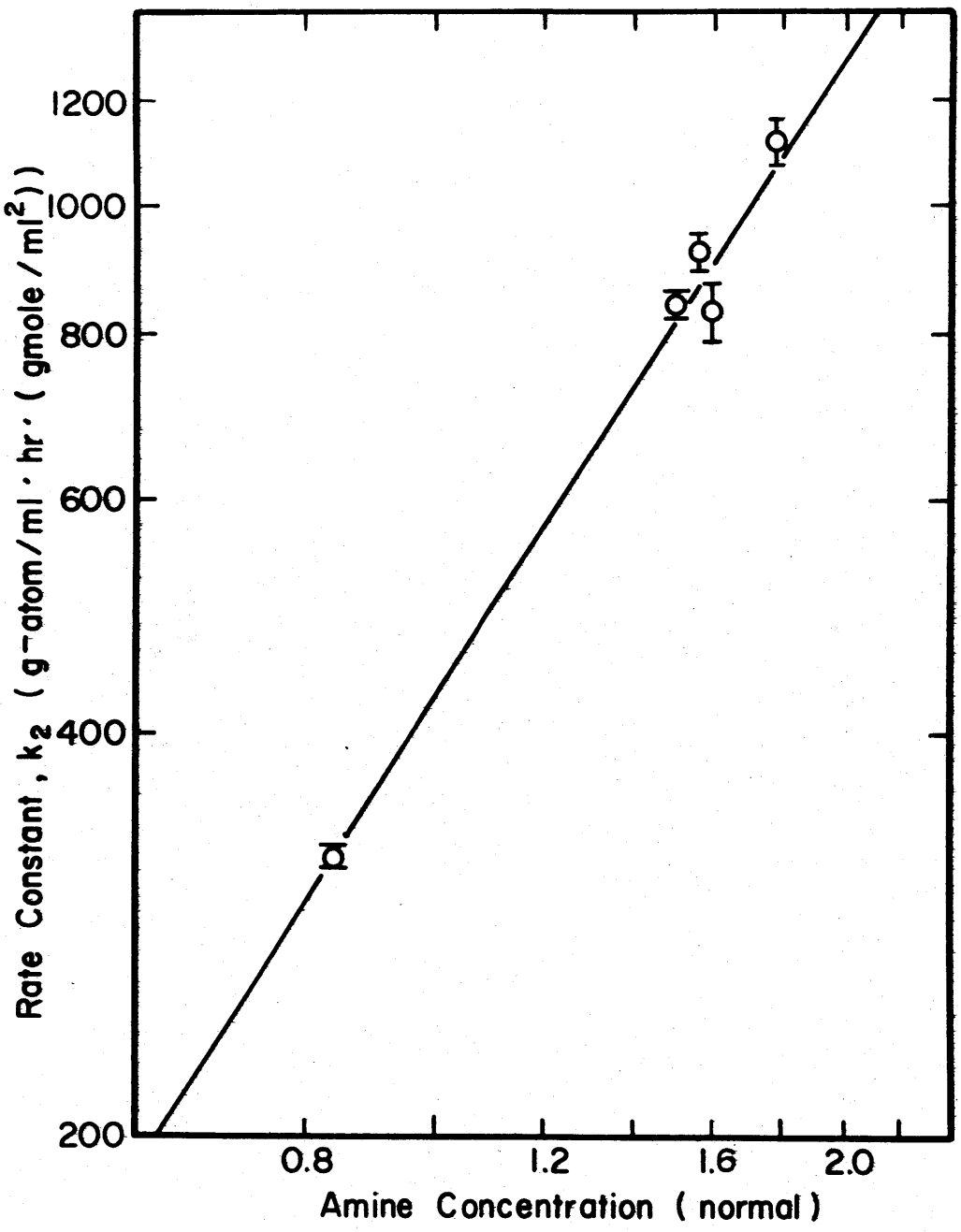

Fig.20 Dependance of Rate Constant k_2 on Amine Concentration at 200 ℃.

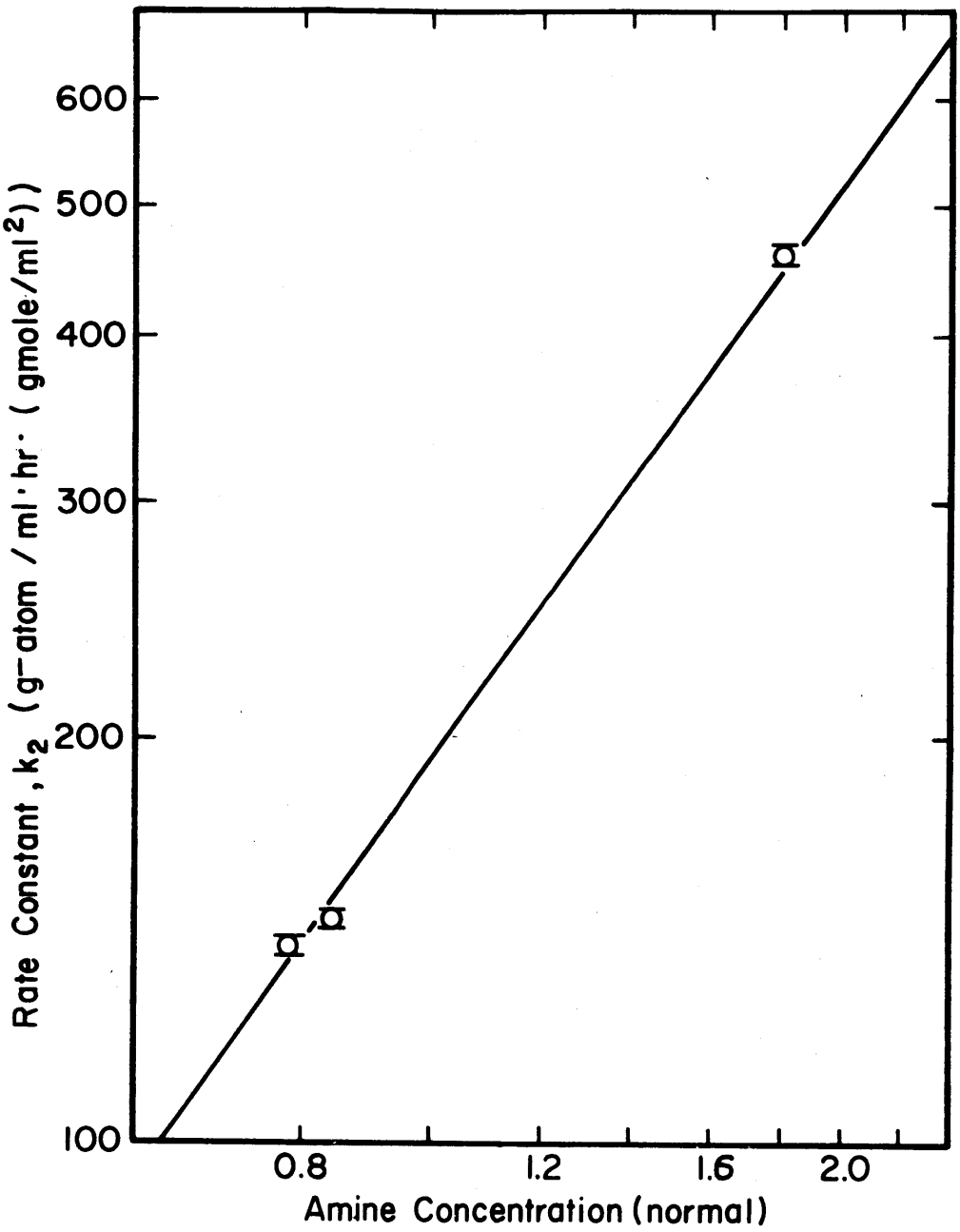

Fig. 21 Dependence of Rate Constant k_2 on Amine Concentration at 150°C.

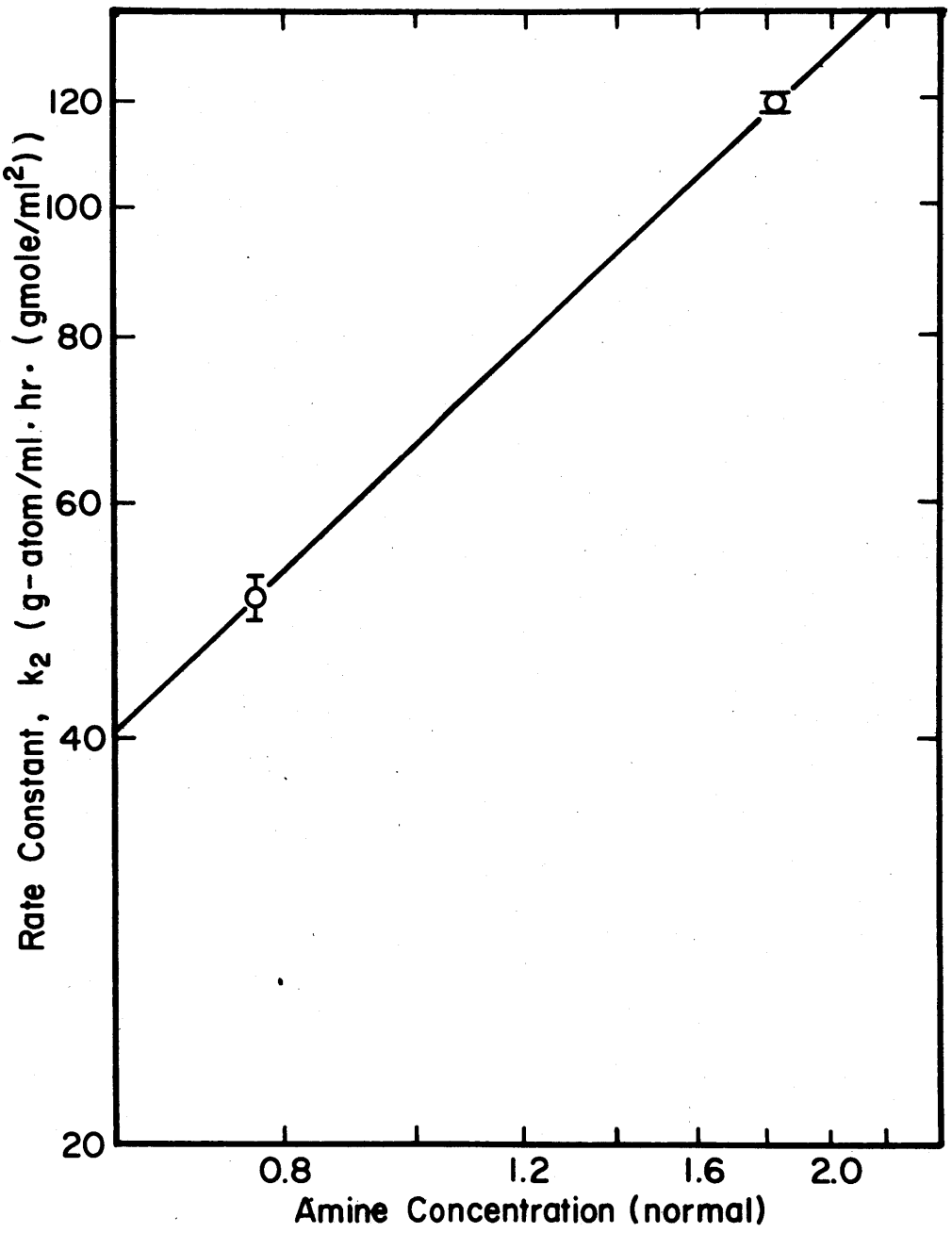

Fig.22 Dependence of Rate Constant k_2 on Amine Concentration at 100 °C.

reaction with respect to the amine concentration was found from slopes of these figures as follows:

At 200°C (from Fig. 20); order $\bar{y}_{200} = 1.58 \pm 0.07$ (69)

At 150°C (from Fig. 21); order $\bar{y}_{150} = 1.46 \pm 0.02$ (70)

At 100°C (from Fig. 22); order $\bar{y}_{100} = 1.07 \pm 0.01$ (71)

If the mechanism of catalysis by hydroxyl ion proposed by Wilmarth et al (A-22) to explain the catalysis of deuterium exchange by KOH were applicable to diethylamine, the slope of these lines should have been 0.5. With diethylamine, hydroxyl ion is obtained from the reaction

$$(C_2H_5)_2NH + H_2O \rightleftharpoons (C_2H_5)_2NH_2^+ + OH^- \qquad (72)$$

with a value of around 10^{-4} for the equilibrium constant K_a defined by

$$K_a \equiv \frac{[(C_2H_5)_2NH_2^+][OH^-]}{[(C_2H_5)_2NH]} \qquad (73)$$

With so small a value of K_a, the concentration of hydroxyl ion at appreciable concentrations of DEA is given by

$$OH^- \doteq (K_a[(C_2H_5)_2NH])^{1/2} \qquad (74)$$

The results tabulated above, however, clearly indicate that the reaction rate depends on the first or higher power of the amine concentration in the system of hydrogen-water-diethylamine in the range of temperature that has been investigated here. This point will be discussed further in

Section 3 of the present chapter.

The rate constant k_2 is expected to depend on temperature as

$$k_2(T) = k_2(T_o)\left[\exp \frac{\Delta E_2}{R_{th}} \left(\frac{1}{T_o} - \frac{1}{T}\right)\right] \qquad (75)$$

where R_{th} is the gas constant, 1.987 calories per gram mole per ^oK, ΔE_2 is the activation energy of the liquid phase reaction

$$HD + H_2O \longrightarrow H_2O + HDO, \qquad (76)$$

and T_o and $k_2(T_o)$ are a reference absolute temperature and the value of k_2 at that temperature. Consequently, a plot of k_2 against 1/T on semilog paper should give a straight line whose slope is $-\Delta E_2/R_{th}$.

Values of k_2 interpolated to amine concentrations of 2.0, 1.6, 1.2 and 0.8 from Figures 20, 21 and 22 have been plotted against 1/T on semilog paper in Figure 23. The fact that the points at 100, 150 and 200°C fall close to straight lines confirms the applicability of Eqn. (75). Average activation energies at the different amine concentrations found from the slopes of the straight lines in Fig. 23 are given in Table VI.

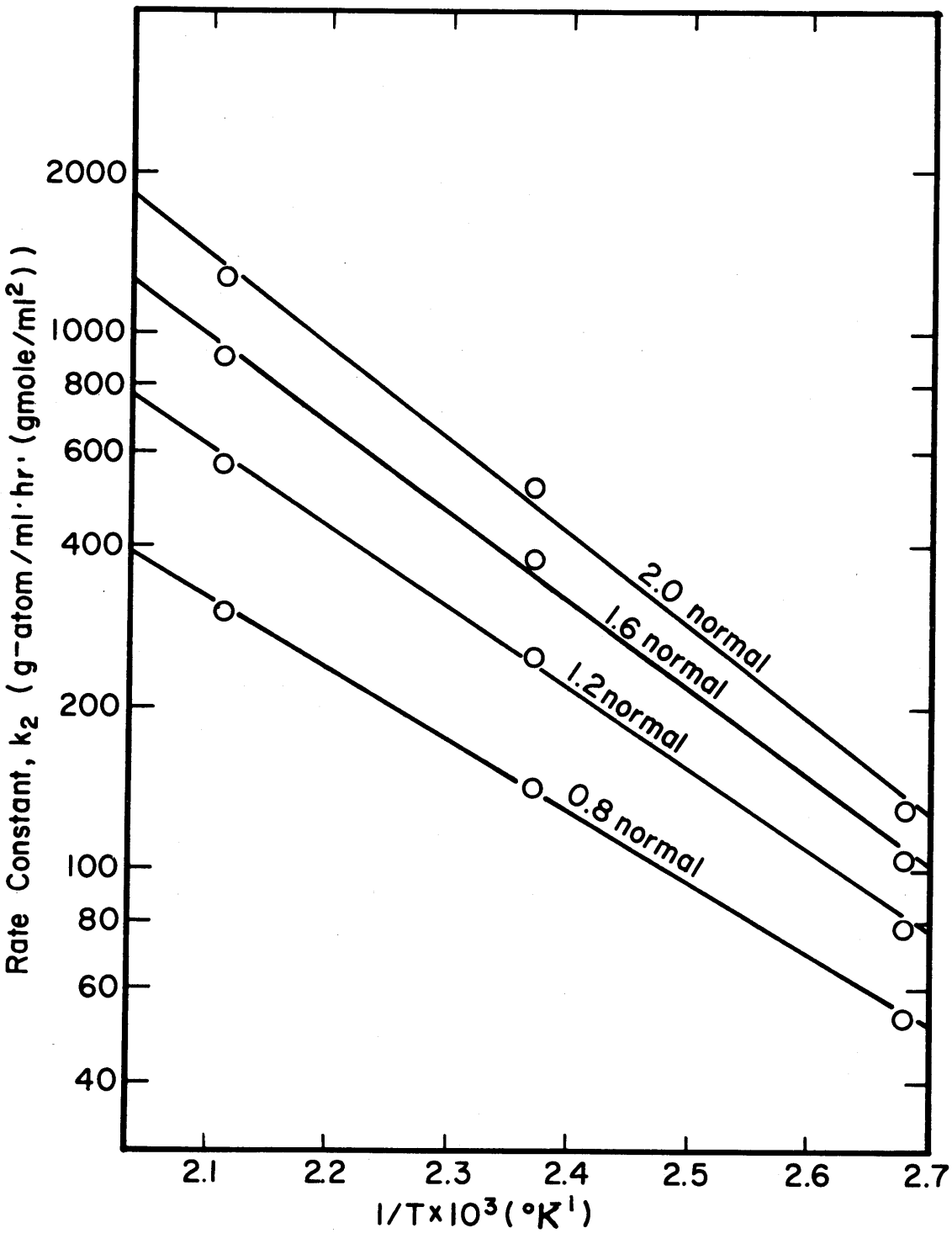

Fig. 23 Rate Constant k_2 as a Function of Temperature at Constant Amine Concentration.

Table VI.

Average Activation Energies of Liquid-phase Reaction, $HD + H_2O \rightarrow H_2 + HDO$, in Presence of Diethylamine at Temperatures between 100 and 200°C

Amine-Concentration (N)	Average Activation Energy, ΔE_2 (Kcal/gmole)
2.0	8.0
1.6	7.5
1.2	6.9
0.8	6.1

The fact that the average activation energy increases with the amine concentration indicates

i) that more than one mechanism is involved in the overall exchange of deuterium, and

ii) that a mechanism whose activation energy is higher than other mechanisms contributes to the total exchange reaction more prominently at higher amine concentrations than at lower.

To aid interpreting these results, reported activation energies of related exchange reactions of isotopes of hydrogen are summarized in Table VII.

This tabulation reveals

i) that the activation energy is about 25 Kcal/gmole for exchange reactions between hydrogen and water catalyzed by OH^-, about 7.5 to 8 Kcal/gmole for those between hydrogen

and ammonia catalyzed by alkali amides, and about 3.5 Kcal for those between hydrogen and alkylamines catalyzed by alkali alkyl amides, and

ii) that magnitudes of the average activation energy ΔE_2 of the reaction (76) in the presence of diethylamine, the results obtained in the present work, resemble more closely those for the exchange reactions between hydrogen and ammonia or alkylamine rather than those for the reactions between hydrogen and water catalyzed by hydroxyl ion.

In every mechanism for reactions (77) to (83) that has been proposed on the basis of experimental observations, a catalyst molecule, which is a base in all cases, first attacks a hydrogen molecule to form an activated intermediate complex (see next section). The complex is, then, attacked by a solvent molecule (water, ammonia or alkylamine) acting as an acid in the Lewis sense from the opposite side of the hydrogen molecule, resulting in stretching and finally cleavage of H-H bond in the H_2 molecule. The observation ii) on Table VII mentioned above then seems to indicate that a predominant mechanism in the exchange reaction under

Table VII

Activation Energies of Related Exchange Reactions

Reaction No.	Reaction	Catalyst	Temp. (°C)	Activation Energy (Kcal/gmole)	Authors and Literature
(8)	$H_2+OH^- \rightarrow H^-+H_2O$	---	25	20 ± 4*	Wilmarth et al (A-22)
(77)	$D_2+H_2O \rightarrow HD+HDO$	KOH	80 ~ 110	25	" "
"	"	NaOH	120	24	(A-4)
(78)	$H_2+D_2O \rightarrow HD+HDO$	KOH	110 ~ 190	28 ± 3	Miller et al (A-23)
(79)	$D_2+NH_3 \rightarrow HD+NH_2D$	KNH_2	-61 ~ -43	7.4 ± 0.3	Bar-Eli and Klein (4)
"	"	$NaNH_2$	"	8.0 ± 0.3	" "
(80)	$HD+NH_3 \rightarrow H_2+NH_2D$	KNH_2	"	7.4 ± 0.3	" "
"	"	KNH_2	-70 ~ -40	10	Dirian et al (5)
(81)	$HT+NH_3 \rightarrow H_2+NH_2T$	KNH_2	-61 ~ -43	7.6 ± 0.6	Bar-Eli and Klein (4)
(82)	$D_2+MeNH_2 \rightarrow HD+MeNHD$	LiNHMe**	-30 ~ -22	3.6 ± 0.2	Bar-Eli and Klein (6)
(83)	$D_2+EtNH_2 \rightarrow HD+EtNHD$	KNHEt**	"	3.5 ± 0.2	" "

Notes: * Theoretical value, calculated from thermodynamic data given in Latimer's "Oxidation Potentials" (A-24).

** Me and Et are denoted to methyl group and ethyl group, respectively.

investigation involves undissociated amine, which is a base, rather than hydroxyl ion.

Further interpretation of the results shown in Table VI concerns itself with possible mechanism of the reaction under investigation. They will be proposed in the following section. Acceptable mechanisms should be able to explain

i) the average order of the reaction with respect to the amine concentration and the dependence of the order on temperature as given in Eqns. (69) to (71) and

ii) the average activation energy of the reaction and its dependence on the amine concentration as shown in Table VI. They also should be compatible with other observations on other related exchange reactions, reported in the literature given in Table VII. These other observations will be summarized in the beginning of the following section.

3. Possible Reaction Mechanisms

Experimental facts and proposed mechanisms of other exchange reactions related to the reaction of interest in the present work will be described in subsection (a). Then, possible mechanisms for the present reaction which are in keeping with these facts and mechanisms will be presented in subsection (b). In the last subsection, (c), the possible mechanisms will be discussed in comparison with the experimental results obtained in the present work.

(a) Mechanisms Proposed for Related Exchange Reactions

When Wilmarth et al (A-22) first reported the catalytic activity of OH^- for the exchange reaction (77),

$$D_2 + H_2O \longrightarrow HD + HDO \qquad (77)$$

they propose a mechanism

$$D_2 + OH^- \longrightarrow D^- + HDO \qquad (6)$$

(rate-controlling)

and $$D^- + H_2O \longrightarrow HD + OH^- \qquad (7)$$

This successfully explained the observed first order dependence of the exchange rate on partial pressure of deuterium gas and hydroxyl ion concentration and the experimental values of activation energy observed by themselves and later by other workers on isotopically similar exchange reactions (see Table VII). A mechanism through an exactly simultaneous attack of a hydrogen molecule by OH^- and a water molecule, which they called "concerted attack" was then excluded on the grounds that attempted catalysis of the exchange reaction (77) by means of strong inorganic acid failed: they maintained that the acid catalysis should not fail if a hydrogen molecule were attacked "concertedly" by the strong base OH^- and a weak acid H_2O in the successful OH^--catalyzed reaction. In the attempted acid-catalysis then, H^+ and H_2O would have acted as a strong acid and a weak base, respectively, and they should have caused some measurable rate of heterolytic cleavage of the H-H bond, thus achieving the exchange.

Attempted acid catalysis by other workers (A-23, A-26) all failed, confirming Wilmarth's observation.

It, however, does not completely exclude the possibility of a mechanism in which an intermediate product is not a simply hydrated hydride ion as shown in reaction (6) but an excited complex in which OH^- and D_2 are partially bound togehter. Such a mechanism may be expressed as follows:

$$H-\underline{\overline{O}}|^{\ominus} + H-H \longrightarrow (H-\underline{\overline{O}}\cdots H-H)^{\ominus} \quad \text{(rate-controlling)} \qquad (84)$$

and

$$(H-\underline{\overline{O}}\cdots H-H)^{\ominus} + D-\underline{\overline{O}}-H \longrightarrow H-\underline{\overline{O}}-H + H-D + |\overset{\ominus}{\underline{\overline{O}}}-H \qquad (85)$$

Since all the mechanisms proposed for the related exchange reactions can be expressed in these forms, this expression of the mechanism is worth receiving more detailed explanation. In these expressions, each of the horizontal and vertical lines around an oxygen atom are used to represent an unshared pair of electrons around the oxygen atom, and a horizontal line drawn between two atomic symbols is used to express a shared pair of electrons in a bond of predominantly covalent or homopolar nature. In the excited intermediate complex, one of the three unshared electron pairs in the original OH^- (or a part of one of these pairs) is used to form a weak bond, which might be called a partial bond, between the original OH^- and H_2. The partial bond is expressed by a dotted line in the symbols in Eqns. (84) and (85). It might be a hybrid of many orbitals of the covalent and ionic nature so that the total negative charge of one unit is placed outside the parentheses. It is clear that, the stronger a base which

might act in the place of OH^- in other base-catalyzed reactions, the more easily the partial bond between the base and hydrogen molecule is formed. The rate of formation of the excited intermediate complex would be proportional to partial pressure of hydrogen and concentration of the base in a form which plays the role of OH^- in the formation of the complex. It also would be a direct function of basicity of the base.

In the second step (reaction (85)), a water molecule would approach the hydrogen atom of H_2 in the complex which is not bound to the oxygen atom of OH^-. Because the covalent bonds in the water molecule are not perfectly covalent, the oxygen atom being a center of a partially negative charge, the deuterium atom in the water molecule is electrophilic, or attracts electrons. As the water molecule approaches the intermediate complex, therefore, the deuterium atom would attract the electron cloud around the negatively charged complex toward itself, reducing the overlap charge of electron between the two adjacent atoms in the complex. At the same time, the denser electron cloud formed between the terminal hydrogen atom and the deuterium atom would pull the nucleus of the terminal hydrogen toward the deuterium atom, thus making the H—H bond of the original H_2 molecule even weaker. This state of the intermediate complex might be called a hydrated intermediate complex or, more generally, a solvated intermediate complex. The hydrated intermediate complex could either go back to the original state by breaking the partial bond between H and D or yield the products as shown

in the forward reaction (85) by breaking the H—H bond. It is clear that, the more acidic or electrophilic a molecule or a cation is which might act in the place of DOH, the more easily is the H—H bond broken. It is also clear that the relative probability of formation of the solvated intermediate complex from the excited intermediate complex in competition with decomposition of the excited intermediate complex into the original reactants is proportional to the concentration of the solvent or, more generally, that of the acid which plays the role of DOH in reaction (85). Thus the forward rate of the overall exchange reaction will be proportional to the concentrations of hydrogen, the base and the acid.

Expressions similar to those of expressions (84) and (85) will be used frequently in the following discussion of mechanisms which have been proposed for other related reactions. The same type of argument as what has been used in connection with reactions (84) and (85) will be implied whenever the similar expressions appear in the following.

Wilmarth and Dayton (A-25) studied the catalytic effect of KNH_2 on exchange of deuterium atoms between liquid ammonia and dissolved hydrogen at -50°C. Concentrations of the catalyst used were rather low ($\sim 10^{-4}$ N). It was found that the rate of exchange is proportional to the concentration of amide ion NH_2^- formed through ionization of KNH_2 (ionization constant $\simeq$ 7×10^{-5} mole/liter).

Bar-Eli and Klein (4) investigated exchange reactions between liquid ammonia and each of dissolved D_2, HD and HT in the presence of KNH_2 or $NaNH_2$ as catalyst in the temperature range of -61 to -43°C. Concentrations of the catalysts used were much higher than those used in Wilmarth's work (5~200 mmole/liter). It was found that the exchange rate depends not only on the activity of NH_2^- but also on the activity of undissociated KNH_2, so that the rate constant k was best represented by

$$k = k_{NH_2^-}[NH_2^-] + k_{KNH_2}[KNH_2] \qquad (86)$$

in which $k_{NH_2^-}$ and k_{KNH_2} are the specific rate constants for the catalysis by NH_2^- and for the catalysis by undissociated KNH_2, respectively. At -61°C, they found that

$$k_{NH_2^-} = (2.18 \pm 0.17) \times 10^6 \text{ ml/mole·min}$$

and

$$k_{KNH_2} = (1.03 \pm 0.10) \times 10^5 \text{ m./mole·min}$$

Both NH_2^- and KNH_2 were stated to act as the base in a mechanism they proposed. Because the ionization constant K_{KNH_2} of potassium amide defined as

$$K_{KNH_2} = \frac{[K^+][NH_2^-]}{[KNH_2]} \simeq \frac{[NH_2^-]^2}{[KNH_2]} \qquad (87)$$

is only 7.3×10^{-5} mole /liter at -61°C, the activity of undissociated amide $[KNH_2]$ in the solution was much higher than the activity of NH_2^- : in the concentrations of

KNH_2 they used, $[KNH_2]$ was up to about 60 times as great as $[NH_2^-]$. Consequently, a plot of k against $[KNH_2]$ looked more like a straight line than a square-root dependent curve. Also, the fact that KNH_2 is a much weaker base than NH_2^- is reflected by the much smaller value of its specific rate constant k_{KNH_2} compared with $k_{NH_2^-}$.

They also found that the catalytic activity of undissociated KNH_2, k_{KNH_2}, is higher than k_{NaNH_2} which, in turn, is higher than k_{LiNH_2}. This is related to the fact that magnitudes of the ionization constant for the three amides as defined in Eqn. (87) are in the order of $K_{KNH_2} > K_{NaNH_2} > K_{LiNH_2}$: the higher ionization constant of an amide implies that the density of the electron cloud around the nitrogen atom in the undissociated amide molecule is higher so that the availability of electrons from the nitrogen atom, a property which has been required of a catalyst of these exchange reactions, is higher. These observations agree with the general hypothesis that the catalytic activity of a base catalyst in an exchange reaction between hydrogen and a solvent is a direct function of the basicity of the catalyst, or the availability of electrons from them. Their proposed mechanism, expressed in the form of Eqns. (84) and (85), is as follows:

$$H-\overset{\ominus}{\underset{\displaystyle H}{\overset{|}{\underset{|}{\overline{N}}}}}| \; + \; D-D \longrightarrow \left(H-\underset{\displaystyle H}{\overset{|}{\underset{|}{\overline{N}}}}\cdots D-D\right)^{\ominus} \quad \text{(rate-controlling)} \qquad (88\text{-a})$$

or

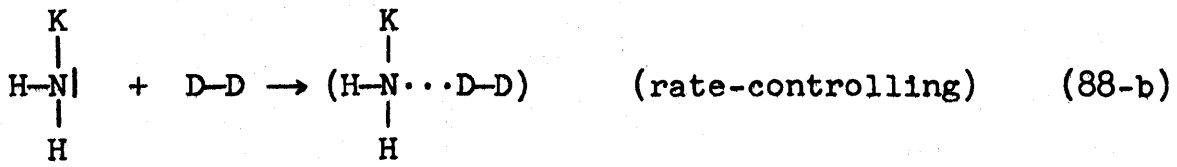

(rate-controlling) (88-b)

then,

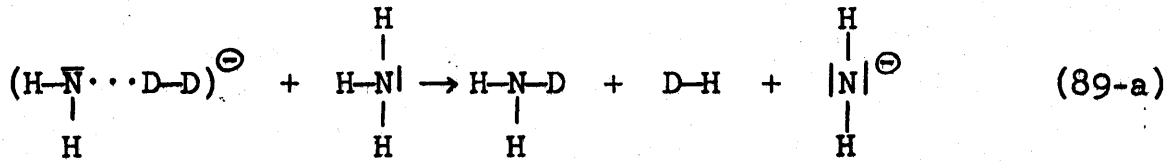

(89-a)

or

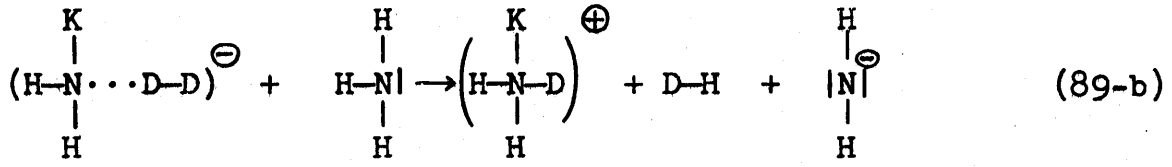

(89-b)

and then,

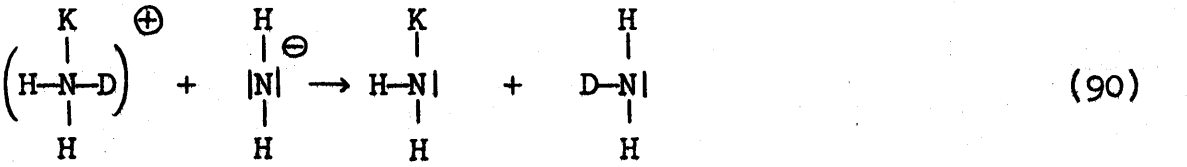

(90)

Reaction (89-a) follows reaction (88-a), and reaction (89-b) follows reaction (88-b). Reaction (90), which follows reaction (89-b) completes the total reaction

$$D_2 + NH_3 \longrightarrow HD + NH_2D$$

and proceeds rapidly. The rate-determining step was claimed to be the formation of the excited intermediate complex reactions (88-a) and (88-b). This mechanism explains the observed facts.

An independent investigation by Dirian et al (5) on the

system of NH_3 + HD in the presence of KNH_2 confirmed the experimental observations of Bar-Eli and Klein (4), but Dirian interpreted the observation in a different manner: both groups of workers found that the exchange rate depended not only on the activity of NH_2^- but also on a quantity which is proportional to the square of the activity of NH_2^- or $[NH_2^-]^2$. Bar-Eli and Klein interpreted the second quantity as $[KNH_2]$, which is right in view of the relation (87). Dirian et al interpreted the same quantity as a product of $[K^+]$ x $[NH_2^-]$, which again is right because of the same relation (87). Thus, Dirian et al fitted the experimental results to a relation

$$K = k_{NH_2^-}[NH_2^-] + k_{K^+NH_2^-}[K^+][NH_2^-] \qquad (91)$$

and proposed a mechanism as follows:

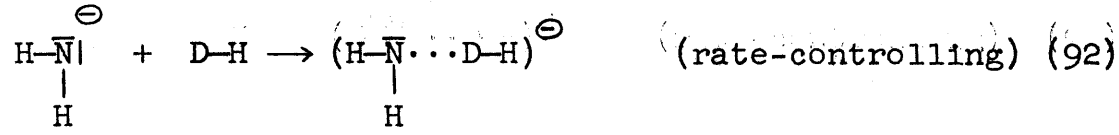

(rate-controlling) (92)

then,

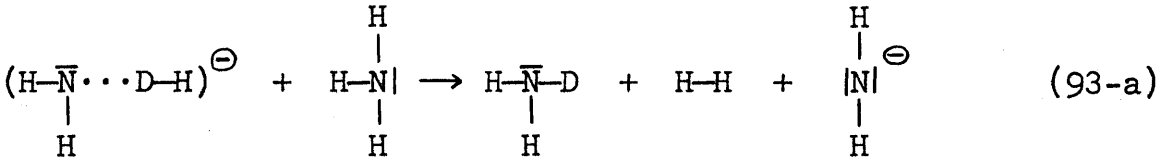

(93-a)

or

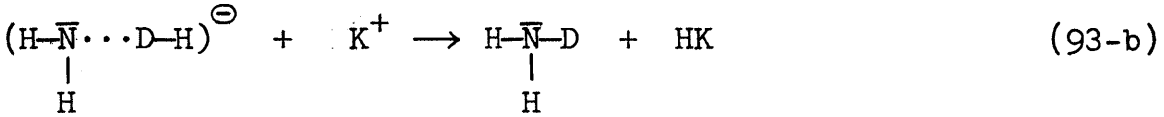

(93-b)

and

$$HK + NH_3 \longrightarrow K^+ + NH_2^- + H_2 \qquad (94)$$

Rate-deterimining step is reaction (92). In these mechanisms, the excited intermediate complex was stated to react either with NH_3 or K^+, both acting as an acid in the Lewis sense. Ammonia is a solvent in the system and its concentration is practically independent of the catalyst concentrations. Therefore, a combination of reactions (92) and (93-a) yields the first term of Eqn. (91). Although the rate-controlling step is reaction (92), the exchange rate through combination of reactions (92) and (93-b) is expected to be proportional both to concentration of NH_2^- and to concentration of K^+. This is because the excited intermediate complex would decompose into HD and NH_2^- in the absence of the acid, K^+. Thus, a combination of reactions (92) and (93-b) yields a rate which is proportional to a product of $[K^+]$ and $[NH_2^-]$ and is represented by the second term in Eqn. (91). Reaction (94) follows reaction (87-b) and proceeds rapidly. This mechanism also can explain Bar-Eli and Klein's observation that $k_{KNH_2} > k_{NaNH_2} > k_{LiNH_2}$, since

$$k_{KNH_2}\,[KNH_2] = k_{K^+NH_2^-}\,[K^+][NH_2^-]$$
$$= k_{K^+NH_2^-}\,K_{KNH_2}\,[KNH_2] \qquad (95)$$

so that

$$k_{KNH_2} = k_{K^+NH_2^-}\,K_{KNH_2}\,. \qquad (96)$$

There is no information available on which one could judge which mechanism, Bar-Eli and Klein's or Dirian et al's, is more likely to happen. This would suggest a possibility of a compromise mechanism in which

i) both NH_2^- and undissociated KNH_2 act as the base to form excited intermediate complexes, as proposed by Bar-Eli and Klein, and then

ii) both NH_3 and K^+ attack the excited intermediate complexes to yield the products, as proposed by Dirian et al.

Such a compromise mechanism would indicate possible presence of an additional term, besides the terms, each proportional to $[NH_2^-]$ and $[KNH_2]$ or $[K^+][NH_2^-]$ in the linear expression for k, such as Eqns. (86) and (91). Such a term would be proportional to the 3/2 power of the concentration of undissociated amine due to the following mechanism:

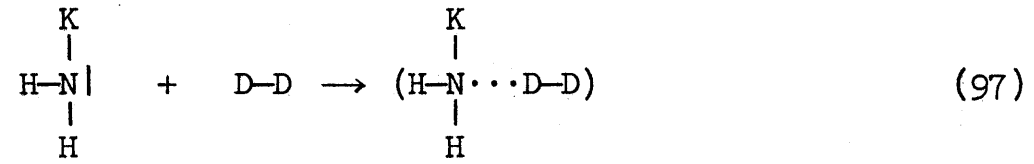

(97)

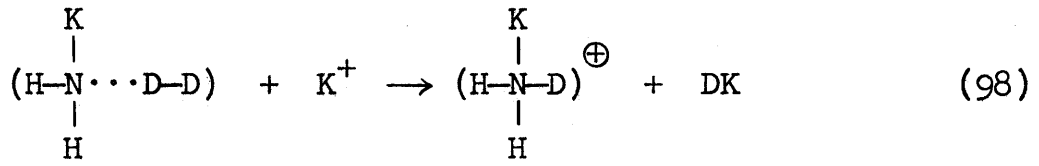

(98)

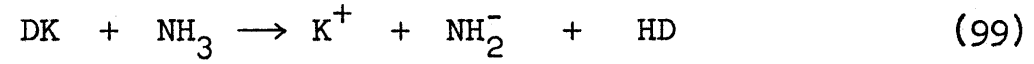

(99)

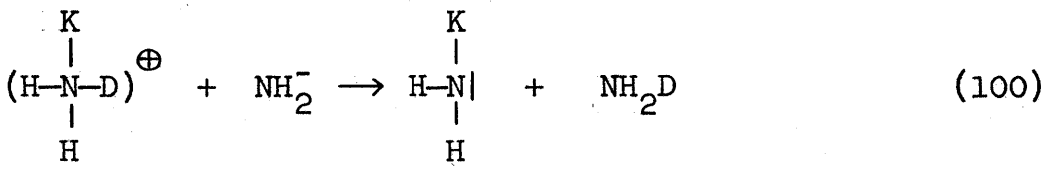

(100)

Each reaction follows the preceding one. Reaction (97) could be

rate-controlling. Reactions (99) and (100) are similar to reactions (94) and (90), respectively, and proceed rapidly. But, contribution of reactions (99) and (100) to the total rate constant k would be very small compared with the first two reactions because of the small concentration of K^+ and the small specific rate constant k_{KNH_2} as observed by Bar-Eli and Klein. If the exchange rate could have been measured for the same system (liquid ammonia and dissolved D_2) in the presence of a higher concentration of K^+ and of KNH_2 at much higher temperatures, the effects of the third reaction might have been observed.

Bar-Eli and Kleir (6) investigated another class of exchange reactions, between liquid alkylamines and dissolved D_2 in the presence of alkali alkylamides at temperatures ranging from -30 to -22°C. Alkali alkylamide dissociates as follows:

$$MNHR \longrightarrow M^+ + \overset{\ominus}{\underset{\displaystyle H}{\underset{|}{\overline{N}}}}\!\!-R \qquad (101)$$

where M and R represent an atom of alkali element and an alkyl group, respectively. It was found that the substituted amide ion RNH^- catalyzes the exchange reaction, and that the exchange rate is proportional to concentration of substituted amide ion RNH^- in the range of its concentration investigated. Solubilities of alkali alkylamides in liquid alkylamines were so small that high enough concentrations could not be obtained to investigate catalytic effects of undissociated alkali alkylamide or combined catalytic effects of RNH^- and K^+. The following mechanism was proposed:

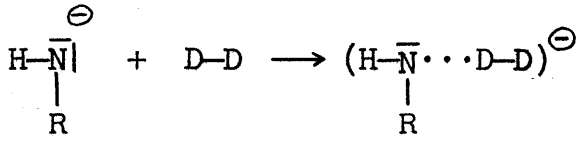

(102)

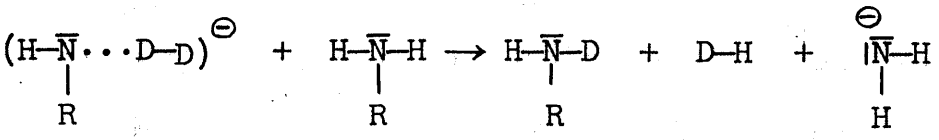

(103)

They also attempted to catalyze exchange between D_2 and liquid CH_3NH_2 with a 10 M solution of $CH_3NH_2 \cdot HCl$ in liquid CH_3NH_2 at $-30^{\circ}C$. They expected that methyl ammonium ion $CH_3NH_3^+$ existing in the solution as a result of ionization of $CH_3NH_2 \cdot HCl$ would act as a strong acid, the role of RNH_2 in reaction (103), and that the solvent molecule CH_3NH_2 would act as a base, the role of RNH^- in reaction (102). The attempt failed; no exchange took place. This result is very similar to that of the attempted acid-catalysis in the system of water and dissolved hydrogen in which the solvent molecule, water, was to act as the base. These observations again confirm the theory that only a strong base can initiate the exchange reaction and that unless the base is sufficiently strong, presence of a strong acid, however strong it is, does not help the situation in any way: initial excitation of the hydrogen molecule, the necessary condition for cleavage of the H–H bond, cannot be accomplished without a strong base.

On the basis of these proposed theories, possible mechanisms for the exchange reaction of present interest, the exchange between water and dissolved hydrogen in the presence of diethylamine in various concentrations, will be discussed in the following subsection.

b) Possible Mechanisms for Present Reaction System

In the following discussion of possible mechanisms for the deuterium exchange reaction between water and dissolved hydrogen in the presence of diethylamine, the overall reaction

$$HD + H_2O \xrightarrow{k_2} H_2 + HDO \ , \qquad (76)$$

will be considered rather than the reverse reaction, since the final data have been tabulated for the rate constant k_2 for this reaction. The treatment would be essentially the same for either reaction.

In this reacting system, the catalyst, diethylamine, is present in various chemical forms because of the dissociation equilibria

$$(C_2H_5)_2NH + H_2O \rightleftharpoons (C_2H_5)_2NH_2^+ + OH^- \qquad (104)$$

with the equilibrium constant K_a defined by

$$K_a = \frac{[(C_2H_5)_2NH_2^+][OH^-]}{[(C_2H_5)_2NH]} = \frac{[(C_2H_5)_2NH_2^+]^2}{[(C_2H_5)_2NH]} = \frac{[OH^-]^2}{[(C_2H_5)_2NH]} \qquad (105)$$

Ethyl group C_2H_5 will be represented by R in the following treatment.

In this reacting system, therefore, two bases and three acids are present which merit consideration:

Bases; OH^- and R_2NH

Acids; $R_2NH_2^+$, H_2O and R_2NH

Although Bar-Eli and Klein d is proved a possibility of

undissociated methylamine and ethylamine being the base-catalyst which initiates attack on the hydrogen molecule at lower temperature, undissociated diethylamine R_2NH is still worth being considered as a base at temperatures above 100°C. This is especially so because diethylamine is a stronger base than methylamine and ethylamine, a fact that could be deduced from its higher ionization constant K_a than the other's, at least at room temperature (see Table A-III in APPENDIX Section A). Thus, $(C_2H_5)_2NH$ being a stronger base than NH_3, CH_3NH_2 and $C_2H_5NH_2$, it is a weaker acid than the other amines. Nevertheless, it is also listed as an acid since it is present in high concentrations in the solutions used in the present work.

A possible mechanism would consist of three major steps. A base first attacks HD to form an excited intermediate complex, which step will be called an excitation step. The excited intermediate complex then decomposes to product species by an action of an acid, which step will be called a decomposition step. Some of the products of the decomposition step will go into rapid chemical reactions which make the overall reaction identical with reaction (76). This step will be called a balance step. Some decomposition reactions require a balance step, and others do not.

The possible mechanisms then are as follows. Reactions (a), (b) and (c) in a balance step follows reactions

(a), (b) and (c) in a decomposition step, respectively.

I. Exchange Initiated by OH^-

(i) Excitation Step

$$H\text{-}\underline{O}|^{\ominus} + D\text{-}H \longrightarrow (H\text{-}\underline{O}...D\text{-}H)^{\ominus} \qquad (106)$$

(ii) Decomposition Step

(a) $$(H\text{-}\underline{O}...D\text{-}H)^{\ominus} + H\text{-}\underline{O}\text{-}H \longrightarrow H\text{-}\underline{O}\text{-}D + H\text{-}H + |\underline{O}^{\ominus}\text{-}H \qquad (107\text{-}a)$$

(mechanism 1)

(b) $$(H\text{-}\underline{O}...D\text{-}H)^{\ominus} + \left(H\text{-}\underset{\underset{R}{|}}{\overset{\overset{H}{|}}{N}}\text{-}R\right)^{\oplus} \longrightarrow H\text{-}\underline{O}\text{-}D + H\text{-}H + \underset{\underset{R}{|}}{\overset{\overset{H}{|}}{N}}\text{-}R \qquad (107\text{-}b)$$

(mechanism 2)

(c) $$(H\text{-}\underline{O}...D\text{-}H)^{\ominus} + H\text{-}\underset{\underset{R}{|}}{\underline{N}}\text{-}R \longrightarrow H\text{-}\underline{O}\text{-}D + H\text{-}H + |\underline{N}^{\ominus}\text{-}R \qquad (107\text{-}c)$$

(mechanism 3)

(iii) Balance Step

(a) No balance reaction

(b) $$R_2NH + H_2O \longrightarrow R_2NH_2^+ + OH^- \qquad (108\text{-}b)$$

(c) $$R_2N^- + H_2O \longrightarrow R_2NH + OH^- \qquad (108\text{-}c)$$

II. Exchange Initiated by R_2NH

(i) Excitation Step

$$R\text{-}\underset{\underset{R}{|}}{\overset{\overset{H}{|}}{N}}| + D\text{-}H \longrightarrow \left(R\text{-}\underset{\underset{R}{|}}{\overset{\overset{H}{|}}{N}}...D\text{-}H\right) \qquad (109)$$

(ii) Decomposition Step

(a) $$\left(R\text{-}\underset{\underset{R}{|}}{\overset{\overset{H}{|}}{N}}...D\text{-}H\right) + H\text{-}\underline{O}\text{-}H \longrightarrow \left(R\text{-}\underset{\underset{R}{|}}{\overset{\overset{H}{|}}{N}}\text{-}D\right)^{\oplus} + H\text{-}H + |\underline{O}^{\ominus}\text{-}H \qquad (110\text{-}a)$$

(mechanism 4)

(b) $(R\text{-}\overset{H}{\underset{R}{N}}\ldots D\text{-}H) + (H\text{-}\overset{H}{\underset{R}{N}}\text{-}R)^{\oplus} \longrightarrow (R\text{-}\overset{H}{\underset{R}{N}}\text{-}D)^{\oplus} + H\text{-}H + \overset{H}{\underset{R}{N}}\text{-}R$

(mechanism 5) (110-b)

(c) $(R\text{-}\overset{H}{\underset{R}{N}}\ldots D\text{-}H) + H\text{-}\overset{\ominus}{\underset{R}{N}}\text{-}R \longrightarrow (R\text{-}\overset{H}{\underset{R}{N}}\text{-}D)^{\oplus} + H\text{-}H + \overset{\ominus}{\underset{R}{N}}\text{-}R$

(mechanism 6) (110-c)

(iii) Balance Step

(a) $R_2NHD^+ + OH^- \longrightarrow R_2NH + HDO$ (111-a)

(b) No balance reaction.

(c) $R_2NHD^+ + R_2N^- \longrightarrow R_2NH + R_2ND$ (111-c1)

$R_2ND + H_2O \longrightarrow R_2NH + HDO$ (111-c2)

Following the theory of other workers for the related exchange reactions, the excitation step is expected to be the rate-controlling step. The exchange rate, however, would depend not only on concentrations of HD and OH^- (or R_2NH), the reactants in the rate-controlling step, but also on concentration of the acid: since an excited intermediate complex could either decompose into HD and OH^- (or R_2NH) or undergo the forward reaction with the acid to form the products of the decomposition step, rate of the forward reaction would be proportional to the acid concentration, too. Reactions of the balance step are expected to proceed so rapidly that they would not be rate-controlling in any cases, and concentrations of the reactants in this step

do not influence the overall reaction rate. The order of the overall reaction rate via different paths with respect to the concentration of undissociated amine, $[R_2NH]$, could be estimated on the basis of this theory: a specific rate constant $k_{2,i}$ for the exchange reaction (76) through a mechanism characterized by i, expressed as gram moles D transferred per milliliter per hour per unit concentrations of HD and H_2O, could be expressed as

$$k_{2,i} = k^{o}_{2,i} [R_2NH]^{y_i} \qquad (112)$$

where y_i is a number to whose power of $[R_2NH]$ $k_{2,i}$ is dependent and $k^{o}_{2,i}$ is a specific rate constant expressed as gram moles D transferred per milliliter per hour per unit concentrations of HD and H_2O per unit concentration of R_2NH raised to the y_ith power. Values of y_i for all the mechanisms are summarized in Table VII.

Table VIII. y for Various Reaction Mechanisms

	y		
Base	H_2O as Acid	$R_2NH_2^+$ as Acid	R_2NH as Acid
OH^-	$y_1 = \frac{1}{2}$	$y_2 = 1$	$y_3 = \frac{3}{2}$
R_2NH	$y_4 = 1$	$y_5 = \frac{3}{2}$	$y_6 = 2$

$k^{o}_{2,i}$ is a function of temperature and, consequently, $k_{2,i}$ is a function of temperature and amine concentration. The total rate constant k_2 would be the sum of $k_{2,i}$'s for

all reaction mechanisms:

$$k_2 = \sum_{i=1}^{6} k_{2,i} = \sum_{i=1}^{6} k^{o}_{2,i}[RNH_2]^{y_i} \qquad (113)$$

The average order of the overall exchange reaction with respect to the amine concentration would be a weighted mean of y_i's, the weights being a function of the relative magnitudes of the contribution of the individual mechanisms: the larger the contribution of a mechanism, the higher the weight of that mechanism.

Assuming again that the excitation step is the rate-controlling step, activation energies for the mechanisms 1, 2 and 3 would be predominantly a characteristics of reaction (106). To a first approximation, then, activation energies for the mechanisms 1, 2 and 3 are expected all equal to the activation energy of reaction (106), denoted by $\Delta E_{2,OH^-}$. Similarly, activation energies for the mechanisms 4, 5 and 6 are expected all equal to the activation energy of reaction (109), denoted by $\Delta E_{2,R_2NH}$. The average activation energy of the overall reaction (76) is then expected to be an average value of $\Delta E_{2,OH^-}$ and $\Delta E_{2,R_2,NH}$, each weighted by relative contributions to the overall reaction of the mechanisms I and II, respectively.

In the following subsection, these possible mechanisms will be compared with the experimental results on the order of the reaction with respect to amine concentration and on activation energies.

(c) Discussion of Possible Mechanisms on the Basis of Experimental Results

Results of the relevant experimental observations in the present work are reproduced below;

Average order of reaction with respect to the amine concentration:

At 200°C, $\bar{y}_{200} = 1.58 \pm 0.07$ (69)

At 150°C, $\bar{y}_{150} = 1.46 \pm 0.02$ (70)

At 100°C, $\bar{y}_{100} = 1.07 \pm 0.01$ (71)

Average activation energy:

At $[R_2NH] = 2.0$ N , $\Delta E_2 = 8.0$ Kcal/gmole

At $[R_2NH] = 1.6$ N , $\Delta E_2 = 7.5$ Kcal/gmole

At $[R_2NH] = 1.2$ N , $\Delta E_2 = 6.9$ Kcal/gmole

At $[R_2NH] = 0.8$ N , $\Delta E_2 = 6.1$ Kcal/gmole

In the following discussion, no distinction will be made between the concentration of undissociated amine, $[R_2NH]$, and the stoichiometric or total concentration of amine, $[R_2NH] + [R_2NH_2^+]$, since $[R_2NH_2^+]$ is always a small fraction (order of a per cent) of $[R_2NH]$.

Let us now examine the possible mechanisms in the light of the experimental results.

The order of the exchange reaction with respect to the amine concentration for an individual mechanism, y_i, ranges from 1/2 to 2, while the average order of the overall exchange reaction observed in the present work ranges from 1.0 to 1.6. It seems, therefore, that the set of six reaction mechanisms presented in the preceding subsection, although possibly not complete, satisfactorily covers the range of the order of the reaction at the temp-

eratures investigated.

As to the activation energy, it has been expected that the average value of the overall reaction is a weighted mean of those of the excitation steps, reactions (106) and (109), that is, $\Delta E_{2,OH^-}$ and $\Delta E_{2,R_2NH}$. And it has been known that E_{2,OH^-} is about 25 Kcal/gmole (see Table VII). Therefore, the present experimental values, ranging from 8 to 6 Kcal/gmole indicated that E_{2,R_2NH} is smaller than 6 Kcal/gmole. Furthermore, the observations that the activation energy increases with amine concentration, would imply that the relative contribution to the total reaction of those mechanisms initiated by OH^- becomes increasingly important as the amine concentration gets higher. Such would be possible only if the average order of the reaction mechanism initiated by OH^- with respect to the amine concentration is higher than the average order of those initiated by R_2NH. That is, a condition

$$\frac{\sum_{i=1}^{3} y_i k^o_{2,i} \left[R_2NH\right]^{y_i}}{\sum_{i=1}^{3} k^o_{2,i} \left[R_2NH\right]^{y_i}} > \frac{\sum_{i=4}^{6} y_i k^o_{2,i} \left[R_2NH\right]^{y_i}}{\sum_{i=4}^{6} k^o_{2,i} \left[R_2NH\right]^{y_i}} \qquad (114)$$

Such a condition could be fulfilled only if mechanism 3 contributed more to the overall rate than 1 and 2, while mechanism 4 contributed more than 5 and 6.

This does not necessarily mean that rate of the excitation step involving OH^- itself should increase more rapidly with increase in the amine concentration than

rate of the excitation step involving R_2NH does. In fact, one would expect that the rate of the latter increases faster than the rate of the former reaction as the amine concentration increases beyond certain limits, the limit being a function of K_a and the relative magnitudes of specific rate constants of reactions (106) and (109). It is the combined rate of forward reactions of the excitation and decomposition steps of the mechanisms 1, 2 and 3 that should increase faster with the amine concentration than the combined rate of the mechanisms 4, 5 and 6. Physically, this would mean that R_2NH primarily acts as an acid rather than a base so that increasing the amine concentration in the solution is practically increasing the acid concentration rather than the base concentration. Such would be the case if the effectiveness of R_2NH as an agent for exciting the hydrogen molecules is not so high as OH^-. This agrees with the observations of the previous workers on the related reactions.

Under the condition of inequality (114), the average activation energy of the present system at infinite dilution of the catalyst would correspond to the activation energy of the excitation step (109) or $\Delta E_{2,R_2NH}$. The observed average activation energy is plotted against the amine concentration in Fig. 24. Extrapolation to zero amine concentration yields $\Delta E_{2,R_2NH} \simeq 4$ Kcal/gmole. This value resembles the value of activation energy in the system of D_2-alkylamine-alkali alkylamide.

In simplest terms, the present experiments suggest that the principal contributors to the observed reaction rate are mechanisms 3 and 4, with 3 the dominant reaction at high temperatures, and 4 at low temperatures. In mechanism 3 the hydrogen molecule is attacked by OH^- acting as a base, and the complex reacts with diethylamine acting as a weak acid. In mechanism 4, the hydrogen molecule is attacked by diethylamine acting as a base, and the complex reacts with water acting as a weak acid.

The only experimental observation which is not fully compatible with the combination of mechanisms postulated is the 1.58 order of the reaction observed at 200°C. As the probable error in $\bar{y}$ is 0.07 and the 95% confidence limit is 0.14, it is possible that the correct value at 200°C could be as low as 1.45 and thus not be incompatible with the combination of mechanisms postulated.

4. Comparison of Diethylamine with Other Catalysts for Deuterium Exchange between Water and Hydrogen

The absolute magnitudes of the deuterium exchange rate constant in the pressence of diethylamine will be compared with other catalysts that have been investigated for the liquid-phase exchange reaction between water and dissolved hydrogen in this section.

Wilmarth et al (A-22) reported that, at 100°C, rate constant K^o defined as gram moles of reaction

$$D_2 + H_2O \longrightarrow HD + HDO$$

per liter of water per hour per unit concentrations of dissolved deuterium and hydroxyl ion each expressed in

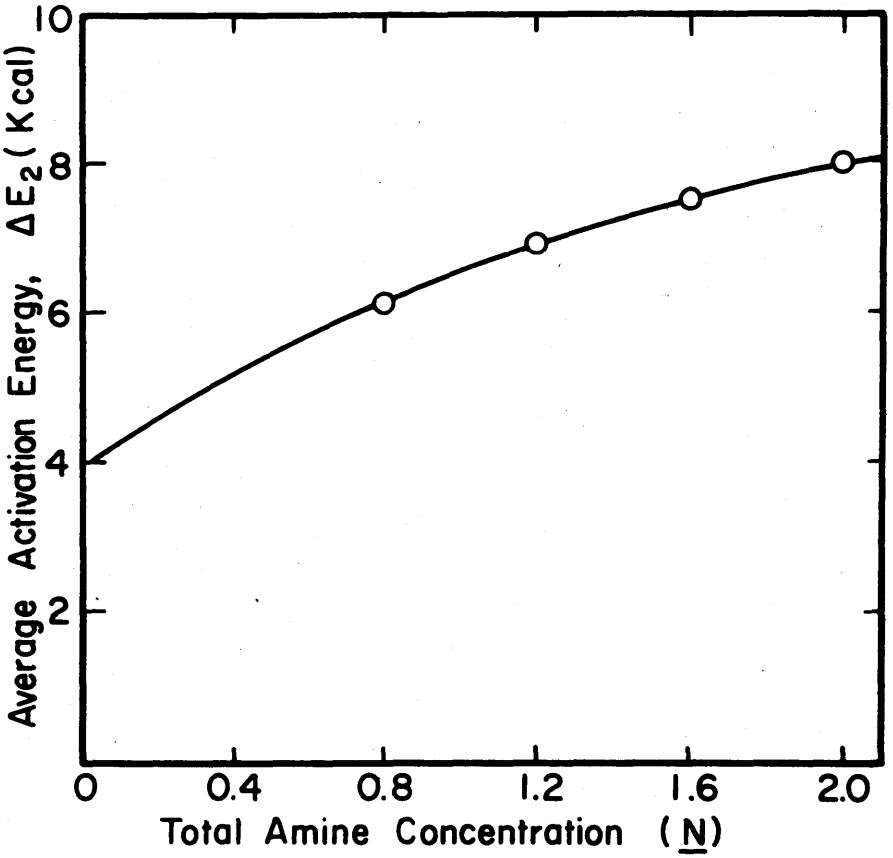

Fig. 24 Average Activation Energy as a Function of Amine Concentration.

gram moles per liter, is 0.344. Assuming that Henry's law constant of D_2 in water at 100°C is 5.7×10^7 mm Hg per unit mole fraction of dissolved D_2 in water, the exchange reaction will proceed at a rate of 3 gram atoms D transferred per hour per liter of one normal KOH solution under a hydrogen pressure of 200 atmospheres.

In the present work, it was found that, at 100°C and with the amine concentration of 1.64 normal, k_2 for the reaction

$$HD + H_2O \longrightarrow H_2 + HDO$$

is 119 gram atoms D transferred per milliliter per hour per unit concentrations of HD and H_2O, each expressed in gram moles per milliliter. Assuming the same value of Henry's law constant for HD as for D_2, the exchange reaction will proceed at a rate of 1 gram atom D transferred per hour per liter of 1.64 normal diethylamine solution under a hydrogen pressure of 200 atmospheres. Neglecting isotopic effect of D_2 vs HD, this is only one third of the rate of the OH^--catalyzed exchange reaction quoted above.

Becker and his collaborators have reported (A-2, A-3) high catalytic activities of platinum-based dispersed catalysts. Under the reaction conditions they investigated, the catalytic activities are so high that the observed rate of exchange of deuterium between water and dissolved hydrogen depends both on the mass transfer rates between the two phases and on the chemical reaction rate in the liquid phase. With most effective sieve plate under a

hydrogen pressure of 200 atmospheres and with an optimized set of working conditions, the values of an overall rate constant k, expressed as gram moles of exchange reaction per hour in the particular experimental setup used, listed in Table IX were reported. Interpolation of these data to 100°C yields k = 170 grams moles per hour. Since Becker's experimental volume was 0.3 liters, 570 gram atom D will be transferred in one hour in one liter of water.

Table IX. Becker's Rate Constant k for Platinum-Based, Dispersed, Catalyst*

Temperature (°C)	k (gram moles per hour)
30	45
45	73
60	98
200	376

* Catalyst used is a suspension of platinized activated charcoal, 50 gram charcoal per liter with a platinum to charcoal weight-ration of 0.10. The total volume of water is 0.3 liters.

Thus, the rate of the diethylamine-catalyzed exchange reaction at 100°C is only 1/570 that of the platinum-catalyzed reaction and seems to be too slow for practical application. It is true that a higher concentration of diethylamine could be used to increase the rate at 100°C since diethylamine and water are completely miscible with each other at this temperature. But too high a concentration of the amine would not be practical because the heat input

required to distil off the amine from water streams leaving a stage of dual-temperature plant would then become too large (see Fig. 2).

At 200°C, the rate constant k_2 is about ten times higher than the value at 100°C at about the same amine concentration and increases approximately as the 3/2 power of the amine concentration. At this temperature, however, solubility of diethylamine is limited to about 2.5 normal. Therefore, the highest exchange rate at 200°C and under the hydrogen pressure of 200 atmosphere one can expect is about 13 gram atoms D transferred per hour per liter. Such a reaction rate would be only about one-tenth that observed by Becker with platinum at 30°C.

As the size of cold tower for the first stage of a dual-temperature heavy water plant using platinum catalyst at 30°C is so large as almost certain to be uneconomic, it is concluded that diethylamine is not sufficiently active as a catalyst to serve in a practical dual-temperature hydrogen-water exchange process for heavy water production.

It would not be practical to operate at a cold-tower temperature above 200°C to obtain a higher reaction rate, because this would be too close to the maximum practical hot-tower temperature, which is limited to around 300°C by the rapid increase in vapor pressure of water with temperature. At 300°C it has already reached 80 atm. Between temperatures of 300 and 200°C the ratio of deuterium exchange equilibrium constants K for reaction (3) is

$$\frac{K_{300}}{K_{200}} = 1.137$$

This is already as low as is practical, and any further increase in cold tower temperature would lead to unacceptably large hydrogen circulating rates and heat loads.

VI. CONCLUSIONS

The rate constant k_2 for the liquid-phase exchange reaction

$$HD + H_2O \rightarrow H_2 + HDO$$

has been measured under various pressures of hydrogen ranging up to 80 atmospheres in the presence of diethylamine at concentrations ranging from 0.76 to 1.83 normal, at temperatures 100, 150, and 200°C. The results are tabulated in Table I.

On the basis of these results, the following conclusions have been drawn with respect to the reaction mechanism and possible practical application of the reaction.

1. Theoretical Aspects

The first order dependence of the rate of this exchange reaction on the partial pressure of hydrogen catalyzed by diethylamine has been confirmed. A similar first-order dependence had been established by other workers on such related liquid-phase exchange reactions as between D_2 and H_2O catalyzed by OH^-, D_2 and NH_3 catalyzed by KNH_2 and D_2 and alkylamides.

The order of the dependence of the exchange reaction rate on the total concentration of diethylamine has been found to be

1.58 ± 0.07 at 200°C,
1.46 ± 0.02 at 150°C,
and 1.07 ± 0.01 at 100°C.

The average activation energy of the exchange reaction has been found to depend on the concentration of diethylamine. Some interpolated values at various concentrations of the amine are as follows:

8.0 Kcal/gram mole at 2.0 N total amine concentration,

7.5 Kcal/gram mole at 1.6 N total amine concentration,

6.9 Kcal/gram mole at 1.2 N total amine concentration,

and 6.1 Kcal/gram mole at 0.8 N total amine concentration.

Reaction mechanisms have been discussed in connection with those that had been proposed for other liquid-phase exchange reactions catalyzed by a base. It has been shown that the magnitudes and the trends of the observed reaction rates with respect to the total amine concentration and the activation energies can be explained with a set of reaction mechanisms which is compatible with the generally accepted theory of the base-catalyzed exchange reaction of hydrogen isotopes between a hydrogenous solvent and dissolved hydrogen.

2. Practical Aspects

It has been found that rate of the diethylamine-catalyzed reaction appears to be too slow for practical application in a dual-temperature exchange process. The rate is definitely too slow for use in the cold tower at a temperature of 200°C or lower. As the hot-tower temperature could not be much over 300°C owing to the large vapor pressure of water at such temperatures, this leaves too little margin between the temperatures of the cold and hot towers for a practical process.

3. Experimental Procedure

The high-pressure apparatus used in these experiments and described in Chapter III performed satisfactorily and is suitable for measuring the rates of reactions of this type.

The thermal-conductivity cell used to analyze hydrogen for deuterium content had several serious deficiencies. Too much time was required to reach thermal equilibrium, and the output voltage was too sensitive to such operating conditions as ambient temperature and gas pressure.

VII. RECOMMENDATIONS

The experience and knowledge gained in this research points to a number of additional topics worthy of further investigation.

1. Further Investigation of Diethylamine

Although reaction rates with diethylamine are probably not rapid enough to justify its use in a practical process for producing heavy water, further investigation of the mechanism by which it catalyzes the deuterium exchange reaction would be of considerable theoretic interest.

a) To help explain how diethylamine catalyzes the exchange between hydrogen and water, the rate of deuterium exchange between pure diethylamine and dissolved hydrogen should be measured. To permit interpretation of such data, the solubility of hydrogen in diethylamine should be determined.

b) Phase equilibria in the system water-diethylamine should be investigated at temperatures up to 300°C. The limits of miscibility of the two liquid phases should be determined, and the composition of the vapor in equilibrium with dilute solutions of diethylamine in water should be measured, in order to permit estimation of the activity of diethylamine in these dilute solutions.

c) The rate of exchange of deuterium between water and dissolved hydrogen in the presence of diethylamine such as was measured in this research at

temperatures of 100, 150 and 200°C should be determined at 250 and 300°C.

d) Additional measurements of the exchange rate in this reaction should be made at 100 and 200°C at diethylamine concentrations below the lowest and above the highest values studied in the present research, in order to obtain more detailed information on how the rate varies with DEA concentration.

2. Engineering Studies of Diethylamine

Although the rate of deuterium exchange with diethylamine catalyst appears to be too low for its use in a practical process, confirmation of this conclusion by engineering analysis of the design of a dual-temperature process using DEA as catalyst would be desirable. The rate data obtained in the present work, extrapolated to higher temperatures if necessary, should be used as the basis for roughing out the design of a dual-temperature process and estimating the cost of producing heavy water in such a process.

3. Other Catalysts

The relatively low catalytic efficiency of diethylamine that has been found in the present work indicates that the other amines surveyed at the start of the present investigation are not likely to be good catalysts, because their dissociation constants are even lower than DEA's.

Tetra-alkyl ammonium hydroxides might be worth an investigation. They ionize almost completely in aqueous solution so that their specific catalytic activities are

expected to be high. The lower homologs dissolve in water easily. Their melting points are high, and so are their boiling points. In almost every aspect they behave like the inorganic hydroxides. If their catalytic activities were found to be high, practical questions regarding their usefulness that would still have to be answered include their corrosiveness on steel walls compared with that of caustic alkali, their rate of dehydration in comparison with the exchange rate at the reaction temperatures of interest, and the ease with which these bases could be separated from water. The most feasible method of separation seems to be cation exchange but the large molecular volume of these bases might present difficulty.

Other possible catalysts for the water-hydrogen exchange reaction are stable and soluble salts of transition elements, such as iron.

4. Refinements of Experimental Procedure

The thermal conductivity method used in the present work to analyze hydrogen for deuterium content gave considerable difficulty and should be modified before additional exchange measurements are made.

Because of the limited amounts of available gas sample, a static rather than a steady flow method was employed. The thermal conductivity cell, made of stainless steel, was connected with the gas purification and gas storage systems, which were made of glass, through ground joints between metal and glass. The cell could be isolated from the rest of the system by closing glass stopcocks on the glass line.

To maintain the ambient temperature of the cell uniform and constant, the cell and its steel supply lines up to just below the glass-metal joint were placed in a thermostated water bath at 50°C. This required long supply lines of small diameter and also left a portion of the cell system and its gas content which was above the water level exposed to lower ambient temperature. As a result of the static method and the long and partially exposed lines, the system required as long as two hours to reach thermal equilibrium. Consequently it took much too long for the bridge-output to reach its steady value. This gave three difficulties: the gas analysis took much too long, it was difficult to tell when the bridge output reached a steady value, and the mechanical plus epoxy resin seal of the bridge-filaments to the body of the thermal conductivity cell sometimes caused small leaks which could contaminate the gas sample being analyzed in the stretch of two hours.

To correct these difficulties, the following alterations are suggested for the static thermal-conductivity method of gas analysis. One alternative is to use a steel cell block with the filaments hermetically sealed to the body. The supply lines to the cell should be made of glass tubing, fused onto the cell-body and equipped with high-vacuum type stopcocks positioned as close to the cell as possible. The entire unit should be placed in an oven thermostated around 50°C and equipped with a forced circulation fan. A second alternative would be to use a system of cells and

supply lines entirely made of glass, with the filaments fused through the glass wall. This system also should be placed in a thermostated oven. In either case, it is recommended that a cell be designed so that heat transmission from the filaments to the walls be least affected by natural convection. This will minimize the effect of gas pressure on the bridge-output.

5. Changes in Computational Procedure

In writing up the results of the present work, it became apparent that certain assumptions made to simplify the reduction of data introduced slight inaccuracies in the computed rate constant and its interpretation. The computational procedure should be modified as described below in any future work. It would be desirable, also, to recompute the results of present measurements with these modifications.

In deriving the material balance equations for estimating amounts of the reactants present at the beginning of each partial run, the total amounts of hydrogen present in both vapor and liquid phases have been approximated by the total amounts of hydrogen present in the vapor phase. In making the material balance calculations in the future, it is recommended that this approximation not be used. This becomes more important at temperatures above 200°C, because the Henry's law constant of hydrogen in water decreases as the temperature increases above 200°C.

In the material balance calculations in the present work, the presence of D_2 in hydrogen has been neglected in estimating the amount of deuterium transferred during each partial run, ΔX_n. This approximation is valid at the start of a run, when the deuterium content of hydrogen is low. But as the system comes closer to equilibrium, a second order term neglected in the formula, Eqn. (48), should be taken into account.

The assumption that water and diethylamine form ideal solutions has introduced a slight error in the calculated DEA concentration in the liquid and the calculated DEA and hydrogen concentrations in the vapor phase. A rough estimate of the activity of DEA in the liquid phase such as can be made from present data on the limits of miscibility of water and DEA would be sufficiently accurate to permit a more refined calculation of these concentrations. This should be done in any recomputation of present measurements or in any future work on DEA.

As the catalytic effect of DEA can probably be interpreted more accurately when correlated with the activity of DEA rather than its concentration, the present rate data should be re-examined with this point in mind. This effort would not be worthwhile, however, until more extensive measurements had been made of the activity of DEA in aqueous solution, such as outlined under 1(b) above.

VIII. APPENDICES

A. Literature Survey on Possible Homogeneous Catalysts

Results of a literature survey on possible homogeneous catalysts for the exchange of deuterium between water and dissolved hydrogen will be presented in this section. These catalysts may be classified into two groups according to the mechanism of catalysis. In the first group are catalysts which mainly activate the reactants to produce radicals as intermediates of the reaction. In the second group are those which catalyze the reaction mainly through ionic intermediate states. These two groups will be described in separate subsections, A-1 and A-2 following.

A-1. Catalysts for Radical Reactions

Noble metals such as platinum and palladium are noted for their high catalytic activities for the reaction between hydrogen and water. They are known to catalyze the reaction by dissociating hydrogen molecules into hydrogen atoms. Colloidal forms of these metals have been especially extensively investigated (A-1, A-2, A-3, A-4). Nickel and stainless steel containing high concentration of nickel have been found to weakly catalyze the reaction between hydrogen and steam (A-5). Their catalytic activity is attributed to a mechanism similar to that of the noble metals. These metallic catalysts are, however, not homogeneous ones in which the present work has interest, so that no further discussion of these will be given here.

In the following subsections, possibilities of radiation-induced exchange reactions, reactions catalyzed by stable radicals and those actuated by salts of the transition elements will be discussed. It has been reported that the exchange reaction does take place when water and hydrogen is exposed to various types of nuclear radiation and that the reaction proceeds through intermediate states which involve radicals generated from water and hydrogen molecules. For catalysis by stable radicals and by salts of the transition elements, however, it has not even been known whether the catalysis will take place or not, but possibilities of catalysis are expected due to similarity with the metal catalysts mentioned in the preceding paragraph.

(a) Radiation-Induced Reactions

If the exchange reaction between water and hydrogen could be induced by nuclear radiation with such a high rate that would be practical but without producing any by-products, this would be a very promising means for use in a dual-temperature exchange process. The process would, then, have no need of a catalyst-recovery process, and the exchange rate could be controlled by merely controlling the radiation dose rate. Radiation-induced reactions, therefore, were rather extensively surveyed. In the following, established facts in the radiolysis of water will be summarized first; in liquid water in which hydrogen gas is dissolved, any direct effect of radiation is mostly on water molecules rather than on hydrogen molecules since concentration of the dissolved

hydrogen is only a minor fraction of that of water. Effect of radiation on the exchange reaction will then be discussed.

The following are among the well-established facts for the radiolysis of water.

(1) Decomposition of water by nuclear radiation yields atomic hydrogen, H·, and hydroxyl radical, ·$\underline{O}$-H, as its primary products. As the primary products diffuse away from the hot points at which they are formed, they either combine by themselves to produce molecular products, H_2 and H_2O_2, or react with any solutes present in water: the solute may be an oxidizing agent which will scavenge hydrogen atoms, or a reducing agent, which will scavenge hydroxyl radicals (A-6, A-7, A-8, A-9, A-10, A-11, A-12).

(2) In pure water, the yield of radicals decreases with increasing ionization density while the yield of H_2 and H_2O_2 increases. For instance (A-11, A-13, A-14),

$G(H) + G(OH) \simeq 6.6$ for gamma rays,

$G(H) + G(OH) \simeq 0$ for fission fragments,

$G(H_2) \simeq 0.4$ for gamma rays

and $G(H_2) \simeq 1.8$ for fission fragments.

where G denotes to the yield of a product, defined as the number of molecules or radicals of that product formed per 100 ev of energy given to the material being irradiated.

(3) The presence of radical scavengers in short period-irradiations reduces the yields of both radicals and molecular products, H_2 and H_2O_2. For prolonged irradiation of water under non-bubbling or non-boiling condition, the

radical scavengers first reduce net yields of the radicals, reducing at the same time the yields of H_2 and H_2O_2. Thus, it takes longer for the system to reach a steady rate of production of radicals and the molecular products, H_2 and H_2O_2. This steady rate would be slower than in the absence of these scavengers if it were not for the fact that the recombination reaction of the molecular products by a chain reaction

$$H + H_2O_2 \longrightarrow H_2O + OH$$

$$OH + H_2 \longrightarrow H_2O + H$$

which might continue without termination in the absence of the scavengers is terminated more easily when concentrations of the radicals are low due to the presence of the scavengers. Consequently, as a net effect, the steady rate of production of the molecular products is higher in the presence of the scavengers than in their absence.

(4) Under boiling or bubbling conditions, the molecular products are stripped from the solution before an appreciable amount of the free-radical-induced recombination sets in. It has been reported (A-15) that net H_2-generation rate increases about forty times when pure water being irradiated by gamma-rays is bubbled with CO_2. Effects of solutes under bubbling conditions have not been specifically investigated.

It follows from these facts that,

i) if a type of radiation is to be selected for the purpose of heavy water production by means of the induced exchange reaction between water and hydrogen, it should be

of lowest possible ionization density, that is, gamma radiation,

ii) a system of water and hydrogen gas exposed to gamma radiation should be as chemically pure as possible, and

iii) increased hydrogen formation in two-phase systems will present a serious difficulty in the practical application of radiation-induced exchange.

Effects of gamma-radiation on the exchange of deuterium

$$D_2 + H_2O \longrightarrow HD + HDO$$

have been investigated (A-9, A-16, A-17, A-18). It has been found that the exchange does take place and that $G(HD) \simeq G(H) \simeq 2.7$. Proposed mechanism is as follows.

$$H_2O \xrightarrow{h\nu} H + OH$$

$$H + D_2 \longrightarrow HD + D$$

$$OH + D_2 \longrightarrow HDO + D$$

$$D + D \longrightarrow D_2$$

When pure water was used, no increase in the amount of gas phase was observed. All the investigations were carried out at room temperature, and there is no report on the effect of temperature on the deuterium-transfer rate in the liquid phase. Effect of solutes in the liquid phase reaction has not been studied. If the proposed mechanism shown in the preceding paragraph is valid, however, presence of any hydroxyl-radical scavenger will reduce the transfer yield

G(HDO) and presence of any hydrogen-atom scavenger will reduce the yield of HD.

Thus, if it is assumed that production of radicals rather than the rate of molecular diffusion of the dissolved gases is the rate-controlling step, the rate of deuterium exchange is proportional to the dose rate of gamma-radiation. Using G(H) = G(HD) = 2.7, a dose rate of 5×10^5 roentgens per hour, which is the maximum value available at a facility in MIT's Department of Food Technology, would induce transfer of 0.14 gram atoms of deuterium in one liter of water in one hour, provided that all production of the radicals contribute to the forward reaction, $D_2 + H_2 \longrightarrow HD + HDO$. The reaction which is most interesting for production of heavy water is the one at lower deuterium enrichment,

$$H_2 + HDO \rightleftharpoons HD + H_2O$$

in which hydrogen gas and water consist of very large portions of H_2 and H_2O and very small portions of HD and HDO, respectively. Therefore, a very small fraction of the radicals produced would contribute to effective transfer of deuterium atoms in either direction. This would, consequently, reduce the net transfer rate.

Results of a probability estimation in which fractional values in the total reaction of all possible reactions initiated by the radiolysis of water were estimated and are summarized in Table A-I. In deriving these results it was assumed that the deuterium enrichment of water and hydrogen

gas was so small that only HDO and H_2O were present in the initial water and only HD and H_2 were present in the initial hydrogen gas. Mole fractions of H_2O in the total water and of H_2 in the total hydrogen gas are represented by ξ_o and ξ_o', respectively, in the table. It was also assumed that the G-value for the breakage of O-H bond was equal to that of O-D bond in any water molecule and that, in case there were possibilities of formations of two sets of products which differ from each other only isotopically for a given set of reactants, the two sets of products would be formed with equal probabilities. For instance, two isotopically similar products in reactions

$$OH + HD \begin{cases} \rightarrow H_2O + D \\ \rightarrow HDO + H \end{cases}$$

were assumed to take place with equal probability. It can be seen that the probabilities for the reactions (1) to (5) add up to be $(1 - \xi_o)$ and the probabilities for the reactions (6), (7) and (8) add up to be ξ_o.

Because of the oversimplification involved in these assumptions, no precise quantitative conclusions should be drawn from the results of Table A-I. For instance, an attempt to determine a state of equilibrium from these would lead to a meaningless result, which might be obvious from the fact that the formulae given are independent of temperature. Nevertheless, a useful order-of-magnitude result can be obtained, as follows.

Table A-I

Probabilities of Reaction Initiated by Radiolysis of Water in Presence of Hydrogen

Reactions	Probability	
	Formulae	$\xi_o = \xi_o' = 0.99$
Reactions initiated with radical formations, $HDO \longrightarrow H + OD$ and $HDO \longrightarrow D + OH$	$(1 - \xi_o)$	0.01
(1) $H_2 + HDO \longrightarrow HD + H_2O$	$\frac{1}{8}(1 - \xi_o)\xi_o'(5 + \xi_o')$	7.4×10^{-3}
(2) $HD + HDO \longrightarrow D_2 + H_2O$	$\frac{1}{8}(1 - \xi_o)(1 - \xi_o')(2 + \xi_o')$	3.74×10^{-5}
(3) $HD + HDO \longrightarrow H_2 + D_2O$	$\frac{1}{4}(1 - \xi_o)(1 - \xi_o')$	2.5×10^{-5}
(4) $2HD \longrightarrow H_2 + D_2$	$\frac{1}{4}(1 - \xi_o)(1 - \xi_o')^2$	2.5×10^{-7}
(5) $HDO \longrightarrow HDO$	$\frac{1}{4}(1 - \xi_o)(1 + \xi_o' - \xi_o'^2)$	2.53×10^{-3}
Reactions initiated with radical formation, $H_2O \longrightarrow H + OH$	ξ_o	0.99
(6) $HD + H_2O \longrightarrow H_2 + HDO$	$\frac{1}{2}\xi_o(1 - \xi_o')$	4.95×10^{-3}
(7) $2HD \longrightarrow H_2 + D_2$	$\frac{1}{4}\xi_o(1 - \xi_o')^2$	4.95×10^{-5}
(8) $H_2O \longrightarrow H_2O$	$\frac{1}{4}\xi_o(1 + 4\xi_o' - \xi_o'^2)$	0.985

Reactions (1) and (2) in Table A-I cause increase in the deuterium concentration of hydrogen gas while reactions (3) and (6) cause decrease in the deuterium content of hydrogen gas. Reactions (4) (or (7)), (5) and (8) do not contribute to any changes in the deuterium concentrations in either water or hydrogen gas. It is obvious from the formulae given in the table that the transfer of deuterium from water to the gas is caused mainly through the reaction (1), while the transfer in the opposite direction is caused mainly through the reaction (6). These points are illustrated in the last column of Table A-I in which values of the probabilities are given for a system consisting of water and hydrogen of 0.5 atom percent deuterium. Consequently, with a dose rate of 5×10^5 roentgens per hour, both the forward and backward reactions would initially proceed with a rate of order of 5×10^{-3} gram-atoms per liter per hour. This is so low as to be of little practical interest.

Thus, in the present work, the idea of using gamma radiation to catalyze the exchange reaction was abandoned because of the following reasons:

i) under bubbling conditions, the dilution by hydrogen gas and contamination by oxygen gas of the gas phase resulting from a significant rate of production of the molecular products of the radiolysis of water will present a serious problem, and

ii) in a practical application, the rate of deuterium exchange in a low region of enrichment would seem to be too slow even with an intense radiation source.

(b) Radicals

It has been known that paramagnetic substances catalyze hydrogenation of unsaturated organic substances (A-19). It was, therefore, expected that the exchange of deuterium would be catalyzed by stable organic radicals which are soluble in water. A literature survey showed, however, that otherwise stable organic free radicals are easily hydrogenated or reduced by hydrogen gas. For instance, quinhydron which is a stable intermediate in the oxidation-reduction between p-benzoquinone and p-benzohydroquinone and can be isolated as green crystals has been known to consist partially of a form called semiquinone

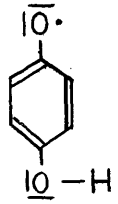

In an aqueous solution, it exists in equilibrium with its dimer, which is held together by hydrogen bonds. Concentration of the monomer, semiquinone, increases with pH of the solution. It has been known that a hydroquinone electrode which is formed by immersing a bright platinum electrode in a solution, usually saturated, of quinhydron reaches equilibrium quickly.

The equlibrium constant for the reaction

$$QH_2 + D_2(g) \longrightarrow QD_2 + H_2(E)$$

where Q represents benzoquinone, has been measured by means of the quinhydron electrode (A-20) and found to be 11.26, but the rate of exchange is not reported. The same paper also shows that equilibrium constants for reactions

$$QH_2(s) \rightleftharpoons Q(s) + H_2(g)$$

and

$$QD_2(s) \rightleftharpoons Q(s) + D_2(g)$$

are $10^{-23.65}$ and $10^{-24.70}$, respectively. This would mean that, in presence of hydrogen, especially at high pressure only negligible amounts of quinone and semiquinone would be present, so that little catalysis could be expected.

(c) Salts of the Transition Elements

As paramagnetic substances of another type, soluble salts of the transition elements were investigated. Those of largest Bohr magneton numbers are among salts of the rare earth elements (A-21), but they might not be economically practical. Besides them, a large number of salts of iron, cobalt, nickel, chromium and manganese are strongly paramagnetic. As a catalyst for the exchange reaction between water and hydrogen, however, a salt also has to be, among other requirements, stable against reduction by hydrogen gas

and hydrolysis at rather high temperatures, probably up to 400 °C. Table A-II shows some of the salts which would probably satisfy the stability conditions.

Table A-II

Some Salts of Transition Elements Which Could Be Used as the Catalyst*

Salts**	Bohr magneton number	ln K***
$Na\left[Fe^{II}EDTA \cdot H_2O\right]$	(5.0)	14.45 at 20°C
$Na\left[Fe^{III}EDTA \cdot H_2O\right]$	5.90	25.1 at 20°C
$Na\left[Cr^{III}EDTA \cdot H_2O\right]$	3.84	(very stable)

* Taken from Martell, A.E. and Calvin, M., "Chemistry of the Metal Chelate Compounds", Prentice-Hall, N.Y.

** EDTA denotes to ethylenediamine tetracetic acid.

*** Natural logarithm of the equilibrium constant for dissociation of the complex with EDTA.

A-2. Catalysts for Ionic Reactions

(a) Pertinent Facts on Acid-Base Catalysis

The exchange of deuterium between water and dissolved molecular hydrogen has been studied for two extreme cases of isotopic composition; one for a system of D_2 and H_2O (A-22), and the other for a system of H_2 and D_2O (A-23). In both cases, the exchange in presence of KOH was found to be catalyzed by hydroxyl ion. The forward reaction in each case is of first order with respect to partial pressure of

hydrogen and concentration of hydroxyl ion.

The activation energy reported is as follows. For the

$$D_2 + H_2O \longrightarrow HD + HDO,$$

it was experimentally found to be about 25 kcal in the temperature range of 80 to 110°C. For the reaction

$$H_2 + D_2O \longrightarrow HD + HDO,$$

it was experimentally found to be 28 $\pm$ 3 kcal in the temperature range of 110 to 190°C. Magnitude of the rate constant for the first reaction is 0.344 liter per gmole per minute at 100°C.

The mechanism proposed for the first reaction is

$$D_2 + OH^- \longrightarrow D^- + HDO$$

$$D^- + H_2O \longrightarrow HD + OH^-$$

and for the second reaction,

$$H_2 + OD^- \longrightarrow H^- + HDO$$

$$H^- + D_2O \longrightarrow HD + OD^- \quad .$$

The rate-controlling step in each case was concluded to be the formation of the negative hydrogen ions D^- or H^- With these mechanisms, the following facts could be explained:

i) the exchange reactions are of the first order with respect to pressure of hydrogen and concentration of hydroxyl ion, and

ii) the entalpy change of the reaction $H_2 + OH^- \longrightarrow H^- + H_2O$ calculated from the data given in Latimer's "Oxidation Potentials" (A-24) is about 20 $\pm$ 4 kcal, which will set a lower limit for the activation energy of the exchange reaction through the stated mechanism (A-22).

A more recent work (A-26) on the catalysis of the exchange between D_2 and H_2O with each of KOH, NaOH and LiOH indicated that the exchange reaction is best represented by the mechanism which has just been described: the heterolytic cleavage of the bond of the molecular hydrogen is nearly complete at the transition state, and the activated complex at this point closely resembles a solvated hydride ion.

An investigation of the catalytic activity of NaOH was made by Institute Francais du Pétrole (A-4) as a part of their extensive work in search of a catalyst for the liquid phase exchange of deuterium between water and dissolved molecular deuterium. They obtained an activation energy of 24 kcal at 120°C, in agreement with other workers. Effects of hydroxyl ion concentration and deuterium pressure were generally in agreement with other workers. They terminated the investigation of alkali-catalyzed exchange for the reason that corrosion of steel at the temperatures used (110 to 200°C) was so serious that this method could not be used in practical applications.

Attempts have been made (A-22, A-23, A-26) to extend

the pH range down to the acid side. It was found that acids do not significantly catalyze the exchange.

(b) Survey of Bases Other than Caustic Alkalis

As mentioned in the preceding subsection, an aqueous solution of caustic alkali attacks steel vessels. The rates of corrosion of aqueous solutions of sodium hydroxide on steel of various types are given in "Engineering Materials Handbook" published by McGraw Hill Book Co. (1958) as a function of temperature and concentration. At 100°C, a 2 N solution etches a wall of a mild steel at a rate of some 20 mils per year. The rate increases rapidly with the temperature and concentration.

A search for less corrosive catalysts among bases other than caustic alkalis revealed that organic amines are much less corrosive than caustic alkalis. For instance, syntheses of ethanolamine and methylamine are conducted in carbon-steel vessels. Aqueous solutions of hexamethylenetetramine form a protective layer on steel surfaces. Aqueous solutions of amine were expected to catalyze the exchange reaction through hydroxyl ion which would be present in the solution in hydrolytic equilibrium with undissociated amine. The undissociated part of the amine also was expected to contribute to the catalysis, as explained in DISCUSSION OF RESULTS Section. A survey of amines to select those expected to be most promising as catalysts will now be presented.

Bases can be qualitatively compared for catalytic activity on the basis of their ionization constants: an amine of higher basicity has a higher value of the ionization constant K_a for reaction

$$RNH_2 + H_2O \longrightarrow (RNH_3)^+ + OH^-$$

$$K_a \equiv \frac{[(RNH_3)^+][OH^-]}{[RNH_2]}$$

where R represents an organic group, aliphatic or aromatic. The possibility that a base of higher basicity would be associated with a higher catalytic activity has been suggested in several works (e.g., (A-22), (A-25)). This criterion almost entirely eliminates the possibility of aromatic amines being catalysts, as they are such weak bases.

Table A-III summarizes physical properties of the amines considered as possible catalysts for the deuterium exchange reaction between water and dissolved hydrogen. Diethylamine has the highest ionization constant K_a, and thus is expected to have the highest specific catalytic activity. Referring to Fig. A-1, diethylamine is completely miscible with water at temperatures below 143.5°C. Above this critical mixing temperature, its solubility, though limited, is at least about 20% (wt.) or about 2.6 normal (diethylamine) at the temperatures of practical interest. This would be sufficiently great for a practical process if its specific catalytic activity is

respectably high. The boiling point of diethylamine (55.5°C) is far enough below that of water so that small amounts of the amine can be distilled from water without great heat input. The same would be true of amines of lower boiling point. Amines with boiling points over 80°C, however, such as triethylamine, iso-amylamine, aniline, pyridine, hydrazine and ethylenediamine either form azeotropes with water, or if separable from water, would require too high a heat input in distillation to be practical.

At the other extreme, low-boiling amines such as ammonia and the methylamines have such high vapor pressures that they would be present in undesirably high concentrations in the vapor phase when present in useful concentrations in the liquid.

For all these reasons, diethylamine stands out as the most promising one of the amines to be investigated for catalytic activity.

All of these amines except hydrazine have adquate chemical stability for use in the water-hydrogen exchange process. All except hydrazine are thermally stable at temperatures up to 300°C, the highest temperature practical for an exchange reaction using water. None are hydrolyzed appreciably by water up to this temperature. Only hydrazine could react with hydrogen at the temperatures and pressures needed for this process.

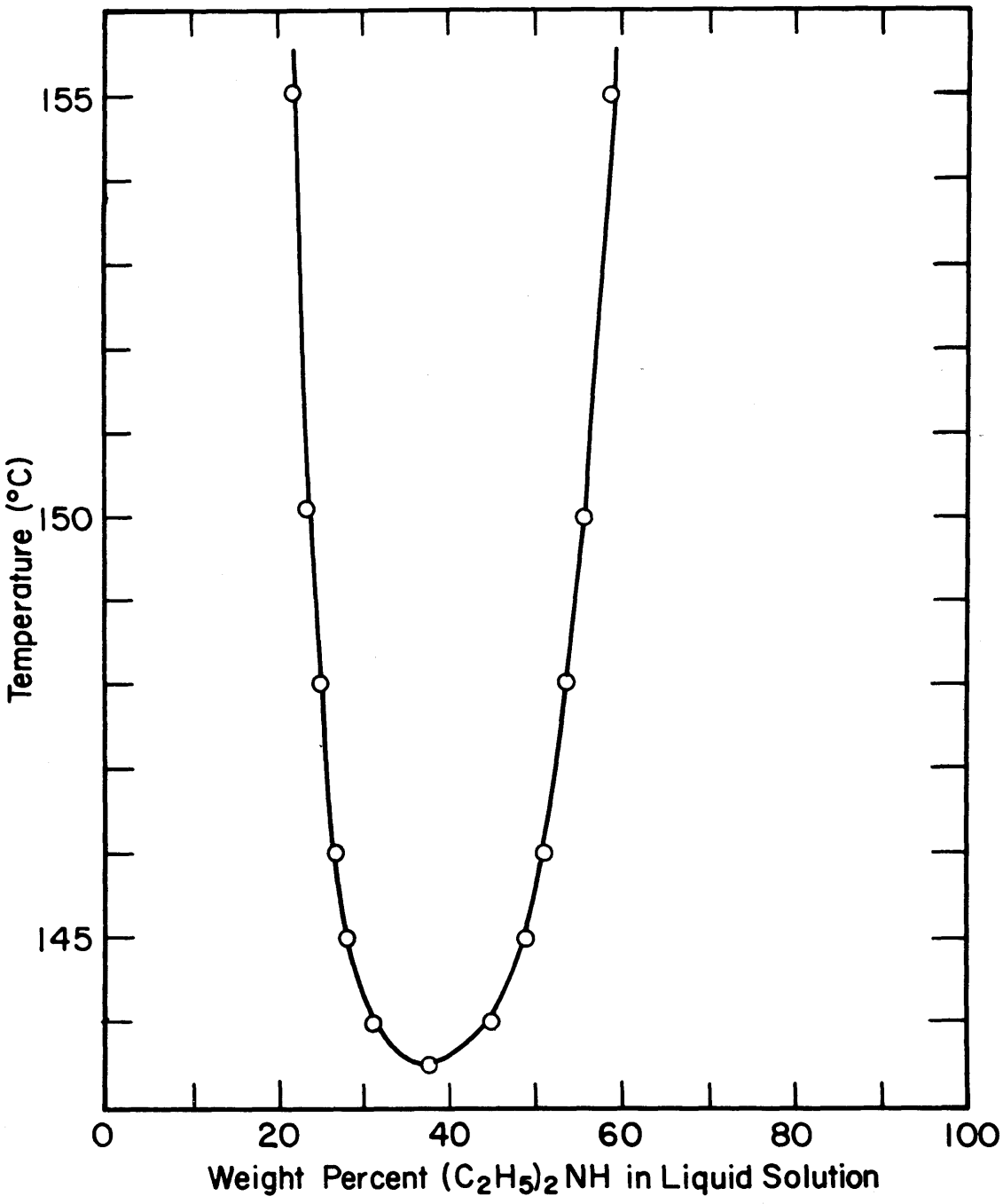

Fig.A-1 Temperature-Composition Diagram under Vapor Pressures for the System $(C_2H_5)_2NH-H_2O$.
(Taken from Ref.(A-27).)

TABLE A-III. PROPERTIES OF TYPICAL AMINES

Amine	Normal B.P. of Pure Amine (°C)	Azeotrope with Water: Temp. (°C)	Azeotrope with Water: Comp. (wt % H_2O)	Thermal Decomp. Temp. (°C)	Solubility in Liquid Water* (g/100ml H_2O)	Molec. Wt.	M.P. (°C)	Density (g/ml)	Ionization Constant at 25°C (K_a)
Methylamine	-6.5	Nonazeotrope		1200-1300	(57.7)	31.06	- 92.5	0.7691 (-70°)	4.1×10^{-4}
Dimethylamine	7.4	Nonazeotrope		820-1120	(38.7)	45.08	- 96.0	0.6804	5.3 "
Trimethylamine	3.5	Nonazeotrope		800-1300	((65.7))	59.11	-124	0.662 (- 5°)	0.6 "
Ethylamine	16.6	Nonazeotrope		1240	(54.1)	45.08	- 80.6	0.7059 (0°)	4.8 "
Diethylamine	55.5	Nonazeotrope***		1170	t_{cm}=143.5°C	73.14	- 50	0.7108 (18°)	11. "
Triethylamine	89.5	75	10	1270	t_{cm}= 18.6°C	101.19	-114.8	0.7229 (25°)	3.8 "
n-Propylamine	48.7	----		----	----	59.11	- 83	0.719	4.1 "
iso-Propylamine	34	----		----	----	59.11	-101.2	0.694 (15°)	4.6 "
n-Butylamine	77.8	----		----	----	73.14	- 50.5	0.7401 (20°)	----
iso-Butylamine	68	----		----	----	73.14	- 85.5	0.736	2.4×10^{-4}
iso-Amylamine	95	----		----	----	87.16	----	0.7505 (20°)	4.2 "
Aniline	184.4	90	80.5	Very high	t_{cm}=165.0°C	93.12	- 6.2	1.022 (20°)	5×10^{-10}
Pyridine	115.3	94	57	Very high	Completely miscible at room temp.	79.10	- 42	0.982	2.3×10^{-9}
Hydrazine	113.5	120	28.5	See text	"	32.05	1.4	1.011 (15°)	$**8.5 \times 10^{-7}$
Ethylenediamine	116	118	20-25	----	Slightly soluble at room temp.	60.10	8.5	0.8994 (20°)	$**0.73 \times 10^{-4}$
Ammonia	-33.4	Nonazeotrope			(52.0)	17.03	-77.7	0.817 (-79°)	0.18×10^{-4}

*All the alkylamines shown are completely miscible with water at room temperature. Those in parentheses are solubility of vapor computed from data on Bunsen absorption coefficient (volume of gas, reduced to STP, dissolved by one volume of the liquid when the partial pressure of the gas is 760 mmHg) at 60°C (ref. A-27) by using a compressibility factor of 0.98 for all amines at STP, so that those shown above are the values at 60 °C and the amine-partial pressure of 1 atm. The value given for trimethylamine is at 25 °C and its partial pressure of 1 atm. Those for which t_{cm}, the critical mixing temperature, is indicated are to be referred to Figs. A-1 to A-3. The value for ammonia is the one under the partial pressure of ammonia of 1 atm. at 25 °C.

**First ionization.

***Reference (A-28).

B. Design, Construction and Performance Tests of Constant Temperature Oil Bath

The constant temperature bath in which the high pressure reaction vessel, autoclave, was placed was required to regulate the temperature within 0.1°C of a set temperature ranging from 100°C to 200°C. It was, of course, also required that it accommodate and suitably position an autoclave whose main body with top cover was 4 3/8 inches in outside diameter and 11 7/8 inches in outside height. Detailed descriptions of the autoclave are in APPENDIX C. Design and Construction of Systems for Handling Superatmospheric Gases. The bath had to be operated continuously for a prolonged period of time, mostly a length of one week at a time. Therefore, all the mechanical and electrical parts had to be dependable and be designed for continuous operation, and the bath fluid had to be of high flash point and low vapor pressure.

Generally the design of a stirring mechanism for precision thermostats by Collins (B-1) was followed. Some modifications of the design were made, and they are explained in the following. A used unit, mostly designed after Collins, was kindly supplied by Professor J. A. Beattie of the Department of Chemistry, and parts from this unit were used whenever possible.

B-1. Bath Fluid

From considerations of cost in addition to the requirements of high flash point and low vapor pressure, General Electric's dimethyl silicone fluid SF-96 Grade No. 50 was

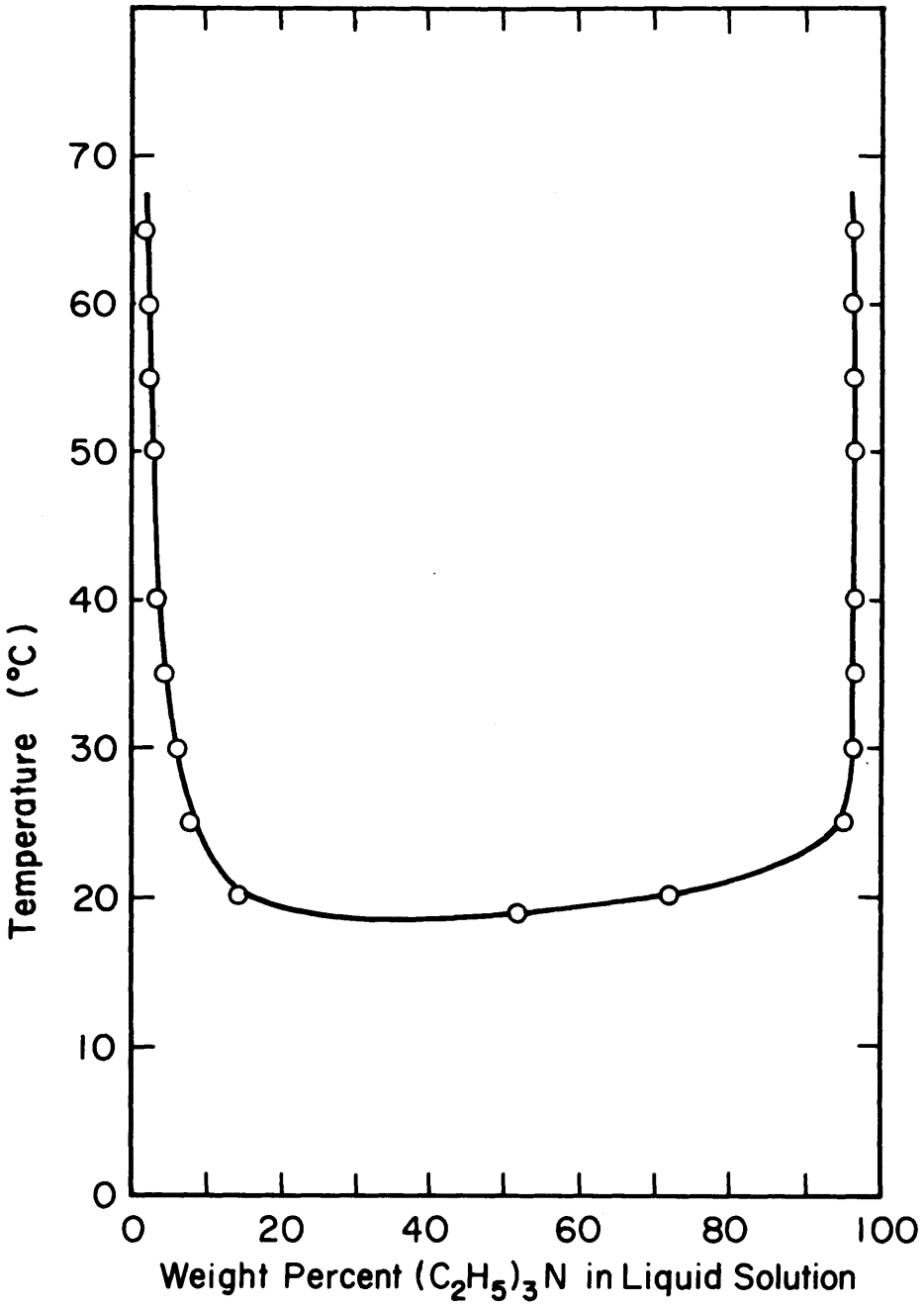

Fig. A–2 Temperature-Composition Diagram under Vapor Pressures for the System Triethylamine-Water (Taken from Ref. (A-27).)

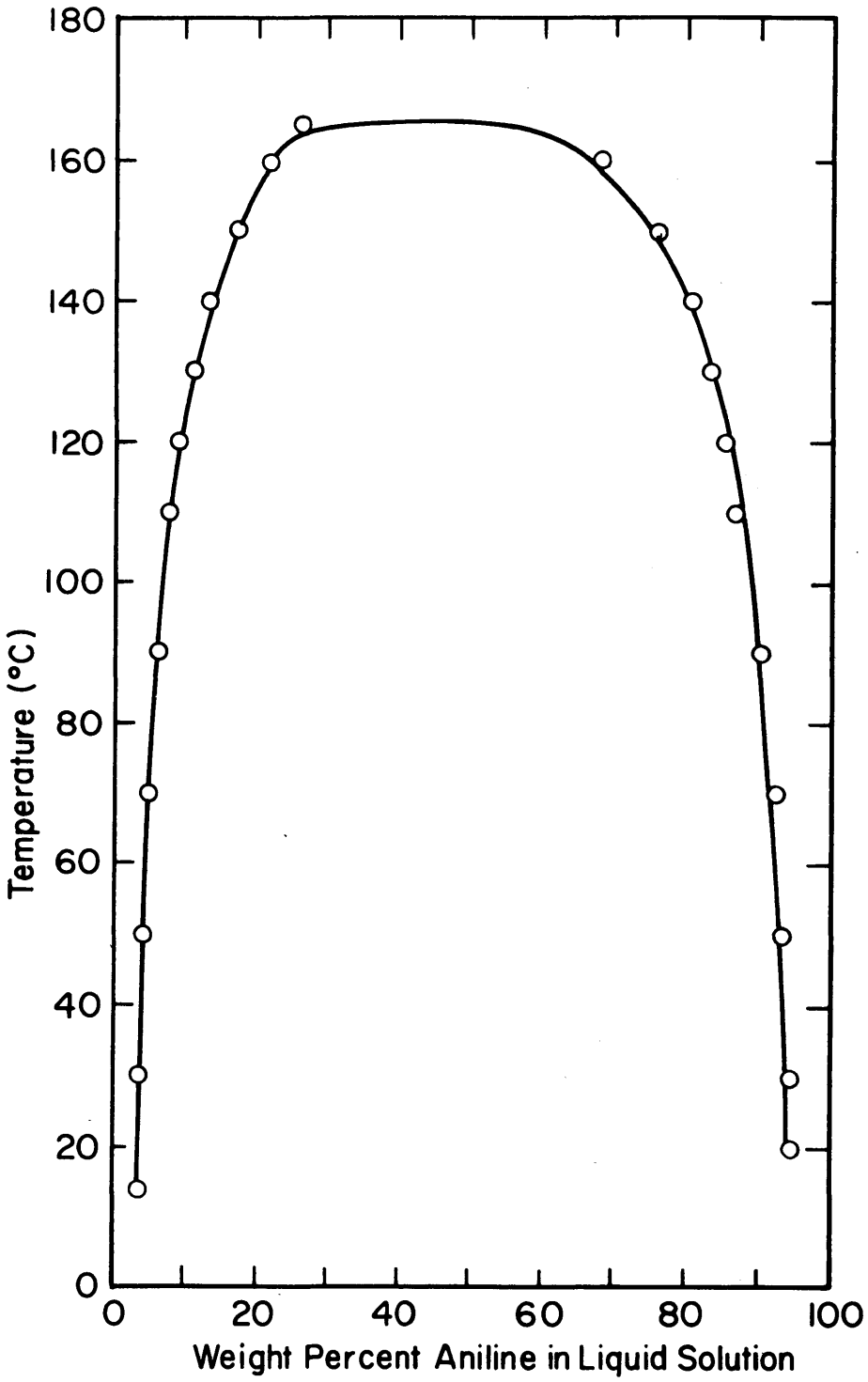

Fig. A-3 Temperature-Composition Diagram under Vapor Pressures for the System Aniline-Water (Taken from Ref.(A-27).)

employed as the bath fluid. This fluid had a very small change of viscosity with temperature, a high resistance to shear breakdown, a high order of thermal and oxidative stability, good electrical properties, and a low order of physiological activity. Its properties are copied from the manufacturer's catalog in Table B-I.

Table B-I. Properties of Bath Fluid

Viscosity at 25°C	50 centistokes
Temperature coefficient of viscosity	0.588 per °C
Pour point	-55°C
Specific gravity at 20°C	0.9701
Surface tension at 25°C	20.8 dynes/centimeter
Thermal conductivity at 49°C	0.0845 BTU/hr·ft·°F
Minimum flash point	315°C
Autoignition point	440°C
Vapor pressure at 220°C	~0.01 mmHg
Volume coeficient thermal expansion	10.55×10^{-4} per °C

According to the manufacturer one-half percent of the fluid would be lost due to evaporation after a two gram sample of the fluid contained in a 50 milliliter beaker was left in a forced-circulation oven at 150°C. Actually, about 12 gallons was needed for the initial charge and since then a total of only about two gallons more of the fluid was required to make up for the evaporation loss during the period of about 300 working days.

B-2. Oil Container

The silicon oil was contained in a steel tank 12.5 inches outside diameter by 25.5 inches high by 1/4-inch thick. This tank is shown at (2) in Fig. B-1. It is also visible in Fig. B-2. On the outside and near its top, an open annular collar was welded. This was made of steel plate 3/16-inch thick, and it was 1 1/2-inches deep and 1 1/4-inches wide. This was to provide a receiver for oil which might be spilled over the edge of the container. It was intended to protect electrical terminal boxes placed underneath the collar as well as to prevent ignition of spilled oil. The tank was supported on three heavy angle-iron legs, each extending 8 inches below the bottom of the oil container, welded to the side of the tank and bolted to the bottom of an outer can.

B.3. Stirring System

Basically, Collins' design, (B-1), was followed. Its essential features are shown in Figs. B-1, 3 and 4.

Referring to Fig. B-1, the entire stirring mechanism was designed to hang under a top plate, shown in Fig. B-1 at (4), which rested on the top edge of the oil container tank (2). The bottom plate, one-half inch thick, was hung from the top plate by six concentrically arranged one-half inch square steel rods (5), and there was a clearance of about one quarter of an inch between the inner bottom of the oil container and the lower side of the bottom plate. This was to provide space for any longitudinal thermal expansion of the supporting rods. Six supporting rods were used, instead of three as specified

Fig. B-1 Constant Temperature Oil Bath

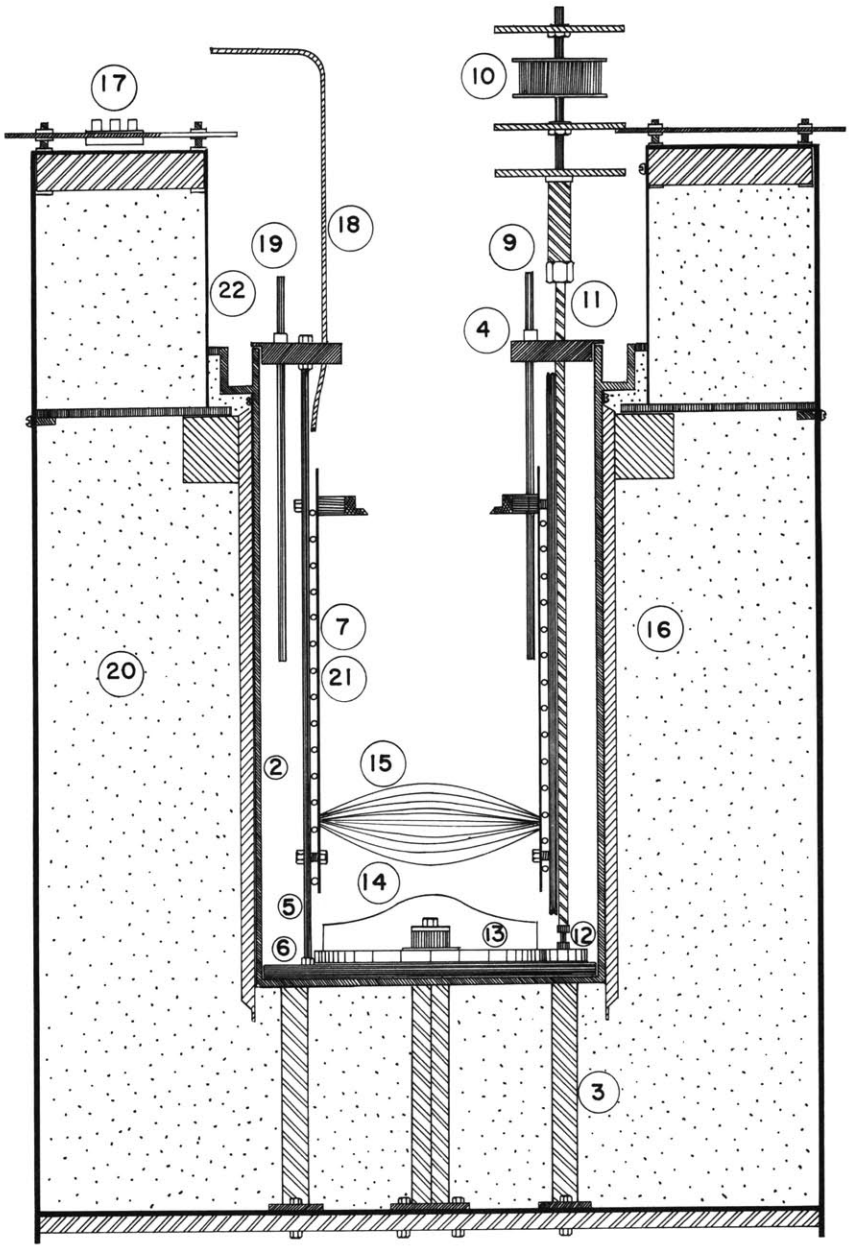

1-Outer can, 2-Oil container, 3-Legs, 4-Top plate, 5-Supporting rod, 6-Bottom plate, 7-Inner cylinder, 8-Autoclave seat, 9-Iron-constantan thermocouple, 10-Pulleys, 11-Flexible shaft, 12-Pinion, 13-Spur gear, 14-Impeller, 15-Stationary vane, 16-External heaters, 17-Terminals for external heaters, 18-Cable for internal heater, 19-Thermistor probe, 20-Asbestos powder, 21-Internal heater, 22-Aluminum cylinder.

Fig. B-2 Oil Container and External Heaters

Fig. B-3 Stirring Mechanism (without Flexible Drive Shaft and Upper Structure)

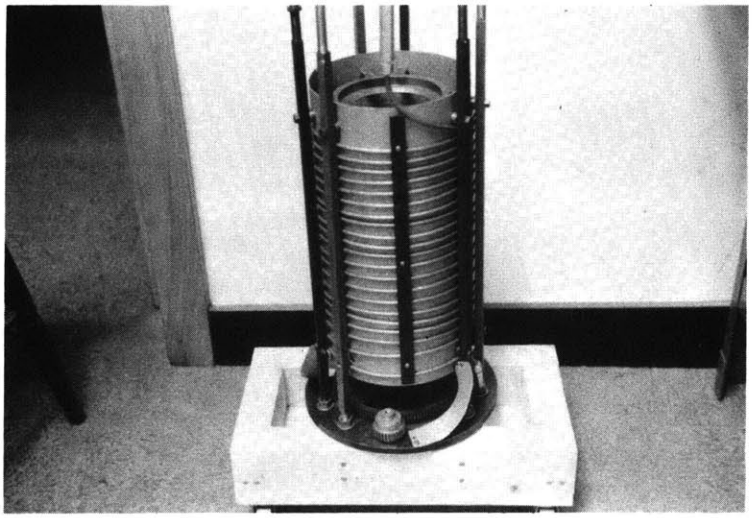

(a) Side View

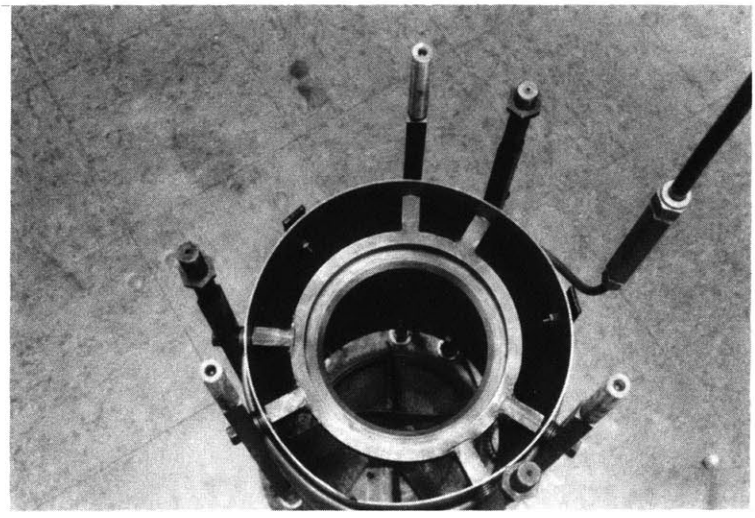

(b) Top View

in the Collins' design, to provide additional support for the heavy autoclave. A cylinder (7), made of 1/16-inch steel plate, 8 1/2 inches in diameter and 18 inches long, was bolted from inside on the six supporting rods (5) with the top edge about 4 1/2 inches below the lower side of the top plate. This cylinder served chiefly to guide the fluid in an orderly circuit. Inside this cylinder and 1 3/8 inches below the edge of the cylinder, an autoclave seat (8) was placed and bolted, through the cylinder, onto the supporting rods. This is clearly shown in Fig. B-3(b). Its inner diameter was such that the clearance between it and the autoclave body was about two thousandths of an inch, so that no additional clamping of the autoclave was necessary. The autoclave was firmly supported in the seat even when the silicone oil was stirred vigorously and the autoclave stirring system was actuated rapidly.

Stirring was performed as follows. Horizontal rotation produced by an AC motor (9), rated 1/4 horse power and 1,750 rpm, was delivered to a vertically mounted drive shaft through a twisted V-belt and a pulley system (10). Speed of rotation was controlled by changing voltage to the motor by means of a variac regulator. The ratio of diameters of the secondary pulley to the one on the motor shaft was 2.35 inches to 1.35 inches, or 1.74. The power was then delivered to a pinion (12) mounted on the bottom plate through a flexible drive shaft (11). The flexible shaft was commercially available and was designed for use at a maximum speed of 1,750 rpm and a torque of 9 pound-inches, and was 25 inches long. This was one of the

modifications of the Collins' design, which used a solid drive shaft. Use of the flexible shaft minimized bearing wear as well as troubles in aligning bearing supports.

An impeller (14), mounted on a spur gear (13), with pitch diameter of 10 inches and 1/2-inch face, caused centrifugal action in the fluid and made it move under some pressure and with considerable angular velocity into the annular space between the cylinder (7) and the walls of the container. Three curved runners, which are not shown in Fig. B-1 but one of which is clearly seen in Fig. B-d-(a), on the right of a pinion on the bottom, assisted in the upward movement of the liquid by reaction with its angular momentum. Having passed through the annular channel, the liquid spilled over the top of the cylinder and flowed downward through it. The cylinder was fitted at its lower end, about 13 inches below the top of the cylinder, with a stationary vane (15), a single strip of sheet iron two inches wide stretched along a diameter and twisted so that its ends made an angle of 90 degrees with each other. The direction of twist was such that the spinning column of liquid was deflected into the impeller rather than away from it. The vane is seen in Fig. B-3-(b), which also shows the impeller. The downward flow of fluid inside the cylinder helped keep the autoclave in position instead of making it float up. With the dimensions of the system as described above, the top of the autoclave cover was immersed about one inch below the surface of silicone oil when the oil surface was kept about 2 inches below the top edge of the oil container.

B-4. Heating and Temperature-Regulating Systems

Two heating systems were installed. One consisted of six strip heaters attached vertically and equally spaced on the outside wall of the oil container, and the other system consisted of a metal-sheathed, ceramic-insulated heating cable coiled around the outside wall of the cylinder in the stirring system. The former was called the external heating system, and the latter was called the internal heating system.

The external heating system was used to roughly maintain a desired temperature level and was kept on steady power throughout a period of operation of the bath. The strip heater unit selected was a Chromalox heater supplied by E. L. Wiegand Company, Pittsburgh, Pennsylvania, Catalog No. SE-2401, which was sheathed with chrome steel. Its maximum sheath temperature could go up to 1200°F. Each was 23 3/4 inches long and 1 1/2 inches wide and had a power of 1,000 watts. Six such units were grouped into three, each group consisting of two units connected in series. This is illustrated in Fig. B-4. The wiring can also be seen in the photograph of Fig. B-2. It shows the strip heating units, their terminal boxes, and lead wires covered partly with ceramic insulator tubelets and partly with asbestos tape, Each strip heater was supported by a small bolt screwed into the wall of the oil tank just below its collar, and its lower end was free to expand downward. They were, however, kept in contact with the wall of the container by means of three steel band clamps. The three groups of heating units could be connected either

in series or in parallel to each other by a flip of a switch, and the input power to these was regulated by means of a voltage regulator. Wiring of the para-series selector switch is shown in Fig. B-5. The induction voltage regulator was kindly supplied by Professor Beattie and was an old product of the General Electric Company, Type MIRS. It had eight terminals, (1) through (8) in Fig. B-6, and when wired up with two double-pole-double-throw (DPDT) switches as shown in Fig. B-6, the regulator could produce outputs as shown in Table B-II. Schematic diagram of windings of the regulator for various combinations of the selector switches are shown in Fig. B-7. Combination of the selector switches most frequently used for the present work was A and C. Fine control of the voltage was achieved by means of rotation of a disk attached on the regulator.

Table B-II. Outputs of Induction Voltage Regulator

Switch Position	Voltage Range	Current Amperes	Primary Windings	Secondary Connections	Disk Rotation to Increase Voltage
A-C	0-120	15	parallel	insulated from primary	either direction from midpoint
B-C	0- 60	30	parallel		
A-D	0-220	15	parallel	in series with primary	Clockwise
B-D	38-170	30	parallel		

The internal heating system was used to closely regulate the temperature, and its power was controlled by an electronically

Fig. B-4 Grouping of External Heating Units

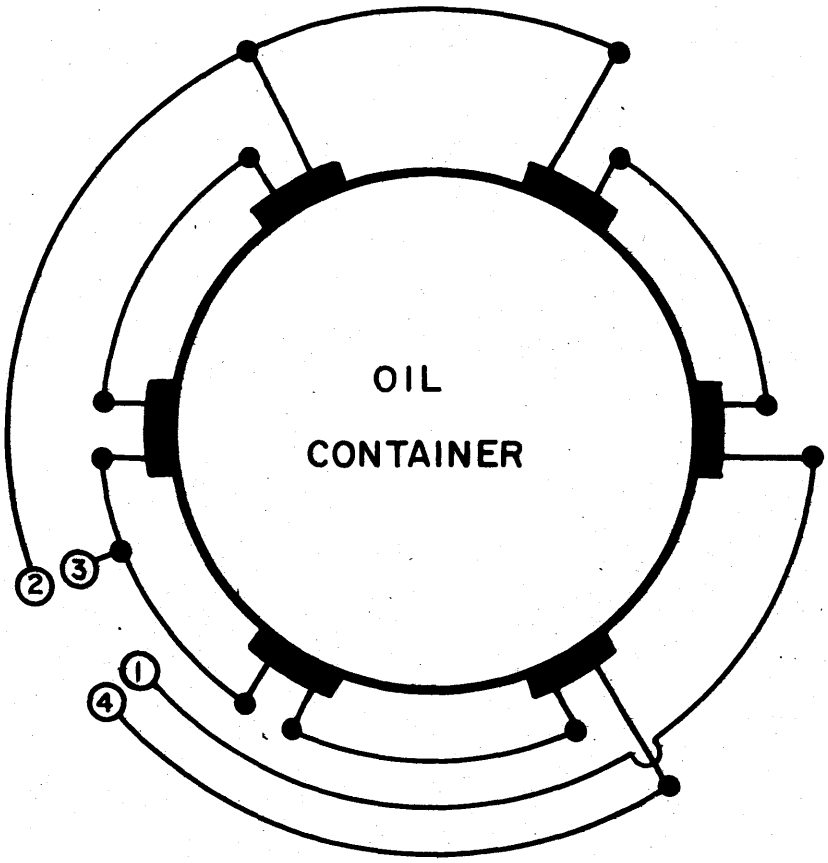

(a) Schematic Top View

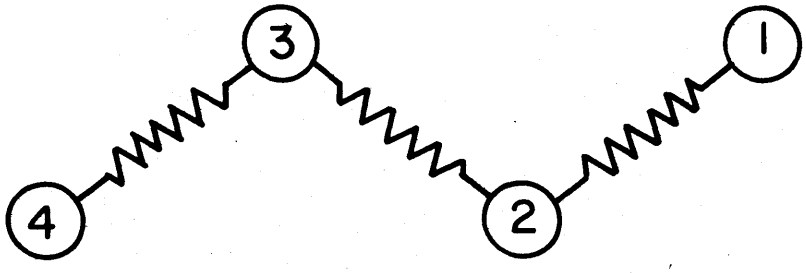

(b) Equivalent Circuit

Fig. B-5 Para-Series Selector Switch Circuit

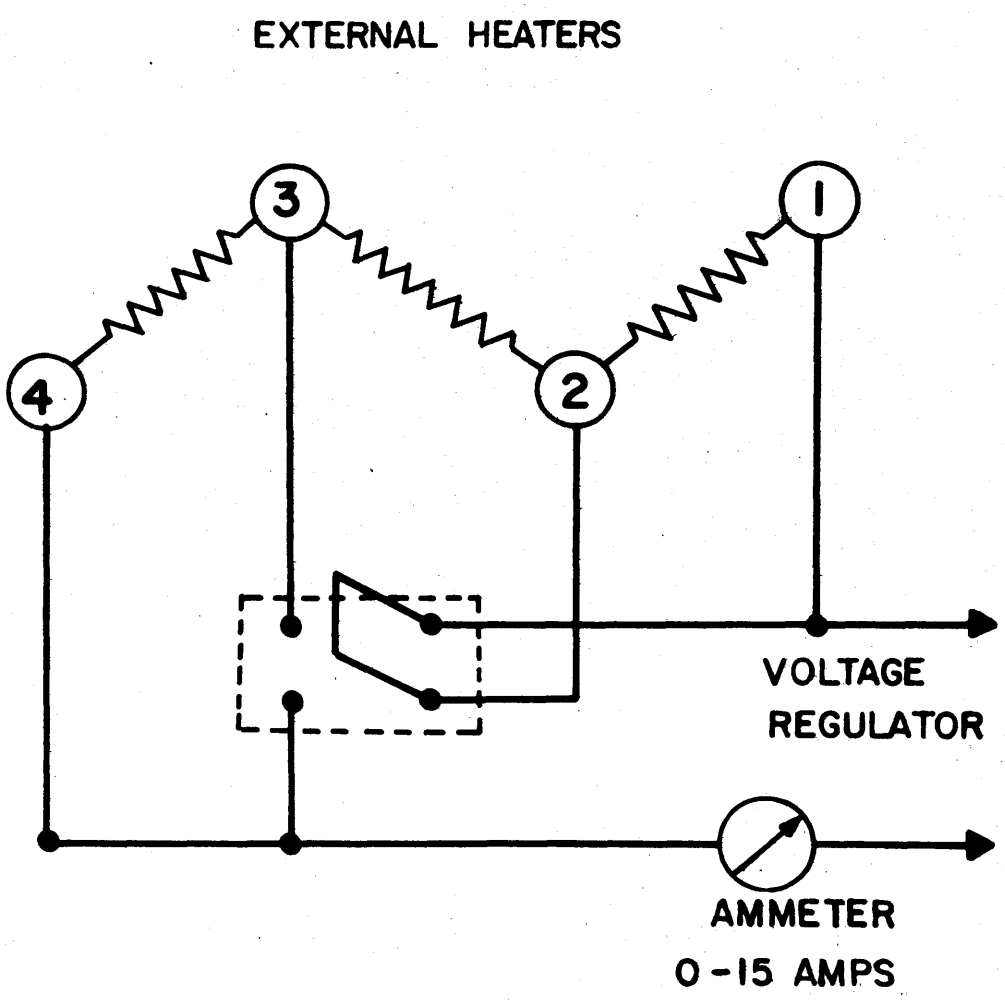

Fig. B-6 Wiring of Voltage Regulator Selector Switches

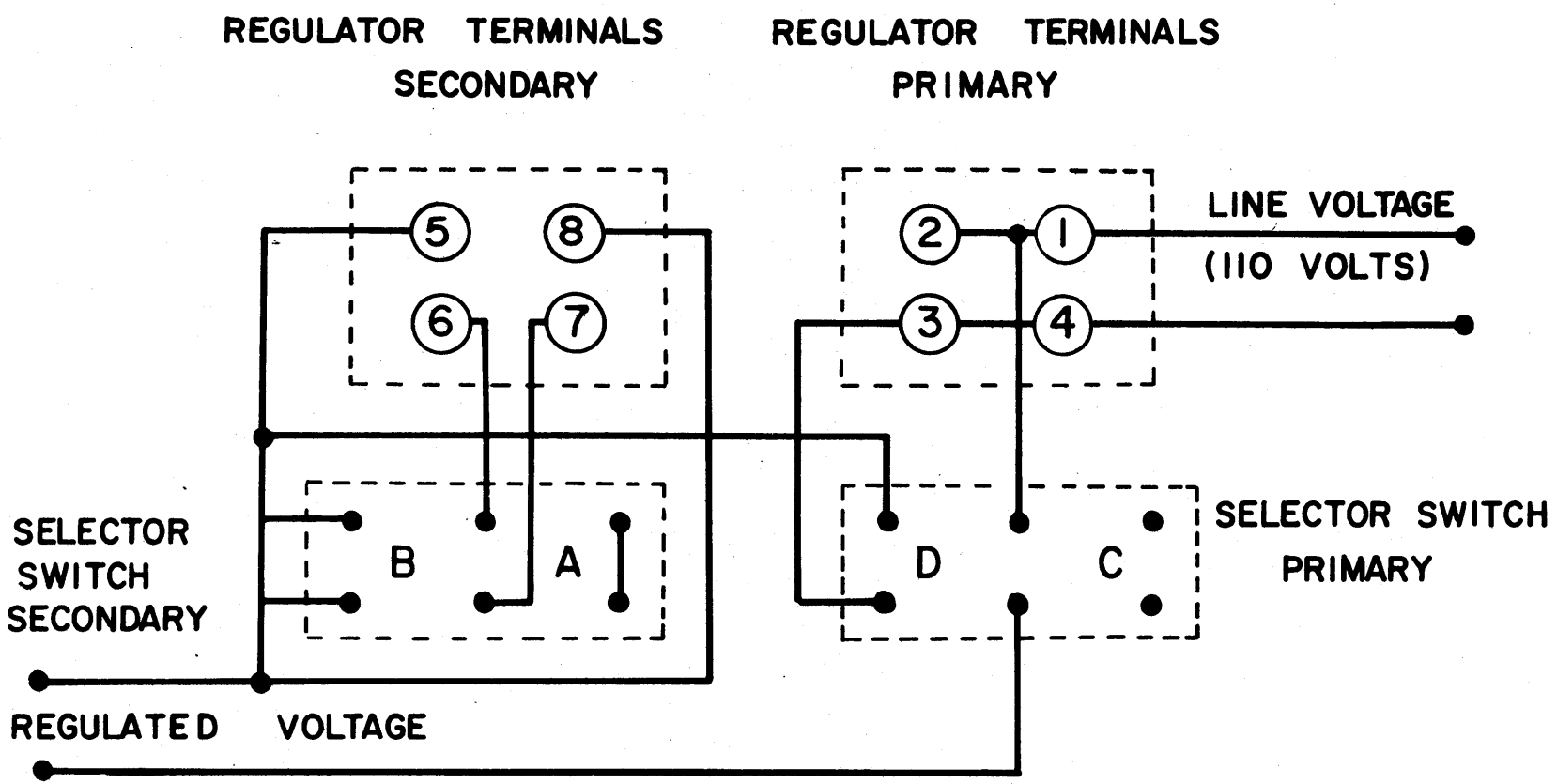

Fig. B-7 Schematic Diagram of Regulator Windings

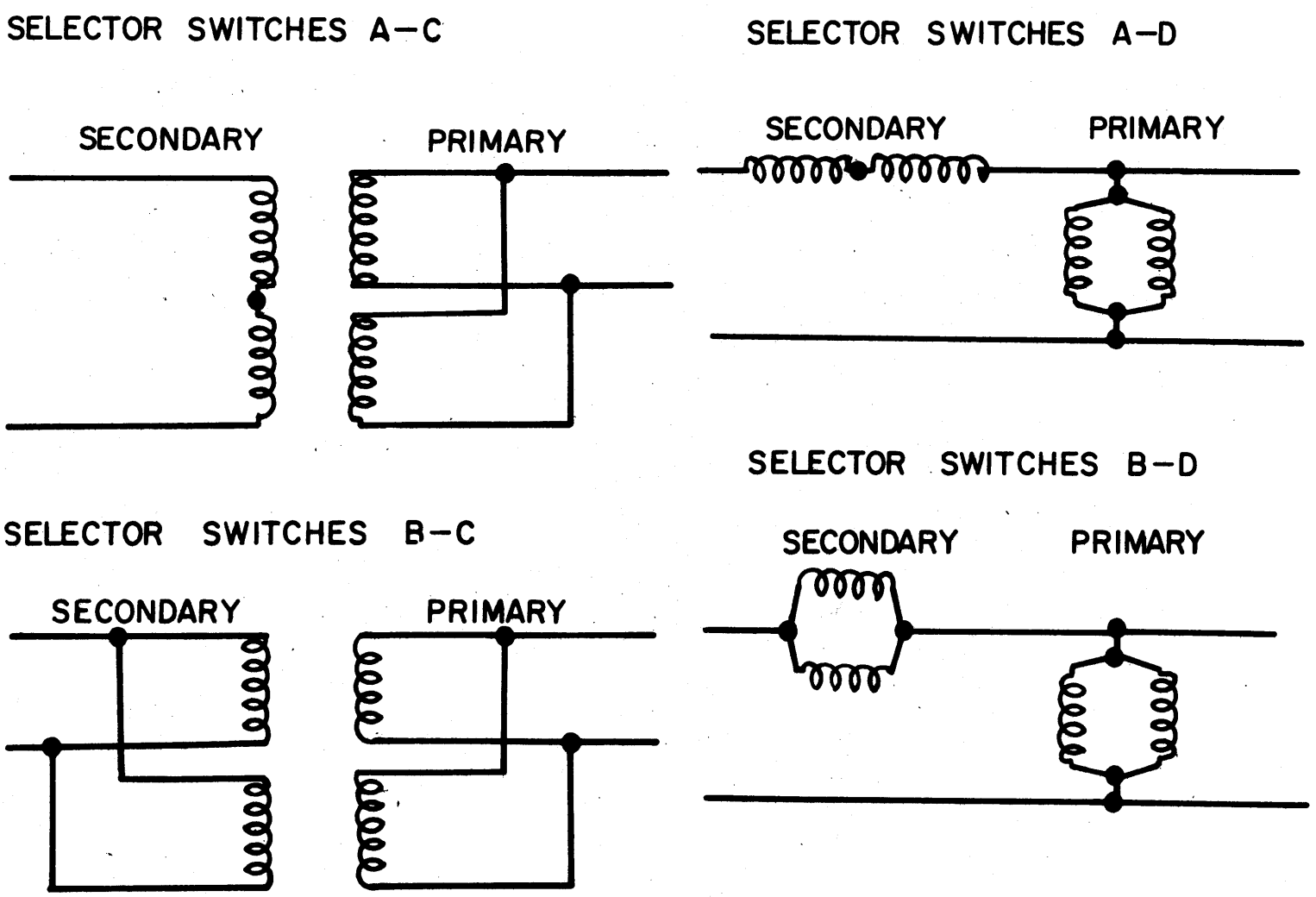

operated temperature-controlling unit which sensed the temperature of the bath fluid by means of a thermistor element. The heating cable employed was a Chromalox heater of the same manufacturer as for the strip heater, which was sheathed in a copper tubing of 0.246 inches in diameter and insulated by a densely compacted ceramic powder. It contained twin resistance wires which were connected together at one end of the cable inside a waterproof end cap. The heated length was 50 feet and the total output was 2.3 kilowatts when operated on 120 volts. It was coiled around the inner cylinder of the stirring system and loosely clamped by means of the supporting rods of the stirring system and three additional clamping plates. The coil is indicated at (21) in Fig. B-1 and is clearly shown in Fib. B-3-(a). Fig. B-3-(b) shows how washers were used to provide enough space for the width of the cable. The cable, when heated, could expand freely both upward and downward. Power input to the coil was regulated by a variac regulator; its imput voltage never exceeded 40 volts, which corresponded to a maximum power of 250 watts. If a higher voltage had been used, the power input would have been too large compared with that of the external heater and, consequently, the overshoot of the bath temperature would have been too large.

Supply of power to the heater was controlled by a temperature controller unit, Model Y-71, manufactured by Yellow Springs Instrument Company, Yellow Springs, Ohio. This unit sensed the bath fluid temperature by means of a thermistor probe and worked on the principle of alternating-current bridge-amplifier-

control relay system, so that its demand was either complete OFF or complete ON. The thermistor sensing element used, Catalog No. 632 of the same manufacturer, had a time constant of 2.5 seconds according to the manufacturer and sensed the temperature ranging from 38°C to 260°C. It orginally had a stainless steel sheath only 8 inches long, and a one-foot length of a 3/16-inch stainless steel tubing had to be silver-soldered on top of its metal sheath before it could be dipped one foot below the surface of silicone oil. The dial of the control unit was graduated in small temperature intervals whose unit division, when used with the No. 632 probe, was found to correspond to a temperature interval of 1.67° C in the range between 100°C and 200°C. With an aid of a vernier fine-set dial attached on the face of the unit, a control of setting to about $\pm$ 0.1°C was possible. Its relay was rated for 10 amperes at 110 volts. There were two pilot lamps provided on the control unit. One was turned on when the heater was on and the other was on when the heater was disconnected.

B-5. Thermal Insulation

The oil container was bolted to the bottom of a larger can, 30 inches in diameter and 42 inches high, (1) in Fig. B-1. The bottom and annular space between the outer can and the oil container was packed with asbestos powder, thus providing insulation 8 1/2 inches thick radially and 8 inches thick on the bottom. The annular space was filled up to the lower end of the collar on the oil container and was covered with an annular-shaped transite board 1/4 inch thick, whose inner edge

rested on top of the terminal boxes of the external heaters while its outer edge rested on small bolts screwed through the outer can. A cylinder, (22) in Fig. B-1, 16 1/2 inches in diameter and 8 1/2 inches long, made of an aluminum sheet 1/8 inch thick, was placed concentrically with the oil container on the transite sheet. The space bounded by the container, the transite sheet and the aluminum cylinder was filled with asbestos powder and covered by an annular-shaped transite sheet. The space between the outer can and the aluminum cylinder was also filled with asbestos powder, and its top surface was covered by an annularly cut wooden plate, 29 3/4 inches in outside diameter, 16 3/4 inches in inner diameter and 1 inch in thickness. The wooden plate was hammered into place and rested on a horizontally placed, square wooden framework whose corners were screwed onto the wall of the outer can. The space directly above the oil container was not covered, even at a price of increased rates of loss of heat and silicone oil, to allow good air circulation in this space to prevent accumulation of silicone oil vapor and hydrogen gas which might come out of the autoclave in case one of the high pressure joints leaked.

B-6. Rough Calibration of Temperature-Setting Dial on the Temperature Control Unit and Recommended Heater Settings

Calibration of the temperature-setting dial on the temperature control unit, Y-71, could not be extremely precise because of the coarse graduations of the dial. Extreme precision

of the calibration was not needed anyway because, once a rough calibration was known, a desired temperature could be easily reproduced within $\pm$ 0.1°C by a trial and error process of manipulating the vernier fine-set dial to find the right setting using an iron-constantan thermocouple to measure temperature, every time a new temperature setting was required. Results of the rough calibration are presented in Table B-III.

Settings of the heaters for roughly attaining a desired temperature were chosen so that the period of time during which the internal heater is turned on would be around fifty percent of the total time of the steady bath operation. Recommended settings for operation at temperatures 100°, 150° and 200°C are tabulated in Table B-IV.

Table B-III. Rough Calibration of Temperature Setting Dial

Dial Setting	Temperature (°C)
4.5	96
6.5	100
8.0	102.5
10.0	105.5
12.0	109
14.0	112.5
16.0	116
18.0	119
20.0	122
22.0	125.5
24.0	128.5
26.0	132
28.5	136
30.0	138
35.0	147
40.1	155
45.0	164
50.0	172
55.0	181
60.0	190
62.5	194
65.0	198.5
66.0	200.5

Table B-IV. Recommended Heater Settings

Temperature (°C)	External Heater			Internal Heater
	Para-Series Switch	Regulator Selector Switches	Total Current (amperes)	Applied Potential (volts)
100	parallel	A-C	5.1	20
150	parallel	A-C	6.8	20
200	parallel	A-C	7.9	30

B-7. Checking Calibration of Iron-Constantan Thermocouple

Bath temperatures were measured with a standard iron-constantan thermocouple, with reference junction in an ice bath, and a Leeds and Northrup Type K potentiometer. The thermocouple was calibrated by comparison in a thermostated water bath with a totally immersed mercury-in-glass thermometer which had been calibrated by the U.S. National Bureau of Standards. Thermocouple millivoltages observed at two temperatures are compared below with millivoltages from a standard table (B-2) for iron-constantan thermocouples.

Temperature (°C)	Millivoltage	
	Observed	Standard
34.0	1.751	1.747
71.48	3.726	3.730

As the differences between observed and standard voltages corresponded to a temperature difference of only 0.05°C, it

was concluded that the table of standard voltages could be used to convert thermocouple readings to temperature with adequate precision for this work.

Thermocouple readings corresponding to the temperatures at which reaction rates were measured were as follows.

Temperature (°C)	Millivolts
100	5.27
150	8.00
200	10.78

B-8. Temperature Fluctuation Test of the Oil Bath

A test for temperature fluctuations of the oil bath was made at 185°C as follows.

The autoclave was placed in position in the oil bath, and all tubing connections including that for cooling water for the autoclave's stirring system were made. Silicone oil level was adjusted to be about one inch above the top of the cover of the autoclave body at 185°C. The iron-constantan thermocouple was immersed in the annular space between the container wall and the inner cylinder of the stirring mechanism.

The temperature setting dial was set at 57.5 which, according to the rough calibration of Table B-III, corresponded to 185°C. The internal heater voltage was set at 30 volts, the external heaters were connected in parallel, the voltage regulator selector switches were set for A-C, and the total current for the external heater was adjusted to 7.8 amperes.

After it was heated up and reached the steady temperature level, the output of the iron-constantan thermocouple was measured every 30 minutes for a period of 31 hours. Values of 62 measurements for the thermocouple were averaged, and the standard deviation of the measured values was calculated. The results were as follows:

average output = 10.0183 millivolts,

corresponding temperature = 186.33°C,

and standard deviation = 0.0028 millivolts.

The standard deviation of 0.0028 millivolts around 186°C for the output of the iron-constantan thermocouple corresponded to a temperature difference of 0.05°C. It was expected that the temperature control was easier at lower temperatures. It was concluded that at all temperatures between 100°C and 200°C the temperature was resetable to within $\pm$ 0.05°C, and the temperature fluctuation could be limited to within 0.05°C of the set temperature.

During this run a copper-constantan couple which was later used to measure temperatures in a thermowell in the autoclave was calibrated by comparison with the iron-constantan couple. At a temperature of 186.33°C as measured by the iron-constantan couple, the copper-constantan couple read 8.5870 millivolts, which corresponded to a temperature of 186.70°C, as read from standard table (B-3). In subsequent use of the copper-constantan couple, 0.37°C was deducted from its indicated temperatures. With this correction, the temperature in the autoclave measured by the copper-constantan thermocouple never

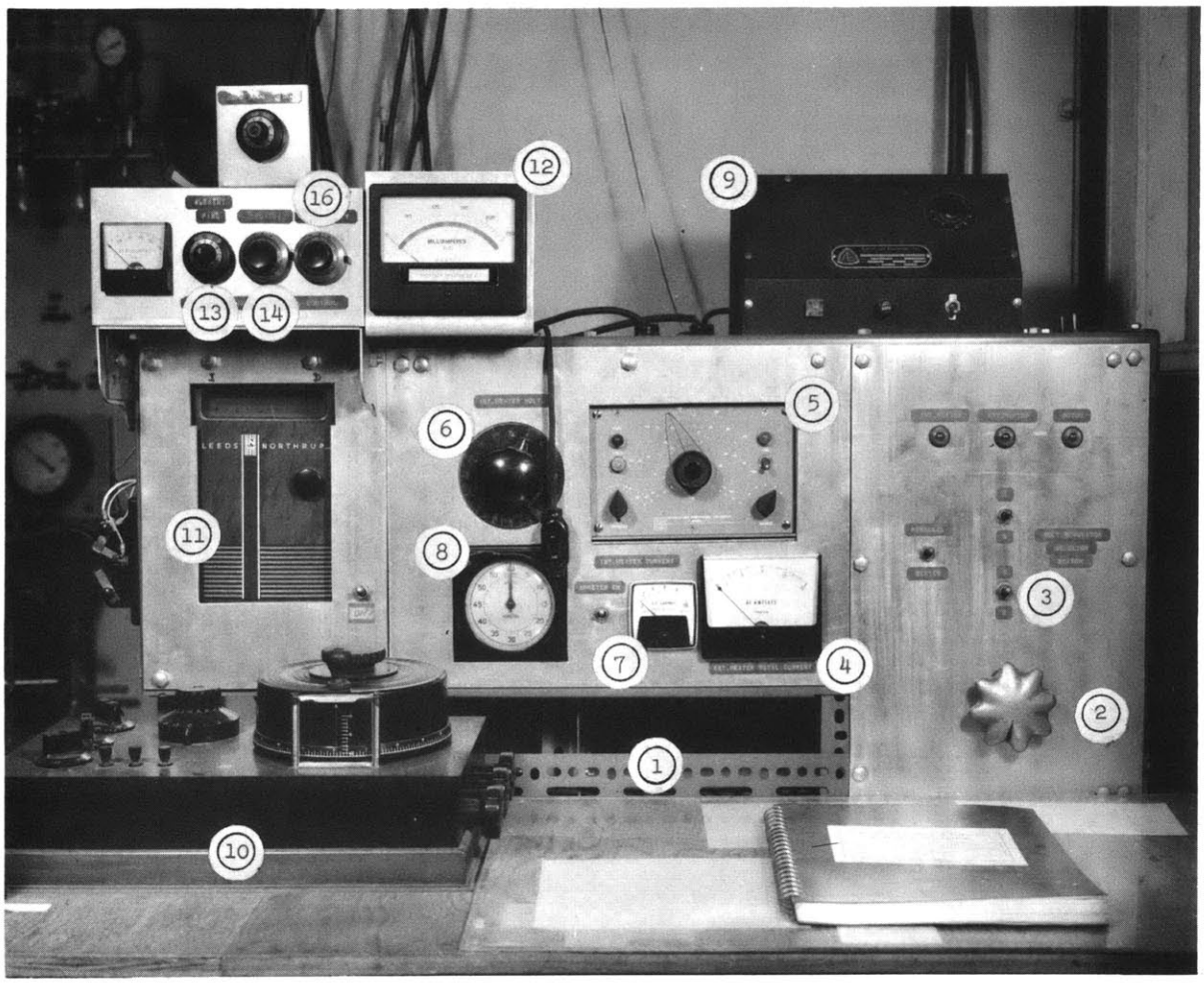

Fig. B-8 Control Board

1. Induction voltage regulator for external heater
2. Knob for controlling the regulator for external heater
3. Selector switches for external heater system
4. AC-Ammeter for total current on external heaters
5. Temperature controlling unit
6. Variac regulator for internal heaters
7. AC-Ammeter for internal heater
8. Timer
9. Controlling unit for autoclave stirrer
10. Precision potentiometer
11. Galvanometer
12. DC-Milliammeter for thermal conductivity bridge
13. Fine control dial for T/C bridge current
14. Coarse zero adjustment dial for T/C bridge
15. Fine zero adjustment dial for T/C bridge
16. Sensitivity dial for T/C bridge

deviated from the bath temperature measured by the iron-constantan thermocouple by more than 0.2°C.

C. Design and Construction of Systems for Handling Superatmospheric Gases

The following systems were required to handle pressures up to about 100 atmospheres:

i) The autoclave, in which the reaction between hydrogen gas and water was carried out under total pressures up to about 90 atmospheres.

ii) The hydrogen-charging system, which was used to charge hydrogen gas from a commercially available hydrogen tank into the autoclave when in position and kept at a reaction temperature in the constant temperature oil bath, to a total pressure of about 90 atmospheres.

iii) The sampling system, through which small portions of the gaseous phase of the reacting mixture was taken while the reaction was in progress.

The following systems were required to handle somewhat lower superatmospheric pressures:

i) The liquid-charging system, which was used to charge degassed amine solution into the autoclave when in its position and kept at reaction temperature in the constant temperature oil bath, and was required to handle pressures of water and amine vapors at the reaction temperature.

ii) The discharging system, which was used to discharge residual contents from the autoclave after a run was over.

Design and construction of these systems are presented in this section.

Material used for construction of these systems was stainless steel of either Type 316 or Type 304, unless stated otherwise. Both types have good resistance to alkaline corrosion. The high-pressure connection used was a type called Ermeto, which was obtained from Autoclave Engineers, Erie, Pennsylvania.

Tubing used to connect various units together was made of stainless steel Type 304, seamless and annealed. Two sizes were used. One was 1/8 inch in outside diameter and 1/16 inch in inside diameter, and the other was 1/4 inch in outside diameter and 1/8 inch in inside diameter. Both were rated for service up to a pressure of 12,000 pounds per square inch.

Valves used were needle valves supplied by Autoclave Engineers, Inc. Two sizes were used, one for 1/8-inch tubings, and the other for 1/4-inch tubings. Valves of both sizes were equipped with Ermeto connections. They were made of stainless steel Type 316. Packing around the stem was made of teflon.

The flowsheet of the systems to handle superatmospheric gas is presented in Fig. C-1.

C-1. Autoclave

The auotclave used was a product of Autoclave Engineers, Inc. Its drawing is shown in Fig. C-2. It was made of stainless steel Type 316, was designed for a maximum working pressure of 5,000 pounds per square inch at 650°F and was hydrostatically tested for pressures up to 8,260 pounds per square inch at

72°F at the factory.

The internal volume of its body, without various service lines inserted, was claimed by the manufacturer to be one liter. A measurement of the internal volume with the service lines inserted, plus internal volumes of tubings connected to the autoclave up to confining valves, was later carried out at room temperature as follows. The autoclave was evacuated, and with all valves around the autoclave closed, a hydrogen-charging vessel (see Section C-2 of APPENDIX) was filled with hydrogen gas to a pressure of 1,500 pounds per square inch. After the temperature of hydrogen gas in the charging vessel settled, a valve HV-2, which separated the autoclave and the charging vessel, was opened. The pressure of the entire system was read after it reached a steady value. The gauge used to read pressures was accurate to $\pm$ 5 pounds per square inch. Using a known internal volume of the hydrogen-charging vessel and the ideal gas law, the internal volume of the autoclave and tube lines directly connected to it was found to be 1001 $\pm$ 11 milliliters.

The autoclave featured a reciprocating agitator which moved up and down along the vertical axis. This provided a means of agitation without a stuffing box. The dasher was actuated by two solenoids mounted one on top of the other and around a solenoid supporting tube, inside which a magnetic core bar assembly was placed. The bar was connected with the dasher. The solenoids were cooled with water running through a blanket around the housing. The section of the

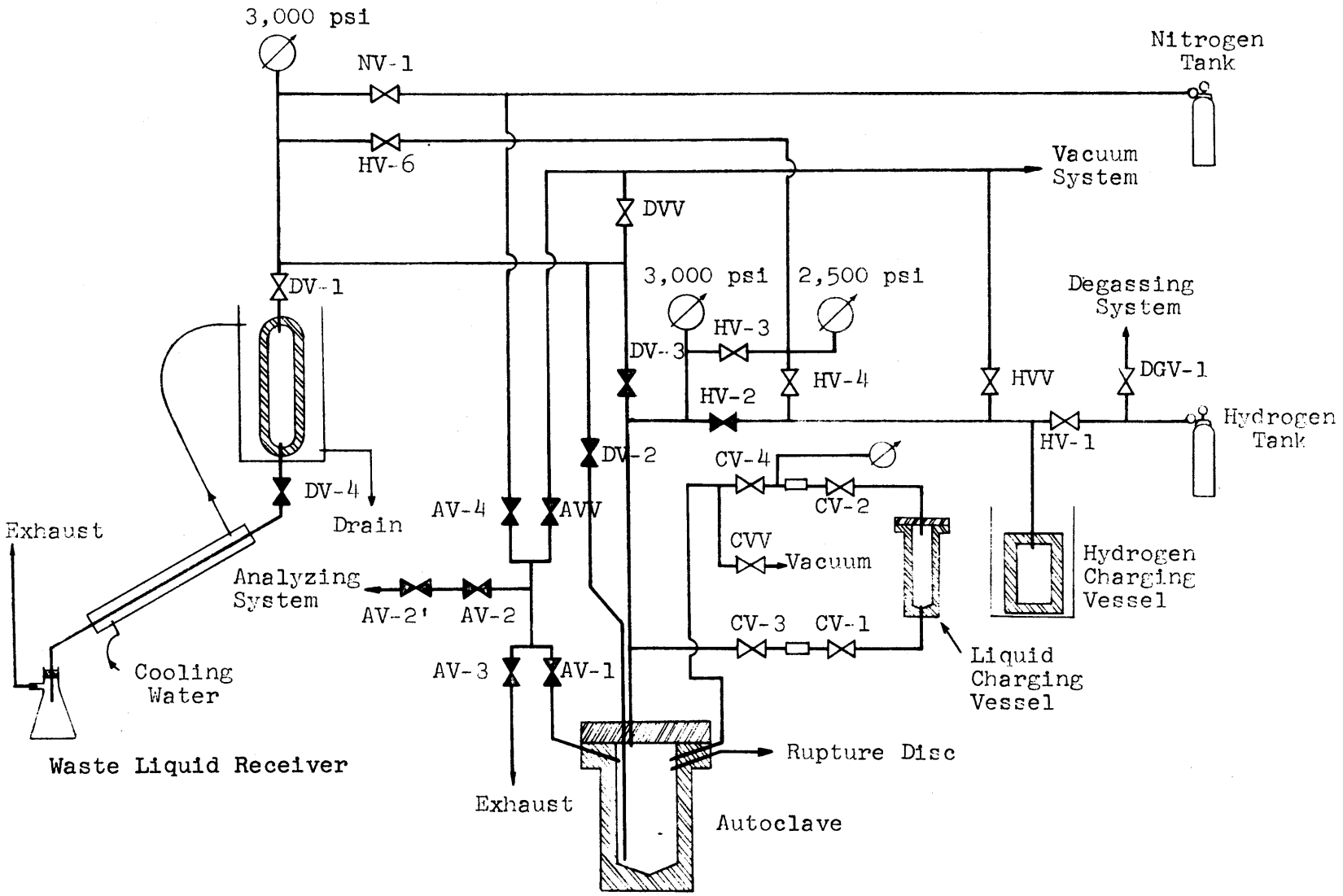

Fig. C-1. Flow Diagram of Systems for Handling Superatmospheric Gases

Fig. C-2 Autoclave
(Courtesy of Autoclave Engineers Inc., Erie, Pa.)

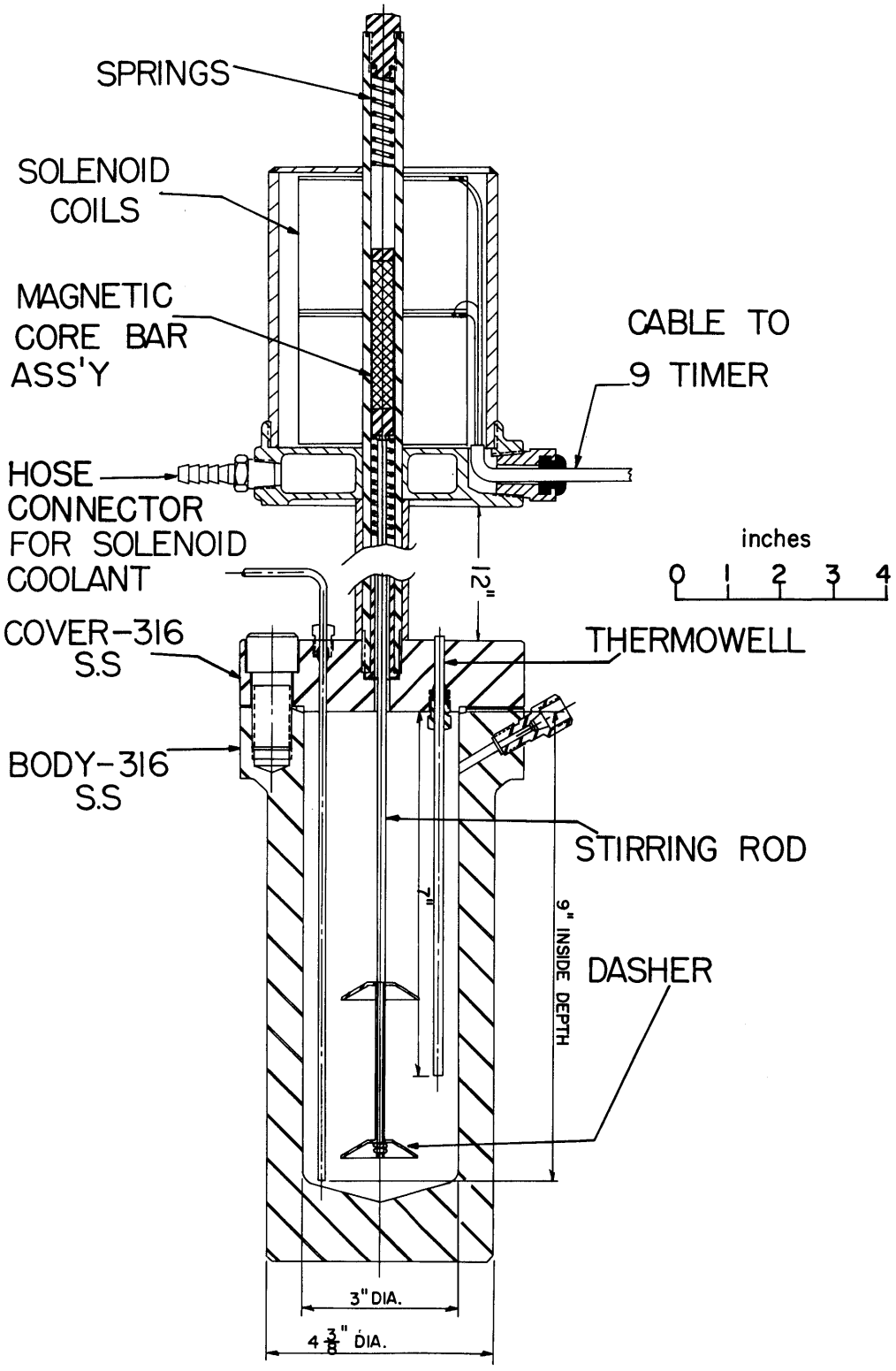

solenoid and housing supports between the bottom end of the housing and top of the cover had to be lengthened from the original 2 1/2 inches to 1 foot. The modification made it possible to keep the solenoids well above the hot oil bath. To provide additional strength to the lengthened solenoid support, the solenoid housing was clamped radially with an aluminum ring clamp which is shown in the photograph, Fig. C-3.

Three service openings were provided in the top cover. One of them was a thermocouple well which extended 7 inches down from the inner surface of the cover. A copper-constantan thermocouple placed there was used to check for temperature changes during the reaction. Another one was an opening for 1/8-inch tubing, which extended down to the bottom of the body and was used to force out, by hydrogen pressure in the autoclave, most of the liquid remaining in the vessel after a run was over. When not in use, a needle valve attached to this line, DV-2, was closed. The third opening was used for connecting a 1/4-inch drainline of the liquid-charging system (See Section C-2 of APPENDIX), as well as for connecting 1/8-inch lines for charging and discharging hydrogen gas.

Three 1/8-inch service openings were provided near the top of the body of the autoclave. They were each used for a vent-line of the liquid-charging system, for a sampling line and a rupture disc assembly. The rupture disc was rated for 3,000 pounds per square inch at 72°F. The assembly was placed outside of the oil bath, and a straight duct leading outdoors was provided on the downstream side of the disc.

C-2. Charging Systems

Charging systems were designed to charge measured amounts of reactants into the autoclave while it was kept in the oil bath at the reaction temperature. There were two charging systems. The liquid-charging system was used to charge a solution of diethylamine in partially enriched heavy water. The hydrogen-charging system was used to charge hydrogen gas.

(a) Liquid-Charging System

The liquid-charging system consisted of a liquid-charging vessel, a Bourdon gauge, five needle valves, CV1, CV2, CV3, CV4 and CVV, and two reusable couplings.

The vessel was required to handle pressures up to about 70 pounds per square inch but, actually, it was designed for pressures up to 1,500 pounds per square inch for safety. The material used had to be resistant to corrosion due to diethylamine in water at temperatures up to 200°C. The system had to be vacuum-tight. The system also had to be able to deliver liquid from the charging vessel into the autoclave solely by gravity.

The liquid-charging vessel was made of steel, with a top cover bolted on the body with eight bolts. Drawings are shown in Figs. C-4-(a) and (b). A picture of the assembled unit is shown in Fig. C-4-(c), which also shows valves CV-1 and CV-2 and parts of the couplings. It was designed for a working pressure of 1,500 pounds per square inch and was hydrostatically tested for pressures up to 2,000 pounds per square inch. Its internal volume was about 500 milliliters. Between the body and the cover was placed a gasket manufactured

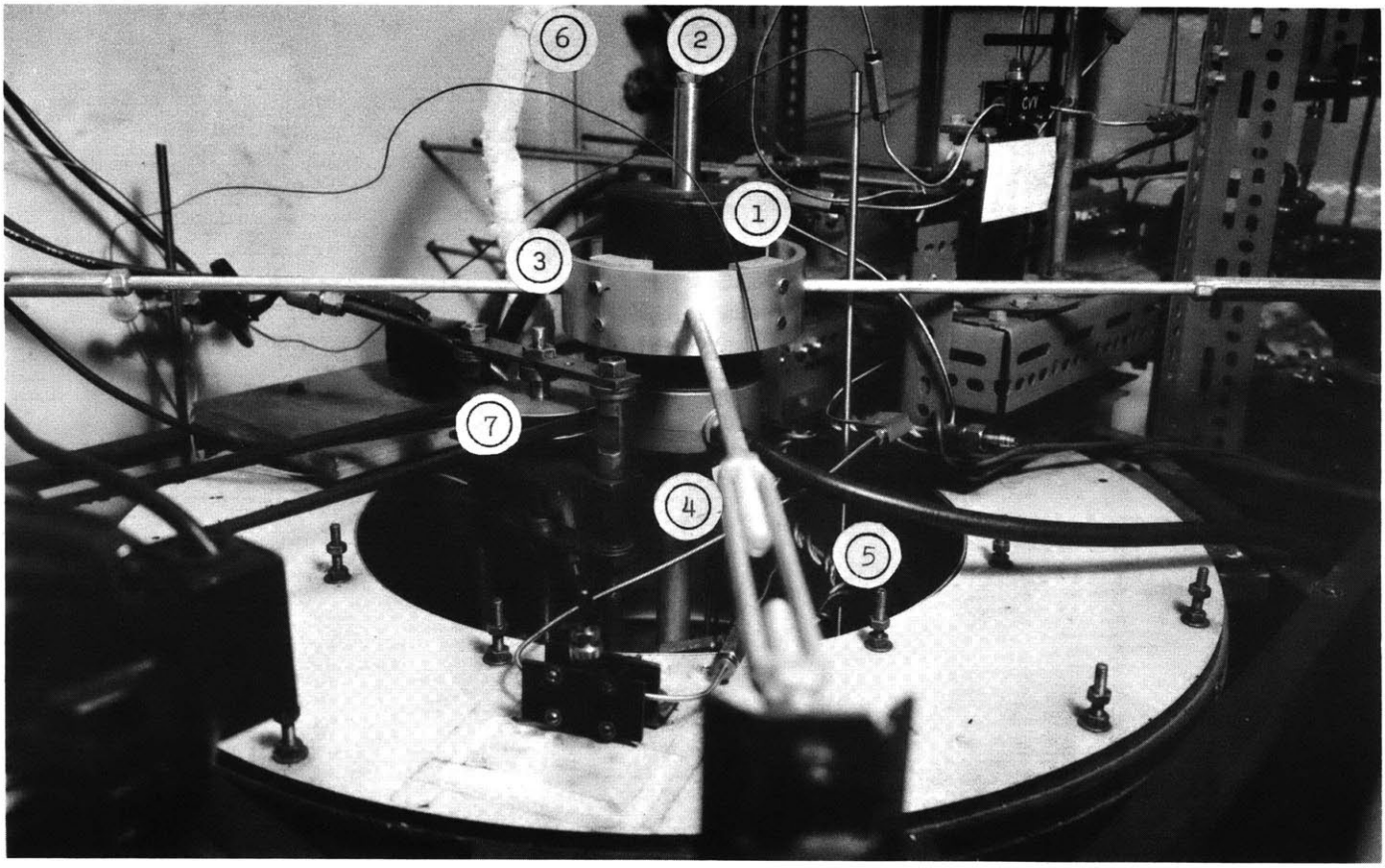

Fig. C-3 Superstructure of Autoclave and Constant Temperature Bath

1. Solenoid-housing
2. Dasher-enclosure
3. Clamp for solenoid-housing
4. Support for solenoid-housing
5. Drain-line of liquid-charging system
6. Ventillation-line of liquid-charging system
7. Pulley for stirring mechanism of oil bath

(a) COVER

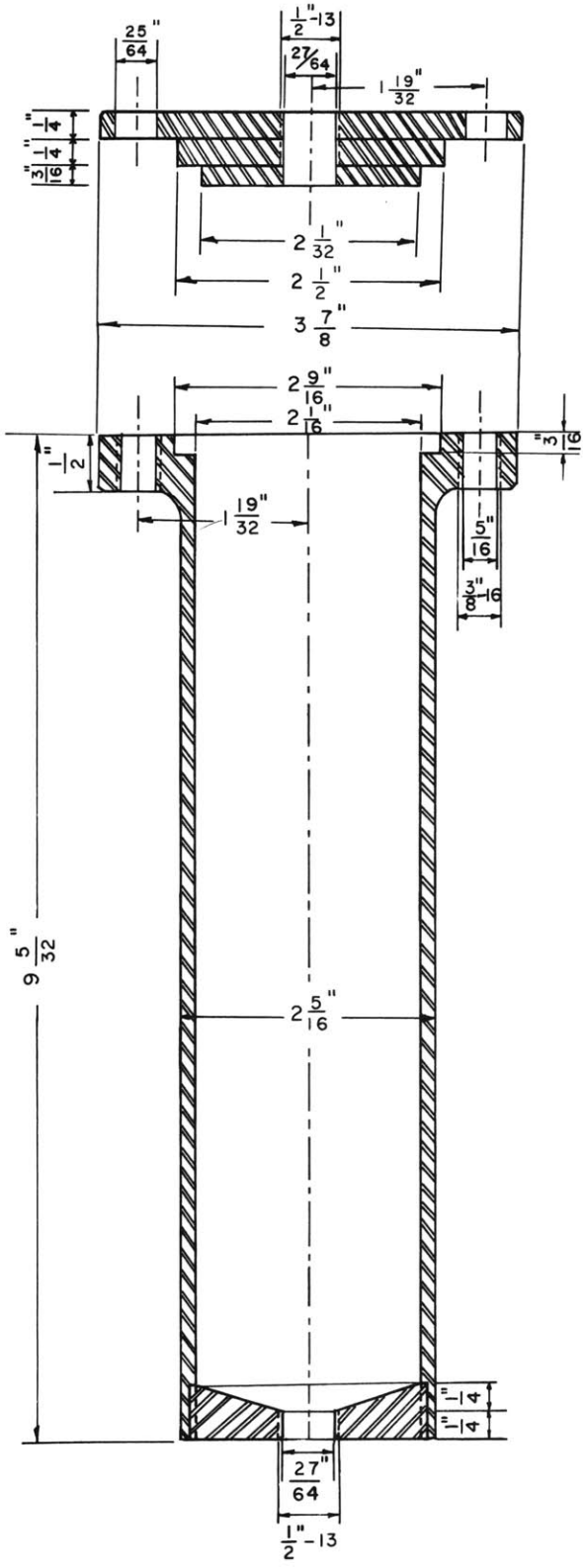

(b) BODY

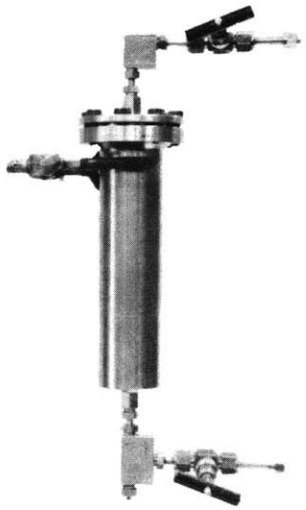

(c) ASSEMBLED UNIT

Fig. c-4 Liquid-Charging Vessel

by Flexitallic Gasket Company, Camden, New Jersey. This gasket was made by spirally winding a thin band of Type 304 stainless steel with Canadian asbestos filler between each round of the metal. The one used was designed for use with an American Standard small-tongue-and groove flange for a nominal pipe size of two inches, rated for a service pressure of 2,500 pounds per square inch. Both inside and outside surfaces of the vessel were plated with nickel to a thickness of five thousands of an inch.

A drain line which connected the bottom of the vessel with the autoclave through valves CV-1 and CV-3 was made of the heavy 1/4-inch stainless steel tubing. This line was cooled with water running through 1/4-inch copper tubing coiled around the stainless steel tubing and silver-soldered to it. This cooling kept the amine solution in the drain line from boiling and, consequently, maintained the driving force needed to drain the solution from the charging vessel drain with a reasonably high rate. The vent line which connected the top cover of the charging vessel with the autoclave through valves CV-2 and CV-4, was made of heavy 1/8-inch stainless steel tubing. This line was covered with a glass-wool blanket to keep vapor from condensing in the line.

A small, compound Bourdon gauge was attached to the vent line between CV-2 and CV-4 to roughly check the pressure of the charging system just before and during the liquid-charging operations, which ranged from vacuum to about 70 pounds per square inch. The gauge could read pressures from vacuum to

150 pounds per square inch. Because the charging of the solution was done before charging hydrogen gas and because the valves CV-2 and CV-4 were to be closed after the liquid had been charged, the gauge was never exposed to higher pressures.

(b) Hydrogen-Charging System

The hydrogen-charging system consisted of a tank of "prepurified" hydrogen with a pressure regulator, a hydrogen-charging vessel, four needle valves, HV-1 through HV-4, and two Bourdon pressure gauges. Its purpose was to charge a known amount of hydrogen gas from a commercial hydrogen tank into the autoclave to a desired pressure of about 1,000 pounds per square inch. The hydrogen-charging vessel was required to be able to handle hydrogen pressures up to about 1,500 pounds per square inch. The pressure gauges were required to be resistant to alkaline corrosion. One of them had to be accurate enough to measure the absolute pressures within about $\pm$ 5 pounds per square inch, which meant that, since the total pressure of the autoclave system was never below 500 pounds per square inch, the accuracy of the pressure readings was to be better than one percent of the readings.

"Prepurified"-grade hydrogen, which was commercially available and came in a tank at a pressure of about 2,200 pounds per square inch, was used after the gas was checked for chemical impurities by procedures described in APPENDIX G. The tank was fitted with a tank-pressure regulator which was designed for service with hydrogen gas and for tank

pressures up to 3,000 pounds per square inch and for delivery pressures up to 2,000 pounds per square inch.

The hydrogen-charging tank was a cylindrical tank made of a mild steel with one opening on top, shown in Fig. C-5. It was designed for service pressures up to 3,000 pounds per square inch and was hydrostatically tested for pressures up to 3,500 pounds per square inch. Dimensions of the design were especially closely followed in machining the vessel so that its internal volume could be calculated from them. It was 502.0 $\pm$ 1.2 milliliters. On the top opening an Ermeto adapter was screwed in and welded on the outside surface.

A standard Bourdon gauge, manufactured by Heise Bourdon Tube Company, Newtown, Connecticut, was used to accurately measure pressures in the hydrogen-charging vessel during the process of hydrogen-charging. This was later used to accurately measure the total pressures of the system in the autoclave during the reacting periods. It had a dial whose diameter measured 8 1/2 inches and which was graduated, in intervals of 5 pounds per square inch, from 0 to 2,500 pounds per square inch. The manufacturer claimed that the gauge was accurate to $\pm$ 2.5 pounds per square inch.

Another Bourdon gauge, which ranged from 0 to 2,000 pounds per square inch but was less accurate, was used to read roughly the total pressure of the autoclave system while hydrogen was being charged from the charging vessel. This was necessary because a definite pressure difference had to be maintained across valve HV-2 while hydrogen gas was being

charged to prevent any back-flow of the contents of the autoclave during the process.

Lines of the hydrogen-charging system were constructed of 1/8-inch stainless steel tubing. Valve HV-1 was used to charge hydrogen gas from the hydrogen tank to the hydrogen-charging vessel. This valve was closed every time before valve HV-2 was opened. Valve HV-2 was used to charge hydrogen gas from the charging vessel to the autoclave. Valve HV-3 was closed and valve HV-4 was opened while hydrogen gas was being charged. The valve HV-3 was opened and valve HV-4 was closed after the charging was over, and they remained so throughout the rest of the run.

C-3. Discharging System

The discharging system was used to safely discharge the contents of the autoclave after a run was over without removing the autoclave from its seat in the oil bath.

The system consisted of two 1/8-inch tubings each connected with the autoclave through needle valves DV-2 and DV-3, a 3,000 milliliter cylindrical tank with a needle valve on each end and a cooling jacket around it, a steel condenser of Liebig type cooled with running water, a receiving flask, and an exhaust gas line.

The 1/8-inch line connected to the autoclave through valve DV-2 went down to the inside bottom of the autoclave and was used to force out most of the liquid content of the autoclave utilizing the high pressure of gas and vapors which occupied the upper space of the autoclave. The line connected

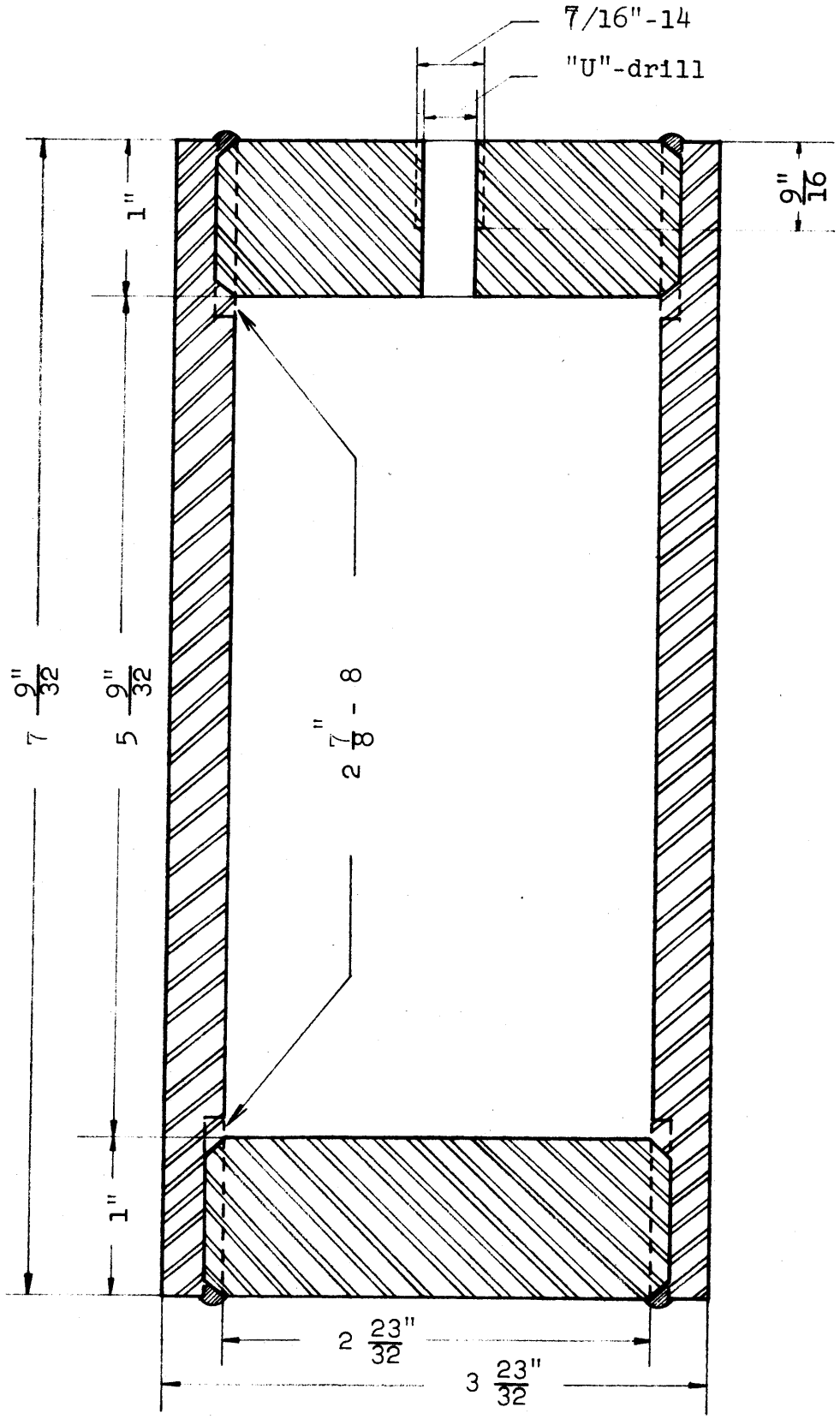

Fig. C-5. Hydrogen-Charging Vessel

through a valve DV-2 was used to distil out the remaining contents as well as to finally flush the autoclave with a stream of nitrogen gas.

The 3000 milliliter cylindrical, stainless steel tank in the discharge line was designed for service pressure of 1,800 pounds per square inch and was a product of Hoke Incorporated, Cresskill, New Jersey. Another steel cylinder was put on the tank and was used as a cooling jacket. The tank thus served both as a pre-cooler of vapors coming out of the autoclave and as a damper for any pressure surge which might happen in case of maloperation of the valves.

The steel condenser was made of mild steel pipes. The inner pipe was 1/2 inch in outside diameter and 5/16 inch in inside diameter. The outer pipe was 1 1/4 inches in outside diameter. Two pipes were welded at each end to an annular steel disc. The cooled length was 15 inches.

An Erlenmeyer flask with a side tube, made of Pyrex glass, was used as receiver for condensed liquid. Uncondensable hydrogen gas was discharged through the side tube, which was connected with a thin-walled rubber tubing to an exhaust line which, in turn, led the gas outdoors. The exhaust line was constructed of hard copper tubing 1/2 inch in outside diameter. In case of a very strong pressure surge which could not be dampened by the 3,000 milliliter tank, the connecting rubber tubing would have been blown off before the glass flask gave way, although such a surge never happened during the present investigation.

C-4. Sampling System

The sampling system was used to safely take a sample of gas phase from the autoclave and deliver it to gas purification equipment in the gas analyzing system. It consisted of a manifold constructed of 1/8-inch tubing and six needle valves AV-1, AV-2, AV-2', AV-3, AV-4 and AVV.

Valve AV-1, which connected the auotclave with the manifold, was placed as close to the autoclave as possible to minimize the amount of reacting materials trapped in the line between autoclave and valve. Two valves, AV-2 and AV-2', were placed in series mainly to protect the analyzing system, which was mostly constructed of glass, against any mal-operation or failure of the valve AV-1. Valve AV-3 was used as an outlet for nitrogen which came in through a valve AV-4 and was used for flushing the manifold. Valve AVV was used to evacuate the manifold after it was flushed. The internal volume of the manifold, as calculated from the cross-sectional area and the total length of the tubing used for the manifold, was about 4 milliliters.

D. Design and Construction of Systems for Handling Subatmospheric Gases

The three systems required to handle gases below atmospheric pressure were the following:

i) The degassing system, which was used to degas the amine solution before charging it into the autoclave.

ii) The analyzing system, which was used to purify the sample gas delivered by the sampling system, to store it while other samples were being analyzed, and to analyze it for its deuterium content by means of the thermal conductivity bridge method.

iii) The chemical gas analysis system, which was used to check the commercially available, bottled hydrogen gas for chemical impurities.

Requirements on the degree of vacuum for each system are discussed in the first section which follows.

Unless stated otherwise, Pyrex-brand glass was used for these systems, and necessary detachable connections were made by means of either standard tapered joints or standard ball-and-socket joints. Use of organic material was avoided on joints which would come in contact with the sample gas before it was analyzed. Where conditions permitted, thick-walled red rubber hoses for use with high vacuum or thick-walled Tygon tubing was used to connect two separate parts. The rubber hose connections were clamped with hose clamps and painted with red glyptal lacquer. The Tygon tubing connections were

painted with red glyptal.

D-1. Pumping Systems

Pumping systems were used to evacuate all systems including those for handling subatmospheric gases as well as for handling superatmospheric gases.

The vacuum requirements for various systems originated in one necessary condition to be fulfilled, that an amount of air present in the systems should not interfere with the analysis of hydrogen gas for its deuterium content. To develop the necessary condition, the following relation was derived.

If p_o and p_a represent partial pressures of H_2 and air, respectively, in millimeters of mercury in a gas sample which was being analyzed, and if κ_o and κ_a represent thermal conductivities of H_2 and air, respectively, in the same gas at the average temperature of the gas in the thermal conductivity cell, then the average thermal conductivity $\overline{\kappa}_a$ of such gas mixtures would be given by

$$\overline{\kappa}_a = \kappa_o \frac{p_o}{p_o + p_a} + \kappa_a \frac{p_a}{p_o + p_a}$$

and the change in the thermal conductivity due to the presence of air would be

$$\Delta\kappa_a \equiv \kappa_o - \overline{\kappa}_a = (\kappa_o - \kappa_a) \frac{p_a}{p_o + p_a} \qquad \text{(D-1)}$$

Similarly, the change in the thermal conductivity, $\Delta\kappa_o'$, due to a presence of D_2 in H_2 with partial pressures, p_o' and p_o, respectively, in a sample gas would be given by

$$\Delta\kappa_o' \equiv \kappa_o - \overline{\kappa}_o' = (\kappa_o - \kappa_o') \frac{p'_o}{p_o + p_o'} \qquad \text{(D-2)}$$

where $\overline{\kappa'_o}$ and κ'_o are the average thermal conductivity of such gaseous mixture and the thermal conductivity of pure D_2, respectively, at the average temperature of the gas in the cell.

The maximum allowable partial pressure of air, p_a, was determined from the condition that it have the same effect on the thermal conductivity of hydrogen as 0.00005 mole fraction D_2, that is

$$\frac{p'_o}{p_o + p'_o} = 0.00005 \qquad \text{(D-3)}$$

At the condition

$$\Delta\kappa_a = \Delta\kappa_o \ , \qquad \text{(D-4)}$$

$$p_a = \frac{\kappa_o - \kappa'_o}{\kappa_o - \kappa_a} \frac{p_o + p_a}{p_o + p'_o} p'_o \qquad \text{(D-5)}$$

as may be seen from Eqs. (D-1), (D-2) and (D-3). The values of these thermal conductivities at 100°C are

$$H_2 : \ \kappa_o = 54.7 \times 10^{-5} \text{ cal/cm.sec.}^\circ\text{C}$$
$$D_2 : \ \kappa'_o = 37.7 \times 10^{-5} \text{ cal/cm.sec.}^\circ\text{C}$$
$$\text{air:} \ \kappa_a = 7.4 \times 10^{-5} \text{ cal/cm.sec.}^\circ\text{C}$$

Hence, from Eqs. (D-3) and (D-5),

$$p_a = 18 \times 10^{-6} \ (p_o + p_a). \qquad \text{(D-6)}$$

As the thermal conductivity of a mixture of H_2 and D_2 would be lowered when equilibrium amounts of HD are formed, (D-1, D-2), this equation was expected to lead to a conservative value of p_a for the equilibrated mixtures of H_2, D_2 and HD

met in this work.

The maximum allowable partial pressures of air, p_a, calculated from this equation for different parts of the apparatus where the total pressure $p_o + p_a$ is stated below are the following:

Unit	Pressure, mm Hg	
	Total, $p_o + p_a$	Max. air, p_a
Analyzing system	50	9×10^{-4}
Purification and Storage systems	380	7×10^{-3}
High pressure systems	6×10^{4}	1.1

For the degassing systems, air dissolved in the amine solution would be released in the autoclave. The partial pressure of the air thus carried into the autocalve had to be less than 1.1 mmHg. To be conservative, a limit of 10^{-1} mmHg was taken, and it was assumed that all hydrogen gas contained in the solution would be discharged into the vapor phase in the autoclave, the volume of which was about 500 milliliters. Then the total number of grammoles of air carried in this way would be

$$\frac{(10^{-1}\ \text{mmHg})\ (500\ \text{ml})}{(760)\ (82)\ (500^{\circ}\text{K})} = 1.6 \times 10^{-6}\ \text{gmoles.} \qquad \text{(D-7)}$$

This amount was to be contained in about 500 grams of aqueous solution consisting of about 25 grammoles. Therefore, the mole

fraction of air dissolved in the "degassed" solution had to be smaller than

$$\frac{1.6 \times 10^{-6}}{25} = 6.4 \times 10^{-8} \qquad \text{(D-8)}$$

Since Henry's law constant for the air in water at a temperature of $10^{o}C$, the temperature of the final stage of the degassing process, was 4.4×10^{7} mmHg per mole fraction H_2 in water, the pressure of air in the space above the solution which was being degassed would have to be lower than

$$p_a = (4.4 \times 10^{7})\ (6.4 \times 10^{-8})$$
$$= 2.8 \text{ mmHg} \qquad \text{(D-9)}$$

To estimate the vacuum requirement for the chemical gas analysis system, a knowledge of how the system worked is necessary. (See Sections D-4 and F-10 for details.) A known amount of sample gas is passed through a train of chemical reactors which is to remove hydrogen gas, and the total amount of impurities is measured by collecting the residual gas into a known, small volume and measuring its pressure. The known, small volume is 2.4 milliliter and the pressure is measured with a mercury U-tube manometer. The total internal volume of the entire system is estimated to be about 350 milliliters. Any air remaining in the system before putting the sample gas into the system would show up as a part of the impurity. Therefore, it was demanded that the initial vacuum be such as would give a final pressure smaller than 0.5 mmHg.

Such vacuum is

$$p_a = \frac{(2.4\ \text{ml}) \times (0.5\ \text{mmHg})}{350\ \text{ml}}$$

$$= 3.5 \times 10^{-3}\ \text{mmHg} \qquad \text{(D-10)}$$

Thus, the strictest vacuum requirement was 3.5×10^{-3}mm for the analyzing system. Such vacuum could be easily achieved by a rotary pump alone.

Two rotary pumps were available for the present work. Both were distributed by Central Scientific Company, Chicago, Illinois. One was their Model HYVAC-7 which was guaranteed for a vacuum of 0.1×10^{-3} mm of mercury. The other one was their Model PRESSOVAC which was guaranteed for a vacuum of 15×10^{-3} mm of mercury.

Utilizing these pumps, two separate pumping systems were constructed. One which used the PRESSOVAC pump, called Pumping System No. 1, was mainly used for evacuating the degassing system, the chemical gas analysis system and the analyzing system. The other one which used the HYVAC-7 pump, called Pumping System No. 2, was mainly used for evacuating the high-pressure systems but could also be used for evacuation of the analyzing system. To reduce the residual pressure of air in the analyzing system below the required 3.5×10^{-3} mmHg with a pump which could produce a vacuum of only 15×10^{-3} mmHg, the analyzing systems were evacuated, flushed with natural hydrogen at a pressure over 10 mmHg, and then evacuated again. This flushing procedure

brought the amount of residual air below the required level.

Flow-diagrams of these pumping systems are shown in Figs. D-1 and D-2. The discharge gauge, PG-1, manufactured by Consolidated Electrodynamics Corporation, Rochester, New York, had three pressure ranges, with a lowest value of 1×10^{-7} mmHg. Lines of these pumping systems were 1/2 inch in inside diameter.

D-2. Degassing System

Flowsheet of the degassing system is shown in Fig. D-3.

The degassing system consisted of three sections. They were a section used to evacuate the system and degas the solution, a section which supplied hydrogen gas at atmospheric pressure, and a section used to transfer the degassed solution from the degassing flask to the liquid-charging vessel.

The degassing section consisted of the following components.

i) A three-necked, round-bottom flask of one liter capacity. All of three necks are standard tapered joints 24/40. This flask was used to contain amine solution to be degassed.

ii) An Allihn condenser, equipped with 24/40 standard tapered joint on each end, with a jacket length of about 40 centimeters. It was used to reflux water and amine vapor.

iii) A liquid nitrogen trap, TDG-1, with a detachable neck having a 40/50 standard joint. It was used to trap any condensable vapors before they reached manometer MM-DG.

iv) A mercury manometer, MM-DG. It consisted of a body tube, about 2.5 centimeters in diameter and 23.5 centimeters in length and an inner tube. The top of the body tube had a

standard taper grinding for the inner tube with a stopper tip. The inner tube had a small hole at its tip through which mercury moved in and out. The ground joint on the inner tube had a narrow trench up to the middle of the length of the taper, on which height an orifice was bored on the side of the outer tube. This device made the use of the manometer extremely fool-proof since it minimized dangers caused by mercury rushing in either direction. The body was graduated from 0 at the bottom to 160 millimeters at the top in 1 millimeter divisions. Pressure was read as a difference of the heights of the inner and outer mercury columns. To read the inner column properly, a level-aligning device was slipped on the outer tube. This manometer was used to measure a residual pressure of the system by closing a stopcock PS-4 once a minute. The system being evacuated was kept for 5 minutes after the manometer showed a pressure less than 1 millimeter of mercury, and then it was presumed that the solution had been degassed sufficiently. Stopcocks DGS-1 and DGS-2 were used to control flow of vapors.

The hydrogen-delivering section was used to supply hydrogen gas at pressures of 0.5 to 1 psig into the degassing flask. The hydrogen pressure was used to transfer the solution into the liquid-charging vessel connected to the right-hand neck of the flask. The pressure regulator PR-DG in the hydrogen delivering section was a product of Hoke, Inc., Cresskill, New Jersey, and was a purely mechanical device. Its delivery pressure could be controlled either by changing its main springs or by adjusting a screw which pushed in or out the selected main

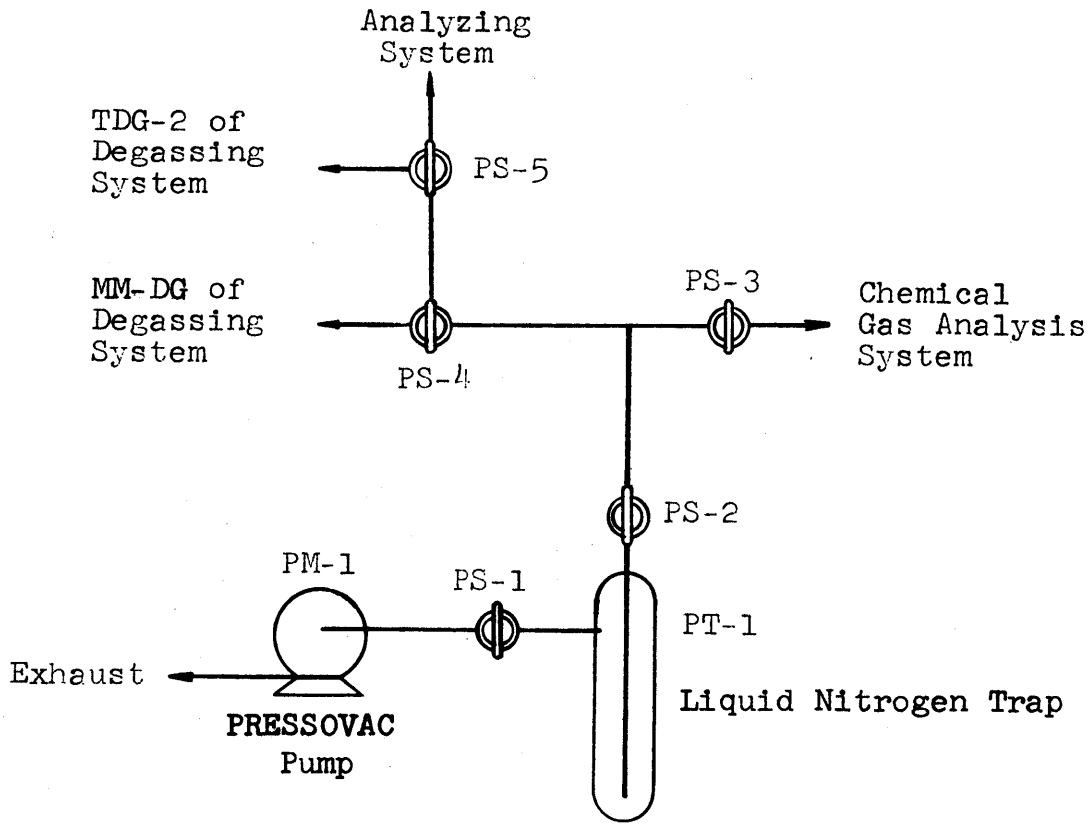

Fig. D-1. Flow Diagram of Pumping System No. 1

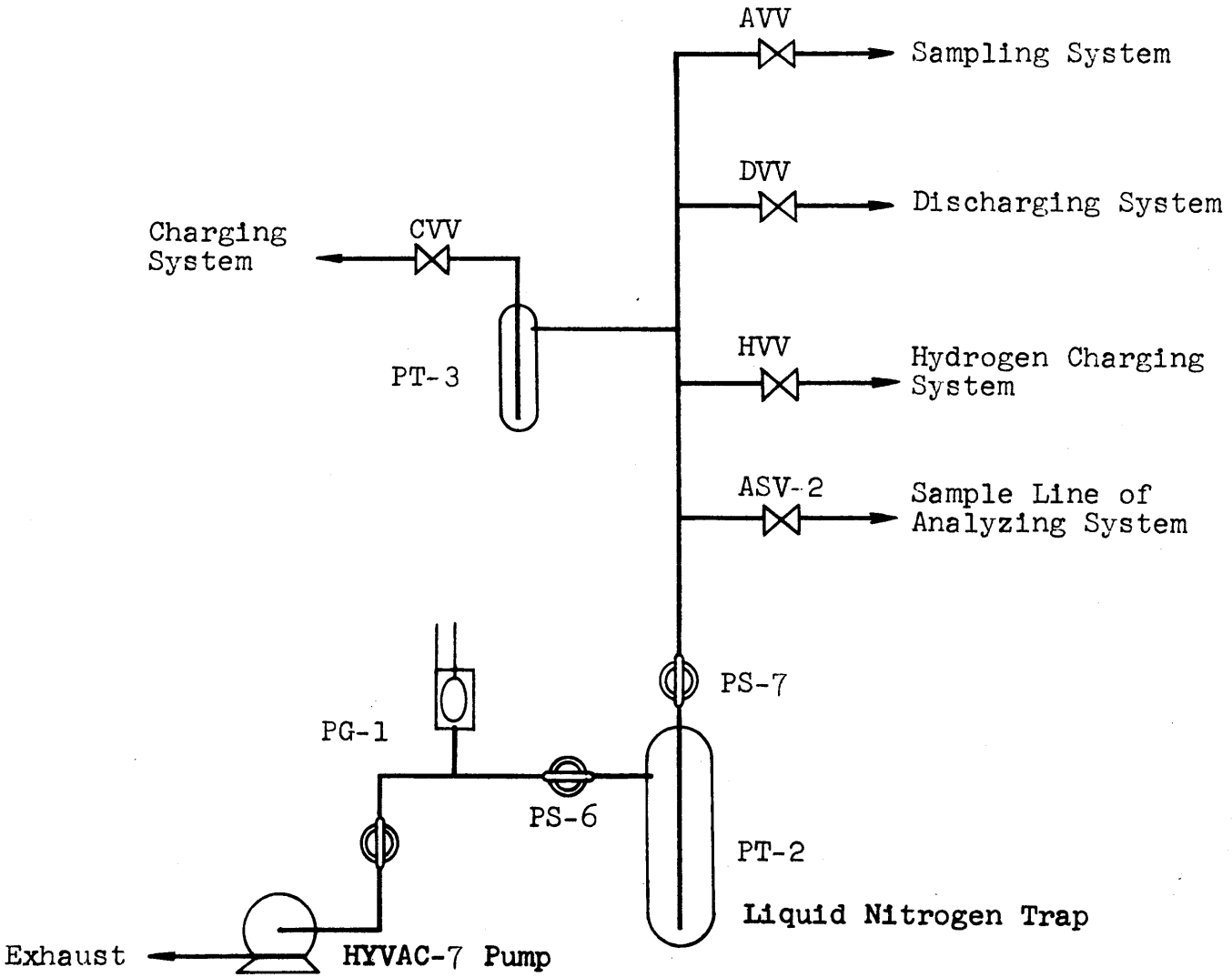

Fig. D-2. Flow Diagram of Pumping System No. 2

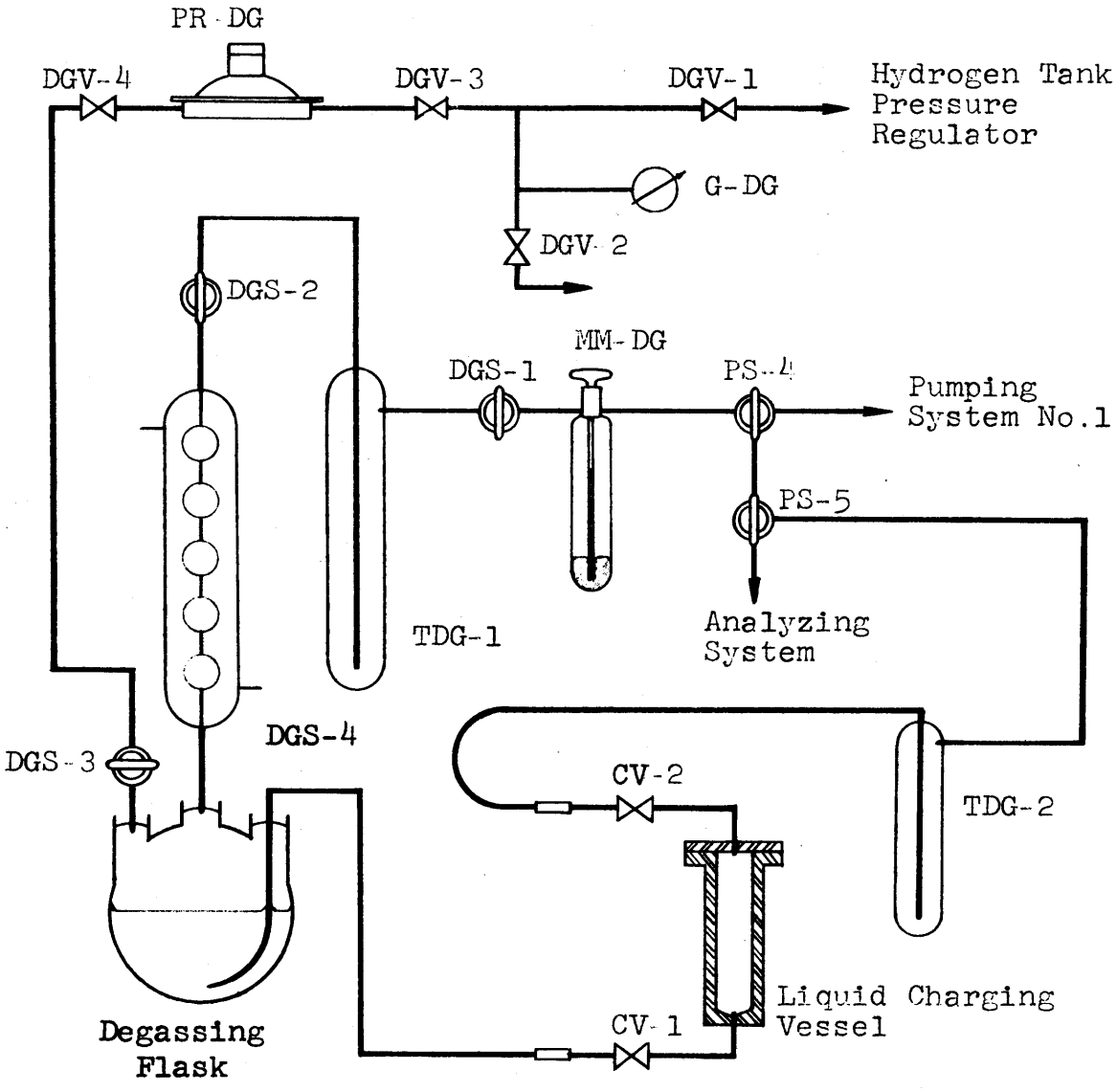

Fig. D-3. Flow Diagram of Degassing System

spring. Its maximum inlet pressure was 250 pounds per square inch. The valves DGV-1, -2, -3, and -4 were used to control pressures as well as the flow of hydrogen gas.

The transfer section consisted of glass tubing fitted on a neck of the flask with its tip extending down to the bottom of the flask, a couple of reusable couplings and a liquid nitrogen trap TDG-2. The couplings were the counterparts of the parts attached adjacent to valves CV-1 and CV-2 of the liquid charging system (Fig. C-1).

D-3. Analyzing System

The analyzing system consisted of two major lines, a reference gas line and a sample gas line. The reference line was used to deliver hydrogen gas of natural isotopic compositions from a tank of "prepurified"-grade hydrogen into the thermal conductivity cell, T/C-cell. The sample line was used to purify the sample gas delivered by the sampling system, to store it while other samples were being analyzed, and to analyze it for its deuterium content by means of the thermal conductivity bridge method. The flow diagram for both lines is shown in Fig. D-4, in which units of the reference line are indicated by letter R while those of the sample line are indicated by letter S.

For convenience of description, the analyzing system is divided into sections and described in turn in the following subheadings of this subsection.

(a) Principle of Analyzing System

The analyzing section consisted of the thermal conductivity

cell, T/C-cell, and adjacent stopcocks, AR-TC1, AR-TC2, AS-TC1 and AS-TC2. The thermal conductivity cell used in this work is shown schematically in Fig. D-5, in plan view at the top of the figure and in vertical section at the bottom. It was modified from a commercial unit purchased from the Gow Mac Instrument Company of Madison, New Jersey, and was designated the "Pretzel" type by the manufacturer, because of the layout of its internal connections.

The cell consisted of a stainless-steel block containing two identical sets of passages, one for the sample gas mixture to be analyzed, the other for a reference gas. Each set of passages contained two nearly identical tungsten filaments, which were connected in the opposite arms of a Wheatstone bridge as shown in Fig. D-6. There the resistances of the two filaments in the passages containing the sample gas are denoted by s_1 and s_2; resistances of the two filaments in the passages containing the reference gas are denoted by r_1 and r_2.

The reference gas used was natural hydrogen. The zero control resistances were adjusted so that the potential difference across terminals 6 and 7 of Fig. D-6 was zero when reference gas was in both the reference and sample passages of the cell. Then when deuterium-containing hydrogen was substituted for reference gas in the sample side of the cell, the temperatures of the two tungsten filaments s_1 and s_2 would be increased because the thermal conductivity of D_2 is lower that that of H_2 (Table D-I), the bridge would be unbalanced,

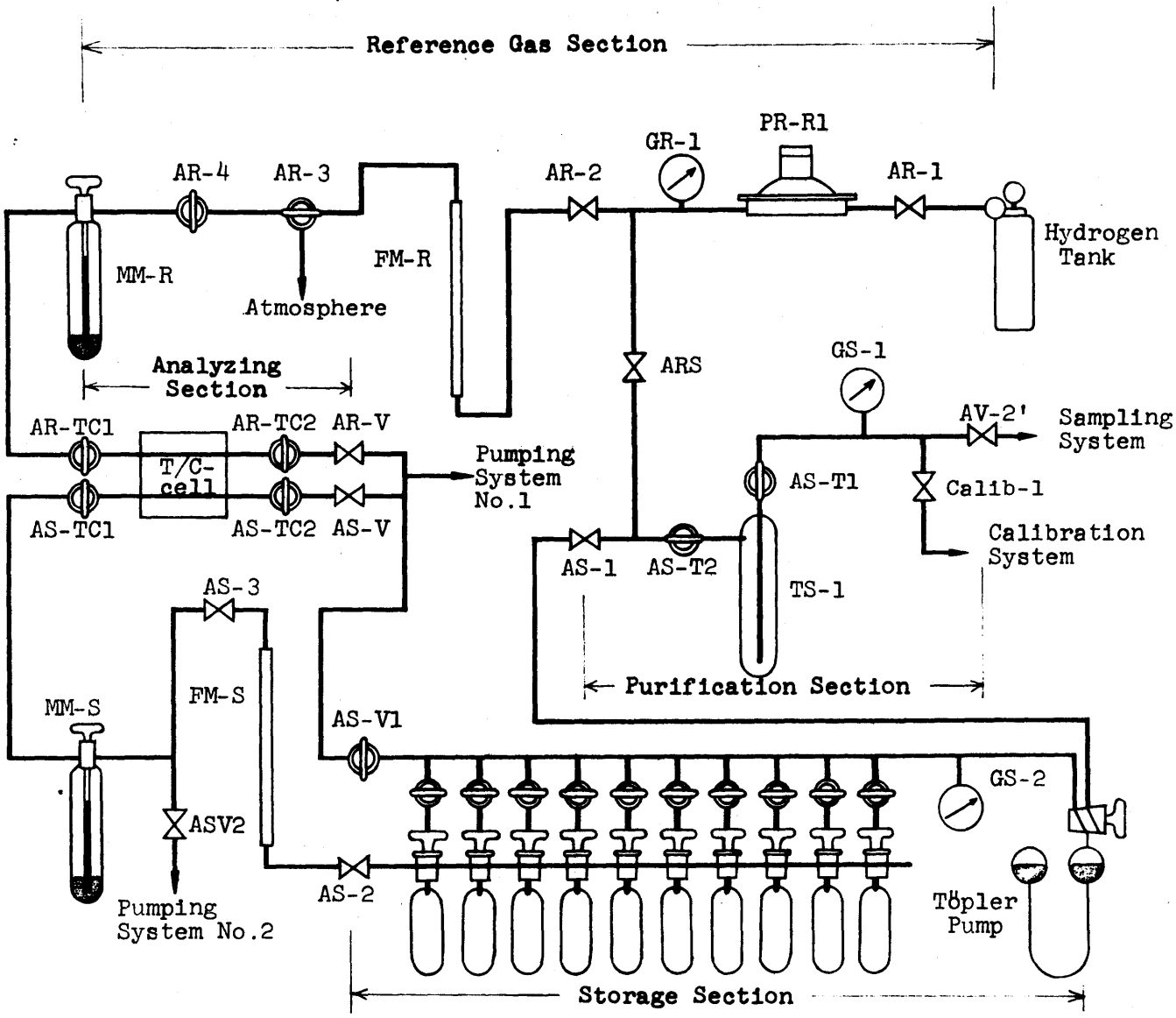

Fig. D-4. Flow Diagram of Analyzing System

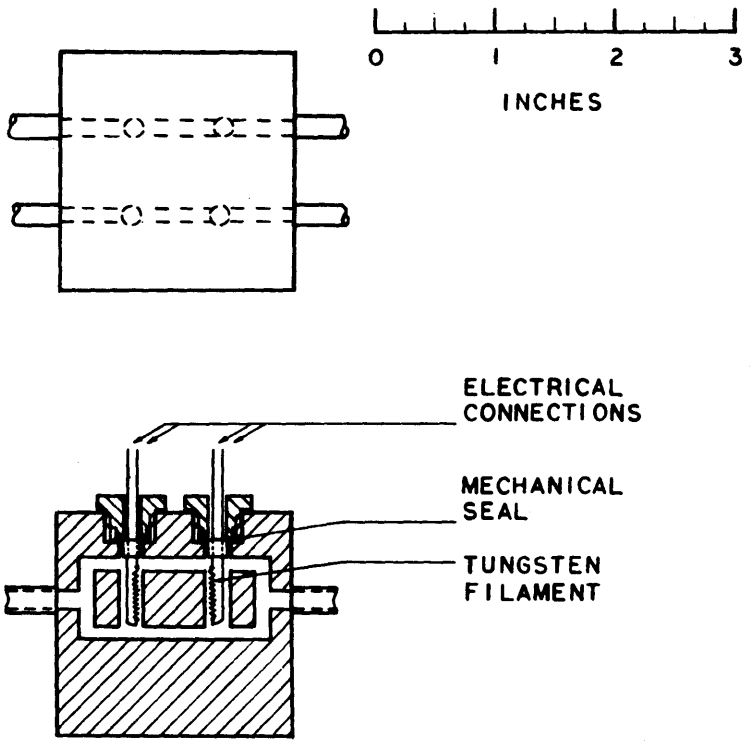

Fig. D-5. Drawing of Thermal Conductivity Cell, "Pretzel"

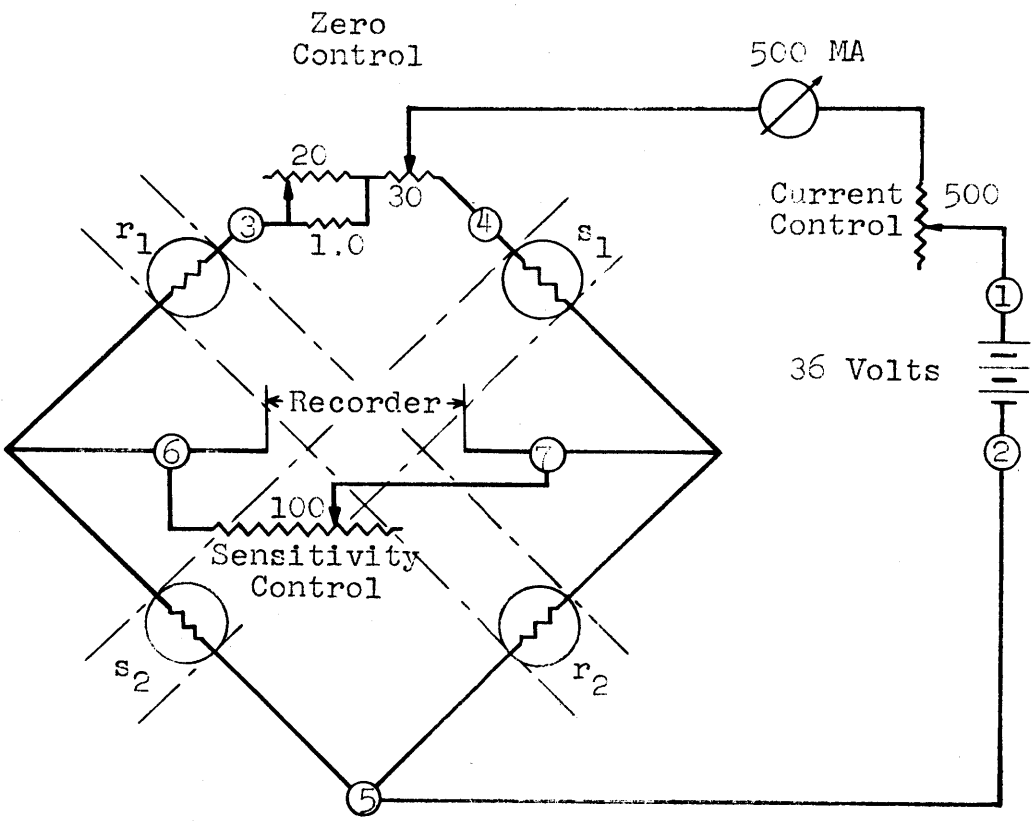

Fig. D-6. Wiring Diagram of Thermal Conductivity Wheatstone Bridge

(Note: Numbers on resistor symbols denote resistances in ohms.)

and a non-zero potential difference would develop between terminals 6 and 7 in Fig. D-6, and would be recorded. The apparatus was calibrated by determining the potential difference between the terminals when samples of known deuterium content were measured, as described in more detail in Section E of APPENDIX. The potential difference was very nearly proportional to the atom ratio of deuterium to hydrogen in the range of low deuterium content that is of interest in the present work.

Table D-I. Thermal Conductivities of Hydrogen and Deuterium*

Temperature (°C)	Thermal Conductivity, cal/cm^2.sec.°C/cm	
	H_2	D_2
-100	21.8×10^{-5}	---
- 50	35.0×10^{-5}	---
0	41.9×10^{-5}	30.6×10^{-5}
20	44.5×10^{-5}	---
100	54.7×10^{-5}	37.7×10^{-5}
200	63.4×10^{-5}	---

*Taken from "Handbook of Physics," Condon, E. U., and Odishaw, H., McGraw-Hill Book Co., N.Y. (1958).

(b) Purification Section of Sample Line

Purification of sample gas was effected by condensing all the condensable components which might be present in the sample

in a liquid nitrogen trap. At the temperature of liquid nitrogen, the only components of sample gas which would pass through the trap were hydrogen, hydrogen deuteride, deuterium and air.

The system consisted of a compound Bourdon gauge GS-1 and a liquid nitrogen trap TS-1 equipped with a stopcock on each of the inlets and outlets. The gauge was used to read pressures in the section which ranged from vacuum to about atmospheric. The stopcock AS-T2 was kept closed when sample gas was being delivered through the valves AV-2 and AV-2'.

(c) Storage Section of Sample Line

The storage section was used to transfer the purified sample gas to one of ten storage bottles and to store it at pressures of around 50 centimeters mercury. Storage was necessary because it took about two hours to analyze one sample, whereas sampling from the autoclave was done more frequently than two hours at the beginning of a run.

The storage section consisted of a manual Töpler pump, a compound Bourdon gauge GS-2, ten storage bottles connected in series, a stopcock AS-V1 and a needle valve AS-1.

The design of the ten storage bottles was all identical. A sketch of one unit is shown in Fig. D-7. It was constructed of Pyrex glass. It consisted of a 100 milliliter bottle, two high-vacuum stopcocks with bottom cap, and two connection arms. The bottom cap was evacuated before use, which held the plug in the barrel of the stopcock. Its use eliminated leak of air through that side of the stopcock. Each connecting arm

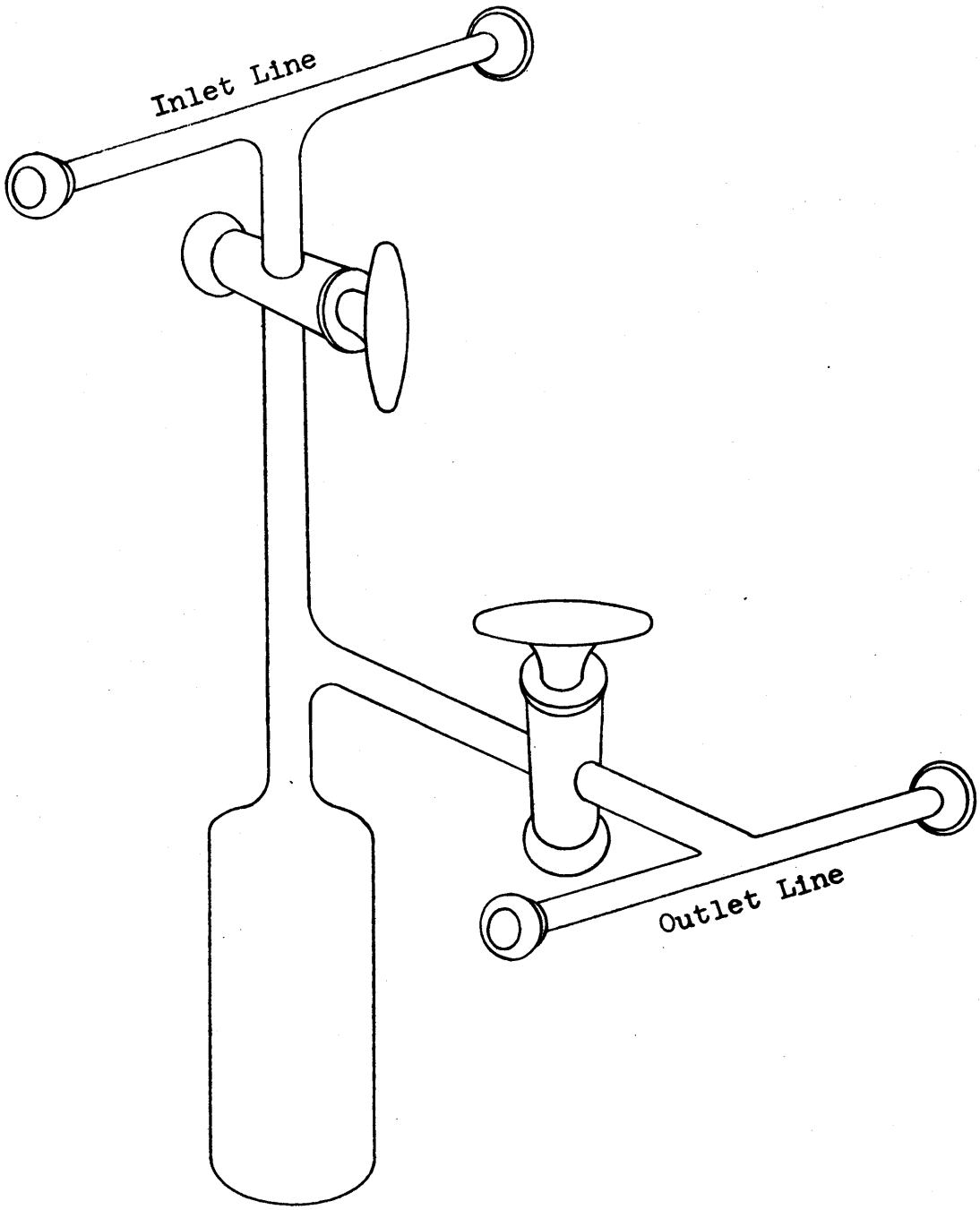

Fig. D-7. Sketch of a Unit Storage Bottle

had two standard ball-and-socket joints 18/9. The overall height of a unit was about 35 centimeters, and the length of the connecting arms was about 10 centimeters. Ten such units were horizontally connected in series. The upper connecting arms were used as inlet line through which the incoming gas was delivered to a desired bottle. One end of the series was fitted with the outlet of the Töpler pump, and the opposite end was connected to the Pumping System No. 1 through a stopcock AS-V1. While delivering purified gas, AS-V1 and the upper "In" stopcocks on all bottle units were closed, except for the bottle into which that particular sample gas was to be stored. The lower connecting arm was used as an outlet line, through which a gas sample was taken out and charged to the thermal conductivity cell. One end of the series was closed, and the opposite end was connected to a line leading to valve AS-2. The lower "Out" stopcock on each bottle unit was closed except for delivery of stored gas to the analyzing section.

(d) Analyzing Section of Sample Line

All the commercially available thermal conductivity cells, including the one employed in the present investigation were, as far as it could be found, designed for uses with continuous flows of reference and sample gases at pressures between one-half atmospheres and one atmosphere. They were primarily designed for use with gas chromatographs. The limited amount of sample gas forced the present work to adopt a static method in which output of the bridge was measured with gases statically

trapped in the thermal conductivity cell. Also, lower pressures ranging between 5 centimeters and 10 centimeters were tried. The particular type of thermal conductivity cell employed was selected because it had one of the smallest internal volumes available in a commercial product, which was 2.45 cubic centimeters for each internal passage including two filament cavities, and had the lowest recommended flow rate, 50 ± 2 cubic centimeters per minute.

The modifications in the working conditions from the ones for which it was originally designed made it necessary to make the cell more completely vacuum tight. The weak spots were at the mechanical seals of the tungsten filament mount, which had to be sealed in by means of Epoxy resin. They could not be silver-soldered because of the delicate construction of the filament. It was also found that there was a significant temperature-dependence of the bridge-output, despite the symmetrical arrangements of the reference and sample channel filaments in the Wheatstone bridge as shown in Fig. D-6. It was therefore necessary to place the thermal conductivity cell in a thermostatic bath. In view of the expectation that the cell would be more sensitive at higher ambient temperature, the water bath surrounding the cell was kept at $50 \pm 0.5^{\circ}C$, instead of making the constant ambient temperature a little higher than room temperature, which would have been much easier to control.

The water bath was constructed as follows. A jar made of Pyrex-brand glass, 12 inches in diameter and 12 inches in

height, was wrapped with a blanket of glass wool to a thickness of 1/2 inch and placed on a 1/4-inch sheet of Transite. The bath was heated by a knife-type 250-watt heater, immersed in water. The temperature was sensed by a mercury thermoregulator which actuated a mercury-plunger-type relay which, in turn, controlled the power to the heater. The bath was stirred by a stainless steel impeller. Water was continuously supplied to make up the evaporation loss from a two-liter beaker filled with water, whose surface level was kept at the desired surface level of water in the bath through a syphon tubing. Surface level of water in the beaker was maintained by a supply of water from a three-liter flask put upside-down in the beaker and clamped in such a way that the edge of its neck was kept at the desired surface level of water. The arrangement made it possible to operate the bath continuously, twenty-four hours a day and seven days a week, and to control the temperature within 0.5°C around 50°C.

The thermal conductivity cell, made vacuum tight and with its electrical lead-wires well insulated so that there could be no short-circuit among the wires through water, was placed upright on the bottom of the water bath. It took about twenty-four hours to establish a steady temperature distribution in the cell block.

The analyzing section of the sample line thus consisted of the sample gas passage of the thermal conductivity cell, a mercury manometer MM-S, a flowmeter FM-S, four valves AS-2, AS-3, AS-V and AS-V2, and two stopcocks AS-TC1 and AS-TC2.

The manometer was of the same type as that described in Section D-2. With the level-aligning device described in the same section, it was possible to read the mercury column within $\pm$ 0.5 millimeter. As shown in APPENDIX E, an unexpectedly large pressure-dependence of the cell output was observed. It was expected that, at pressures higher than that at which the mean-free path of the gas molecules were comparable with the dimension of the wire-cavity in the cell, the thermal conductivity of the gas and, consequently, the output of the bridge would be independent of the pressure. Since the diameter of the cavity was about 3 millimeters while the mean-free path of hydrogen at 20°C and a pressure of 7.5 centimeters mercury was about 1.7×10^{-3} millimeters, it was expected that the pressures around 5 centimeters mercury could be regarded as infinitely high as far as this matter was concerned. The pressure-dependent phenonemon was attributed to natural convection in the cell in which the gases were trapped. This is discussed in more detail in APPENDIX E. After it had been decided that the pressures of both reference and sample gases in the cell would be always 5 centimeters mercury, readings of the inner mercury column of the manometer, that would be given by the difference in the heights of the inner and outer mercury columns of 5 centimeters, were carefully measured once and for all for both manometers, MM-S and MM-R. The pressures were then adjusted, using the inner column readings only, without needing to read the outer columns. The calibration curves were obtained by adjusting pressures in the same way. This procedure

cut the error in pressure readings into one-half of the error which would be caused by measuring the pressure as a difference of two readings. The resulting precision in the pressure adjustment, 0.5 mm, was satisfactory for the present purpose.

Before deciding on the static gas method, attempts were made to operate the thermal conductivity cell under various continuous-flow conditions with very limited amounts of sample gas. It required additional equipment in both reference and sample lines, such as a specially designed Cartesian-type line pressure regulator. It was found that the output of the thermal conductivity bridge was so unstable, even when the flows were controlled to better than $\pm$ 0.5 milliliters per minute around 15 milliliters per minute at 10 centimeters mercury, that the flow method could not be used for the present purpose. Several flow components for the attempted flow method were kept for use with the static method, even though the flow method itself had to be abandoned. These in the sample line were the rotameter FM-S and a metering needle valve AS-3. The former was generally used in the static method to detect any flow in the section, which, for instance, was helpful in finding how well evacuation was progressing. The valve AS-3 was useful in fine adjustment of the sample gas pressure in the cell.

The valves AS-V2 and AS-V were mainly used to evacuate the section between AS-TC1 and the outlet line of the storage section and the section inside the sample gas passage of the cell, respectively.

(e) Reference Line of Analyzing System

The reference line of the analyzing system was used to deliver hydrogen gas of natural composition from the "prepurified"-grade bottled hydrogen at a high pressure around 2,000 pounds per square inch and to charge it into the reference gas channel of the thermal conductivity cell at a closely adjusted pressure of about 5 centimeters mercury.

It consisted of a tank of hydrogen gas whose chemical purity had been tested, a tank pressure regulator, a line pressure regulator PR-R1, a compound Bourdon gauge GR-1, a flowmeter, a mercury manometer MM-R, the reference passages of the thermal conductivity cell, four needle valves, one of which, AR-2, being a metering valve, and four stopcocks. The hydrogen tank was a different one from that used for delivering hydrogen gas into the autoclave. One and the same hydrogen tank was used exclusively for the reference gas and for blending the standard gases to maintain an identical standard of composition for the reference gas throughout the entire investigation. The tank pressure regulator was used to deliver hydrogen at pressures around 200 pounds per square inch, which was below the maximum inlet pressure for the pressure regulator PR-R1. This line pressure regulator was of the same design as that used in the degassing system. A valve ARS was used to introduce the reference gas into the sample line, which operation was necessary to set a zero point of the thermal conductivity bridge. Uses of the other components were similar to corresponding components in the sample line.

(f) Calibration System

The calibration system was used to make mixtures of hydrogen gas of various known concentrations of deuterium by mixing measured quantities of pure D_2 and pure H_2 and establishing the equilibrium $H_2 + D_2 \rightleftharpoons 2\ HD$. The flow diagram is presented in Fig. D-8. It consisted of a deuterium tank, a mercury manometer MM-Calib, a Bourdon gauge for vacuum G-Calib, a mixing tube called an equilibrator, and three stopcocks and a valve Calib-1.

The deuterium was obtained from Texas Nuclear Corporation, Austin, Texas. According to the manufacturer the purity of deuterium gas was higher than 99.8 percent and the impurity was hydrogen gas H_2. Deuterium from one tank was tested for chemical impurity by using the chemical gas analysis system described in Section D-4, and its chemical purity was found to be better than 99.95 percent. The deuterium gas was used without further checking for its purity and, in computing concentrations of deuterium in blended hydrogen, the deuterium gas used was assumed 100 percent pure. As it was introduced in the equilibrator tube, its pressure was read on the mercury manometer MM-Calib.

The manometer was made of Pyrex and consisted of two parts, an inner tube and an outer tube, joined together with a ground tapered joint 14/35. The pressure of the system connected to a side arm extending out from the upper part of the outer tube was measured as the difference in heights of the inner and outer mercury columns. The outer tube was

12 millimeters in outside diameter and about 57 centimeters long. The inner tube was 5 millimeters in outside diameter and just about as long as the outer tube. The inner tube had a thick-walled bulb of about two millimeters internal volume fused on its top, which served as a damper against a surge of mercury. The inner tube had four glass horns fused radially on the wall near its lower tip, which kept the inner tube from being unevenly attracted to one side of the outer tube. The manometer was also used to read the total pressure of the mixture of H_2 and D_2 when it was low enough to be measured by the manometer.

Hydrogen gas was supplied from the reference hydrogen tank. It was introduced through valves and stopcocks, ARS, AS-T2, AS-T1 and Calib-1. Pressure of pure hydrogen in the right side, in Fig. D-8, of stopcock Calib-2, was read on a vacuum Bourdon gauge G-Calib, having a four-inch dial and calibrated against the manometer MM-Calib.

The equilibrator was a Pyrex glass tube, 16 millimeters in inside diameter and 21 centimeters long, having two side tubes and a wire stretched along its axis with its ends going through the ends of the glass tubing. Referring to Fig. D-9-(a), the axial wire assembly consisted of two different materials. The sections which were fused to the glass wall were pieces of tungsten wire of 0.030 inches in diameter. The fusing-in was done by the standard technique of cleaning the tungsten surface by heating it to white heat and touching it with a piece of potassium nitrite and then

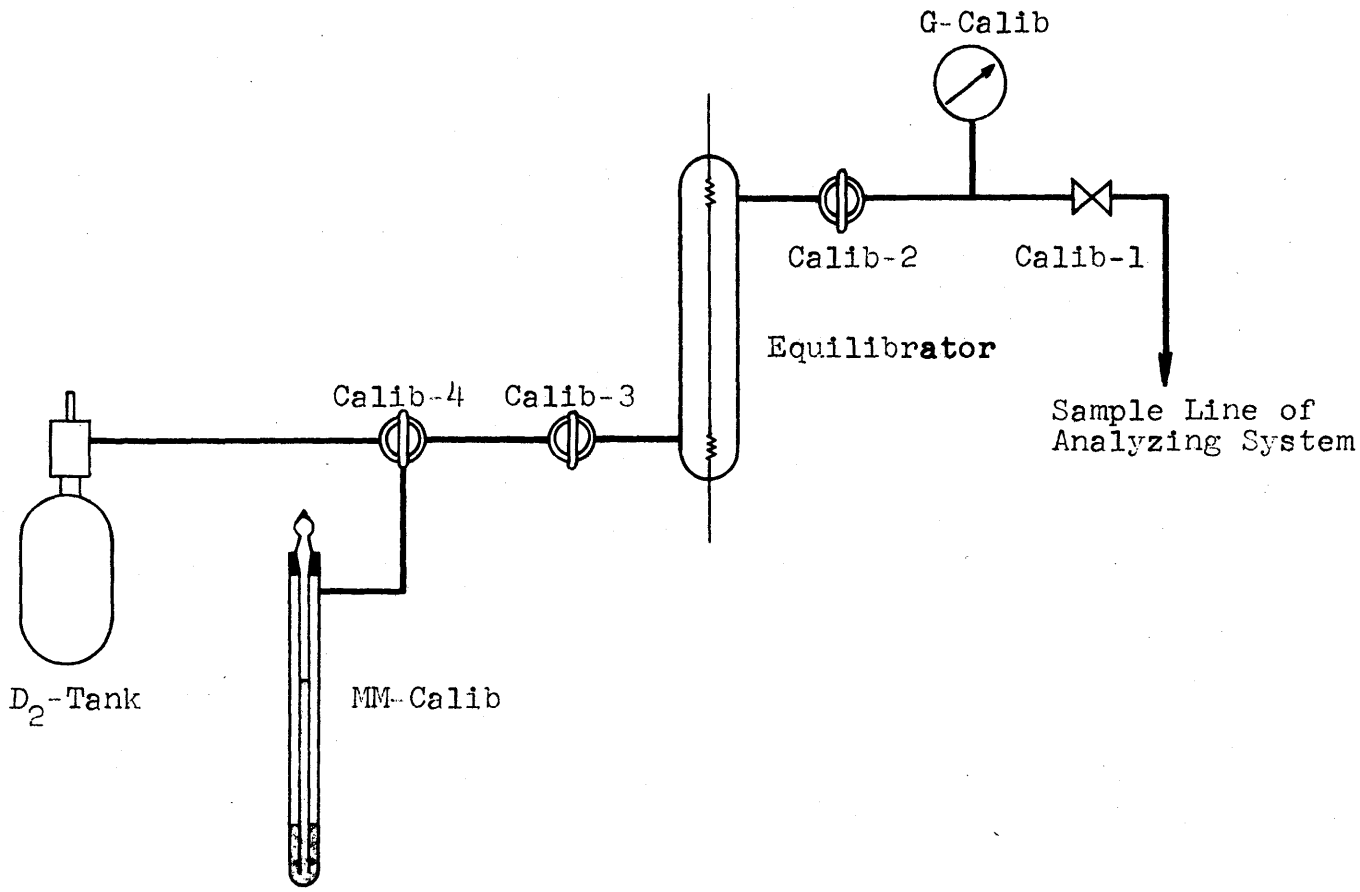

Fig. D-8. Flow Diagram of Calibration System

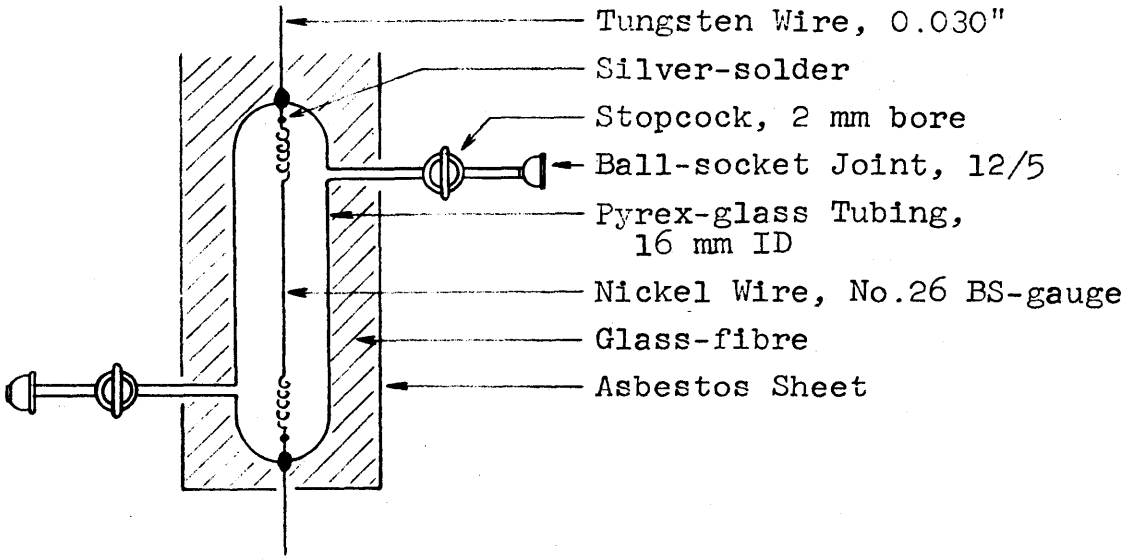

(a) Mechanical Construction

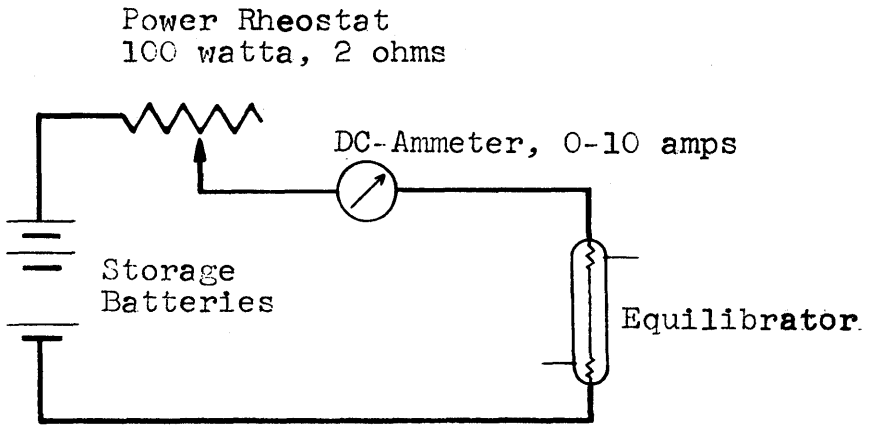

(b) Electrical Connections

Fig. D-9. Equilibrator

fusing a thin glass sleeve before fusing it on a hole blown on the end of the sealed tubing. The coiled sections and the central section were nickel wire of No. 26 B+S gauge. The length of nickel wire estimated from a measurement of its electrical resistance was about 55 centimeters. The nickel and tungsten wires were connected with silver solder. The equilibrator was designed not only to mix H_2 and D_2 uniformly in it but also to catalyze equilibrium in the reaction

$$H_2 + D_2 \rightleftharpoons 2HD$$

This reaction is catalyzed on a heated nickel surface, especially markedly at the temperatures above 600°C (D-1, D-2). The axial nickel wire in the equilibrator was provided for this purpose. The temperature of the nickel wire was estimated from its electrical resistance, computed by using directly-measured values of the current and the potential drop across the wire. Five 6-volt storage batteries connected in series were used to heat the wire. A current of 4 amperes was needed to heat the wire to 600°C when the equilibrator was evacuated. Currents of 6.4 and 7.5 amperes were needed for the same temperature when the tube was filled with 135 and 300 millimeters of mercury and hydrogen gas, respectively.

In principle, a mixture of known composition was made as follows. Deuterium gas was introduced up to the stopcock Calib-2, and its pressure, up to about 10 cmHg, was read on the manometer MM-Calib. The deuterium tank was then isolated from the rest by turning the stopcock Calib-4 so that

MM-Calib was connected only with the equilibrator. Hydrogen gas was introduced up to the stopcock Calib-2. Its pressure, read on the gauge G-Calib, was measured and maintained near atmospheric. The stopcock Calib-2 was cracked momentarily and was closed. The mixed gas filling the equilibrator and the manometer MM-Calib connected with it was left standing for about one hour to allow for complete mixing. The pressure of the mixture was read on the manometer MM-Calib, and the stopcock Calib-3 was closed. The mechanical mixture trapped in the equilibrator was then catalyzed to attain the isotopic equilibrium. The atom fraction deuterium in the mixture was taken to be the ratio of the pressure of deuterium to the pressure of the mixed deuterium and hydrogen.

D-4. Chemical Gas Analysis System

The chemical gas analysis system was used to check the total chemical impurities in the "prepurified"-grade hydrogen that was commercially available. According to the manufacturer, Air Reduction Company, New York, New York, a hydrogen purity of 99.95 percent was guaranteed, and a typical analysis of prepurified hydrogen showed the following impurities: 0.001 w/o CO_2, 0.006 w/o O_2, 0.002 w/o CO, 0.039 w/o CH_4 and 0.017 w/o N_2. These compositions would correspond to the ratio of partial pressures of total impurities to that of hydrogen of 6.4×10^{-5}, a value which barely exceeded the upper limit of 2×10^{-5} set in APPENDIX D-1 for the desirable value of molar ratio of air to hydrogen in any system of the present investigation. The higher value of this magnitude

would, however, be satisfactory if the calibration curves of the analyzing system were made by using hydrogen of identical compositions for both the reference and standard gases and if that same hydrogen was used as reference gas throughout the investigation. This is what actually was done as explained in Section D-3 of APPENDIX. A slight variation of impurities from one tank to another of hydrogen used for charging the autoclave could be taken care of by subtracting the output reading of the T/C cell for the first sample of a run from outputs for all other samples of the run. This procedure is illustrated in APPENDIX K. However, such was permissible only when the amounts of impurities did not exceed the upper limit very much. For this reason hydrogen gas was tested against the impurities for each new hydrogen tank before it was used. Procedures of the analysis are described in Section G-10 of APPENDIX, and the apparatus and the principle only are explained here.

Flow diagram of the system is presented in Fig. D-10. It consisted of an electric furnace through which a Pyrex tube packed with cupric oxide passed, a manual Töpler pump, a liquid nitrogen trap, an empty bulb, a mercury U-tube manometer, a compound Bourdon gauge, four stopcocks and four needle valves. The connecting lines on the right side of two metal-glass joints in Fig. D-10 were made of 1/4-inch copper tubing, while all the rest of the system was connected with Pyrex tubing. The metal-glass joints were each made with a set of standard ground tapered joints 10/30, consisting of a

glass female part and a brass male part machined to the standard specification.

The electric furnace was a product of Hevi-Duty Electric Company, Milwaukee, Wisconsin, and was primarily designed for organic combustion analysis. It had a heated length of 22 inches in which a combustion tube could be placed. A temperature of 500°C was easily achieved by adjusting six control dials. The temperature was roughly checked by means of an iron-constantant thermocouple with the reference point at room temperature.

The Pyrex tube in the furnace was 5 millimeters in inside diameter and 30 inches in length, and was equipped with a ball-and-socket joint on each end. Its central section was packed with about 20 inches of reagent-grade cupric oxide. The amount of the cupric oxide was approximately equivalent to one gram equivalent. The central section was then wrapped with asbestos tape along a length of 26 inches.

This setup was expected to convert hydrogen and oxygen to steam, carbon monoxide to carbon dioxide, methane and its homologues to carbon dioxide and water vapor, and not to affect oxygen, carbon dioxide and nitrogen. Water vapor produced was removed from the stream when it left the furnace and entered the liquid nitrogen trap. Therefore, after passing through the furnace and the trap, hydrogen and oxygen originally present in the gas stream would completely disappear and carbon dioxide and nitrogen, which were originally present, would show up downstream of the trap

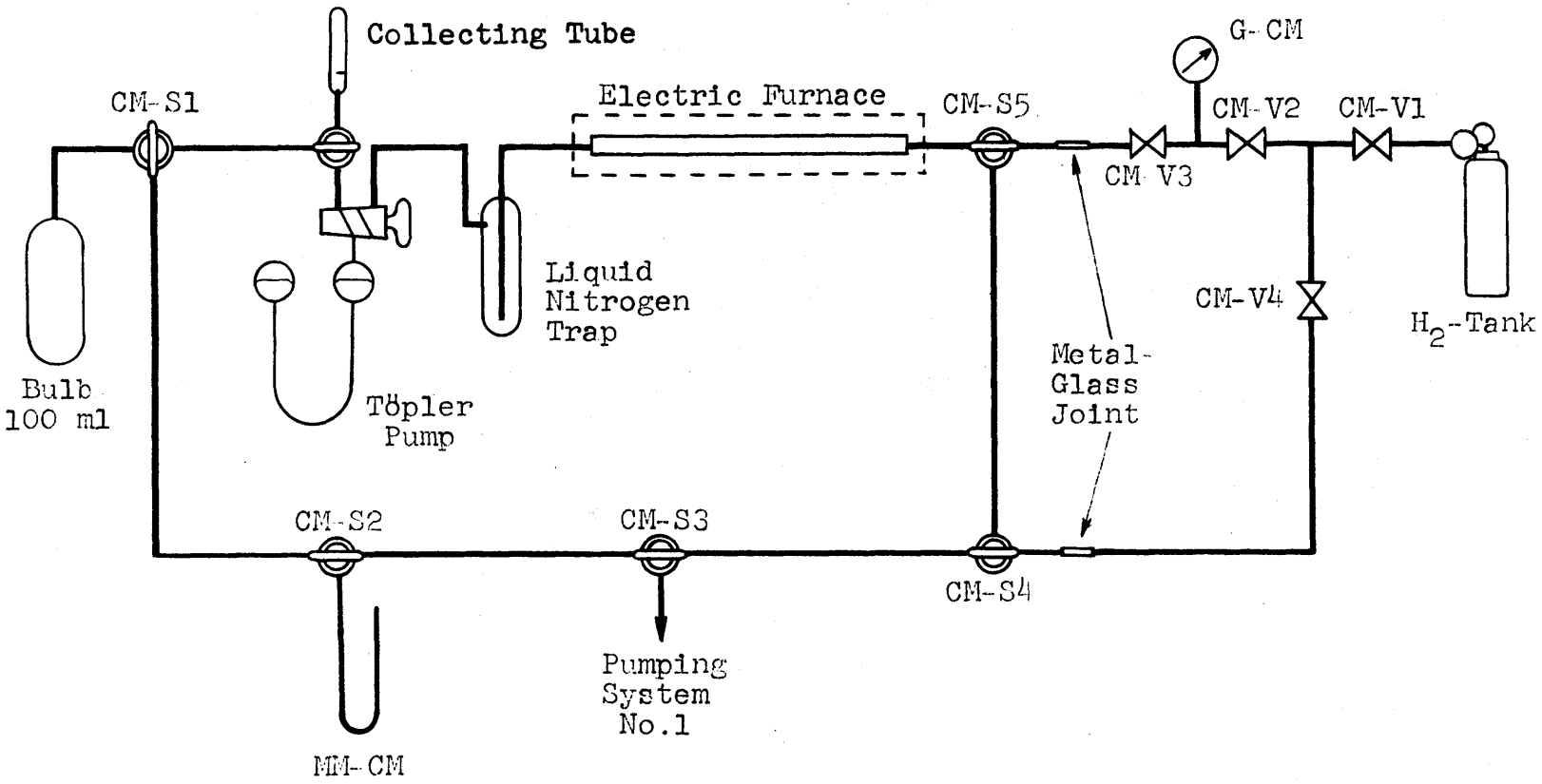

Fig. D-10. Flow Diagram of Chemical Gas Analysis System

without being affected. One grammole of carbon monoxide in the original gas would have been converted to one grammole of carbon dioxide after it passed the trap. One grammole of the original methane would be converted to three grammoles of gaseous molecules after passing through the furnace, but the number would have been reduced to one again after passing through the trap. Therefore, if the original total number of grammoles of a sample gas were known, the fractional amount of total CO_2, CO, CH_4 and N_2 impurities could be calculated by finding the number of grammoles of residual gas after passing through the furnace and the trap. The number of grammoles was obtained from measurement of the initial and final pressures trapped in known volumes. Although the method used would not detect oxygen, the fact that the amount of the other impurities found was always small and the fact that oxygen was not one of the principal impurities listed by the manufacturer, provide reasons to believe that the hydrogen employed was sufficiently pure.

The initial volume of the sample gas was known because it was initially contained in the empty bulb whose internal volume plus the volume of its step up to the stopcock CM-S1 was known to be 100 millliliters within probably 1 millliliter.

It was determined by adding internal volumes of the bulb and the tubing which were each measured before being fused together, by weighing water that filled each section. The initial pressure was read on the manometer MM-CM which could show pressures up to 23 cmHg.

To assure the complete removal of hydrogen, a sample gas was circulated along the loop shown in Fig. D-10 several times by means of the Töpler pump.

The residual pressure was obtained by trapping the residual gas into a small collecting bulb attached on top of the Töpler pump. It had a grading line near its bottom end which marked the lower end of that section of the bulb whose internal volume was known to be 2.4 milliliters. The bulb was equipped with a tapered joint 10/30, and its internal volume was measured by weighing water that filled the marked section. The levelling bulb of the Töpler pump was raised until the surface level of mercury in the other branch reached the grading line. The residual pressure was obtained as a difference in the surface levels in the two branches of the Töpler pump.

E. Calibration of Thermal Conductivity Bridge

Calibration curves were constructed by plotting outputs of the thermal conductivity bridge, described in subsection D-3 of APPENDIX, against known concentrations of deuterium atoms in the standard hydrogen gas blended as described under (f) in that subsection. Standard working conditions finally decided on were the following:

Reference gas	natural hydrogen
Pressure	50 mmHg
Flow rate	zero
Total bridge current	190 milliamperes
Ambient temperature	50°C

The time required for isotopically equilibrating a mechanical mixture of hydrogen gases, H_2 and D_2, in the equilibrator under various equilibrating conditions was obtained by comparing outputs of the thermal conductivity bridge on sample gases blended for various periods of time. The results are given in Table E-I. It is known (D-1, D-2) that equilibrium is attained instantaneously on the surface of a heated nickel wire at 600°C. One may conclude from the results of Table E-I that, at 600°C, the equilibrium throughout the gas volume was reached after one minute, but that at 400°C, equilibrium was not obtained even in ten minutes. One minute, however, seemed to be somewhat too short to establish equilibrium if molecular diffusion of hydrogen molecules toward and away from the heated surface of nickel

Table E-1. Blending Period and Degree of Equilibrium

(Total pressure of gaseous mixture $\simeq$ 40 mmHg at room temperature)

Temperature of Ni wire (°C)	Atom Fraction Deuterium (%)	Blending Period (min)	T/C-Output* (mV)	Output/At.Fr.D (mV/%)
600	7.20 ± 0.24	0	4.78 ± 0.05	0.663 ± 0.035
600	7.50 ± 0.25	0	4.75 ± 0.05	0.633 ± 0.035
600	7.50 ± 0.25	0	4.70 ± 0.05	0.627 ± 0.035
600	7.41 ± 0.25	1	6.40 ± 0.05	0.865 ± 0.034
600	7.51 ± 0.25	1	6.60 ± 0.05	0.878 ± 0.034
600	7.55 ± 0.25	5	6.62 ± 0.05	0.877 ± 0.034
600	7.78 ± 0.26	30	6.80 ± 0.05	0.874 ± 0.034
400	7.48 ± 0.25	1	4.65 ± 0.05	0.622 ± 0.035
400	7.47 ± 0.25	10	4.75 ± 0.05	0.636 ± 0.035

* Obtained under the standard conditions mentioned in the beginning of the present section and with sensitivity "1".

were the only mechanism of mass transfer. The short equilibrium period was attributed to extensive turbulence which could have been caused by the coiled sections of nickel wire which were originally installed to keep the straight section of the wire under tension but were actually heated, when the electric current was put through, to much higher temperatures than the temperature of the straight part. In obtaining the calibration curves, the condition one minute at 600°C, was used throughout.

E-1. Output Versus Deuterium Concentration

Results obtained under the conditions, total bridge current = 190 milliamperes and pressures of gases = 50 millimeters Hg, are shown in Figs. E-1 and E-2, in the form of a plot of bridge output in millivolts against the atom ratio of deuterium to hydrogen. This plot was fitted with the best straight line through the origin, using the least-squares method (E-3) in which uncertainties in both variables are taken into account. In the relation,

$$r' = \gamma E$$

where r' and E are the isotopic ratio of deuterium to hydrogen in a sample hydrogen gas and the corresponding output in millivolts, respectively, it was found that

$\gamma = 0.02175\ mV^{-1}$ for the lower sensitivity, setting "1" (Calibration 1)

and $\gamma = 0.01225\ mV^{-1}$ for the higher sensitivity, setting "2" (Calibration 2).

The probable error in the measured output used in these calculations was 0.05 millivolts for both sensitivity settings. The probable error in the atom ratio deuterium of standard gases was taken to be 0.0010 for the gas mixtures used in calibrations at sensitivity setting "1" and 0.0020 for the sensitivity setting "2", most of the uncertainties being due to those in measuring values of the partial pressures of deuterium.

This calibration was checked at the end of the present investigation and, as shown in Fig. E-2, was found to have remained unchanged.

E-2. Effect of Current on Calibration

The effect of total bridge current on the T/C cell calibration was checked by measuring the bridge output E for various values of the bridge current i under a given set of conditions. The simple theory of this cell predicts that E is proportional to i^3, if all heat were removed by molecular conduction. The results of this check are given in Table E-II. As the ratio E/i^3 is not constant, it seems that current dependence was somewhat different from the simple theory.

Table E-II. Effect of Current

Sensitivity 2.5

Standard gas 10.0% atom ratio deuterium to hydrogen

Pressures 50 mmHg

Run Number	Current, i (ma)	Output, E (mV)	E/i^3 (mV/ma^3)
1	140	2.62	$(9.55 \pm 0.55) \times 10^{-7}$
2	150	3.70	$(9.56 \pm 0.49) \times 10^{-7}$
3	160	4.95	$(12.07 \pm 0.58) \times 10^{-7}$
4	170	6.40	$(13.04 \pm 0.58) \times 10^{-7}$
5	180	7.90	$(14.35 \pm 0.60) \times 10^{-7}$

At 190 ma, the current used for analysis, dE/di was 0.07 mV/ma and 0.14 mV/ma for the sensitivity settings of "1" and "2", respectively. Since the current could be controlled to within 0.5 ma at 190 ma, the error

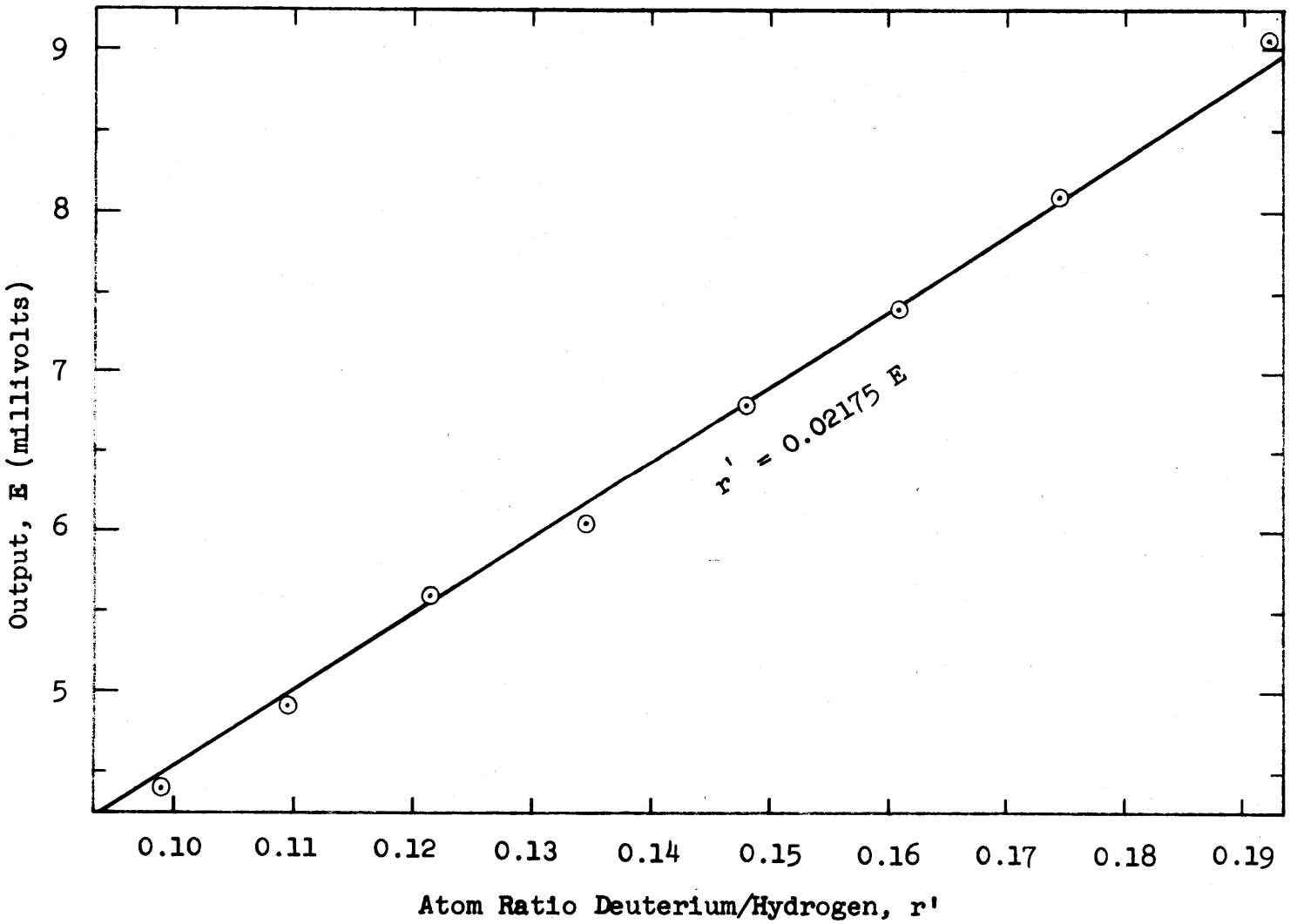

Fig. E-1 Calibration of Thermal Conductivity Bridge (1)
(Sensitivity: 1 Current: 190 ma Pressures: 50 mmHg)

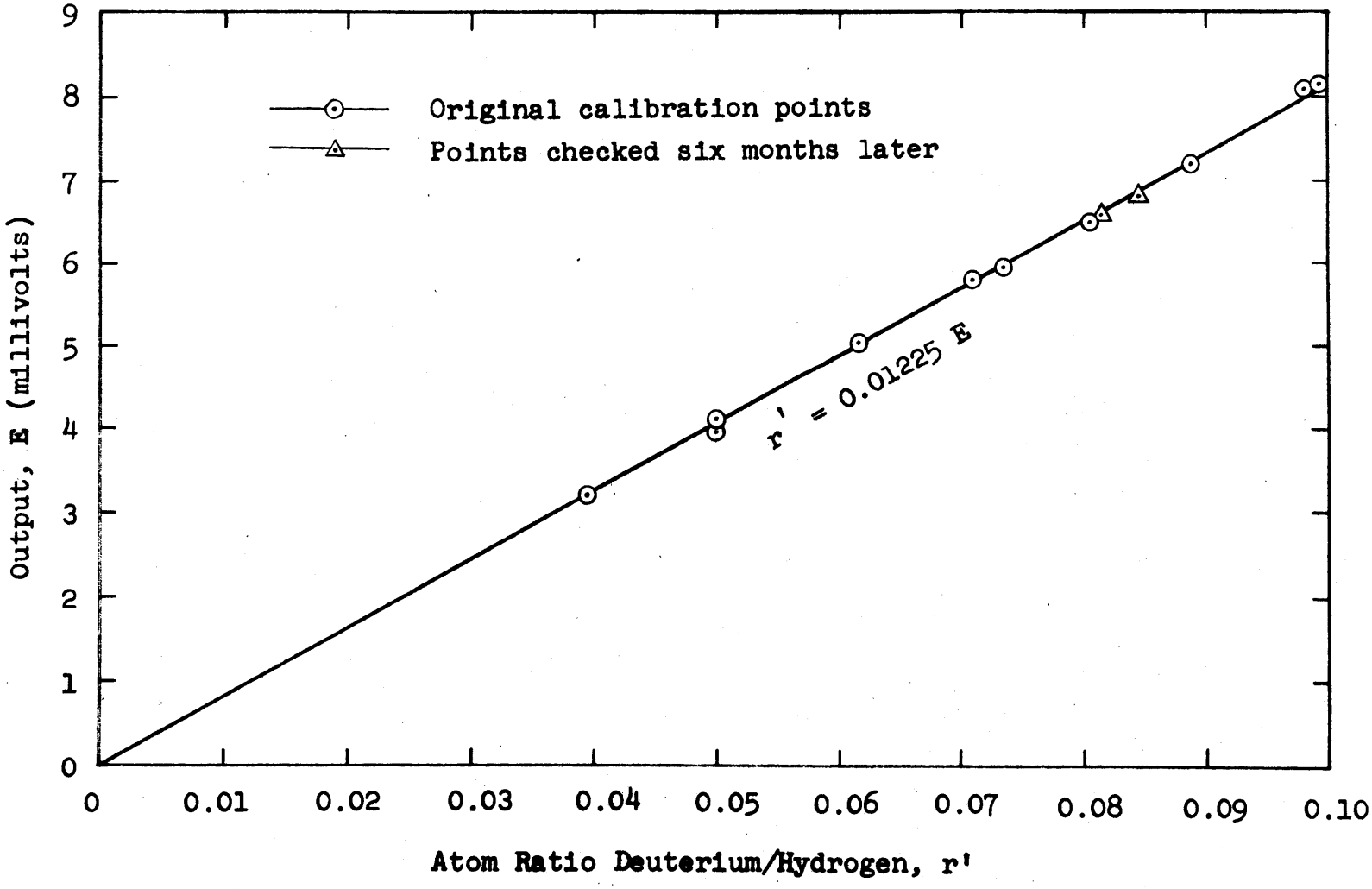

Fig. E-2 Calibration of Thermal Conductivity Bridge (II)
(Sensitivity: 2 Current: 190 ma Pressure: 50 mm Hg)

introduced by nonuniformities in the current was 0.035 mV and 0.07 mV for the sensitivity settings of "1" and "2", respectively. These correspond to an uncertainty of about 0.0008 in atom fraction deuterium.

E-3. Effect of Pressure on Calibration

The effects of varying the static pressures of the reference and sample gases in the thermal conductivity cell were determined by measuring the output with various values of the pressure of natural hydrogen in one passage of the cell while keeping the pressure of natural hydrogen in the other passage constant at 50 millimeters Hg and other operating conditions at their standard values. The results are presented in Fig. E-3. This showed that a deviation in the output of 0.06 millivolts should be expected for an error of one millimeter Hg made in adjusting the pressure of one of the gases at sensitivity setting "2", while the deviation would be 0.04 millivolts for an error of one millimeter Hg at sensitivity setting "1".

As pointed out in Section D-3 of APPENDIX, pressure adjustments for the rest of the work were made by using only readings of the inner mercury columns in the manometers MM-R and MM-S (Fig. D-4) instead of measuring the pressures as a difference in heights of the inner and outer mercury columns. This halved the error introduced in pressure adjustment. Thus, it was sufficient to use for MM-R and MM-S the manometers of the same type as what was described in Section D-2 of APPENDIX and could measure the pressure

to 0.5 millimeters Hg with the level-aligning devices. By using the level-aligning devices described in Section D, the pressure could be measured with a precision of 0.5 millimeters.

A series of measurements at supposedly the same conditions were reproducible within a standard deviation of 0.05 millivolts, at either setting of the sensitivity.

E-4. Effect of Ambient Temperature

An experiment was performed to find the effect of a nonuniform ambient temperature on a zero point. The cell was placed in the atmosphere and was charged with natural hydrogen at the pressure of 50 millimeters Hg in each passage. Air was blown from an electric fan on the side of the cell in which the reference line was running. It was found that an increase in the output of up to about three millivolts were possible depending on how strongly the reference channel was cooled when the sensitivity was 2 and the total current was 190 milliamperes.

Another test was made to find an effect of changing a uniform ambient temperature on a zero point. Results of two measurements of the output with the cell containing natural hydrogen at 50 millliliters Hg in each passage were compared. One measurement was done on the cell placed in the atmosphere at room temperature around 22°C. The other measurement was done on the cell being operated under the same condition except that it was placed in the water bath described in Section D-3 of APPENDIX and kept at 50°C. It was found that

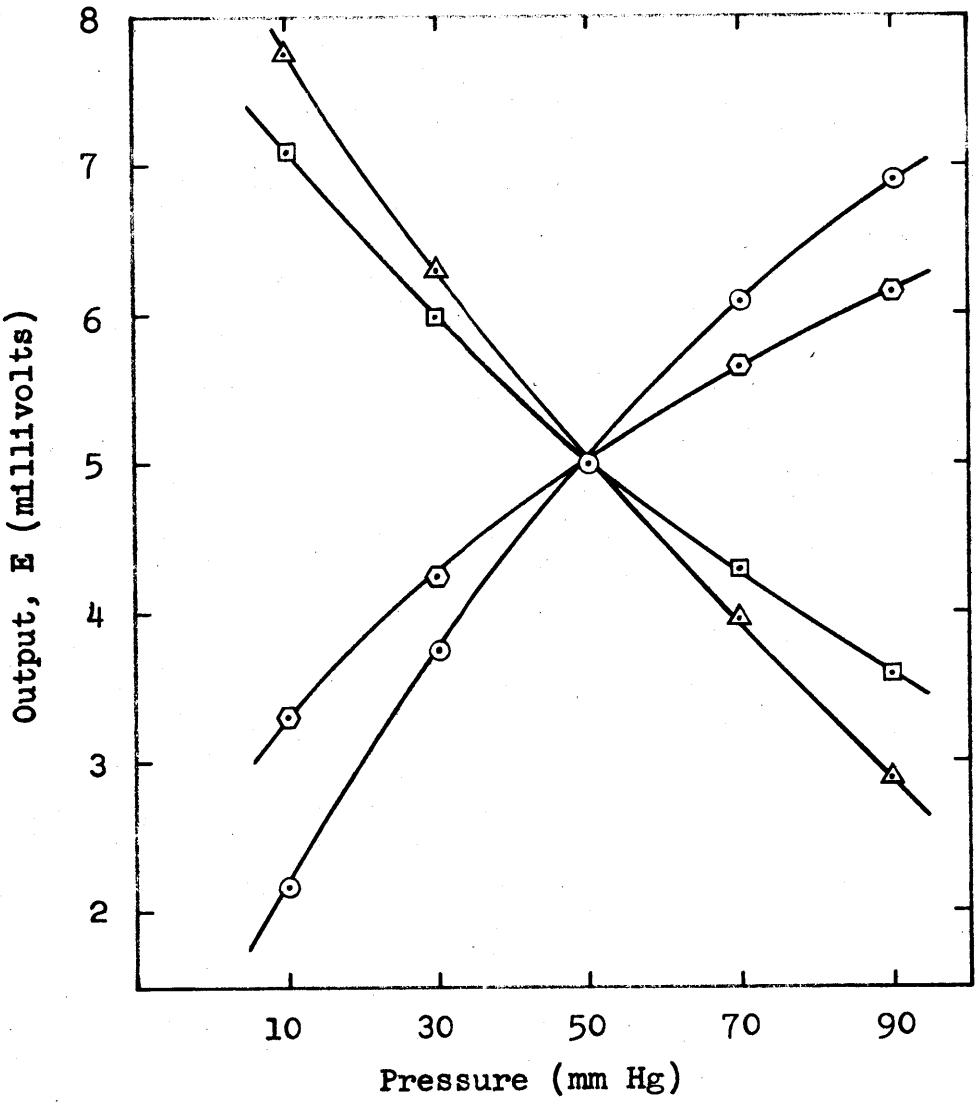

Fig. E-3. Effect of Pressure on Zero Point

Current: 190 ma Gas in both passages: H_2

Common zero point: arbitrary

Sensitivity: 1

—⊙— Reference pressure varying; Sample pressure=50mmHg

—△— Sample pressure varying; Reference pressure=50mmHg

Sensitivity: 2

—⊙— Reference pressure varying; Sample pressure=50mmHG

—⊡— Sample pressure varying; Reference pressure=50mmHg

the latter setup gave an output which was higher than the output for the former setup by 0.7 $\pm$ 0.2 millivolts when the sensitivity setting was 2. The deviation given, 0.2 millivolts, was a limit of fluctuations of the output in the former setup, presumably caused by a nonuniform ambient temperature.

Thus, fluctuation of an output caused by the fluctuation of the uniform temperature in the water bath would be at most 0.03 millivolts per degree centigrade. The temperature-controllability of the water bath described in Section D-3 of APPENDIX, 0.5°C, was therefore sufficient for the present purpose.

F. General Safety Precautions

Since the present work was to deal with hydrogen under considerable pressure, safety considerations were essential in every step of design and operation of the equipment. Precautions taken in design of the oil bath and the higher pressure systems are mentioned in Sections B and C of APPENDIX. Particular operating precautions are pointed out in Sections C, D and G of APPENDIX. This section discusses general safety measures.

The systems for handling high-pressure gases were located at a corner of the laboratory with one side facing a brick wall about one and half inches thick, a second side facing outdoors with a large window and the other two sides facing the rest of the laboratory. The ceiling of the compartment was constructed of two separate layers of plywood under the roof of a one-story building. To provide a primary shield for smaller fragments in case of an explosion, the two sides of the compartment which faced the rest of the laboratory were shielded with two parallel rows of quarter-inch steel boiler plate with labyrinth-type access between them. The steel plate thus protected the rest of the laboratory from flying debris which might be formed in a possible explosion. In addition, the ceiling and the window would have acted as blowout panels.

All the systems for handling the high pressure hydrogen, shown in Fig. C-1, except the hydrogen tank and its pressure

regulator, and the Pumping System No. 2 were placed inside the boiler plate. Some of the high-pressure needle valves used while high-pressure hydrogen was being handled were remotely controlled from outside of the steel wall by means of an extension rod attached to the handle of each of such valves by a universal joint and inserted through a hole on the steel wall. These valves are indicated in Fig. C-1 with dark-shadowed symbols. Two peep holes were provided on the steel wall, each placed directly in front of the Bourdon gauges of the hydrogen-charging system.

All the exhaust gases were discharged to the outdoors. Two exhaust lines were provided. One was used for the two pumping systems and was made of 3/4-inch copper tubing. The other was used for the rest of the systems and was made of 1/2-inch tubing. The latter was flushed with nitrogen every time hydrogen-containing gas was discharged.

G. Details of Procedures

The purposes and principles of operations of the various systems are explained in Sections B, C and D of APPENDIX. Step-by-step procedures only will be described in this section.

G-1. Starting-up and Levelling-off the Constant Temperature Oil Bath

Turn on the ventilation fan. Put on the cooling water for the solenoid housing on the autoclave. Put on the cooling water for the drain line of the liquid-charging system. Turn on the motor for the oil bath-stirring system. See that the pilot lamp is on and the bath oil is being circulated. Check that the dial on the Variac voltage-regulator for the internal heater is at zero and the fine-adjusting knob of the voltage regulator for the external heater is at midpoint. Set the dial on the temperature controller at a temperature about 20° C below the steady bath temperature that is to be finally attained (Table B-III). Set the para-series switch on the side of "parallel." Set the voltage-regulator-selector-switches on A and C. Put the external heater switch on. See that the pilot lamp is on and the total current on the external heater is about zero. Put the Variac regulator for the internal heater on. Put the temperature controller on. See that the controller-power-pilot-lamp is on. See that the "COOL"-lamp on the controller is on and that, after about ten seconds, it is turned off and the "HEAT"-lamp is

turned on. Slowly increase the total current on the external heater to 9 amperes by turning the fine-control knob clockwise. Increase voltage to the internal heater to the value recommended for the final steady temperature to be attained (Table B-IV).

Pack the Dewar-jar which contains the reference junction of the copper-constantan thermocouple with finely crushed ice. Keep on adding ice for the rest of the period of the bath-operation.

Fill Dewar jars containing the traps PT-1, PT-2 and PT-3 (Figs. D-1 and D-2) with liquid nitrogen. Open PS-1, PS-2, PS-6 and PS-7 (Figs. D-1 and D-2) which have been closed during the period of shutdown.

When the bath temperature-recorder connected with the standard iron-constantan thermocouple inserted in the bath-oil shows that the temperature is levelling off, watch the "HEAT" and "COOL" lamps on the temperature recorder. When the "HEAT"-lamp is turned off and the "COOL"-lamp is turned on, decrease the total current on the external heater to an amperage about 0.5 amperes smaller than the recommended value for the final temperature (Table B-IV). Reset the controller dial at a temperature about 2°C below the final temperature to be attained (Table B-III). See that the "HEAT"-lamp is turned on again.

When the "HEAT"-lamp is turned off next time, readjust the total current on the external heater and the control dial at the values corresponding to the final steady temperature (Tables B-III and B-IV).

When the "HEAT"-lamp is turned off again, the oil bath has just reached the steady temperature for a first time.

G-2. Preparing Autoclave for a Run

Normally following the discharge of the remaining contents of the autoclave and the flushing of discharge and exhaust lines with nitrogen, as described in Subsection G-8 of APPENDIX, evacuate the autoclave for about one hour through valve CVV with valve HV3 kept open.

Fill the cleaned liquid-charging vessel with distilled water by replacing air in it with water through valve CV1 attached to it with valve CV2 open. (The cover of the liquid-charging vessel was removed only for the purpose of occasional thorough cleaning of its interior.) Connect the vessel with the rest of the liquid-charging system. Open CV1, CV2, CV3 and CV4 to allow distilled water to drain into the autoclave. Increase the external heater power if necessary. After letting it stand for one hour, close the four valves on the drain and ventilating lines. Turn on the autoclave-stirring system. Remove the charging vessel.

After half an hour, turn off the autoclave-stirring system. Turn on the cooling water for the discharging system. Slowly open DV2. Check that valves AV1 through AV4, AVV and HV4 are closed. Open the regulator valves on the nitrogen tank. Release excess nitrogen through valve NV-1. Close NV-1. Close AV1 and AV4. Slowly open CVV. Keep evacuating the autoclave for at least one hour. Then close HV3.

In the meanwhile, level off the bath temperature by adjusting the temperature-control dial and powers on the heaters and by measuring the autoclave temperature with the copper-constantan thermocouple. (It was recommended that the temperature of oilbath at this stage be raised to about 20°C higher than the desired reaction temperature, since the procedure saved time in levelling-off the temperature again after the aqueous solution of diethylamine was charged.)

Adjust the dial for the autoclave-stirrer at the desired stirring rate.

G-3. Degassing and Analyzing Aqueous Solution.

Evacuate the degassing section as follows. Fill the Dewar jar containing the traps TDG-1 and TDG-2 (Fig. D-3) with liquid nitrogen. Disconnect Swagelok connections on the liquid-charging vessel. Close stopcock DGS-4. Open DGS-3. Put on cooling water for Allihn-type condenser. Close stopcocks DGS-1, DGS-2 and DGS-3. Turn stopcock PS-4 so that the manometer MM-DG is connected to the Pumping System No. 1 but not with stopcock PS-5. Slowly open DGS-1. After the system up to stopcock DGS-2 is evacuated, slowly open DGS-2. Check that valve DGV-4 is closed. Open DGS-3. Keep evacuating.

Meanwhile, prepare about 700 millliliters of an aqueous solution of diethylamine by mixing in a conical flask roughly known volumes of triple-distilled diethylamine and partially-enriched heavy water of known deuterium concentration.

Charge the solution into the degassing flask as follows.

Close stopcocks DGS-1 and DGS-2. Insert the end of the free Swagelok coupling that is connected to the stopcock DGS-4 through Tygon tubing to the bottom of the conical flask held in a tilted position. Open DGS-4. Close DGS-4 just before a last portion of the amine solution in the conical flask is sucked into the degassing flask.

Start degassing the solution as follows. Open stopcock DGS-2 very slowly. Open stopcock DGS-1 very slowly. Keep evacuating.

Meanwhile, evacuate the liquid-charging vessel as follows. Make up the Swagelok connection next to valve CV-2. (The vessel should have been cleaned and emptied.) Open valve CV-2 but keep valve CV-1 closed. Keep evacuating the degassing section for five more minutes after the manometer MM-DG showed a pressure below one millimeter Hg. Turn stopcock PS-4 so that PS-5 is connected to the Pumping System No. 1 but not to MM-DG. Note the time. Turn stopcock PS-5 so that the trap TDG-2 is connected to PS-4 but not to the analyzing system.

See if manometer MM-DG indicates any pressure buildup of more than one millimeter Hg after the system has been isolated for more than three minutes. Evacuate the degassing section for five more minutes and then disconnect it from the pumping system again. Repeat this until no more pressure buildup is observed. (Actually, two evacuation steps were found to be sufficient. If further evacuations were necessary, it should rather be interpreted as an indication of a leak in

the system.) Close stopcock DGS-2. (During this period the solution in the flask keeps boiling. No aids for smooth boiling were necessary. It was desirable to make the period during which the stopcock DGS-2 was open as short as possible, since excessive transfer of water and amine into the trap causes blockage of the trap and also changes the amine concentration in the flask markedly from the originally intended value.)

Keep evacuating the liquid-charging vessel and trap TDG-2 for five more minutes.

Transfer the degassed solution of the charging vessel as follows: Open regulator valves on the hydrogen tank. Adjust pressure between 50 and 100 pounds per square inch. Open valve DGV-1. See that the pressure-reading on gauge G-DG is in the pressure range just mentioned. Open valve DGV-3. Slowly open valve DGV-4. (This operation had to be done very carefully or the solution in the flask would rush up to the stopcock DGS-4, causing breakage of the glass part.) With the loose end of Tygon tubing, attached to stopcock DGS-4, inserted in a receiving flask, crack the stopcock DGS-4 for a second or two, just enough to replace the solution which has been trapped in the Tygon tubing with the degassed solution. Quickly connect the loose end of the Tygon tubing with the liquid-charging vessel. With stopcock DGS-4 still closed, open valve CV-1 and keep evacuating the transfer section for another minute. Close valve CV-2. Slowly open stopcock DGS-4. When the level of the degassed solution

in the degassing flask stops going down, check if the liquid-charging vessel has been really filled by cracking valve CV-2 for a second and seeing that droplets of solution spatter out of the downstream side of the valve. Close valves CV1 and CV2. Turn stopcock PS-5 to disconnect trap TDG-2 from the pump. Disconnect the vessel, which is now ready for charging. Wipe off any liquid hanging on its outside surface. Determine its total weight and record it.

Analyze the degassed solution for the amine-concentration as follows. Take about a 50-milliliter portion of the degassed solution in a breaker by slowly opening stopcock DGS-4. Pipet a 10-milliliter portion from it. Add two or three drops of 0.17% alcoholic solution of hydrochloric acid of either 1.0 or 0.2 normality, depending upon the concentration of amine. The end point of the titration is indicated by a change of color of the solution from blue to yellow at pH of 6.0 to 7.6. Repeat the titration three times and obtain an average value. (It is recommended that three titrations be finished within two or three minutes after the degassed solution is taken out of the degassing flask, because, otherwise, the difference in the vapor pressures of the amine and water would make the titration result considerably smaller than the initial value. The test showed that the apparent concentration of amine became 0.2 and 1.0 percent lower than the initial value after one normal solution was left standing in a 100 milliliter beaker for two and five minutes, respectively.) Calculate the amine concentration from the result, and record it.

Clean the used degassing system as follows. Isolate the degassing section by turning stopcock PS-4. Slowly open stopcock DGS-2 to fill the degassing section with hydrogen to a pressure a little over atmospheric. Close stopcocks DGS-1, DGS-2 and DGS-3. Close the regulator valves on the hydrogen tank. Close valves DGV-1, DGV-3 and DGV-4. Remove the Dewar jars on two traps. Detach the lower side of trap TDG-2 from the upper side and clean it. Carefully loosen the clamp which holds the lower side of trap TDG-1. It would be pushed down by the internal hydrogen pressure which had by then been raised much above the delivery pressure of the line-pressure regulator PR-DG. Take it off and clean it. (It would not be necessary to empty and clean the degassing flask if the next run would be for an amine concentration of roughly the same composition as the earlier one and with water of the same enrichment as the earlier one.)

G-4. Charging Aqueous Solution in Autoclave

Connect the liquid-charging vessel filled with degassed amine solution on the drain and ventillation lines of the charging system. Open valves CV-3 and CV-4 (Fig. C-1). Keep evacuating the autoclave for 30 minutes. Close valve CVV, and wait for about 30 minutes. See that a reading on the compound Bourdon gauge connected on the line between valves CV2 and CV4 roughly shows that the system has been evacuated. (If any amounts of liquid large enough to cause a large error in estimating the amounts of water and amine in the reaction vessel have been left over in the autoclave from the preceding

run, they would cause a large enough vapor pressure to be shown on the gauge.) Recheck that valves AV1, DV2, HV2, HV3 and CVV are closed.

Open valves CV1 and CV2. After one hour close valves CV1, CV2, CV3 and CV4. Disconnect the liquid-charging vessel (plus valves CV1 and CV2). After the charging vessel has been cooled to room temperature, weigh it and record the result. Subtract this weight from the weight measured before charging the content, and record the result, which is the weight of the solution charged.

Turn on the autoclave stirrer. Level off the temperature of the oil bath and the contents of the autoclave by changing and adjusting the temperature-controller dial and powers on the heaters following procedures similar to the one described in Subsection G-1 of APPENDIX. Then the system is ready for charging of hydrogen.

G-5. Charging Hydrogen Gas into Autoclave

Normally, the hydrogen-charging vessel is filled with natural hydrogen gas at pressures around 1,000 pounds per square inch from the preceding run, as mentioned later in this section. Open HV-4 (Fig. C-1). (Since HV4 is now open and HV-3 is closed, the standard gauge (0-2,500 psi) shows the pressure of hydrogen in the hydrogen-charging vessel, while another gauge (0-3,000 psi) on the other side of valve HV3 shows the pressure in the autoclave.) Check that the temperature is steady at the desired level. Put more hydrogen into the hydrogen-charging vessel to as

high a pressure as possible from the hydrogen tank. Close valve HV1. Wait until the temperature and, consequently, the pressure in the hydrogen-charging vessel attains a steady level. Read and record the pressure on the standard (test) gauge connected on the charging vessel. Carefully crack valve HV2. When the pressure in the autoclave becomes about 100 pounds per square inch below that in the charging vessel, close HV2. If the total pressure in the autoclave has not reached the desired value, recharge the hydrogen-charging vessel and repeat the charging procedures until the pressure in the autoclave becomes sufficiently high.

Close valve HV4, and open valve HV3. Read and record the total pressure in the autoclave on the standard gauge. (This pressure is used in computations for the liquid-vapor equilibria in the autoclave.)

Keep the hydrogen gas remaining in the charging vessel until the next run, because it reduces leakage through HV-2 during a run.

G-6. Starting a Run, Sampling and Storing Samples

Evacuate the sampling manifold and the purification section in the sample line of the analyzing system (Figs. C-1 and D-4) by opening valve AS-1, stopcocks AS-T2 and AS-T1 and valves AV2, AV2' and AVV. Close AVV. Close stopcock AS-T2 and valves AV2 and AV2'. Open and close valve AV1. Crack valves AV2 and AV2', and then close them. If the pressure reading on compound gauge GS-1 is lower than -15 inches Hg, repeat the sampling starting with opening and closing of

valve AV1. Read and record the total pressure in the autoclave on the standard gauge (0-2,500 psi). (This pressure is referred to as $p_{o,1}$ and is used to compute quantities of the reaction participants existing in the system just after the first sample is taken, these quantities being indicated by a subscript "1".) Leave the sample gas in the trap for about five minutes.

Meanwhile, turn on the autoclave-stirrer. Note and record the time. (This time is the time zero of the run.)

Evacuate storage bottle No. 1, the one on the extreme left in Fig. D-4, plus the stationary bulb of the Töpler pump through stopcock AS-V1 with stopcock AS-V1 and the "In"-stopcock on the bottle open and with the "Out"-stopcock on the bottle and "In"-stopcocks on all other storage bottles closed. Close stopcock AS-V1.

Open stopcock AS-T2 and valve AS-1. Manipulate the Töpler pump repeatedly until the pressure in the storage bottle No. 1 reaches about -10 inches Hg. Close the "In"-stopcock in storage bottle No. 1. (The sample thus stored is called sample No. 1.)

Open stopcock AS-V1 and "In"-stopcock on storage bottle No. 2 to evacuate storage bottle No. 2 and the stationary bulb of the Töpler pump. Keep evacuating until sample No. 2 has been trapped in TS-1. (Do not forget to close the stopcock AS-V1 when sample No. 2 becomes ready for storage.)

Flush the sampling manifold with nitrogen by opening the regulator valves on the nitrogen tank (Fig. C-1) and

valve AV-4 and then opening valves AVV and AVV3 in turn several times.

Start evacuating the sampling manifold and the purification section of the analyzing system through valve AVV about five minutes before the next sampling is scheduled.

G-7. Analyzing Samples

Zero point of the thermal conductivity is obtained as follows. The reference hydrogen gas normally fills the reference line between a hydrogen tank (Fig. D-4) and valve AR-2, the pressure in the part between line-pressure regulator PR-R1 and valve AR-2 being a little over atmospheric. Evacuate the reference line downstreams to valve AR-2 through AR-V. Evacuate the sample line downstream to the storage bottles through AS-V. Keep valve AR-2 closed. See that stopcock AS-V1 in the sample line is closed. Turn stopcock PS-5 in Pumping System No. 1 (Fig. D-1) so that the analyzing system is isolated from the pumping system. Open valve AR-2 so that the lines confined by AR-2, AS-3, AS-V1 and PS-5 are filled with hydrogen gas to a uniform pressure of about ten millimeters mercury. Evacuate the system again by opening stopcock PS-5. Close it and open valve AR-2 again to fill the system with hydrogen gas to a uniform pressure a little over 50 millimeter Hg. Close valves AR-V and AS-V. Open stopcock PS-5. Adjust the pressure in the sample line at 50 millimeters Hg by manipulating valve AS-V and metering valve AS-3 while watching manometer MM-S. Close stopcocks AS-TC1 and AS-TC2. Adjust

the pressure in the reference line at 50 millimeters Hg by manipulating valve AR-V and metering valve AR-2. Close stopcocks AR-TC1 and AR-TC2.

Turn the thermal conductivity-bridge-current on. Adjust it at 190 milliamperes by means of coarse and fine control dials and the Weston precision millimeter which has a backing mirror on the dial. Set the sensitivity at a desired value. Connect the bridge-output-terminals with the rectangular chart recorder. (The output for a zero-setting run normally starts with a high value and approaches a steady value from the higher side. This is caused by the way hydrogen gas is introduced into the sample line: since a larger amount of hydrogen gas is passed through the reference gas passage in the thermal conductivity cell than an amount of hydrogen which is passed through the sample gas passage, the reference channel is expected to be cooler than the sample channel in the beginning.) It normally takes two to four hours for an equilibrium value to be attained in a zero-setting run.

When a zero-setting run is over, turn off the current and then evacuate both lines. (It is important to turn off the current first because, otherwise, excessive heating of the filaments in the cell due to a decreased rate of heat loss might damage the filaments and might change the calibration.)

It is recommended that a zero-setting run be done once in every ten hours and every time the sensitivity settings are to be changed.

To analyze a sample gas, first evacuate all the sections in the sample line downstream to the storage section and the reference line downstream to valve AR-2.

Close valves AS-V and AR-V. Put a small amount of the sample to be analyzed from its storage bottle into the sample gas passage of the cell to a pressure of about 10 millimeters Hg. Open valve AS-V to evacuate the sample line again. Close AS-V and fully open the "Out"-stopcock on the storage bottle in which the sample to be analyzed is stored. Close valve AS-3. Adjust the pressure in the sample line at 50 millimeters Hg in the same manner as that used for the zero-setting run. Close stopcocks AS-TC1 and AS-TC2.

Fill the reference line with natural hydrogen gas and adjust its pressure at 50 millimeters in a manner similar to that used for the sero setting run. Close stopcocks AR-TC1 and AR-TC2.

Turn the bridge current on. Adjust it at 190 milli-amperes. Always use the same sensitivity-setting as that used in the last zero-setting run. It takes up to two or two and a half hours for a steady value to be reached in an analyzing run.

When an analyzing run is over, turn off the current and then evacuate both lines.

Perfect electrical insulation of the lead wires for the filaments is essential. Output oscillation with frequencies higher than once in every ten seconds and amplitude of around 0.5 millivolts are indications of faulty insulation.

G-8. Terminating a Run and Discharging Remaining Contents

Stop the autoclave-stirrer. Turn on cooling water for the discharging system (Fig. C-1).

Before the start of the discharging operation, valves NV-1 and NV-6 are closed, and valves DV-1 and DV-4 are open. Carefully crack valve DV2 and adjust it so that the waste liquid comes out of the cooling system with a rate around two drops per second. When the rate starts to decrease, open DV2 completely. Leave it open for about thirty minutes. Then close it.

Check that valves AV2, AV2', Av3, AVV and NV1 are closed. Open the regulator valves on the nitrogen tank. Open valves AV4 and AV1. Adjust pressure to around 220 pounds per square inch. Open valve DV2 as wide as possible without blowing off the rubber tubing connecting the steel condenser with the waste receiver. Keep DV-2 open for about ten minutes and then close it. Open valve DV3. Keep it open for about five minutes. Close it and turn off the cooling water for the discharging system.

G-9. Shutting Down the Constant Temperature Oil Bath

Turn the Variac regulator for the internal heater off. Turn the fine control know for the external heater-regulator to the midpoint. See that the external heater-current is close to zero. Turn off the temperature controller. Turn the internal heater-Variac off. Turn the external heater off. See that pilot lamps for the external heater and the controller are off and only that for the bath-stirrer is on. Note the time.

If no more samples remain to be analyzed, close the stopcocks PS-1, PS-2, PS-6 and PS-7.

One hour after the heaters are shut off, turn off the oil bath-stirrer. See that the pilot lamp is off. Turn off all the cooling water.

Turn off the room-exhuast fan.

G-10. Analyzing Hydrogen Gas for Chemical Impurities

The principle of analysis is described in Sections D-1 and D-4 of APPENDIX.

To analyze hydrogen gas in a tank against total chemical impurities, first connect the tank with the chemical gas-analyzing system by making a copper-to-copper joint between the tank-pressure regulator and needle valve CM-V1 (Fig. D-10).

With the tank-regulator valves closed and the levelling bulb of the Töpler pump raised so that the stationary bulb is filled with mercury to its top, open all the stopcocks and valves in the system except stopcock CM-S3 so that all parts in the system are interconnected, and then evacuate the entire system through stopcock CM-S3. (When opening stopcock CM-S2 to connect the manometer with the rest of the system, care should be taken lest mercury in the manometer rush in either direction, depending on relative pressures.) Turn on the electric furnace to heat it up to about 600°C, reading the temperature with an iron-constantan thermocouple. Keep evacuating for 48 hours. Turn off the furnace.

Turn stopcock CM-S3 so that only the line on its right in Fig. D-10 is connected with the pumping system. Turn

stopcock CM-S4 so that only the line on its right in Fig. D-10 is connected with stopcock CM-S3. Close valves CM-V3 and CM-V4. Open the tank valve. Open slightly the tank-regulator valves so that the delivered pressure reads between 10 and 16 pounds per square inch above atmospheric on compound gauge G-CM. Close valve CM-V1. Open valve CM-V4. When the gauge shows near vacuum, close valve CM-V4. Repeat more than five times the process of flushing the line between the hydrogen tank and its pressure regulator by opening and closing valve CM-V1 followed by opening and closing valve CM-V4.

Flush the entire system with hydrogen gas as follows. When the temperature of the electric furnace becomes below 200°C, turn stopcock CM-S3 so that the system is disconnected from the pumping system but the lines on its left and right in Fig. D-10 are interconnected. Also, turn stopcock CM-S4 so that all of three lines extending from it are connected together. Open and close valve CM-V1. Carefully open valve CM-V3. When manometer MM-CM shows steady pressure, close valve CM-V3. Evacuate the entire system for one hour. Repeat the flushing.

Place a Dewar jar containing liquid nitrogen around the liquid nitrogen trap. (The jar has to be refilled repeatedly during the rest of the operation to make up loss due to warm gas coming out of the furnace.) Turn on the furnace and bring the temperature up to 500°C while the system is kept evacuated. Then the system has been conditioned and is ready for analysis.

Charge a sample portion of hydrogen gas to be tested to the 100 millliliter bulb, as follows. Turn stopcock CM-S1 so that the 100 millliliter bulb is connected only with the line extending down from stopcock CM-S1 in Fig. D-10. Turn stopcock CM-S3 so that two horizontal lines on it in the figure are interconnected but isolated from the pump. Turn stopcock CM-S4 so that two horizontal lines on it in the figure are interconnected but disconnected from the vertical line extending from the stopcock. Open valve CM-V1. Adjust the tank-regulator so that delivered pressure read on gauge G-CM becomes about 20 pounds per square inch. Close valve CM-V1. Carefully open valve CM-V4. Read the pressure of hydrogen in the bulb on manometer MM-CM. Repeat the charging of hydrogen again using 20 pounds per square inch as the source pressure. The manometer should read more than 10 centimeters Hg. Read the pressure as accurately as possible, and record the result. Turn stopcock CM-S1 so that the bulb is isolated from the rest of the system. Turn stopcock CM-S3 to evacuate parts of the system, except the bulb, that are filled with hydrogen. Close the stopcock so that the system is isolated from the pump. Turn stopcock CM-S4 so that the lines on its left are connected only with the vertical line extending from the stopcock. Now all parts in a square-shaped loop in Fig. D-10, consisting only of glass parts and going through stopcocks CM-S1, CM-S4 and CM-S5 should be interconnected in either way, except that an inlet line on Töpler pump is not directly connected with an outlet line on it.

Perform an analysis as follows. Turn stopcock CM-S1 so that all of three lines extending from it are interconnected. Circulate the gas, manipulating the Töpler pump so that the gas flows to the left in the upper horizontal line in Fig. D-10 and to the right in the lower horizontal line in the figure. Repeat the operations of suction and discharge of the gas through the pump about ten times. Turn the three-way stopcock, which is on the outlet line of the pump and just below a collecting tube and is called collecting tube-stopcock, so that the collecting tube is connected only to the outlet line of the pump. Collect any residual gas remaining in the loop and in the 100 milliliter bulb in the collecting tube by repeating the pump operation. Every time a portion of gas is pushed out, raise the levelling bulb until the mercury level in the other branch of the pump reaches a line marked on the collecting tube, and measure pressure of the collected gas by reading a difference in mercury levels in two branches of the pump. Repeat the collecting operation until no more increase in the pressure is obtained by further repetition. Record the final pressure. Then release the collected gas by turning the collecting tube-stopcock so that the three lines extending from it are all interconnected. Repeat the entire procedure described above starting with the circulation of the released gas. Record a final pressure of residual gas collected in the collecting-tube for the second time. If the pressure of the residual gas collected for the second time is smaller

than that in the first collection, repeat the entire procedure, although the first two trials are usually sufficient.

Compute the total mole fraction of the impurities in the sample gas by using the perfect gas law and the known volumes of the sample gas (100 milliliters) and the residual gas (2.4 milliliters) and the measured values of the pressures of the sample and residual gases.

Evacuate the system, and repeat the analysis with another portion of hydrogen gas being tested.

H. Evaluation of the Thermodynamic Properties of Water, Diethylamine, and the Mixture of Water and Diethylamine

The following thermodynamic properties had to be evaluated to process the measured data:

Specific volume of liquid at various temperatures, v_f ml/g

Specific volume of vapor at various temperatures and pressures, v_g ml/g

Vapor pressure of liquid at various temperatures, π atm.

The temperature range was from 100°C to 200°C, and the pressure range was from vacuum to about 16 atmospheres. In evaluating these properties, no attempt was made to treat the various isotopic species of a chemical compound separately. It was assumed that intensive and molar properties of a compound of the natural enrichment represented those of higher enrichment. The assumption was justified because, first, the highest enrichment of deuterium that occurred in the entire system was about 27% atom fraction deuterium in water, and, secondly, these properties thus obtained were used only in calculating the liquid-vapor phase equilibria. It was also assumed that hydrogen gas behaved as an ideal gas in both the gaseous phase and the dissolved state.

Data on water were taken from the Steam Tables (H-1). Available data on diethylamine were mostly limited to the temperatures below its normal boiling point or to conditions along its vapor pressure curve. It was therefore necessary to obtain properties of pure diethylamine by applying the

principle of corresponding states to known data on ammonia. Subscripts 0, 1, and 2 were used to represent properties of hydrogen gas, water, and diethylamine, respectively.

H-1. Properties of Pure Water

Data in the Steam Tables were converted to the units of the present work as shown in Table H-I.

Table H-I

Properties of Saturated Water

Temperature (^{o}C)	π_1 (atm)	v_{f_1} (ml/g)	$v^s_{fg_1}$ (ml/g)	$v^s_{g_1}$ (ml/g)
100	1.000	1.045	1735.6	1736.8
150	4.69	1.091	391.37	392.5
200	15.35	1.158	126.03	127.18

For a superheated steam, an equation taken from the Steam Table was used.

$$v_{g1} = \frac{4.555\ T}{P_o} + \beta_1 \qquad \text{(H-1)}$$

$$\beta_1 = 1.80 - \frac{2641.6}{T}\ 10^{\frac{80870}{T^2}} \qquad \text{(H-2)}$$

H-2. Properties of Pure Diethylamine

(a) Vapor Pressure

An empirical formula was obtained form "Advances in Chemistry Series, No. 29; Physical Properties of Chemical Compounds, III", (H-2).

$$\log_{10} p \text{ (mmHg)} = 7.14099 - \frac{1209.9}{t(^{\circ}C) + 229}$$

This was modified so that the equation goes through the critical point, $T_c = 223.5^{\circ}C$ and $P_c = 36.2$ atmospheres as follows:

$$\log_{10} p \text{ (mmHg)} = 7.14099 - \frac{1209.9}{t(^{\circ}C) + 224} \qquad \text{(H-3)}$$

Results obtained by using Eqn. (H-3) are tabulated in Table H-II.

Table H-II

Vapor Pressure of Diethylamine

Temperature ($^{\circ}C$)	Vapor Pressure, π_2, (atm)
100	3.73
150	10.93
200	25.31

(b) Specific Volume of Diethylamine Vapor

There were no data available on superheated diethylamine, and it had to be obtained by applying the principle of corresponding states to ammonia. To prove that diethylamine and ammonia have properties identical with each other at the same reduced temperature and pressure, Eqn. (H-3) was converted to Eqn. (H-4) which was expressed in terms of reduced temperature, T_r, and reduced pressure, P_r, and the latter was compared with numerical data on the vapor pressure of ammonia taken from the National Bureau of Standards, Circular No. 142, (H-3).

$$\log_{10} p_r = 2.702 - \frac{1210}{496.6\ T_r - 44} \qquad \text{(H-4)}$$

The critical data used are tabulated in Table H-III.

Table H-III

Critical Data of Ammonia and Diethylamine

	Critical Temperature (°C)	Critical Pressure (atm)
Ammonia	132.4	111.5
Diethylamine	223.5	36.2

The comparison is illustrated in Fig. (H-1). It is seen that the agreement was very good. To prove the point still another way, empirical formulae for the density of saturated vapor of diethylamine, obtained from the same source as the vapor pressure data, (H-2), were compared with numerical data taken from the NBS Circular No. 142. The empirical formulae are given by Eq's (H-5) and H-6).

$$\log_{10}\rho_g = 1.456 - \frac{1137}{496.6\ T_r - 49} \quad \text{for } -15^\circ C \leqslant t \leqslant 80^\circ C \qquad \text{(H-5)}$$

$$\log_{10}\rho_g = 1.291 - \frac{1137}{496.6\ T_r - 49} + \frac{0.0640}{1.1 - T_r} \quad \text{for } 80^\circ C \leqslant t \qquad \text{(H-6)}$$

The comparison was illustrated in Fig. (H-2). It is seen that the agreement again is satisfactory.

Upon these bases a formula for the specific volume of superheated ammonia (H-4) is given by

$$v_g = \frac{4.555\ T}{p} + \beta_2 \qquad \text{(H-7)}$$

where

$$\beta_2 = 2.653 - \frac{2355.8}{T}\ 10^{\frac{31820.3}{T^2}} \qquad \text{(H-8)}$$

was converted for use with diethylamine. It is given by

$$v_{g_2} = \frac{1.205\ T}{p_2} + \beta_2 \qquad \text{(H-9)}$$

where

$$\beta_2 = 2.653 - \frac{2890}{T}\ 10^{(\frac{219}{T})^2} \qquad \text{(H-10)}$$

Equations (H-9) and(H-10) were used to compute v_{g_2} at a given temperature and a partial pressure of diethylamine.

(c) Specific Volume of Diethylamine in the Liquid State

The specific volume of the saturated liquid of diethylamine was used for the liquid under other pressures. It was obtained by means of the compressibility factor, z_{f_2}, discussed by Meissner and Paddison (H-5). The results are tabulated in Table H-IV.

Table H-IV

Properties of Saturated Liquid of Diethylamine

Temperature (°C)	z_{f_2}	v_{f_2} (ml/g)
100	0.014	1.572
150	0.044	1.923
200	0.115	2.415

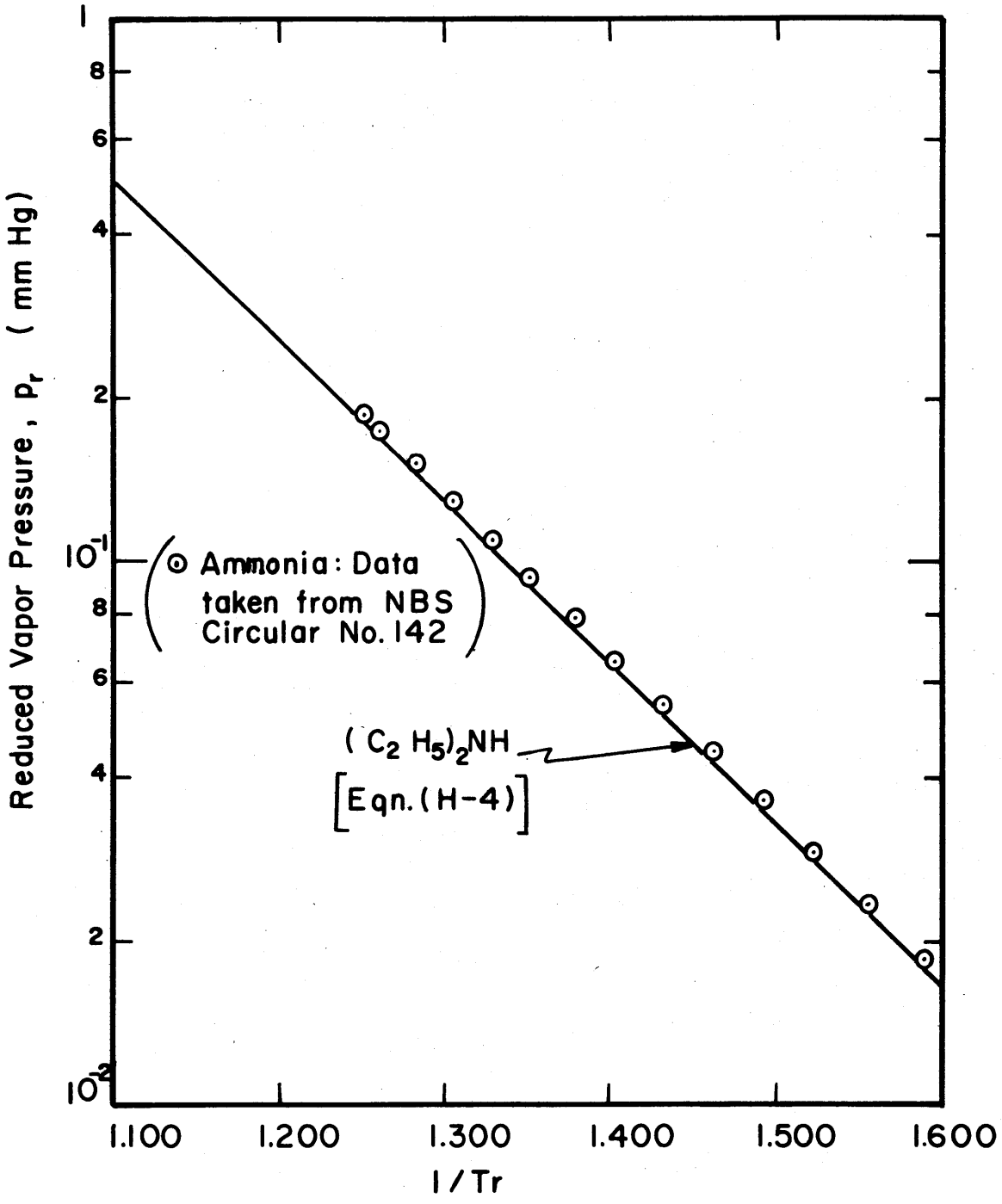

Fig. H-1 Comparison of Vapor Pressures of Ammonia and Diethylamine

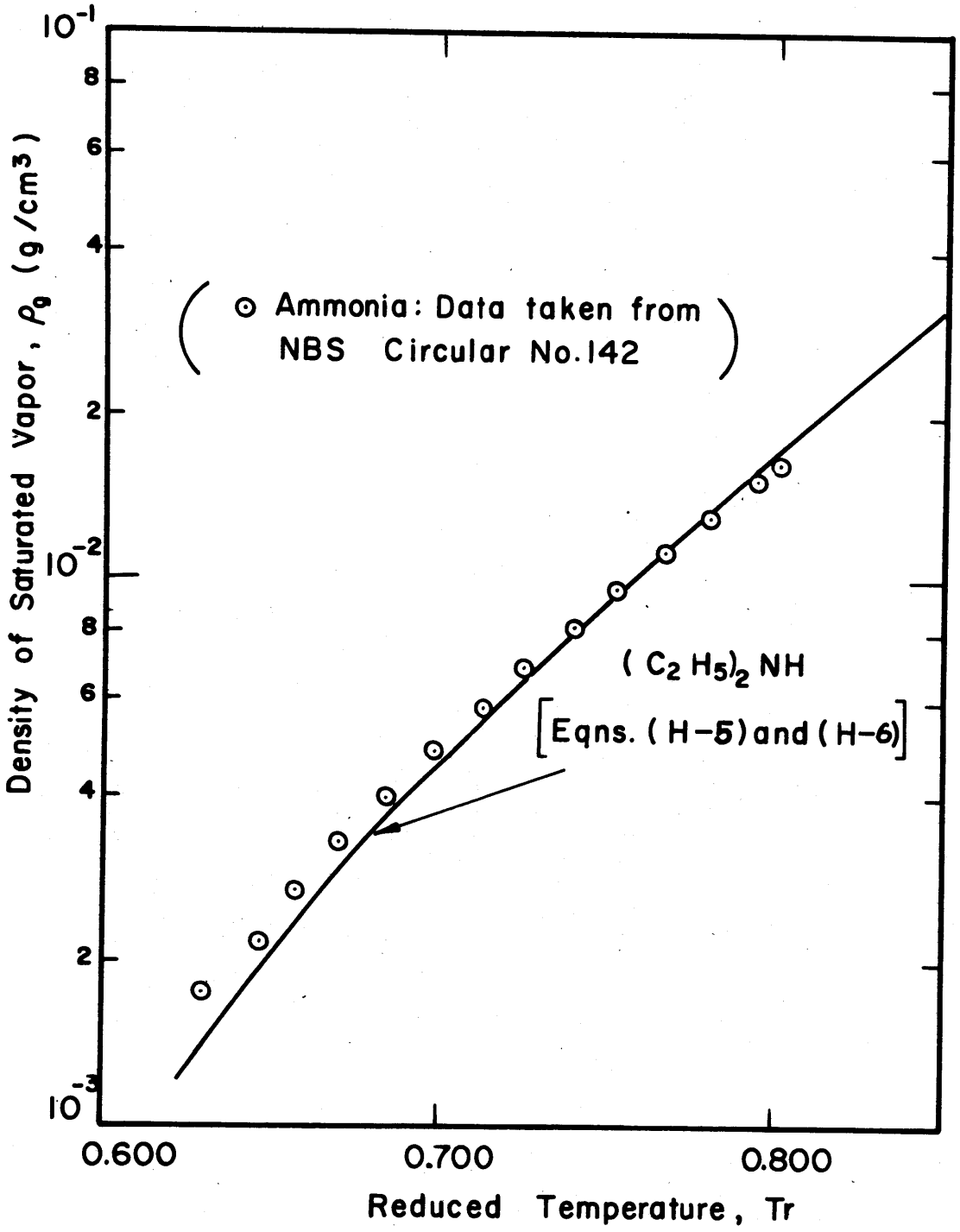

Fig. H-2 Comparison of Densities of Saturated Vapors of Ammonia and Diethylamine

With these values of v_{f_2} and those values of v_{g_2} obtained from Eqn. (H-9), v_{fg_2} was computed by

$$v_{fg_2} = v_{g_2} - v_{f_2} \qquad \text{(H-11)}$$

H-3. Properties of Mixture of Water and Diethylamine

Both liquid and vapor phases were assumed to be ideal because there was no other alternative. The assumption is discussed in APPENDIX, Section L. It was found that the assumption of ideality was satisfactory for the present problem.

In analyzing the experimental data, it was necessary to know the atom fraction of exchangeable deuterium, f_d, charged to the autoclave. This was determined as follows. A mixture of light and heavy water of known deuterium atom fraction, j, was prepared by mixing measured weights of natural water and heavy containing 99.95 atom percent deuterium. This water was mixed with natural diethylamine, and the normality, N, of amine in the mixture was determined by titration with standard hydrochloric acid using bromthymol-blue as the indicator. The f_d, j and N are related by

$$f_d = \frac{j}{1 + \frac{(18.02 + 2j)\ N}{2\ (1000\rho - 73.14N)}} \qquad \text{(H-11-a)}$$

To find a relation between the density, ρ, and normality of amine, N, an experiment was carried out, which is described below.

A dilute amine solution in water of a known enrichment, the same enrichment as the one used for the exchange reaction, was placed in a measuring cylinder which was deep enough for use with an hydrometer about 14 inches long. The measuring cylinder was placed in a deep glass jar which was filled with water at room temperature, 25°C, whose level was kept several inches higher than the level of the amine solution inside the smaller cylinder. When the temperature reached a steady value, room temperature, a five milliliter portion of the solution was pipetted out and titrated for amine content with a standard solution of hydrochloric acid of either one or 0.2 normality, depending on the concentration of amine, using bromthymol blue as indicator. At the same time that a sample for titration was taken, a specific gravity value was read on the hydrometer. The hydrometer used was graduated from 0.940 to 1.010 specific gravity with 0.001 specific gravity intervals. The hydrometer reading had to be multiplied by the density of water at 60°F, which was 0.999. More amine was then added to the remaining solution. The solution was stirred well and left standing until the temperature settled down to room temperature. The pipetting and the hydrometer reading were then repeated. These procedures were repeated until the desired range of the amine concentration had been covered.

Because two different initial enrichments were used for heavy water in the exchange reaction, two series of such experiments were performed. The results were tabulated in Tables H-V and H-VI.

Table H-V

Experimental Results on Relation between Amine Concentration and Density of a Solution--1N Runs*

Amine Concentration (Normal)	Density (g/ml at 25°C)
0.607	1.0091
1.052	1.0010
1.518	0.9940
1.765	0.9899

* Heavy Water used was of 22.85% atom fraction deuterium.

Table VI

Experimental Results on Relation between Amine Concentration and Density of a Solution--2N Runs*

Amine Concentration (Normal)	Density (g/ml at 25°C)
0.420	1.0070
0.836	1.0005
1.176	0.9945
1.604	0.9870
1.944	0.9800

* Heavy Water used was of 26.67% atom fraction deuterium.

The best fit linear relations were obtained through the standard method of the least-squares analysis. For runs which employed heavy water of 22.85 atom % deuterium.

$$\rho = - 0.01637N + 1.0188 \qquad \text{(H-12)}$$

and for runs which used heavy water of 26.67 atom % deuterium,

$$\rho = - 0.01767N + 1.0149 \qquad \text{(H-13)}$$

Using Eq's (H-11-a), (H-12) and (H-13), f_d was computed as follows. For "1N" and "blank" runs (using water containing 22.85 atom % D).

$$f_d = \frac{0.2285}{1 + \frac{N}{0.1084\ (1000\rho - 73.14N)}} \qquad \text{(H-14)}$$

For 2N runs (using water containing 26.67 atom % deuterium)

$$f_d = \frac{0.2667}{1 + \frac{N}{0.1080\ (1000\rho - 73.14N)}} \qquad \text{(H-15)}$$

H-4. Henry's Law Constant of Hydrogen in Water-Diethylamine

The values of Henry's law constant of hydrogen gas in pure water were available in the International Critical Tables (H-6) for the temperatures ranging from zero to 100°C. It showed that the constant exhibited a sharp increase with temperature from 0°C until at 55°C the constant took on a maximum value of $c = 5.81 \times 10^7$ mmHg/mole fraction H_2, after which the constant slowly decreased. The plot is shown in Fig. (H-3). An extrapolation to higher temperatures gave rough estimates of the value of the constant at 150°C and 200°C. The results are tabulated in Table H-VII. An estimated probable error of $P(c) = 0.05 \times 10^7$ was a very conservative one. We conclude that

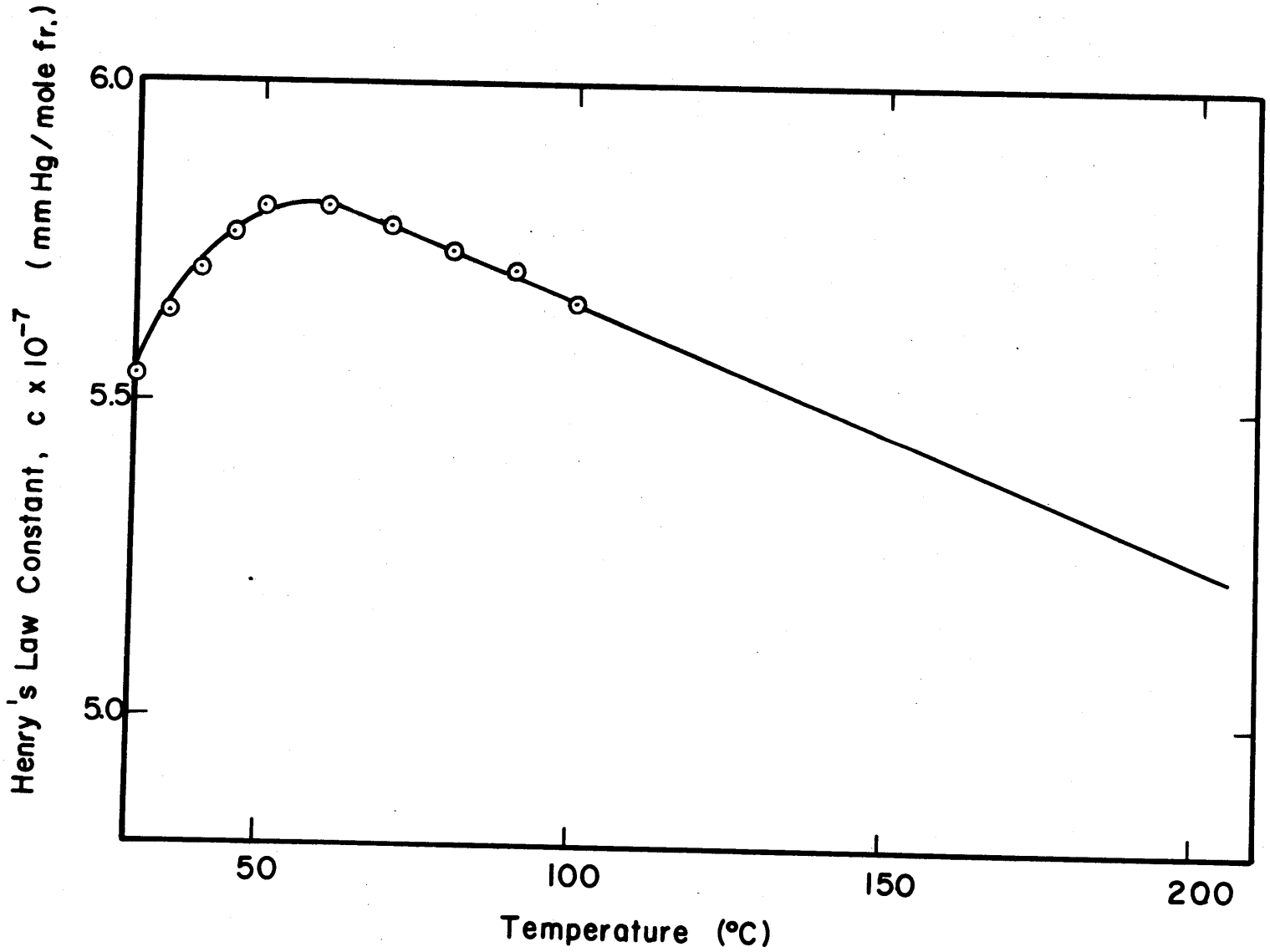

Fig. H-3 Henry's Law Constant for Hydrogen in Water

$$\frac{P(c)}{c} \cong 0.01 \qquad \text{(H-16)}$$

Table H-VII

Henry's Law Constant

Temperature (°C)	Constant (mm Hg/mole fr. H_2)
100	5.66×10^7
150	5.46×10^7
200	5.26×10^7

There were no data available for hydrogen gas in an amine solution, but data for hydrogen and aqueous solutions of organic acid of comparable degrees of ionization, available in the International Critical Tables (H-7), indicated that the effect of addition of weak electrolytes such as acetic acid, monochloracetic and, presumably, diethylamine on Henry's law constant was negligibly small.

H-5. Equilibrium Constants of Isotopic Exchange Reactions

Values of the equilibrium constant K for the liquid-phase reaction

$$H_2(l) + HDO(l) \rightleftharpoons HD(l) + H_2O(l)$$

were needed in working up experimental data. These were obtained from the equilibrium constant 1/K' for the reverse gas-phase reaction

$$HD(g) + H_2O(g) \rightleftharpoons H_2(g) + HDO(g)$$

quoted by Kirschenbaum (H-8) and plotted in Fig. H-4. The

relationship between K and K' is

$$K = K' \left(\frac{\pi_{HDO}}{\pi_{H_2O}}\right)\left(\frac{c_{H_2}}{c_{HD}}\right) \qquad \text{(H-17)}$$

The ratio of the vapor pressure of HDO to H_2O ($\pi HDO/\pi_{H_2O}$) is given in Table J-1. It has been assumed that Henry's law contants (c) for H_2 and HD are equal. Table H-VIII gives values of 1/K' interpolated from Fig. H-4 to the temperatures used in this work and value of K calculated from Eqn. (H-17).

Table H-VIII

Equilibrium Constant for the Reaction,

$H_2 + HDO \rightleftharpoons HD + H_2O$

Obtained from Kirschenbaum (H-8)

Temperature (°C)	1/K'	K
100	2.63	0.370
150	2.29	0.433
200	2.09	0.478

Kirschenbaum's equilibrium constants were obtained from values calculated from spectroscopic data by Kimball and Stockmayer (H-9) and Libby (H-10). More recent experimental data by Cerrai et al (H-11) give values of 1/K', about 5% lower than Kirschenbaum. As this difference is within the experimental error of the measured values and as there is

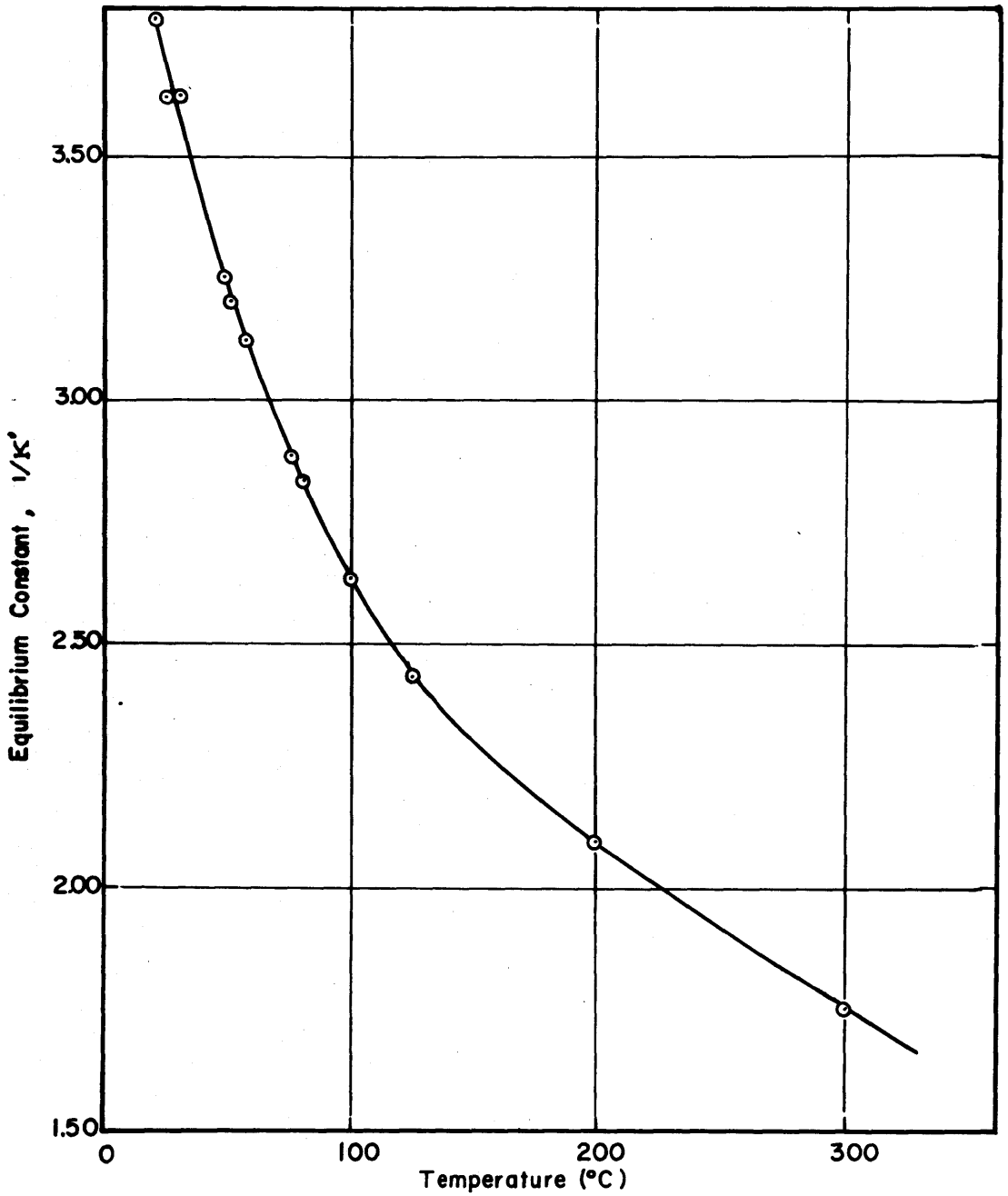

Fig, H-4 Equilibrium Constant for a vapor phase reaction
$HD + H_2O = H_2 + HDO$

some reason to believe that the calculated values are more precise, the calculated values have been used in the primary reduction of the present reaction-rate data. To show the effect on the reaction-rate constant of using a different value of the equilibrium constant, the reaction-rate data have also been worked up with a value of K obtained from Cerrai's experimental data and Eqn. (H-17). The three sets of values of K are given in Table H-IX.

Table H-IX

Three Sets of Equilibrium Constants K

for Liquid Phase Reaction

$H_2 + HDO \rightleftharpoons HD + H_2O$

Temperature (°C)	K	
	Cerrai, Measured	Kirschenbaum, Calculated
100	0.382	0.370
150	0.446	0.433
200	0.501	0.478

Values of the equilibrium constant, K_w, of the reaction

$$H_2O\ (l) + D_2O\ (l) \rightleftharpoons 2HDO\ (l)$$

were obtained by extrapolation to higher temperatures of the data available for the temperatures below 125°C. The data are tabulated in Table H-X.

Table H-X

Equilibrium Constant, K_W, of the Reaction

H_2O (l) + D_2O (l) = 2HDO (l)

Temperature (°C)	K_W **
0	3.76
25	3.80
50	3.83
75	3.85
100	3.87
125	3.89
150	3.91 *
175	3.93 *
200	3.95 *

* These are the values obtained by extrapolation.

** K_W tends to 4.00 as the temperature increases. The data are taken from Kirschenbaum (H-8).

I. Derivation of Formulae for Liquid-Vapor Equilibrium of the System, Hydrogen-Water-Diethylamine

To interpret experimental results properly it was necessary to know the compositions of liquid and vapor phases in equilibrium with each other in the system, hydrogen-water-diethylamine. The procedure used for calculating these compositions for given values of the temperature, T, the pressure, P, the total volume, V^o, and the total amounts of water, w_1, and diethylamine, w_2, will be described. Because of the lack of equilibrium data for the system of water-diethylamine, the ideal laws were assumed for the solutions in both phases. The evaluation of the thermodynamic properties of the pure components are presented in Section H of the APPENDIX. The same value was used for a thermodynamic property for all isotopic species of a chemical compound. The validity of the ideal laws of the solution are discussed in Section L of the APPENDIX. Sample calculations are shown in Section K of the APPENDIX.

For an ideal gaseous solution,

$$V_g' = V^o - m_1 v_{f1} - m_2 v_{f2} = \frac{n_o' RT}{p_o} \qquad \text{(I-1)}$$

$$= (W_1 - m_1)\, v_{g1} \qquad \text{(I-2)}$$

$$= (W_2 - m_2)\, v_{g2} \qquad \text{(I-3)}$$

If both phases are ideal,

$$p_o = p - (\pi_1 x_1 + \pi_2 x_2) \qquad \text{(I-4)}$$

where

$$x_1 = \frac{\frac{M_2}{M_1} m_1}{\frac{M_2}{M_1} m_1 + m_2} \qquad \text{(I-5)}$$

$$x_2 = 1 - x_o - x_1 \simeq 1 - x_1 \qquad \text{(I-6)}$$

Eqn. (1-2) could be approximated by

$$V^o - m1v_{f1} - m_2v_{f2} = (W_1 - m1)\ v^s_{g1}$$

since the mole fraction of water in the liquid phase was always in the vicinity of 0.98. Then, setting

$$v^s_{g1} - v_{f1} \equiv v_{fg1} \qquad \text{(I-7)}$$

and

$$W_1v^s_{g1} - V^o \equiv \Delta V_1 \qquad \text{(I-8)}$$

this relation becomes

$$v_{fg1}m_1 - v_{f2}m_2 = \Delta V_1 \qquad \text{(I-9)}$$

Similarly, from Eqn. (I-3),

$$- v_{f1}m_1 + v_{fg2}m_2 = \Delta V_2 \qquad \text{(I-10)}$$

where

$$v_{g2} - v_{f2} \equiv v_{fg2} \qquad \text{(I-11)}$$

$$W_2v_{g2} - V^o \equiv \Delta V_2 \qquad \text{(I-12)}$$

Solving Eqs. (I-9) and (I-10) for m_1 and m_2,

$$m_1 = \frac{v_{fg2}\ \Delta V_1 + v_{f2}\ \Delta V_2}{v_{fg1}\ v_{fg2} - v_{f1}\ v_{f2}} \qquad \text{(I-13)}$$

$$m_2 = \frac{v_{fg1}\,\Delta V_2 + v_{f1}\,\Delta V_1}{v_{fg1}\,v_{fg2} - v_{f1}\,v_{f2}} \qquad \text{(I-14)}$$

Estimation of m_1, or m_2, involved a trial and error procedure because the specific volume of the vapor of diethylamine was a function of its partial pressure, which in turn was a function of the concentration in the liquid phase. The relation is given by Eqn. (H-9).

Other equilibrium quantities were obtained by using thus obtained values of m_1 and m_2 as follows:

$$m_1' = W_1 - m_1 \qquad \text{(I-15)}$$

$$m_2' = W_2 - m_2 \qquad \text{(I-16)}$$

$$n_o' = \frac{p_o V'}{RT} \qquad \text{(I-17)}$$

where p_o and V' were obtained by using Eqns. (I-1) and (I-4). The amount of hydrogen gas dissolved in the liquid phase was calculated by using Henry's law constant c. By definition

$$x_o = \frac{760\ p_o}{c}$$

and

$$x_o = \frac{n_o}{n_o + n_1 + n_2} \simeq \frac{n_o}{n_1 + n_2}$$

Therefore,

$$n_o = \frac{760\ p_o\ (n_1 + n_2)}{c} \qquad \text{(I-18)}$$

The same equations applied for blank runs if W_2 and m_2 were set to be zero. It was assumed that not only the total amounts of water and diethylamine in the system but also their distribution between two phases remained unchanged

throughout a run, in spite of the fact that some gaseous samples were taken out of the system. This assumption was proved to be acceptable by actually calculating the equilibrium quantities of water and amine in the system after every sampling in Runs 9 through 16, using the total pressure data after the sampling. The calculation is illustrated in Section K of the APPENDIX. However, the amounts of hydrogen gas did have to be re-evaluated after every sample was taken because the amount of sample gas needed for flushing the sample line and for analyzing was so large that the total pressure of the system went down appreciably and the decrease could not be neglected. Therefore, the initial conditions had to be re-evaluated for each sample of a run. The procedure is discussed in Section J of the APPENDIX.

J. Derivation of Formulae for the Rate Constant of the Exchange Reaction

Processing the data of this work required that three problems be solved consecutively. These were first, to calculate the chemical compositions of liquid and vapor in equilibrium with each other for a given set of conditions and total charge in the reactor system; second, to find the isotopic compositions of thus distributed water and diethylamine, thus determining the initial conditions; and third, to solve a rate equation for the exchange reaction and see if the data fit the presupposed theory. The first problem was treated in Section I of the APPENDIX. The last two problems are discussed in this section.

J-1. Basic Formulae for the Rate Constant

(a) Equilibria between Isotopic Species of Water and Diethylamine

The following equilibria in the liquid phase were taken into consideration

$$\underset{(1-\xi_1)}{(C_2H_5)_2NH} + \underset{(\xi_1)}{HDO} = \underset{(\xi_1)}{(C_2H_5)ND} + \underset{(\xi_o)}{H_2O} \qquad \text{(J-1)}$$

$$\underset{(1-\xi_1)}{(C_2H_5)_2NH} + \underset{(1-\xi_o-\xi_1)}{D_2O} = \underset{(\xi_1)}{(C_2H_5)_2ND} + \underset{(\xi_1)}{HDO} \qquad \text{(J-2)}$$

$$\underset{(\xi_o)}{H_2O} + \underset{(1-\xi_o-\xi_1)}{D_2O} = \underset{(\xi_1)}{2HDO} \qquad \text{(J-3)}$$

The symbols under each chemical formula indicate the mole fraction of that isotopic species in the chemical compound. As discussed in Section L of the APPENDIX, hydrogen atoms in the ethyl group do not undergo exchange with water. The equilibrium condition for Eqn. (J-3) is

$$k_w = \frac{\xi_1^2}{\xi_o (1 - \xi_o - \xi_1)} \qquad \text{(J-4)}$$

No experimental data were available for the isotopic exchange equilibria involving diethylamine. It was assumed that the separation factor of the deuterium-exchange reactions between water and diethylamine was unity at the temperatures used; that is, the isotope effect was negligible for the reactions involving such large molecules as diethylamine. This assumption is justified in Section L of the APPENDIX, based on the findings on isotopic exchange reactions between water and other amines.

Thus,

$$r_a = \frac{\zeta_1}{1 - \zeta_1}$$

and

$$r_w = \frac{\xi_1 + 2 (1 - \xi_o - \xi_1)}{2\xi_o + \xi_1}$$

Equating r_a and r_w,

$$\zeta_1 = \frac{2 - (\xi_1 + 2\xi_o)}{2} \qquad \text{(J-5)}$$

From the material balance on deuterium atoms in the system,

$$\left[\xi_1 + 2 (1 - \xi_o - \xi_1) \right] n_1 + \zeta_1 n_2 = r_d \qquad \text{(J-6)}$$

Eliminating ξ_1 and ζ_1 from Eqns. (J-4), (J-5), and J-6),

$$(4-Kw)\eta^2 + \left[K_w - 2f_d\ (4-K_w)\right]\eta + 2f_d\ (2f_d - K_w) = 0 \qquad \text{(J-7)}$$

where $\eta = 1 - \xi_o$

and $$f_d = \frac{n_d}{2n_1 + n_2} \qquad \text{(J-8)}$$

The value of f_d was computed by Eqn. (H-11-a) using the known atom fraction deuterium in water, j, and the normality of the amine solution, N, obtained from acid-base titration of a sample taken from an amine solution which was later charged in the autoclave for the run.

The coefficients on the terms of η^2 and η of Eqn. (J-7) were positive for the experimental conditions used, while the last term was negative. Therefore, one root of Eqn. (J-7) was positive and the other was negative. Using the positive root for η, values for the mole fraction of H_2O (ξ_o) and of HDO (ξ_1) in total water may be obtained from

$$\xi_o = 1 - \eta \qquad \text{(J-9a)}$$

$$\xi_1 = 2\ (\eta - f_d) \qquad \text{(J-9b)}$$

$$\zeta_1 = f_d \qquad \text{(J-9c)}$$

Using these values, the inital amounts of the reactants corresponding to the equilibrium conditions before taking the zero point sample of a run were calculated as follows.

Initial amount of H_2 : $A_0 = n'_{o,0}$ (J-10a)

Initial amount of HDO : $B_0 = \xi_1(n_{1,0} + n_{1,0})$ (J-10b)

Initial amount of HD : $C_0 = 0$ (J-10c)

Initial amount of H_2O : $D_0 = \xi_o\ (n_{1,0} + n'_{1,0})$ (J-10d)

Initial amount of $(C_2H_5)_2NH$: $E_0 = (1 - \xi_1)\ (n_{2,0} + n'_{2,0})$ (J-10e)

Initial amount of $(C_2H_5)_2ND$: $G_0 = \xi_1(n_{2,0} + n'_{2,0})$ (J-10f)

In the symbols used above, the first subscript represents a compound while the second one refers to a sample number. As mentioned in Section I of the APPENDIX, the initial conditions had to be re-evaluated for each of all the other samples. This is treated in the last part, Part (c), of the present subsection.

The portion of deuterium that was initially taken up by diethylamine represented about 1% of the total deuterium atoms and had been known to undergo rapid exchange with hydrogen atoms in water. Therefore, the deuterized amine was regarded as an additional source of deuterium available for exchange with hydrogen gas, delivering deuterium atoms continuously and rapidly to water.

(b) Rate Equation and Its Solution

The rate of the overall reaction

$$H_2 + HDO \longrightarrow HD + H_2O$$

is to be considered. To this reaction is coupled the equilibrium in the liquid phase, among isotopic species of water and diethylamine.

Thus,

$$\underset{(A-X)}{H_2} + \underset{(B-Y)}{HDO} \rightleftharpoons \underset{(C+X)}{HD} + \underset{(D+Y)}{H_2O} \qquad \text{(J-11)}$$

$$\underset{(E+Z)}{(C_2H_5)_2NH} + \underset{(B-Y)}{HDO} \rightleftharpoons \underset{(G-Z)}{(C_2H_5)_2ND} + \underset{(D+Y)}{H_2O} \qquad \text{(J-12)}$$

The quantities A, B, C, D, E and G represent amounts of the indicated species present initially at time zero. Also, X is the number of gram atoms of deuterium transferred to H_2 from HD. Y is the number of gram atoms of deuterium transferred from HDO, and Z is the number of gram atoms of deuterium transferred from $(C_2H_5)_2ND$. The quantities in the parentheses represented the amounts of reaction participants existing in the system at time t after startup. The equilibrium (J-12) was considered to be reached instantaneously and, therefore, the equilibrium condition that $r_a = r_w$ was satisfied at every moment. From material balance on deuterium atoms,

$$Z = X - Y \qquad \text{(J-13)}$$

Therefore Eqn. (J-12) can be written as

$$\underset{(E+X-Y)}{(C_2H_5)_2NH} + \underset{(B-Y)}{HDO} \rightleftharpoons \underset{(G-X-Y)}{(C_2H_5)_2ND} + \underset{(D+Y)}{H_2O} \qquad \text{(J-14)}$$

From the equilibrium condition,

$$\frac{G}{E} = \frac{B}{B + 2D} \qquad \text{at time zero}$$

and

$$\frac{G - X + Y}{E + X - Y} = \frac{B - Y}{B - Y + 2(D + Y)} \qquad \text{at time t.}$$

Solving the last two equations for Y,

$$Y = \frac{2(B + D)X}{(E + G) + 2(B + D)} = FX \tag{J-15}$$

where

$$F \equiv \frac{2(B + D)}{(E + G) + 2(B + D)} \tag{J-15a}$$

Thus, the net reaction which controls the rate can be written as follows:

	H_2	+	HDO	$\rightleftharpoons$	HD	+	H_2O
Initially	A		B		C		D
At time t	(A-X)		(B-FX)		(C+X)		(D+FX)
Participating in liq. phase	λ_o(A-X)		λ_{11}(B-FX)	$\underset{k_2}{\overset{k_1}{\rightleftharpoons}}$	λ_o(C+X)		λ_1(D+FX)
Participating in vap. phase	λ'_o(A-X)		λ'_{11}(B-FX)	$\underset{k_2'}{\overset{k_1'}{\rightleftharpoons}}$	λ'_o(C+X)		λ'_1(D+FX)

(J-16)

where λ_o, λ_1 and λ_{11} are the fractions of hydrogen gas (H_2 or HD), H_2O and HDO, respectively, present in the liquid phase, and

$$\lambda'_o = 1 - \lambda_o \tag{J-16a}$$

$$\lambda'_1 = 1 - \lambda_1 \tag{J-16b}$$

and $$\lambda'_{11} = 1 - \lambda_{11} \tag{J-16c}$$

are the fractions present in the liquid phase.

The reaction taking place in the liquid phase is the one being catalyzed by the added catalyst, while the reaction in the

vapor phase is the one being catalyzed on the surface of the inside wall of the autoclave. The reaction mechanisms as well as the catalytic activities of the catalysts are different from each other, so that different rate constants are used. Each rate constant is expressed as grammoles of deuterium transferred per unit time per unit volume per unit molar concentration of each reactant concerned. They are related to the equilibrium constants as follows:

$$\frac{k_1}{k_2} = K$$

and

$$\frac{k_1'}{k_2'} = K'$$

where

$$K' = K \frac{\pi_{H_2O}}{\pi_{HDO}} = K\alpha^*$$

According to Armstrong (J-1), the values of the ratio of the vapor pressures of H_2O to HDO are as follows.

Table J-I

Ratio of the Vapor Pressures of H_2O to HDO

Temperature (°C)	$\alpha^* = \pi_{H_2O}/\pi_{HDO}$
100	1.026
150	1.011
200	1.0025

Assuming that the rate of reaction is proportional to the concentration of reacting species, the rate of transfer of deuterium to H_2 is

$$\frac{dX}{dt} = V\left\{k_1\left[\frac{\lambda_o(A-X)}{V}\right]\left[\frac{\lambda_{11}(B-FX)}{V}\right] - k_2\left[\frac{\lambda_o(C+X)}{V}\right]\left[\frac{\lambda_1(D+FX)}{V}\right]\right\} \quad \text{(J-17)}$$

$$+ V'\left\{k_1'\left[\frac{\lambda_o'(A-X)}{V'}\right]\left[\frac{\lambda_{11}'(B-FX)}{V'}\right] - k_2'\left[\frac{\lambda_o'(C+X)}{V'}\right]\left[\frac{\lambda_1'(D+FX)}{V'}\right]\right\}$$

But λ_1' and λ_{11}' are related by

$$\frac{\lambda_{11}'}{\lambda_1'} = \frac{1}{\alpha^*} \quad \text{(J-17a)}$$

and, since both λ_1' and λ_{11}' were smaller than 10^{-2} in their magnitudes,

$$\frac{\lambda_{11}}{\lambda_1} = \frac{1-\lambda_{11}'}{1-\lambda_1'} \simeq 1 \quad . \quad \text{(J-17b)}$$

Therefore, Eqn. (J-17) can be reduced to

$$\frac{dX}{dt} = \left[\frac{\lambda_o\lambda_1 k_2}{V} + \frac{\lambda_o'\lambda_1' k_2'}{V'}\right]\left[K(A-X)\ (B-FX) - (C+X)\ (D+FS)\right] \quad \text{(J-18)}$$

In this equation, let an overall reaction rate constant $\langle k_2 \rangle$ be defined by

$$\frac{\langle k_2 \rangle}{V^o} \equiv \lambda_o\lambda_1\frac{k_2}{V} + \lambda_o'\lambda_1'\frac{k_2'}{V} \quad \text{(J-19)}$$

and factor the quadratic form into

$$K(A-X)\ (B-FX) - (C+X)\ (D+FX) = F(K-1)\ (X-\alpha)\ (X-\beta) \qquad (J\text{-}20)$$

Then Eqn. (J-18) simplifies to

$$\frac{dX}{dt} = \frac{\langle k_2 \rangle}{V^o} F(K-1)\ (X-\alpha)\ (X-\beta) \qquad (J\text{-}21)$$

α and β are related to A, B, C and D by

$$\alpha \equiv \frac{-\delta_1 - \sqrt{\delta_1^2 - \delta_2}}{2F(1-K)} \qquad (J\text{-}22)$$

$$\beta \equiv \frac{-\delta_1 + \sqrt{\delta_1^2 - \delta_2}}{2F(1-K)} \qquad (J\text{-}23)$$

$$\delta_1 \equiv K(AF + B) + (CF + D) \qquad (J\text{-}24)$$

$$\delta_2 \equiv -4F(1-K)\ (KAB - CD) \qquad (J\text{-}25)$$

As $K < 1$ and $KAB > CD$, α is negative and β is positive. β has the physical significance of the number of gram atoms of deuterium which could be transferred to HD by the time equilibrium was reached and the reaction rate dX/dt became zero.

The result of integrating Eqn. (J-21) from time zero, with X = 0, to time t is

$$\frac{1}{\beta - \alpha} \ln \frac{\beta(X-\alpha)}{\alpha(X-\beta)} = \frac{\langle k_2 \rangle}{V^o} F(1-K)\ t \qquad (J\text{-}26)$$

Thus, if a plot is made of the quantity L defined as

$$L \equiv \frac{1}{\beta - \alpha} \ln \frac{\beta(X - \alpha)}{\alpha(X - \beta)} \qquad \text{(J-27)}$$

against time t, the result should be a straight line whose slope S is related to the overall reaction rate constant $\langle k_2 \rangle$ by

$$\langle k_2 \rangle = \frac{SV^o}{F(1 - K)} \qquad \text{(J-28)}$$

The preceding integration of the rate equation (J-19) is applicable only when the total amount of hydrogen (H_2, HD and D_2) and water (H_2O, HDO and D_2O) in the system remains constant. In the present experiments the amount of hydrogen removed in gas samples to be analyzed was large enough to require use of a modified form of the integrated rate equation. Consequently, an integrated rate equation equivalent to Eqn. (J-26), but applicable also to a system from which gas samples are withdrawn, will be derived.

Consider first a system in which the inventory remains constant. Suppose that the number of gram atoms of deuterium transferred to HD is determined at the end of time intervals t_1, t_2, etc. The number of gram moles of reactants and products present at the beginning of each time interval, the corresponding values of α and β, and the number of gram atoms of deuterium transferred to HD are to be represented by the nomenclature of Table J-II. From material balance considerations,

Table J-II

Nomenclature for Ideal Case

Interval	Duration	Initial conditions: Gram Moles of H_2	HD	HDO	H_2O	α	β	Gram Atoms D Transferred to HD: In Interval	Total
1	Δt_1	A_1^o	C_1^o	B_1^o	D_1^o	α_1^o	β_1^o	ΔX_1^o	X_1^o
2	Δt_2	A_2^o	C_2^o	B_2^o	D_2^o	α_2^o	β_2^o	ΔX_2^o	X_2^o
3	Δt_3	A_3^o	C_3^o	B_3^o	D_3^o	α_3^o	β_3^o	ΔX_3^o	X_3^o
.	.	.	.	.	.	.	.	.	.
.	.	.	.	.	.	.	.	.	.
.	.	.	.	.	.	.	.	.	.
i	Δt_i	A_i^o	C_i^o	B_i^o	D_i^o	α_i^o	β_i^o	ΔX_i^o	X_i^o
.	.	.	.	.	.	.	.	.	.

Note: The superscript (^{o}) is used as a reminder that no material is withdrawn from the system.

it is clear that

$$A_n^o = A_1^o - \sum_{i=1}^{n-1} \Delta X_i^o \qquad \text{(J-30)}$$

$$C_n^o = C_1^o + \sum_{i=1}^{n-1} \Delta X_i^o \qquad \text{(J-31)}$$

$$B_n^o = B_1^o - F \sum_{i=1}^{n-1} \Delta X_i^o \qquad \text{(J-32)}$$

and

$$D_n^o = D_1^o + F \sum_{i=1}^{n-1} \Delta X_i^o \qquad \text{(J-33)}$$

α_n^o and β_n^o may be determined from these values of A_n^o, B_n^o, C_n^o and D_n^o, by means of (J-22), (J-23), (J-24) and (J-25).

During each interval Δt_n, the integrated rate equation (J-26), applies in the form

$$\frac{1}{\beta_n^o - \alpha_n^o} \ln \frac{\beta_n^o(\Delta X_n^o - \alpha_n^o)}{\alpha_n^o(\Delta X_n^o - \beta_n^o)} = \frac{\langle k_2 \rangle}{V^o} F(1 - K)\Delta t_n \qquad \text{(J-34)}$$

The sum of these equations is

$$\sum_{n=1}^{r} \frac{1}{\beta_n^o - \alpha_n^o} \ln \frac{\beta_n^o(\Delta X_n - \alpha_n^o)}{\alpha_n^o(\Delta X_n^o - \beta_n^o)} = \frac{\langle k_2 \rangle}{V^o} F(1 - K)t_r \qquad \text{(J-35)}$$

where

$$t_r = \sum_{n=1}^{r} \Delta t_n \qquad \text{(J-36)}$$

We will now show that the left side is identically equal to

the left side of Eqn. (J-26), that is, that

$$\sum_{n=1}^{r} \frac{1}{\beta_n^o - \alpha_n^o} \ln \frac{\beta_n^o(\Delta X_n^o - \alpha_n^o)}{\alpha_n^o(\Delta X_n^o - \beta_n^o)} = \frac{1}{\beta_1^o - \alpha_1^o} \ln \frac{\beta_1^o(X_r^o - \alpha_1^o)}{\alpha_1^o(X_r^o - \beta_1^o)} \tag{J-37}$$

where

$$X_r^o = \sum_{n=1}^{r} \Delta X_n^o \tag{J-38}$$

To do this, we recall that α_n^o and β_n^o are obtained by factoring the quadratic form analogous to Eqn. (J-20):

$$K\left[A_n^o - \Delta X_n^o\right]\left[\beta_n^o - F\Delta X_n^o\right] - \left[C_n^o + \Delta X_n^o\right]\left[D_n^o + F\Delta X_n^o\right] \tag{J-39}$$

$$\equiv F(K - 1)\ (\Delta X_n^o - \alpha_n^o)\ (\Delta X_n^o - \beta_n^o)$$

Substitution for A_n^o, B_n^o, C_n^o and D_n^o from Eqns. (J-30), (J-31), (J-32) and (J-33) yields

$$K\left[A_1^o - (\sum_{i=1}^{n-1}\Delta X_i^o + \Delta X_n^o)\right]\left[B_1^o - F(\sum_{i=1}^{n-1} \Delta X_i^o + \Delta X_n^o)\right]$$

$$- \left[C_1^o + (\sum_{i=1}^{n-1} \Delta X_i^o + \Delta X_n^o)\right]\left[D_1^o + F(\sum_{i=1}^{n-1} \Delta X_i^o + \Delta X_n^o)\right] \tag{J-40}$$

$$= F(K - 1)\ (\Delta X_n^o - \alpha_n^o)\ (\Delta X_n - \beta_n^o)$$

But the left side of this equation may also be factored into

$$F(K - 1)\ (\sum_{i=1}^{n-1} \Delta X_i^o + \Delta X_n^o - \alpha_1^o)\ (\sum_{i=1}^{n-1} \Delta X_i^o + \Delta X_n^o - \beta_1^o)\ .$$

Comparison with Eqn. (J-40) shows that

$$\alpha_n^o = \alpha_1^o - \sum_{i=1}^{n-1} \Delta X_i^o \tag{J-41}$$

and

$$\beta_n^o = \beta_i^o - \sum_{i=1}^{n-1} \Delta X_i^o \tag{J-42}$$

Substitution for α_n^o and β_n^o in the left side of Eqn. (J-37) yields

$$\sum_{n=1}^{r} \frac{1}{\beta_n^o - \alpha_n^o} \ln \frac{\beta_n^o(\Delta X_n^o - \alpha_n^o)}{\alpha_n^o(\Delta X_n^o - \beta_n^o)}$$

$$= \frac{1}{\beta_1^o - \alpha_1^o} \sum_{n=1}^{r} \ln \frac{(\beta_1^o - \sum_{i=1}^{n-1} \Delta X_i^o)(\sum_{i=1}^{n} \Delta X_i^o - \alpha_1^o)}{(\alpha_1^o - \sum_{i=1}^{n-1} \Delta X_i^o)(\sum_{i=1}^{n} \Delta X_i^o - \beta_1^o)}$$

$$= \frac{1}{\beta_1^o - \alpha_1^o} \ln \prod_{n=1}^{r} \frac{(\beta_1^o - \sum_{i=1}^{n-1} \Delta X_i^o)(\sum_{i=1}^{n} \Delta X_i^o - \alpha_1^o)}{(\alpha_1^o - \sum_{i=1}^{n-1} \Delta X_i^o)(\sum_{i=1}^{n} \Delta X_i^o - \beta_1^o)}$$

$$= \frac{1}{\beta_1^o - \alpha_1^o} \ln \frac{\beta_1^o}{\alpha_1^o} \frac{\sum_{i=1}^{r} \Delta X_i^o - \alpha_i^o}{\sum_{i=1}^{r} \Delta X_i^o - \beta_i^o}$$

$$= \frac{1}{\beta_1^o - \alpha_1^o} \ln \frac{\beta_1^o(X_r^o - \alpha_1^o)}{\alpha_1^o(X_r^o - \beta_1^o)} \tag{J-43}$$

Thus the identity (J-37) is established.

If we define the extent of reaction in the n-th time interval by

$$\Delta L_n^o \equiv \frac{1}{\beta_n^o - \alpha_n^o} \ln \frac{\beta_n^o(\Delta X_n^o - \alpha_n^o)}{\alpha_n^o(\Delta X_n^o - \beta_n^o)} \qquad \text{(J-44)}$$

Eqn. (J-43) shows that

$$\sum_{n=1}^{r} \Delta L_n^o = L_r^o \qquad \text{(J-45)}$$

where L_r^o, defined by Eqn. (J-27), is the extent of reaction occuring between conditions (α_1^o, β_1^o) at time zero and time t_r.

We have shown that when no material is withdrawn from the system, the reaction rate constant $\langle k_2 \rangle$ may be obtained either from the integral of the differential rate equation over the complete time interval from zero to t_r, in the form

$$L_r^o \equiv \frac{1}{\beta_1^o - \alpha_1^o} \ln \frac{\beta_1^o(X_r^o - \alpha_1^o)}{\alpha_1^o(X_r^o - \beta_1^o)} = \frac{\langle k_2 \rangle F(1 - K)}{V^o} \qquad \text{(J-46)}$$

or in terms of the integrals of the differential rate equation over all individual time intervals, in the form

$$\sum_{n=1}^{r} \Delta L_n^o \equiv \sum_{n=1}^{r} \frac{1}{\beta_n^o - \alpha_n^o} \ln \frac{\beta_n^o(\Delta X_n^o - \alpha_n^o)}{\alpha_n^o(\Delta X_n^o - \beta_n^o)} = \frac{\langle k_2 \rangle F(1 - K)}{V^o} \qquad \text{(J-47)}$$

When no material is withdrawn these expressions are mathematically identical.

When gas samples are withdrawn at the end of each time interval, to be analyzed for deuterium content, material balance relations (J-30) and (J-31) for H_2 and HD,

respectively, no longer hold. Consequently, α_n and β_n are no longer given by Eqns. (J-41) and (J-42), and expressions (J-46) and (J-47) are no longer equivalent. However, the differential rate equation (J-19) may still be integrated during each time interval Δt_n between the taking of samples, so that the integrated rate equation (J-34) still is applicable during each time interval. To distinguish this case, in which samples are withdrawn at the end of each time interval from the ideal case, the equation is rewritten without the superscript (^{o}) as follows.

$$\Delta L_n \equiv \frac{1}{\beta_n - \alpha_n} \ln \frac{\beta_n(\Delta X_n - \alpha_n)}{\alpha_n(\Delta X_n - \beta_n)} = \frac{\langle k_2 \rangle}{V^o} F(1 - K)\Delta t_n \qquad \text{(J-48)}$$

Summation of the equations over all time intervals gives an integrated rate equation for the actual case in which samples are withdrawn, analogcus to the second form, Eqn. (J-47), of the integrated rate equation for the ideal case in which no samples are taken:

$$\sum_{n=1}^{r} \Delta L_n \equiv \sum_{n=1}^{r} \frac{1}{\beta_n - \alpha_n} \ln \frac{\beta_n(\Delta X_n - \alpha_n)}{\alpha_n(\Delta X_n - \beta_n)}$$

$$= \frac{\langle k_2 \rangle}{V^o} F(1 - K) \sum_{n=1}^{r} \Delta t_n \qquad \text{(J-49)}$$

or

$$L_r = \frac{\langle k_2 \rangle}{V^o} F(1 - K)\, t_r \qquad \text{(J-50)}$$

where

$$t_r \equiv \sum_{n=1}^{r} \Delta t_n \qquad \text{(J-51)}$$

and

$$L_r \equiv \sum_{n=1}^{r} \frac{1}{\beta_n - \alpha_n} \ln \frac{\beta_n(\Delta X_n - \alpha_n)}{\alpha_n(\Delta X_n - \beta_n)} \qquad \text{(J-52)}$$

It is important to note that in the actual case, when samples are taken

$$L_r \neq \frac{1}{\beta_1 - \alpha_1} \ln \frac{\beta_1(X_r - \alpha_1)}{\alpha_1(X_r - \beta_1)}$$

By plotting L_r, defined by Eqn. (J-52) against t_r and determining the slope S of the best straight line, $\langle k_2 \rangle$ may be obtained from

$$\langle k_2 \rangle = \frac{SV^o}{F(1 - K)} \qquad \text{(J-53)}$$

This is the procedure used in these experiments.

The rate constant k_2 for the homogeneous liquid phase reaction was obtained from the observed overall rate constant $\langle k_2 \rangle$ by correcting for the heterogeneous reaction occurring on metal surfaces in contact with the gas phase through

$$k_2 = \frac{V}{\lambda_o \lambda_1} \left(\frac{\langle k_2 \rangle}{V^o} - \frac{\lambda_o' \lambda_1' k_2'}{V^o} \right) \qquad \text{(J-54)}$$

derived from Eqn. (J-19). The fraction of hydrogen λ_o dissolved in the liquid phase was $n_o/(p_o V'/RT)$. Using Eqn. (I-18),

$$\lambda_o = 760(n_1 + n_2) \frac{RT}{cV'} \qquad \text{(J-55)}$$

The fraction of water present in the liquid phase was

$$\lambda_1 = \frac{m_1}{m_1 + m_1'} = \frac{m_1}{W_1} \qquad \text{(J-56)}$$

The rate constant k_2' for the heterogeneous reaction was determined from $\langle k_2 \rangle$ observed in a blank run made in the absence of catalyst, in which k_2 was zero, so that

$$k_2' = \frac{\langle k_2 \rangle V'}{(1 - \lambda_o)(1 - \lambda_1)V^o} \qquad \text{(J-57)}$$

Errors in estimation of k_2 or k_2' from the average value of $\langle k_2 \rangle$ for a complete run were computed by using formulae given in subsection J-4 of the APPENDIX.

(c) Material Balance Calculations

The quantities α_n and β_n appearing in Eqn. (J-48) are evaluated from the number of grammoles of H_2, HD, HDO and H_2O present in the system at the beginning of each time interval, A_n, C_n, B_n and D_n, respectively. The way in which these and ΔX_n were obtained from measured quantities will now be described.

From the known total volume of the reacting system V^o and the measured pressure p_o and weights of water W_1 and diethylamine W_2 charged to the system, the procedure of Section I of the APPENDIX permits calculation of the number of grammoles of hydrogen $n'_{o,0}$ present in the gas phase before taking the zero-point sample and the total number of grammoles of water $(n_{1,0} + n'_{1,0})$ and diethylamine $(n_{2,0} + n'_{2,0})$ present at this time. From the known atom fraction f_d of deuterium in the mixture of water and diethylamine charged to the system, the mole fractions of HDO (ξ_1) and H_2O (ξ_o) in water and of $(C_2H_5)_2ND$ (ζ_1) in diethylamine are computed by Eqn's

(J-9a), (J-9b), (J-9c) and (J-7). From these quantities, with the aid of Eqns. (J-10a) through (J-10f), one then computes the number of moles of each of the individual isotopic species present before the zero point sample is taken:

$$\begin{aligned} H_2 &: A_0 \\ HDO &: B_0 \\ HD &: C_0 \\ H_2O &: D_0 \\ (C_2H_5)_2NH &: E_0 \\ (C_2H_5)_2ND &: G_0 \end{aligned}$$

The fraction of exchangeable deuterium present in water, F, is computed from Eqn. (J-15a) with these values of B, D, E and G; it is assumed to remain constant throughout the run, as the fraction of the charge of water and diethylamine removed via gas phase samples is very small.

The zero-point sample is taken as soon as possible after charging hydrogen, and the pressure $p_{(1)}$ prevailing during the first partial run is measured. At time t_1 at the end of the first partial run, gas-phase sample No. 1 is taken, and the atom fraction of deuterium $f'_{d,1}$ in this sample is determined from the output of the thermal conductivity cell by using calibrations of the T/C cell described in Section E of the APPENDIX.

The number of moles of hydrogen $n'_{o,1}$ in the gas phase during partial run No. 1 is determined from $p_{(1)}$ by the procedure of Section I of the APPENDIX, and the number of moles of $H_2(A_1)$, HDO (B_1), HD (C_1) and H_2O (D_1) present at the beginning

of partial run No. 1 are determined from Eqns. (J-10a) through (J-10d). α_1 and β_1 are evaluated from A_1, B_1, C_1 and D_1 by Eqns. (J-22) through (J-25). The amount of H_2 present before the sample No. 1 is taken is

$$A_1 - \Delta X_1 = n'_{o,1}(1 - f'_{d,1})^2$$

so that

$$\Delta X_1 = 2\, n'_{o,1}\left[f'_{d,1} - \left(\frac{f'_{d,1}}{2}\right)^2 \right] \qquad \text{(J-58)}$$

As $f'_{d,1} \ll 1$ in this work, this has been approximated by

$$\Delta X_1 = 2\, n'_{o,1}\, f'_{d,1} \qquad \text{(J-59)}$$

After sample No. 1 is taken, the amount of hydrogen in the gas phase is reduced to $n'_{o,2}$, which remains constant during the second partial run. The number of grammoles of each reactant present at the beginning of partial run No. 2 is

$$H_2 : \quad A_2 = n'_{o,2}(1 - f'_{d,1})^2$$

$$HD : \quad C_2 = 2\, n'_{o,2}(1 - f'_{d,1}) f'_{d,1}$$

$$HDO : \quad B_2 = B_1 - F\Delta X_1$$

$$H_2O : \quad D_2 = D_1 + F\Delta X_1$$

Analysis of gas sample No. 2 taken at the end of the second partial run gives $f'_{d,2}$, the atom fraction deuterium at that time. The amount of hydrogen present at the end of the second partial run, before the sample No. 2 is taken is

$$A_2 - \Delta X_2 = n'_{o,2}(1 - f'_{d,2})^2$$

so that

$$\Delta X_2 = n'_{o,2}\left[2(f'_{d,2} - f'_{d,1}) - (f'_{d,2})^2 + (f'_{d,1})^2\right] \quad \text{(J-60)}$$

This has been approximated by

$$\Delta X_2 = 2\, n'_{o,2}(f'_{d,2} - f'_{d,1}) \ .$$

The procedure of taking sample No. n, making partial run No. n at constant inventory, taking sample No. (n+1), etc., is continued until the end of the run. The general equations used to extend the material-balance calculations through the run are

$$H_2 : \quad A_n = n'_{o,n}\left[1 - f'_{d,(n-1)}\right]^2 \quad \text{(J-61)}$$

$$HD : \quad C_n = 2\, n'_{o,n}\left[1 - f'_{d,(n-1)}\right] f'_{d,(n-1)} \quad \text{(J-62)}$$

$$\text{D transferred to } H_2: \quad \Delta X_n \simeq 2\, n'_{o,n}\left[f'_{d,n} - f'_{d,(n-1)}\right] \quad \text{(J-63)}$$

$$HDO : \quad B_n = B_{n-1} - F\Delta X_{n-1} \quad \text{(J-64)}$$

$$H_2O : \quad D_n = D_{n-1} + F\Delta X_{n-1} \quad \text{(J-65)}$$

Here $n'_{o,n}$ is the grammoles of hydrogen of all isotopic species present in the gas phase during the n-th partial run, as calculated from the pressure measured at the beginning of of the n-th partial run, after sample No. (n-1) is taken.

In case a sample, No. (n-1), was taken but was disregarded either because the sample was lost due to maloperations of the stopcocks or because it was contaminated somehow, a value of $n'_{o,(n-1)}$, the total grammoles of hydrogen gas which was present in the system after the (n-2)-nd sample was taken,

was used, along with quantities associated with the (n-2)-nd sample, for computing initial conditions for the n-th partial run. Although this procedure did not exactly represent what was happening in the reaction vessel in connection with the change of the hydrogen pressure in the system, this procedure was adequate enough for the present purpose because the decrease in the pressure due to one sampling was always only a small fraction of the total hydrogen pressure.

J-2. Source and Evaluation of Errors

There were three classes of possible sources of errors in the final results. They are the experimental errors, uncertainties of the constant used for computation and errors introduced by the assumptions made. The last two are treated in Section L of the APPENDIX. The experimental errors which might contribute error in the quantity

$$\Delta L_n = \frac{1}{\beta_n - \alpha_n} \ln \frac{\beta_n(\Delta X_n - \alpha_n)}{\alpha_n(\Delta X_n - \beta_n)}$$

were the errors in the thermal conductivity analysis and errors in the estimates of the volume, the pressure, and the total amounts of water and amine. Repeated measurements of the output from the thermal conductivity cell with a sample gas of supposedly constant composition showed that 0.05 mV was a fair estimate for the probable error of an output. Using a capital P for a probable error,

$$P(E^{\circ}) = 0.05 \text{ mV} \qquad \text{(J-66)}$$

The superscript ($^{\circ}$) was to indicate a probable error for one output measurement.

There was no experimental basis on which the probable error could be estimated for $P(V')$, $P(p_o)$, $P(W_1)$ and $P(N)$. The first one was roughly estimated in APPENDIX L-1 as

$$P^2(V') = 1 \text{ ml} \tag{J-67}$$

The standard gauge used to read the total pressure of the system could be read off to ± 5 psi. To be conservative, therefore, $P(p_o)$ was estimated to be

$$P(p_o) = 5 \text{ psi} = 0.344 \text{ atmospheres} \tag{J-68}$$

For $P(W_1)$, a value of one gram was assigned from consideration of the fact that the balance used could weigh to $\pm$ 0.5 grams.

$$P(W_1) = 1 \text{ gram} \tag{J-69}$$

For the titration error, 1% of the normality of the amine was used.

$$P(N) = 0.01 \text{ N normal} \tag{J-70}$$

These errors were propagated to the calculation of β by the following formulae. Subscripts n outside the square brackets mean that the quantity appearing in the square brackets is to be computed on the n-th sample, or the n-th partial run.

$$P(f_d) = \begin{cases} \dfrac{0.256N}{(110.5 - 8.7N)^2} & \text{for "1}\underline{N}\text{" runs} \qquad \text{(J-71)} \\ \dfrac{0.295N}{(109.7 - 8.8N)^2} & \text{for "2}\underline{N}\text{" runs} \qquad \text{(J-72)} \end{cases}$$

$$\left[\frac{P(n_o')}{n_o'}\right]_n^2 = \left[\frac{P(V')}{V'}\right]^2 + \left|\frac{P(p_o)}{p_o}\right|_n^2 = \left(\frac{1}{V'}\right)^2 + \left(\frac{0.344}{p_o}\right)_n^2 \tag{J-73}$$

$$\left[P(f_d')\right]_n^2 = \frac{\left[EP(\gamma)\right]_n^2 + \left[\gamma P(E)\right]_n^2}{(1 + E\gamma)_n^2} \tag{J-74}$$

$$\left[\frac{P(A)}{A}\right]_n^2 = \left[\frac{P(n_o')}{n_o'}\right]_n^2 + \left[\frac{2P(f_d')}{1 - f_d'}\right]_{(n-1)}^2 \tag{J-75}$$

$$\left[\frac{P(C)}{C}\right]_n^2 = \left[\frac{P(n_o')}{n_o'}\right]_n^2 + \left[\frac{(1 - 2f_d')P(f_d')}{f_d'(1 - f_d')}\right]_{(n-1)}^2$$

$$\left[\frac{(1 - 2f_d')P(f_d')}{f_d'(1 - f_d')}\right]_{(n-1)}^2 \tag{J-76}$$

$$\left[\frac{P(\Delta X)}{\Delta X}\right]_n^2 = \left[\frac{P(n_o')}{n_o'}\right]_n^2 + \frac{\left[P(f_d')\right]_n^2 + \left[P(f_d')\right]_{(n-1)}^2}{\left[f_{d,n}' - f_{d,(n-1)}'\right]^2}$$

$$\simeq \frac{\left[P(f_d')\right]_n^2 + \left[P(f_d')\right]_{(n-1)}^2}{(\Delta f_{d,n})^2} \tag{J-77}$$

$$\left[\frac{P(F)}{F}\right]^2 = \frac{(E_1 + G_1)^2\left[\frac{P(B_1 + D_1)}{B_1 + D_1}\right]^2 + P^2(E_1 + G_1)}{\left[(E_1 + G_1) + 2(B_1 + D_1)\right]^2}$$

$$\simeq \frac{\left(\frac{W_2}{M_2}\right)^2\left[\left(\frac{1}{W_1}\right)^2 + \left(\frac{1}{W_1 + W_2}\right)^2\right]}{(E_1 + G_1) + 2(B_1 + D_1)^2} \tag{J-78}$$

$$P^2(B_1) \simeq \left(\frac{B_1}{W_1}\right)^2 \tag{J-79}$$

$$\left[P(B)\right]_n^2 = \left[P(B)\right]_{(n-1)}^2 + \left[FP(\Delta X)\right]_{(n-1)}^2 + \left[\Delta X P(F)\right]_{(n-1)}^2$$

$$\simeq \left[P(B)\right]_{(n-1)}^2 + \left[FP(\Delta X)\right]_{(n-1)}^2 \qquad (n \geqslant 2) \tag{J-80}$$

$$\left[P(D_1)\right]^2 \simeq \left(\frac{D_1}{W_1}\right)^2 \tag{J-81}$$

$$\left[P(D)\right]_n^2 = \left[P(D)\right]_{(n-1)}^2 + \left[FP(\Delta X)\right]_{(n-1)}^2 + \left[\Delta X P(F)\right]_{(n-1)}^2$$

$$\left[P(D)\right]_{(n-1)}^2 + \left[FP(\Delta X)\right]_{(n-1)}^2 \qquad (n \geqslant 2) \tag{J-82}$$

$$\left[P(\delta_1)\right]_n^2 = K^2\left[F^2P^2(A) + A^2P^2(F) + P^2(B)\right]_n$$

$$+ \left[F^2P^2(C) + C^2P^2(F) + P^2(D)\right]_n$$

$$\simeq K^2\left[F^2P^2(A) + P^2(B)\right]_n + \left[F^2P^2(C) + P^2(D)\right]_n \tag{J-83}$$

$$\left[\frac{P(\delta_2)}{\delta_2}\right]_n^2 = \left[\frac{P(F)}{F}\right]^2 + \frac{K^2\left[A^2P^2(B) + B^2P^2(A)\right]_n + \left[C^2P^2(D) + D^2P^2(D)\right]_n}{(KAB - CD)_n^2}$$

$$\simeq \frac{\left[KBP(A)\right]_n^2 + \left[DP(C)\right]_n^2}{(KAB - CD)_n^2} \tag{J-84}$$

$$\left[\frac{P(\beta)}{\beta}\right]_n^2 = \left[\frac{P(F)}{F}\right]^2 + \left[\frac{P(\delta_1)}{\sqrt{\delta_1^2 - \delta_2}}\right]_n^2 + \left[\frac{1}{4F(1-k)\sqrt{\delta_1^2 - \delta_2}}\,\frac{P(\delta_2)}{\beta}\right]_n^2 \tag{J-85}$$

$$\left[P(\Delta L_n)\right]^2 \simeq \left[\frac{\Delta X}{\alpha(\beta - \Delta X)}\right]_n^2 \left\{\left[\frac{(2\beta - \Delta X)P(\beta)}{\beta}\right]_n^2 + \left[\frac{P(\Delta X)}{\Delta X}\right]_n^2\right\}$$

$$\simeq \left[\frac{\Delta X}{\alpha(\beta - \Delta X)}\right]_n^2 \left[\frac{P(\Delta X)}{\Delta X}\right]_n^2 \tag{J-86}$$

J-3. Least Squares Fit and Estimate of Its Reliability

The quantity L_n defined by Eqn. (J-52),

$$L_n \equiv \sum_{i=1}^{n} \Delta L_i \equiv \sum_{i=1}^{n} \frac{1}{\beta_i - \alpha_i} \ln \frac{\beta_i(\Delta X_i - \alpha_i)}{\alpha_i(\Delta X_i - \beta_i)} \tag{J-52}$$

was plotted against the time t_n defined by Eqn. (J-51),

$$t_n = \sum_{i=1}^{n} \Delta t_i \qquad \text{(J-51)}$$

These points should lie on a straight line going through the origin if the theory that the rate was of the first order with respect to the pressure of hydrogen was valid. The least-squares procedures and a criterion on the linear fit of the experimental points are described in this section.

The probable error of L_n is

$$P^2(L_n) = \sum_{i=1}^{n} P^2(\Delta L_n) \qquad \text{(J-87)}$$

In applying the theory of the least squares here, each point was weighted according to

$$w_n = \frac{P^2(L_1)}{P^2(L_n)} \qquad \text{(J-88)}$$

where w_n was the weight of the n-th sample and a subscript M represented the sample number of the last sample of the run. According to the theory then, the slope of the best-fit straight line, S was given by

$$S = \frac{\sum^{M} w_n t_n L_n}{\sum^{M} w_n t_n^2} \qquad \text{(J-89)}$$

and its probable error by

$$P(S) = \frac{P(\bar{L}) \sqrt{\sum^{M} w_n^2 t_n^2}}{\sum^{M} w_n t_n^2} \qquad \text{(J-90)}$$

where

$$P(\bar{L}) \equiv 0.675 \sqrt{\frac{\sum_{n}^{M} w_n (L_n - St_n)^2}{(M-1)\sum_{n}^{M} w_n}} \qquad \text{(J-91)}$$

To ascertain whether the deviation of the plot of L vs t from the straight line predicted for a second-order reaction could be attributed to experimental errors in the determination of L, a comparison was made between $P(\bar{L})$ from Eqn. (J-91), which represents the probable error in L determined from the deviations of the measured values from the best straight line, and $\overline{P(L)}$, the mean error in L anticipated from errors in measuring the quantities entering into the calculation of L. $\overline{P(L)}$ is given by

$$\overline{P(L)} \equiv \sqrt{\frac{\sum_{n}^{M} w_n P^2(L_n)}{(M-1)\sum_{n}^{M} w_n}} \equiv \sqrt{\frac{MP^2(L_1)}{(M-1)\sum_{n}^{M} w_n}} \qquad \text{(J-92)}$$

For brevity, $P(\bar{L})$ will be called the observed probable error in L and $\overline{P(L)}$ the predicted probable error.

For most runs, the observed probable error $P(\bar{L})$ was smaller than the predicted probable error $\overline{P(L)}$. Although this would suggest that the estimates of measurement errors entering into the calculation of $\overline{P(L)}$ were somewhat too great, it indicates that the assumption of a second order reaction mechanism is confirmed within experimental error. The same point has been indicated graphically in Figs. 3 to 19 where each measurement of L_n with its estimated error is

compared with the straight line expected for a second-order reaction.

J-4. Formulae for the Liquid-Phase Rate Constant from the Overall Rate Constant

Rate constant k_2 for the liquid phase reaction at a given temperature was obtained from the overall rate constant $\langle k_2 \rangle$ as follows. From Eqn. (J-54),

$$k_2 = \frac{V^o - V^1}{\lambda_o \lambda_1} \left[\frac{\langle k_2 \rangle}{V^o} - \frac{(1-\lambda_o)\ (1-\lambda_1)\ k_2'}{V'} \right] \qquad \text{(J-92)}$$

where k_2' was the rate constant for the reaction occurring on metal surfaces in contact with the vapor phase and obtained from a blank run made in the absence of catalyst and at the same temperature, and λ_o and λ_1 were obtained from Eqns. (J-55), (J-56), respectively.

The rate constant k_2' for the vapor phase reaction was determined from

$$k_2' = \frac{V'}{(1-\lambda_o)\ (1-\lambda_1)} \langle k_2 \rangle \qquad \text{(J-93)}$$

where $\langle k_2 \rangle$ was obtained from a blank run.

The quantities in Eqn. (J-92) whose errors might contribute to error in k_2 are V', λ_o, λ_1, $\langle k_2 \rangle$ and k_2'. However, as the term in k_2' is only a small correction, this term can be neglected. Then,

$$\left[\frac{P(k_2)}{k_2}\right]^2 \simeq \left[\frac{P(\langle k_2 \rangle)}{\langle k_2 \rangle}\right]^2 + \left[\frac{P(V')}{V^o - V'}\right]^2 + \left[\frac{P(\lambda_o)}{\lambda_o}\right]^2 + \left[\frac{P(\lambda_1)}{\lambda_1}\right]^2$$

(J-94)

For the conditions of these runs, $V^o - V' \simeq 500$, so that

$$\left[\frac{P(V')}{V^o-V'}\right]^2 \simeq 4 \times 10^{-6} \qquad \text{(J-95)}$$

λ_o may be written as

$$\lambda_o \simeq 760 \frac{(V^o-V')\rho}{V'} \frac{RT}{c} \qquad \text{(J-96)}$$

where ρ is the molar density of the liquid phase and c is Henry's law constant for hydrogen. The principal uncertainties are in V' and c.

$$\left[\frac{P(\lambda_o)}{\lambda_o}\right]^2 \simeq \left[\frac{V^o}{V^o-V'}\right]^2 \left[\frac{P(V')}{V'}\right]^2 + \left[\frac{P(C)}{C}\right]^2$$
$$= 4 \times 4 \times 10^{-6} + 1 \times 10^{-4}$$
$$\simeq 1.2 \times 10^{-4} \qquad \text{(J-97)}$$

As

$$\lambda_1 = 1 - \frac{m_1'}{w_1}$$
$$= 1 - \frac{v_{g1}^s V'}{w'} \quad , \qquad \text{(J-98)}$$

$$\left[\frac{P(\lambda_1)}{\lambda_1}\right]^2 = \left[\frac{1-\lambda_1}{\lambda_1}\right]^2 \left\{ \left[\frac{P(V')}{V'}\right]^2 + \left[\frac{P(W_1)}{W_1}\right]^2 \right\} \qquad \text{(J-99)}$$

As $V' \simeq 500$ and $W_1 \simeq 425$ for these runs,

$$\left[\frac{P(\lambda_1)}{\lambda_1}\right]^2 \simeq \left[\frac{1-\lambda_1}{\lambda_1}\right]^2 (4 \times 10^{-6} + 6 \times 10^{-6})$$
$$= 10^{-5} \left[\frac{1-\lambda_1}{\lambda_1}\right]^2 \qquad \text{(J-100)}$$

The highest value of $(1 - \lambda_1)$ existing in these runs was 0.01, at 200°C. Therefore,

$$\left[\frac{P(\lambda_1)}{\lambda_1}\right]^2 \leqslant 10^{-9} \qquad \text{(J-101)}$$

and can be neglected.

Finally, for these runs, using

$$\left[\frac{P(\langle k_2\rangle)}{\langle k_2\rangle}\right]^2 = \left[\frac{P(S)}{S}\right]^2 , \qquad \text{(J-102)}$$

$$\left[\frac{P(k_2)}{k_2}\right]^2 = \left[\frac{P(S)}{S}\right]^2 + 1.2 \times 10^{-4} \qquad \text{(J-103)}$$

A similar error analysis for k_2', obtained from Eqn. (J-93), shows that the only term contributing significantly is

$$\left[\frac{P(k_2')}{k_2'}\right]^2 = \left[\frac{P(\langle k_2\rangle)}{\langle k_2\rangle}\right]^2 = \left[\frac{P(S)}{S}\right]^2 \qquad \text{(J-104)}$$

K. Sample Calculations

To minimize computation error due to rounding off of figures more than adequate decimal places were kept for every step of the calculations.

K-1. Phase Equilibrium

Run No. 16 is used for the illustration. This was a run at 200°C, so that the constants used for the phase equilibrium calculation were as follows.

Table K-I

Constants Used for Run 16

Specific volume of water in the liquid phase;	$v_{f1} = 1.158$ ml/g
Specific volume of saturated steam;	$v^s_{g1} = 127.18$ ml/g
Change in specific volume of water associated with vaporization of liquid to saturated steam;	$v_{fg1} = 126.03$ ml/g
Specific volume of diethylamine in the liquid phase;	$v_{f2} = 2.415$ ml/g
Correction term in Eqn. (H-9);	$\beta_2 = -7.35$ ml/g
Vapor pressure of water;	$\pi_1 = 15.35$ atm.
Vapor pressure of diethylamine;	$\pi_2 = 25.31$ atm.

Concentration of diethylamine in the solution charged was 1.60 normal, and the total amount of the solution charged was 443 grams. Total pressure after taking each sample was as given in Table K-II. These values also appear in the fourth column of Table M-VIII.

Table K-II

Total Residual Pressures in Run 16

Sample Number	Total Pressure, p (atmospheres)
Before taking zero point sample (sample No. 0)	78.55
After taking sample No. 0	77.87
" 1	77.19
" 2	76.17
" 3	75.14
" 4	73.78
" 5	71.74
" 6	69.70
" 7	65.63
" 8	62.20
" 9	58.82

(a) Computing the Total Amounts of Water and Amine Charged, W_1 and W_2

The density of the solution charged was obtained from Eqn. (H-13),

$$\rho = -0.01767N + 1.0149 \qquad \text{(K-1)}$$

where ρ is the density of the solution charged in grams per milliliter and N is the normality of diethylamine in the solution. Therefore,

$$\rho = -(0.01767 \times 1.60) + 1.0149$$

$$= 0.9866 \text{ grams/ml.} \qquad \text{(K-2)}$$

The total amount of water charged was obtained by

$$W_1 = G\left(1 - 0.07314\,\frac{N}{\rho}\right) \qquad \text{(K-3)}$$

where W_1 is the total amount of water charged in grams,

G is the total amount of the solution charged in grams,

N is the normality of diethylamine in the solution charged,

and ρ is the density of the solution charged in grams per milliliter.

Therefore,

$$W_1 = 443 \times \left(1 - \frac{0.07314 \times 1.60}{0.9866}\right)$$

$$= \underline{388.8 \text{ grams}} \qquad \text{(K-4)}$$

and

$$W_2 = G - W_1$$

$$= \underline{54.2 \text{ grams}}. \qquad \text{(K-5)}$$

(b) Computing the Equilibrium Amounts of Water and Diethylamine in Liquid and Vapor Phases, m_1, m_1', m_2, and m_2'

After several trial-and-error processes, a trial value of x_2, the mole fraction of diethylamine in the liquid phase, of 0.0331 was examined as follows. The partial pressure of diethylamine was obtained from

$$p_2 = \pi_2 x_2 \qquad \text{(K-6)}$$

where p_2 is the partial pressure of diethylamine in atmospheres,

π_2 is the vapor pressure of pure diethylamine in atmospheres, and

x_2 is the mole fraction of diethylamine in the liquid phase.

Therefore,

$$p_2 = 25.31 \times 0.0331 = 0.8375 \text{ atmospheres.} \qquad \text{(K-7)}$$

The specific volume of diethylamine in the vapor phase was obtained from Eqn. (H-9),

$$v_{g2} = \frac{1.205T}{p_2} + \beta_2 \qquad \text{(K-8)}$$

where v_{g2} is the specific volume of diethylamine vapor in milliliter per gram,

T is the absolute temperature in degrees Kelvin,

p_2 is the partial pressure of diethylamine in atmospheres, and

β_2 is a correction term for gas imperfections in milliliter per gram.

Therefore,

$$v_{g2} = \frac{1.205 \times 473.1}{0.8375} - 7.35 = 673.22 \text{ ml/gram.} \qquad \text{(K-9)}$$

Then,

$$v_{fg2} = v_{g2} - v_{f2}$$

$$= 673.22 - 2.42 = 670.80 \text{ ml/gram.} \qquad \text{(K-10)}$$

Using Eqn. (I-8),

$$\Delta V_1 = W_1 v_{g1}^s - V$$

$$= 388.8 \times 127.18 - 1000 = 48,435 \text{ ml.} \qquad \text{(K-11)}$$

Using Eqn. (I-12),

$$\Delta V_2 = W_2 v_{g2} - V$$

$$= 54.2 \times 673.22 - 1000 = 35,488 \text{ ml.} \qquad \text{(K-12)}$$

Using Eqn. (I-13),

$$m_1 = \frac{v_{fg2}\Delta V_1 + v_{f2}\Delta V_2}{v_{fg1}v_{fg2} - v_{f1}v_{f2}}$$

$$= \frac{670.80 \times 48,435 + 2.415 \times 35,488}{126.03 \times 670.80 - 1.158 \times 2.415}$$

$$= 385.32 \text{ grams.} \qquad \text{(K-13)}$$

Using Eqn. (I-14),

$$m_2 = \frac{v_{fg1}\Delta V_2 + v_{f1}\Delta V_1}{v_{fg1}v_{fg2} - v_{f1}v_{f2}}$$

$$= \frac{126.03 \times 35,488 + 1.158 \times 48,435}{126.03 \times 670.80 - 1.158 \times 2.415}$$

$$= 53.57 \text{ grams.} \qquad \text{(K-14)}$$

Using Eqn. (I-5) with these values of m_1 and m_2,

$$x_1 = \frac{\frac{M_2}{M_1} m_1}{\frac{M_2}{M_1} m_1 + m_2}$$

$$= \frac{4.061 \times 385.32}{4.061 \times 385.32 + 53.57} = 0.9669. \qquad \text{(K-15)}$$

Therefore, from Eqn. (I-6),

$$x_2 = 1 - x_1$$

$$= 1 - 0.9669 = 0.0331, \qquad \text{(K-16)}$$

which coincides with the trial value of x_2. Thus, the values of m_1, m_1', m_2, m_2' to be used for computing the initial conditions for the first partial run of Run 16 are

m_1 = 385.32 grams

m_1' = 3.48 grams

m_2 = 53.57 grams

and m_2' = 0.63 grams.

(c) Computing the Vapor Phase Volume V' and Amount of Hydrogen in the Vapor Phase n_o'

The partial pressure of hydrogen consistent with these values of the amount of the condensable components of the system found in the preceding subsection was obtained from Eqn. (I-4),

$$p_o = p - (\pi_1 x_1 + \pi_2 x_2) \qquad \text{(K-17)}$$

where p_o is the partial pressure of hydrogen in atmospheres and p is the total pressure of the system before taking the zero point sample (sample No. 0) in atmospheres. Therefore,

$$p_o = 78.55 - (15.35 \times 0.967 + 25.31 \times 0.033)$$
$$= 62.94 \text{ atmospheres}. \qquad \text{(K-18)}$$

The volume of the vapor phase was obtained from the first half of Eqn. (I-1),

$$V' = V - m_1 v_{f1} - m_2 v_{v2} \qquad \text{(K-19)}$$

where V_g is the volume of the vapor phase in milliliters and V is the total volume of the system in milliliters. Therefore,

$$V' = 1{,}000 - 385.32 \times 1.158 - 53.57 \times 2.415$$
$$= 424.9 \text{ milliliters}. \qquad \text{(K-20)}$$

The amount of hydrogen in the vapor phase was obtained from the last half of Eqn. (I-1),

$$n_o' = \frac{p_o V'}{RT} \qquad \text{(K-21)}$$

where n_o' is the number of grammoles of hydrogen gas in the vapor phase

and R is the gas constant in ml.atmospheres/grammole·°K. Therefore,

$$n_o' = \frac{62.94 \times 424.9}{82.06 \times 473.1} = \underline{0.689 \text{ grammoles}}. \qquad \text{(K-22)}$$

This value was entered as "Total Amount of H_2 Charged: $n_{o,o}'$" in Table M-VIII.

(d) Computing the Total Amounts of Water and Diethylamine Existing during the First Partial Run, $W_{1,1}$ and $W_{2,1}$

In estimating the total amounts of water and diethylamine remaining in the system after the zero-point sample was taken, it was assumed that there was no material transfer occurring between the two phases and that the vapor phase volume remained unaffected by the sampling. Although the phase equilibria were disturbed by the sampling of a portion of the vapor phase mixture, the time period required for taking the sample was a matter of one second or two, enough to crack and close a needle valve, during which hardly any material transfer could occur. Therefore, just after taking the zero-point sample, the amount of hydrogen remaining in the system $n_o'^*$ was given by

$$n_o'^* = \frac{V' p_o^*}{RT} \qquad \text{(K-23)}$$

where p_o^* was the partial pressure of hydrogen just after taking the zero-point sample and was given by

$$p_o^* = p^* - \pi_1 x_1 - \pi_2 x_2 \qquad \text{(K-24)}$$

in which p^* was the total residual pressure of hydrogen just after taking the zero-point sample and x_1 and x_2 were the values of the mole fractions of water and diethylamine, respectively, as calculated in the preceding subsections for equilibria existing before the zero-point sample was taken. It was also assumed that the sample taken was representative of the composition of the vapor phase chemically as well as isotopically, so that

$$\frac{m_1'^*}{m_1'} = \frac{m_o'^*}{m_o'} = \frac{n_o'^*}{n_o'} = \frac{p_o^*}{p_o} \qquad \text{(K-25)}$$

where the quantity with a superscript * represents that quantity remaining in the vapor phase just after sampling, while one without the superscript * represents the equilibrium quantity before the sampling. Combining Eqn's (K-24) and (K-25),

$$m_1'^* = \frac{p_o^*}{p_o} m_1'$$

$$= \frac{p^* - (\pi_1 x_1 + \pi_2 x_2)}{p - (\pi_1 x_1 + \pi_2 x_2)} (W_1 - m_1) \qquad \text{(K-26)}$$

Similarly,

$$m_2'^* = \frac{p^* - (\pi_1 x_1 + \pi_2 x_2)}{p - (\pi_1 x_1 + \pi_2 x_2)} (W_2 - m_2) \qquad \text{(K-27)}$$

Thus, with these values of $m_1'^*$ and $m_2'^*$, the total amounts of water and diethylamine remaining after the zero-point sampling, $W_{1,1}$ and $W_{2,1}$, were

$$W_{1,1} = m_1'^* + m_1 \qquad \text{(K-28)}$$

and $$W_{2,1} = m_2'^* + m_2 \qquad \text{(K-29)}$$

Using Eqn. (K-2) and the value of $p^* = 77.87$ atmospheres from Table K-II,

$$p_o^* = 77.87 - 15.61 = 62.26 \text{ atmospheres.} \qquad \text{(K-30)}$$

Using Eqn. (K-1),

$$n_o'^* = \frac{62.26 \times 424.9}{82.06 \times 473.1} = 0.681 \text{ grammoles.} \qquad \text{(K-31)}$$

Using Eqn's (K-26) and (K-27),

$$m_1'^* = 3.34 \text{ grams} \qquad \text{(K-32)}$$

and $$m_2'^* = 0.628 \text{ grams.} \qquad \text{(K-33)}$$

Therefore, using Eqn's (K-28) and (K-29),

$$W_{1,1} = 3.34 + 385.32 = 388.66 \text{ grams} \qquad \text{(K-34)}$$

and $$W_{2,1} = 0.628 + 53.57 = 54.195 \text{ grams.} \qquad \text{(K-35)}$$

(e) Computing the Phase Equilibrium Quantities during Each Partial Run

Using the values of Eqn's (K-34) and (K-35) in place of W_1 and W_2 in the formulae in the previous subsection (b), another series of the trial-and-error procedures yielded

$$m_1 = 385.28 \text{ grams} \qquad \text{(K-36)}$$

and $$m_2 = 53.56 \text{ grams} \qquad \text{(K-37)}$$

which represented amounts of water and diethylamine existing in the liquid phase during the partial run No. 1. Using these values with the equations in the previous subsection (c), it was found that, for the period of the partial run No. 1,

$$p_o = 62.26 \text{ atmosphere} \qquad \text{(K-38)}$$

$$V' = 424.7 \text{ milliliters} \qquad \text{(K-39)}$$

and $$n_o' = 0.681 \text{ grammoles}. \qquad \text{(K-40)}$$

This value of n_o' was entered in Table M-VIII as $n_{o,1}'$. Equations in the preceding subsection (d) yielded

$$W_{1,2} = 388.63 \text{ grams} \qquad \text{(K-41)}$$

and $$W_{2,2} = 54.186 \text{ grams} \qquad \text{(K-42)}$$

which were further used for calculating the equilibrium quantities to be used for computing initial conditions for partial run No. 2. The same procedures were repeated for all the other partial runs, with the results summarized in Table K-III. It is seen that the phase equilibrium quantities of water and amine and the vapor phase volume remained nearly constant throughout the run while the amount of hydrogen changed considerably. To illustrate the point further, results on the similar calculations for a blank run, Run 13, are summarized in Table K-IV.

This shows that the repeated calculations of the phase equilibria for every sample were not necessary and only one calculation for the first sample was sufficient for all equilibrium quantities except the amount of hydrogen gas,

Table K-III

Summary of the Phase Equilibrium Calculations

for Run 16 at 200°C

Partial Run No.	Water		Diethylamine		Hydrogen	
	m_1 (grams)	m_1' (grams)	m_2 (grams)	m_2' (grams)	n_o' (gmoles)	V' (ml)
Before starting	385.32	3.48	53.57	0.63	0.689	424.9
1	385.28	3.48	53.56	0.63	0.681	424.7
2	385.25	3.48	53.55	0.63	0.674	425.0
3	385.19	3.48	53.54	0.63	0.663	425.1
4	385.13	3.48	53.53	0.63	0.652	425.2
5	385.11	3.48	53.52	0.63	0.637	425.2
6	385.09	3.48	53.51	0.63	0.615	425.3
7	385.08	3.48	53.50	0.63	0.593	425.3
8	385.07	3.48	53.50	0.63	0.548	425.3
9	385.06	3.48	53.49	0.63	0.473	425.4

Table K-IV

Summary of the Phase Equilibrium Calculations for Blank Run 13 at 100°C

Partial Run No.	Water		Hydrogen	
	m_1 (grams)	m_1' (grams)	n_o' (gmoles)	V' (ml)
Before starting	459.74	0.26	1.366	520.8
1	459.74	0.26	1.354	520.7
2	459.73	0.26	1.308	520.7
3	459.73	0.26	1.296	520.7
4	459.73	0.27	1.250	520.7
5	459.73	0.27	1.220	520.7
6	459.73	0.27	1.180	520.7
7	459.72	0.27	0.949	520.7
8	459.72	0.28	0.891	520.6

which was computed from Eqn. (I-1) and an approximation formula for Eqn. (K-24),

$$p_o = p - (\pi_1 x_1 + \pi_2 x_2) \qquad \text{(K-43)}$$

where p is the total residual pressure after the preceding sample was taken and the quantity in parentheses is assumed to be constant and equal to that for the first sample. The values of n_o' thus calculated was entered in Tables M-I to M-XVII as "Amount of Hydrogen after Sampling".

K-2. Rate Constant

Run No. 24 is used for the illustration. This was a run at 150°C with a concentration of diethylamine in the solution charged of 0.78 normal. Results of the phase equilibrium calculations, together with the outputs of the thermal conductivity bridge are summarized in Table K-V. The theoretical equilibrium constant, $K_{150°C} = 0.433$, was used.

(a) Computing the Atom Fraction Deuterium in Hydrogen Gas, f_d'

The T/C-cell output millivoltages for samples No. 6 and 8 are obviously too high compared with the other samples. This is attributed to contamination of the sample by air, and these two results were disregarded. Since the analyses were made with a sensitivity "1", calibration No. 1 was used to compute the atom fraction deuterium in hydrogen;

$$f_d' = \frac{0.02175E}{1 + 0.02175E} \qquad \text{(K-44)}$$

where f_d' is the atom fraction deuterium in hydrogen gas and E is the thermal conductivity cell bridge output in millivolts.

Table K-V

Results of Phase Equilibrium Calculations and Thermal Conductivity Analyses of Run 24

m_1 = 424.3 grams m_1' = 1.20 grams

m_2 = 26.32 grams m_2' = 0.16 grams

V' = 487 milliliters

Sample Number (n)	Amount of Hydrogen after Sampling $n'_{o,(n+1)}$ (gmole)	T/C-cell Output E_n (millivolts)*
0	1.17	0
1	1.15	0.25
2	1.12	0.52
3	1.11	0.78
4	1.09	1.20
5	1.07	1.55
6	1.06	4.43
7	1.03	3.62
8	0.99	8.70
9	0.89	3.65

*The sensitivity used was "1", so that the calibration curve to be used was No. 1.

Using the values of E in Table K-V, f'_d was calculated for each sample. The results are tabulated in Table K-VI.

Table K-VI

Atom Fraction Deuterium in Hydrogen Gas for Samples of Run 24

Sample Number (n)	Atom Fraction Deuterium in Hydrogen Gas, $f'_{d,n}$
0	0
1	0.0054
2	0.0112
3	0.0167
4	0.0254
5	0.0326
6	----
7	0.0729
8	----
9	0.0735

Values in the seventh column of Table M-XII are identical with the values in Table K-VI except that the former are expressed in percent.

(b) Computing the Initial Amounts of H_2 and HD and the Amount of Reaction for Each Partial Run, A_n, C_n and ΔX_n

For the system before taking the zero-point sample, using Eqn's (J-10a) and (J-10c),

$$A_o = n'_{o,o} = 1.22 \qquad \text{(K-45)}$$

and $$C_o = 0 \qquad \text{(K-46)}$$

and, also,

$$\Delta X_o = 0. \qquad \text{(K-47)}$$

For the first partial run, using Eqn's (J-61), (J-62) and (J-63),

$$A_1 = n'_{o,1}(1 - f'_{d,o})^2$$

$$= 1.17 \times (1 - 0)^2 = 1.170 \text{ grammoles} \qquad \text{(K-48)}$$

$$C_1 = 2n'_{o,1}f'_{d,o}(1 - f'_{d,o})$$

$$= 2 \times 1.17 \times 0 = 0 \text{ grammoles} \qquad \text{(K-49)}$$

and $$\Delta X_1 = 2n'_{o,1}(f'_{d,1} - f'_{d,o})$$

$$= 2 \times 1.17 \times (0.0054 - 0) = 0.0126 \text{ gmoles.} \qquad \text{(K-50)}$$

For the second partial run using Eqn's (J-61), (J-62) and (J-63),

$$A_2 = n'_{o,2}(1 - f'_{d,1})^2$$

$$= 1.15 \times (1 - 0.0054)^2 = 1.138 \text{ grammoles} \qquad \text{(K-51)}$$

$$C_2 = 2n'_{o,1}f'_{d,1}(1 - f'_{d,1})$$

$$= 2 \times 1.15 \times 0.0054 \times (1 - 0.0054) = 0.0124 \text{ gmoles} \qquad \text{(K-52)}$$

and $$\Delta X_2 = 2n'_{o,2}(f'_{d,2} - f'_{d,1})$$

$$= 2 \times 1.15 \times (0.0112 - 0.0054) = 0.0133 \text{ gmoles.} \qquad \text{(K-53)}$$

The procedures were the same for all other samples. For sample No. 7, since the result of the analysis of sample No. 6 was disregarded, the result of the analysis of sample No. 5 had to be used. Thus, for the partial run No. 7,

$$A_7 = n'_{o,7}(1 - f'_{d,5})^2$$

$$= 1.07 \times (1 - 0.0326)^2 = 1.001 \text{ grammoles} \qquad \text{(K-54)}$$

$$C_7 = 2n'_{o,7}f'_{d,5}(1 - f'_{d,5})$$

$$= 2 \times 1.07 \times 0.0325 \times (1 - 0.0326) = 0.0675 \text{ gmoles} \qquad \text{(K-55)}$$

and $$\Delta X_7 = 2n'_{o,7}(f'_{d,7} - f'_{d,5})$$

$$= 2 \times 1.07 \times (0.0729 - 0.0326) = 0.0863 \text{ gmoles.} \qquad \text{(K-56)}$$

A similar procedure was used for computing A_9, C_9 and ΔX_9. These results for ΔX_n, A_n and C_n were entered in columns 8, 9 and 13, respectively, in Table M-XII.

(c) Computing the Initial Amounts of HDO and H_2O for Each Partial Run, B_n and D_n

For computing the atom fraction deuterium in the total exchangeable atoms of hydrogen isotopes in the liquid before exchange was started, f_d, Eqn. (H-14) was used,

$$f_d = \frac{0.2285}{1 + \frac{N}{0.1084(1000 - 73.14N)}} \qquad \text{(K-57)}$$

where ρ is the density of the solution charged. This was calculated from Eqn. (H-12) and the value of normality of

the solution, N = 0.78, to be 1.0060 grams per milliliter. Thus,

$$f_d = 0.226. \tag{K-58}$$

Equation (J-7),

$$(4 - K_w)\eta^2 + [K_w - 2f_d(4 - K_w)]\eta + 2f_d(2f_d - K_w) = 0 \tag{K-59}$$

was solved with $K_w = 3.91$ and $f_d = 0.226$ to find

$$\eta = 0.405. \tag{K-60}$$

From Eqn's (J-9-a), (J-9-b) and (J-9-c),

$$\xi_o = 1 - \eta$$
$$= 0.596 \tag{K-61}$$

$$\xi_1 = 2(\eta - f_d)$$
$$= 0.356 \tag{K-62}$$

and $$\xi_1 = f_d$$
$$= 0.226. \tag{K-63}$$

Also, from the total amounts of water and diethylamine charged,

$$W_1 = 425.5 \text{ grams} \tag{K-64}$$

and $$W_2 = 26.48 \text{ grams}, \tag{K-65}$$

the quantities $(n_{1,o} + n'_{1,o})$ and $(n_{2,o} + n'_{2,o})$ were calculated as follows.

Total number of grammoles of water charged; $n_{1,o} + n'_{1,o} = \frac{W_1}{M_1} = \frac{425.5}{18.45} = 23.08$ (K-66)

Total number of grammoles of amine charged; $n_{2,0} + n'_{2,0} = \frac{W_2}{M_2} = \frac{26.48}{73.14} = 0.362.$ (K-67)

Thus, using Eqn's (J-10-b), (J-10-d), (J-10-e) and J-10-f);

Initial amount of HDO

$$B_0 = \xi_1(n_{1,0} + n'_{1,0})$$

$$= 0.356 \times 23.08 = 8.200 \text{ grammoles} \quad \text{(K-68)}$$

Initial amount of H_2O;

$$D_0 = \xi_0(n_{1,0} + n'_{1,0})$$

$$= 0.596 \times 23.08 = 13.735 \text{ grammoles} \quad \text{(K-69)}$$

Initial amount of $(C_2H_5)_2NH$;

$$E_0 = (1 - \xi_1)(n_{2,0} + n'_{2,0})$$

$$= 0.774 \times 0.362 = 0.280 \text{ grammoles} \quad \text{(K-70)}$$

and Initial amount of $(C_2H_5)_2ND$;

$$G_0 = \xi_1(n_{2,0} + n'_{2,0})$$

$$= 0.226 \times 0.362 = 0.082 \text{ grammoles.} \quad \text{(K-71)}$$

Therefore, from Eqn. (J-15a),

$$F = \frac{2(B_0 + D_0)}{(E_0 + G_0) + 2(B_0 + D_0)}$$

$$= \frac{2 \times (8.200 + 13.735)}{0.362 + 2 \times (8.200 + 13.735)} = 0.993. \quad \text{(K-72)}$$

For other samples, using Eqn's (J-64) and (J-65),

$$B_1 = B_0 - F\Delta X_0$$

$$= 8.200 - 0.993 \times 0 = 8.200 \text{ grammoles} \quad \text{(K-73)}$$

$$B_2 = B_1 - F\Delta X_1$$

$$= 8.200 - 0.993 \times 0.0126 = 8.187 \text{ grammoles} \quad \text{(K-74)}$$

and so on for other B_n, and

$$D_1 = D_0 - F\Delta X_0$$

$$= 13.735 - 0.993 \times 0 = 13.735 \text{ grammoles} \quad \text{(K-75)}$$

$$D_2 = D_1 + F\Delta X_1$$

$$= 13.735 + 0.993 \times 0.0126 = 13.748 \text{ grammoles} \quad \text{(K-76)}$$

and so on for other D_n. These values of B_n and D_n are entered in columns 10 and 11 in Table M-XII.

(d) Computing ΔL_n and L_n

For quantities δ_1 and δ_2 for each partial run, Eqn's (J-24) and (J-25) were used. For instance, for partial run No. 1,

$$\delta_{1,1} = K(A_1F + B_1) + (C_1F + D_1)$$

$$= 0.433 \times (1.170 \times 0.993 + 8.200) + (0 \times 0.993 + 13.735)$$

$$= 17.794 \text{ grammoles} \quad \text{(K-77)}$$

and

$$\delta_{2,1} = -4F(1 - K)(KA_1B_1 - C_1D_1)$$

$$= 4 \times 0.993 \times (0.567) \times (0.433 \times 1.170 \times 8.200 - 0 \times 13.735)$$

$$= -9.356(\text{grammole})^2. \quad \text{(K-78)}$$

For quantities α and β for each sample, Eqn's (J-22) and (J-23) were used. For instance, for partial run No. 1,

$$\alpha_1 = \frac{-\delta_{1,1} - \sqrt{\delta_{1,1}^2 - \delta_{2,1}}}{2F(1 - K)}$$

$$= \frac{-17.794 - \sqrt{(17.794)^2 - (-9.356)}}{2 \times 0.993 \times (0.567)}$$

$$= -31.835 \text{ grammoles} \qquad \text{(K-79)}$$

and

$$\beta_1 = \frac{-\delta_{1,1} + \sqrt{\delta_{1,1}^2 - \delta_{2,1}}}{2F(1 - K)}$$

$$= \frac{-17.794 + \sqrt{(17.794)^2 - (-9.356)}}{2 \times 0.993 \times (0.567)}$$

$$= 0.2318 \text{ grammoles.} \qquad \text{(K-80)}$$

These values of δ_1, δ_2, α and β for each partial run are summarized in Table K-VII. These values of β are entered in Column 12 in Table M-XII.

The value of ΔL_n for each partial run was then computed by Eqn. (J-48),

$$L_n \equiv \frac{1}{\beta_n - \alpha_n} \ln \frac{\beta_n(\Delta X_n - \alpha_n)}{\alpha_n(\Delta X_n - \beta_n)} \qquad \text{(K-81)}$$

For instance, for the first partial run,

$$L_1 = \frac{1}{0.2318 - (-31.835)} \ln \frac{0.2318 \times [0.0126 - (-31.835)]}{(-31.835) \times [0.0126 - 0.2318)]}$$

$$= 0.00176 \text{ grammole}^{-1} \qquad \text{(K-82)}$$

A similar calculation for the second partial run yielded

$$L_2 = 0.00200 \text{ grammole}^{-1} \qquad \text{(K-83)}$$

Table K-VII

Values of δ_1, δ_2, α and β for Each Partial Run of Run 24

Partial Run No.	δ_1 (gmole)	δ_2 (gmole^2)	α (gmole)	β (gmole)
1	17.794	-9.356	-31.835	0.2318
2	17.799	-8.700	-31.829	0.2156
3	17.801	-7.962	-31.813	0.1974
4	17.810	-7.414	-31.816	0.1838
5	17.822	-6.543	-31.826	0.1622
6	---	---	---	---
7	17.829	-5.838	-31.812	0.1447
8	---	---	---	---
9	17.899	-2.583	-31.855	0.0639

The value of L_n through each partial run was obtained by Eqn. (J-52) or

$$L_n \equiv \sum_{i=1}^{n} \Delta L_i . \qquad \text{(K-84)}$$

Thus, for the first partial run,

$$L_1 = \Delta L_1$$
$$= 0.00176 \text{ grammole}^{-1} \qquad \text{(K-85)}$$

and, for the second partial run,

$$L_2 = \Delta L_1 + \Delta L_2$$
$$= 0.00176 + 0.00200$$
$$= 0.00376 \text{ grammole}^{-1} . \qquad \text{(K-86)}$$

These results are shown in columns No. 14 and 15 in Table M-XII.

(e) Computing Weight for L_n; w_n

For computing errors of L_n which were later used for obtaining the weight, w_n, of each experimental point, the experimental errors only were taken into account, that is, equations in subsection (J-2) of the APPENDIX were used. The results are summarized in Table K-VIII.

The first term in Eqn. (J-74), used for computing $P(f'_{d,n})$,

$$\left[P(f'_d)\right]_n^2 = \left[EP(\gamma)\right]_n^2 + \left[\gamma P(E)\right]_n^2 \qquad \text{(K-87)}$$

was, for the case of the calibration "1", equal to

$$\left[EP(\gamma)\right]_n^2 = (1.56 \times 10^{-4})^2 E_n^2$$
$$= 2.43 \times 10^{-8} E_n^2 \qquad \text{(K-88)}$$

which was, at most, 3.25×10^{-7} in Run 24, while the second term containing P(E) was always of the order of 10^{-6} as shown below in Eq. (K-90). It is, therefore, seen that the first term was negligible in most cases.

According to Eqn. (J-73),

$$P(E^{o}) = 0.05 \text{ millivolts} \qquad \text{(K-89)}$$

for a single measurement of the bridge output. Almost always, however, the result of analysis of the zero-point sample was found to deviate slightly from exactly zero output, thus making it necessary to deduct the output for the zero-point sample from the output for other samples. Therefore, the corrected outputs listed in Tables M-I to M-XVII are mostly differences of two observations. Some of them are results of even three or four observations as it was sometimes necessary to repeat a zero setting or to change sensitivities in going from one sample to the next in the same run. Thus, and effective value of P(E) of an output value which was obtained as a result of q observations was given by $0.05\sqrt{q}$, where q was the number of observations. The point will be best illustrated in an actual example of Run 24.

In Run 24, samples No. 0, 1, 2 and 3 were analyzed with one zero-setting and the remaining four samples were analyzed with a renewed zero setting since there was a prolonged interruption between analyses of the two groups of samples. Also, since the output of the zero-point sample was -0.05 mV relative to the first zero-setting, all other output values

had to be augmented by 0.05 mV. The output values appearing in Tables K-V and M-XII are the ones which have been corrected in this manner. Thus, the value of q for samples No. 1, 2 and 3 was 2. That for the remaining four samples, however, was 3 because there was an additional uncertainty in the second zero reading, relative to the first, obtained as a result of the second zero-setting.

Therefore, the second term of Eqn. (J-74) was

$$\left[\gamma P(E)\right]_n^2 = (0.02175 \times 0.05 \times 2)^2 = 2.36 \times 10^{-6} \text{ for samples No. 1, 2 and 3} \qquad \text{(K-90)}$$

and

$$\left[\gamma P(E)\right]_n^2 = (0.02175 \times 0.05 \times 3)^2 = 3.55 \times 10^{-6} \text{ for samples No. 4, 5, 7 and 9.} \qquad \text{(K-91)}$$

These values were used to compute values of $P(f_{d,n}^{\circ})$ which appear in the fourth column of Table K-VIII.

It was noticed that P(F) was as small as

$$P(F) = 2.62 \times 10^{-5} \qquad \text{(K-92)}$$

or

$$\left[\frac{P(F)}{F}\right]^2 = 6.95 \times 10^{-10} \qquad \text{(K-93)}$$

so that terms containing P(F) in Eqn's (J-80), (J-82), (J-83), (J-84) and (J-85) are negligible compared with other terms.

It may be also seen, as from Table K-VIII, that $P(\Delta L_n)$ is mostly due to the error in ΔX rather than due to the error in β (see Eqn. (J-86)).

Table K-VIII

Summary of Error Calculations for Run 24

Partial Run Number (n)	$\left[\frac{P(n_o')}{n_o'}\right]_n^2$	q_n^*	$P(f_{d,n}')$	$P^2(A_n)$	$P^2(C_n)$	$P^2(B_n)$	$P^2(D_n)$	$P^2(\delta_{1,n})$	$P^2(\delta_{2,n})$
1	2.1×10^{-5}	2	1.5×10^{-3}	2.9×10^{-5}	0	3.7×10^{-4}	1.0×10^{-3}	1.1×10^{-3}	1.9×10^{-3}
2	2.2 "	2	1.5 "	4.0 "	1.2×10^{-5}	3.8 "	1.1 "	1.1 "	1.4×10^{-2}
3	2.3 "	2	1.5 "	3.9 "	1.1 "	4.1 "	1.1 "	1.2 "	1.3 "
4	2.3 "	3	1.8 "	3.8 "	1.1 "	4.3 "	1.1 "	1.2 "	1.3 "
5	2.4 "	3	1.8 "	4.1 "	1.4 "	4.6 "	1.1 "	1.2 "	1.7 "
7	2.5 "	3	1.7 "	3.9 "	1.3 "	4.9 "	1.2 "	1.3 "	1.5 "
9	2.6 "	3	1.7 "	3.2 "	9.5×10^{-5}	5.2 "	1.2 "	1.3 "	1.2 "

Partial Run Number (n)	$\left[\frac{P(\beta)}{\beta}\right]_n^2$	$P^2(\Delta X_n)$	$\left[\frac{(2\beta - \Delta X)P(\beta)}{\beta}\right]_n^2$	$\left[\frac{P(\Delta X)}{\Delta X}\right]_n^2$	$P(\Delta L_n)$	$P^2(L_n)$	w_n
1	2.4×10^{-5}	1.3×10^{-5}	5.0×10^{-6}	8.0×10^{-2}	5.1×10^{-4}	2.6×10^{-7}	1.00
2	1.9×10^{-4}	2.5 "	3.4×10^{-5}	1.4×10^{-1}	7.7 "	8.6 "	0.31
3	2.1 "	2.3 "	3.0×10^{-5}	1.5×10^{-1}	8.2 "	1.5×10^{-6}	0.17
4	2.3 "	2.8 "	2.8×10^{-5}	7.4×10^{-2}	1.0×10^{-3}	2.6 "	0.10
5	3.9 "	3.2 "	3.7×10^{-5}	1.3×10^{-1}	1.2 "	4.0 "	0.07
7	4.5 "	2.9 "	1.9×10^{-5}	3.9×10^{-3}	3.2 "	1.4×10^{-5}	0.02
9	1.7×10^{-3}	5.1 "	2.8×10^{-5}	3.9×10^{1}	3.8 "	2.9 "	0.009

(f) Computing Slope and Rate Constants; S, $\langle k_2 \rangle$ and k_2

The slope of a best-fit straight line for the plot of the quantity L against time was obtained by Eqn. (J-89), and the probable error of the slope was estimated from Eqn's (J-90) and (J-91). The last point in Run 24 had such a low weight compared to the first point of the run (see the last column in Table K-VIII) that this point was neglected in the least-squares calculation. The results are summarized in Table K-IX.

Table K-IX

Least-Squares Fit Calculation for Run 24

Sample Number	w	L (gmole^{-1})	t (hr)	wt (hr)	St (gmole^{-1})	$(L-St)^2$ (gmole^{-2})
1	1.00	1.76×10^{-3}	0.5	0.500	1.77×10^{-3}	0.0001×10^{-6}
2	0.31	3.76 "	1.0	0.310	3.54 "	0.0485 "
3	0.17	5.78 "	1.5	0.255	5.30 "	0.230 "
4	0.10	9.29 "	2.5	0.250	8.85 "	0.193 "
5	0.07	12.47 "	3.5	0.245	12.40 "	0.0005 "
7	0.02	40.91 "	12.0	0.240	42.50 "	2.53 "

(Table K-IX is continued on the following page.)

$$S = \frac{\sum_{n=1}^{M} w_n t_n L_n}{\sum_{n=1}^{M} w_n t_n^2} = \frac{18.714 \times 10^{-3}}{5.305} = 3.54 \times 10^{-3} \quad \text{gmole}^{-1}\text{hr}^{-1} \qquad \text{(K-94)}$$

$$P(\bar{L}) = 0.675 \sqrt{\frac{\sum_{n=1}^{M} w_n (L_n - St_n)^2}{(M-1) \sum_{n=1}^{M} w_n}}$$

$$= 0.675 \times \sqrt{\frac{0.1244 \times 10^{-6}}{5 \times 1.67}} = 8.25 \times 10^{-5} \quad \text{gmole}^{-1} \qquad \text{(K-95)}$$

$$P(S) = \frac{P(\bar{L}) \sqrt{\sum_{n=1}^{M} w_n^2 t_n^2}}{\sum_{n=1}^{M} w_n t_n^2}$$

$$= \frac{(8.25 \times 10^{-5}) \sqrt{0.592}}{5.305} = 1.20 \times 10^{-5} \quad \text{gmole}^{-1}\text{hr}^{-1} \qquad \text{(K-96)}$$

The predicted probable error $\overline{P(L)}$ was found from Eqn. (J-92) to be

$$\overline{P(L)} = \sqrt{\frac{MP^2(L_1)}{(M-1) \sum_{n=1}^{M} w_n}}$$

$$= \sqrt{\frac{6 \times (26.3 \times 10^{-8})}{5 \times 1.67}}$$

$$= 4.35 \times 10^{-4} \quad \text{gmole}^{-1} \qquad \text{(K-97)}$$

which value was larger than the observed probable error $P(\overline{L})$ in Table K-IX. This indicates that the experimental points fit a straight line better than predicted from the errors estimated for the measured quantities entering the calculations of L.

To calculate $\langle k_2 \rangle$, using Eqn. (J-53),

$$\langle k_2 \rangle = \frac{SV^o}{F(1 - K)}$$

$$= \frac{(3.54 \times 10^{-3})(10^3)}{(0.993)(0.567)}$$

$$= 6.29 \quad \text{ml/gmole.hour} \qquad \text{(K-98)}$$

Error in $\langle k_2 \rangle$ was computed from Eqn. (J-102),

$$P(\langle k_2 \rangle) = \frac{P(S)\, V^o}{F(1 - K)}$$

$$= \frac{(1.2 \times 10^{-5})(10^3)}{(0.993)(0.567)}$$

$$= 0.0223 \quad \text{ml/gmole.hour} \qquad \text{(K-99)}$$

The value of the rate constant for the liquid phase, k_2, was computed from Eqn. (J-92),

$$k_2 = \frac{V}{\lambda_o \lambda_1} \left(\frac{\langle k_2 \rangle}{V^o} - \frac{\lambda_o' \lambda_1' k_2'}{V'} \right) \qquad \text{(K-100)}$$

where k_2' was obtained from a blank run at the same temperature, 150°C, Run No. 9, and was equal to 62.0 $\pm$ 0.8 ml/gmole.hour. Values of λ_o and λ_1 were obtained from Eqn's (J-55) and (J-56).

$$\lambda_o = \frac{760RT\left(\frac{m_1}{M_1} + \frac{m_2}{M_2}\right)}{cV'}$$

$$= \frac{760 \times 82.06 \times 423 \times \left(\frac{424.3}{18.45} + \frac{26.32}{73.14}\right)}{(5.46 \times 10^7) \times (487)}$$

$$= 0.0231 \qquad \text{(K-101)}$$

and

$$\lambda_1 = \frac{m_1}{W_1}$$

$$= \frac{424.3}{425.5} = 0.9972. \qquad \text{(K-102)}$$

Also,

$$\lambda_o' = 1 - \lambda_o = 0.9769 \qquad \text{(K-103)}$$

and

$$\lambda_1' = 1 - \lambda_1 = 0.0028. \qquad \text{(K-104)}$$

Thus,

$$k_2 = \frac{513}{(0.0231)(0.9972)}\left[\frac{6.29}{10^3} - \frac{(0.9769)(0.0028)(62.0)}{487}\right]$$

$$= 132.2 \quad \text{ml/gmole·hour} \qquad \text{(K-105)}$$

The probable error of this value of k_2 was estimated from Eqn. (J-103).

$$\left[\frac{P(k_2)}{k_2}\right]^2 = \left[\frac{0.0223}{6.29}\right]^2 + 12 \times 10^{-5}$$

$$= 13 \times 10^{-5}$$

$$P(k_2) = \sqrt{13 \times 10^{-5}} \times 132.2 = 1.5 \quad \text{ml/gmole-hr.}$$

L. Considerations on Reliability of the Values of Physical Properties

L-1. Estimate of Errors in the Rate Constant due to Uncertainties in Physical Properties

In deriving equations for the probable errors ΔX, β, L and $\langle k_2 \rangle$ in Section J of the APPENDIX, Eqns. (J-47) to (J-62), it was assumed that there were no uncertainties in the values of the physical properties given in Section H of the APPENDIX. This section shows that uncertainties in the physical properties used have no appreciable effect on ΔX, β, L and $\langle k_2 \rangle$.

There were two classed of uncertainties in physical properties. One is uncertainties in the values for the pure substances and the other is the error introduced in using these values for the pure substance directly for the component in a solution. The second uncertainty is treated in the next subsection, L-2, of the APPENDIX.

The first uncertainty is discussed in this section. It was treated by assigning to each property a numerical value of a limit of uncertainty within which the true value, taking into account the way by which the constant was estimated, could be said to lie with a reasonably high confidence, say, more than 50%. We might even assume that the distribution of error is normal. The effect of the uncertainties was then propagated in the standard manner. The effect of uncertainties in physical properties, however, could not be separated from the effect of the experimental errors in propagating the

errors. And, in treating them together, the limits of uncertainty, $P_o(q)$, which were somewhat vaguely defined quantities, had to be mixed up with the probable errors, $P(q)$. Since the total effect on the errors in the values of which resulted from this mixing turned out to be still negligible compared to the probable error in ΔX which was entirely caused by the experimental errors, which fact made the use of the approximation formula of Eqn. (J-86) acceptable, this procedure which had no theoretical ground was useful in proving the point. The effect of the uncertainties on evaluation of the rate constant from the slope was then estimated.

The effect of uncertainty in the value of the equilibrium constant, K, was treated in the DISCUSSION. The theoretical set of equilibrium constants were used for the present calculations. It was found that the effects of uncertainties in the physical properties of the magnitude assumed here were negligible compared with the experimental errors and did not affect the final results on the rate constants and their estimated errors.

The numerical values of the limits of uncertainty of the physical properties used are tabulated in Table L-I. A limit of uncertainty of a quantity q is represented by $P_o(q)$.

Results of the error estimation on the liquid-vapor equilibrium calculation are sumarized in Table L-II. It was found that the error in m_2, the amount of diethylamine in the liquid phase, did not contribute appreciably to the final error in k_2. Error in the partial pressure of hydrogen gas,

Table L-I

Assigned Limits of Uncertainty of the Constant Values

$P_o(v^s_{gl}) = P_o(v_{fgl})$	= 0.5 milliliter per gram
$P_o(v_{g2}) = P_o(v_{fg2})$	= 1 milliliter per gram
$P_o(v_{fl}) = P_o(v_{f2})$	= 0.01 milliliter per gram
$P_o(\pi_1) = P_o(\pi_1)$	= 0.05 atmospheres
$P_o(c)$	= 5×10^5 millimeter Hg per mole fraction H_2
$P_o(K_w)$	= 0.01

Table L-II

Uncertainties in Liquid-Vapor Equilibria due to Uncertainties in Physical Properties

Run Number	$P_o^2(m_1)$, $(gtm.)^2$	$P_o^2(V')$, $(ml)^2$
9	1.5	2.4
10	2.9	2.8
11	2.9	2.8
12	2.9	2.9
13	1.7	2.7
14	1.5	2.6
15	2.5	3.6
16	2.4	2.7
17	2.4	3.5
19	1.1	2.4
21	2.8	2.5
24	1.4	2.8
25	1.0	2.6
26	1.2	2.0
27	2.5	3.8
28	1.5	2.4
29	1.3	2.5

$P_o(p_o)$, due to these uncertainties was found to be smaller than that due to the error in reading the total pressure. It is seen from Table L-II that the assigned value of 1 ml for $P(V')$, employed in Section J of the APPENDIX for estimation of the effects of the direct experimental error, was not far from these calculated values, especially considering the fact that those in Table L-II consisted of the effects of experimental errors as well as the uncertainties in physical properties.

Thus, the uncertainties in the constant values used were found not affecting calculation of the slope S, at least through the basic probable errors assigned by Eqns. (J-67) to J-70). There was, however, one more route through which the uncertainty in these constant values might affect the slope calculations. It was due to the uncertainty in the value of K_w. It might have a significant effect on the calculation of the initial amounts of HDO and H_2O, B_o $(=B_1)$ and D_o $(=D_1)$. (See Eqns. (J-7) to (J-10d).) This, in turn, might significantly influence the value of F and subsequent values of B_n and D_n. (See Eqns. (J-62) to (J-65).)

The effect of small uncertainties in the value of the isotope equilibrium constant among the water molecules, K_w, was unimportant, as most of the deuterium was present as HDO at the atom fractions of deuterium used.

Equation (J-78) was replaced by

$$\left[\frac{P(F)}{F}\right]^2 \simeq \frac{\left(\frac{W_2}{M_2}\right)^2 \left\{\left(\frac{1}{W_1}\right)^2 + \left(\frac{1}{W_1 + W_2}\right)^2 + \left[\frac{P(\eta)}{1 + \eta - 2f_d}\right]^2\right\}}{\left[(e_1 + g_1) + 2(b_1 + d_1)\right]^2} \qquad \text{(L-1)}$$

Thus, P(F) for Run 24 became 2.82×10^{-5} in place of 2.62×10^{-5}, the value calculated in Section K of the APPENDIX without any uncertainty in the value of K_w.

Combined effects of these results were as follows. The term $P(F)/F^2$ was still negligible compared with other terms in all the equations for the error calculation. In Eqn. (J-83), the terms $F^2P^2(A_n)$, $A_n^2P^2(A_n)$, $A_n^2P^2(F)$, $F^2P^2(C_n)$ and $C_n^2P^2(F)$ became negligible compared with other terms. In Eqn. (J-84), the term $C_n^2P^2(D_n)$ was still negligible but the term $A^2P^2(B_n)$ became comparable with the term $B_n^2P^2(A_n)$. In Eqn. (J-85), the term of P(F) was still negligible. And, finally, in Eqn. (J-86), it was found that the term of $P(\beta)/\beta$ was still negligible compared with the term of $P(\Delta X)/\Delta X$. But, ΔX and $P(\Delta X)$ were purely experimental quantities and were not influenced by the uncertainties in the constants.

Thus, it was found that uncertainties in the physical properties of the order of magnitude listed in Table L-I did not significantly influence the weights of each point on the plot for determining the slope S, thus keeping the value of S and, therefore, $\langle k_2 \rangle$ unaffected.

L-2. <u>On the Ideality of the System, Hydrogen-Water-Diethylamine</u>

In deriving equations for liquid-vapor equilibria in the system, hydrogen-water-diethylamine, four ideal laws were assumed. These were (1) the ideality of the liquid solution of diethylamine in water, (2) Raoult's law for the vapor pressures of water and diethylamine, over the liquid mixture,

(3) Gibbs-Dalton's law for the partial pressures in the vapor, and (4) Henry's law for the solubility of hydrogen gas in the liquid. The applicability of Henry's law is discussed in Section H of the APPENDIX.

To find out the extent to which the first three laws were valid in the present case, measured values and calculated values based on the ideal laws were compared for two quantities. These were the density of the mixture of water and diethylamine and the total amount of hydrogen gas charged.

The density of the solutions was related to the normality of amine by Eqns. (H-12) and (H-13) which were obtained from actual measurements of both quantities. If the solution were really ideal, the volumes would have been additive so that a relation

$$\frac{NM_2}{\bar{\rho}} + \frac{(1000\bar{\rho} - NM_2)}{\bar{\rho}} = 1000 \qquad \text{(L-2)}$$

had to be satisfied. Solving this for $\bar{\rho}$,

$$\bar{\rho} = \bar{\rho}_1 - \frac{NM_2}{1000}\left(\frac{\bar{\rho}_1}{\rho_2} - 1\right) \qquad \text{(L-3)}$$

Using $M_2 = 73.14$, $\rho_2 = 0.705$ grams per milliliter at 25°C and $\bar{\rho}_1 = 1.024$ grams per milliliter for the "1N" runs and $\bar{\rho}_1 = 1.028$ grams per milliliter for the "2N" runs, this relation became

$$\bar{\rho} = 1.024 - 0.0332N \qquad \text{for the "1N" runs} \qquad \text{(L-4)}$$

and

$$\bar{\rho} = 1.028 - 0.0335N \qquad \text{for the "2N" runs} \qquad \text{(L-5)}$$

These were compared with Eqns. (H-12) and (H-13). For the "1N" runs,

$$\frac{\Delta\rho}{\rho} \equiv \frac{\rho - \bar{\rho}}{\rho} = \frac{0.0168N - 0.005}{1.0188 - 0.0164N} \qquad \text{(L-6)}$$

Therefore, when N was 0.5, $\Delta\rho/\rho$ = + 0.0034 and, when N was 1.0, $\Delta\rho/\rho$ = + 0.0118. For the "2N" runs,

$$\frac{\Delta\rho}{\rho} \equiv \frac{\rho - \bar{\rho}}{\rho} = \frac{0.0158N - 0.013}{1.0149 - 0.0177N} \qquad \text{(L-7)}$$

Therefore, when N was 1.5, $\Delta\rho/\rho$ = + 0.0108 and, when N was 2.0, $\Delta\rho/\rho$ = + 0.0190. Thus the ideal law always gave too small a density, as expected, but the deviation from the true value never exceeded two percent.

The total amount of hydrogen charged for each run was calculated as $n'_{o,o}$ through equations for the liquid-vapor equilibrium while figuring out the liquid-vapor equilibria for conditions existing before taking the zero-point sample. This value was compared with a value computed from change of the pressure in the hydrogen charging vessel before and after charging of hydrogen into the autoclave. The ideal gas law was applied for that, and an internal volume of the charging vessel of

$$\frac{(3.14) \times (2.719)^2 \times (5.28)}{4} = 30.65 \text{ in}^3$$

$$= 502 \text{ milliliters}$$

and the room temperature which ranged for 19° C to 25°C depending on the date of charging were used as the volume and the

temperature of hydrogen gas, respectively. The results are presented in Tables L-III to L-V. The values based on the data of the pressure drop in the charging vessel were called "Measured" in these tables. It was found that there was no regular trend among the extents of deviation of the calculated values from the measured values. This was attributed to the roughness of estimation of the final pressures of hydrogen in the charging vessel. As mentioned in Section G of the APPENDIX, the temperature of hydrogen remaining in the charging vessel after delivering about one-half of the original content of the vessel to the autoclave dropped considerably due to the adiabatic expansion, and it took ten to fifteen minutes for the residual pressure to recover to its steady, final value. Because at least two successive chargings were necessary to bring the autoclave pressure up to a desired level of 1,000 psig and it was feared that an appreciable amount of reaction might take place in the autoclave, even in the absence of mechanical agitation of the liquid while waiting for the recovery of the charging pressure, the waiting time was cut as reasonably short as possible. Consequently, the readings of the final pressure were apt to be too low, thus making the pressure difference too large. This was one of the reasons why the "Measured" value was not used for calculating the initial conditions of the first sample. It was, however, noted that a deviation from Raoult's law and Gibbs-Dalton's law would generall be such that which would make the deviation in $n'_{o,o}$ negative, that is, the calculated value of $n'_{o,o}$ would be too small compared

Table L-III

Comparison of Calculated and Measured Values of the Amount of Hydrogen Charged for Blank Runs

Temperature (°C)	Number	Calculated $n'_{o,o}$ (gmole)	Measured $n'_{o,o}$ (gmole)	Deviation (percent)
200	10	0.834	---*	---
200	11	0.875	---*	---
200	12	0.791	0.815	-2.9
150	9	1.18	1.24	-4.8
100	13	1.37	---*	---
100	14	1.37	1.39	-1.44

* The final pressure of the charging vessel could not be taken since a valve, HV-1, which connected the charging vessel to the source hydrogen tank was forgotten to be closed.

Table L-IV

Comparison of Calculated and Measured Values of the Amount of Hydrogen Charged for the "1N" Runs

Temperature (°C)	Run Number	Calculated $n'_{o,o}$ (gmole)	Measured $n'_{o,o}$ (gmole)	Deviation (percent)
200	21	0.920	0.962	-4.4
150	24	1.22	1.26	-3.2
150	28	0.936	0.962	-2.7
100	25	1.46	1.50	-2.7

Table L-V

Comparison of Calculated and Measured Values of the Amount of Hydrogen Charged for the "2N" Runs

Temperature (°C)	Run Number	Calculated $n'_{o,o}$ (gmole)	Measured $n'_{o,o}$ (gmole)	Deviation (percent)
200	15	0.769	0.780	-1.4
200	16	0.689	0.716	-3.8
200	17	0.749	0.773	-3.1
200	26	0.456	0.471	-3.2
200	27	0.710	0.745	-4.7
150	29	0.930	0.955	-2.6
100	19	1.42	1.47	-3.4

with a real value. For sake of the argument that follows, therefore, the deviation of calculated value from real value was set to be minus four percent.

Thus, referring to equations in Section I of the APPENDIX, the quantity $(m_1 v_{f1} + m_2 v_{f2})$ in Eqn. (I-1) was too large by some two percent, and the resulting value of n_o' was too small by some four percent. The two-percent error in the liquid-volume terms only affected terms in the succeeding equations that were negligibly small in magnitude compared with other terms anyway. They were the terms v_{f1} in Eqn. (I-7), $v_{f2}m_2$ in Eqn. (I-9), $v_{f1}m_1$ in Eqn. (I-10), and v_{f2} in Eqn. (I-11). Therefore, the resulting values of m_1 and m_2 were practically unaffected by the nonideality.

Effect of a four-percent increase in n_o' for every sample of a run would be as follows. The quantities of A_n, C_n, ΔX_n and $\delta_{2,n}$ would have to be increased by four percent, but the quantities B_n, D_n and practically $\delta_{1,n}$ would remain unchanged. Therefore, β_n was defined by Eqn. (J-23) and which could be approximated by

$$\beta_n \simeq \frac{\delta_{2,n}}{4F(K-1)\,\delta_{1,n}} \qquad \text{(L-8)}$$

would increase by four percent, but α_n remained practically unchanged. Thus, the quantity

$$\Delta L_n = \frac{1}{\beta_n - \alpha_n} \ln \left[\frac{\beta_n(\Delta X_n - \alpha_n)}{\alpha_n(\Delta X_n - \beta_n)}\right] \simeq \frac{1}{|\alpha_n|} \ln \frac{\beta_n}{\beta_n - \Delta X_n} \qquad \text{(L-9)}$$

would remain unchanged. Thus, the small deviations from

Raoult's law and Gibbs-Dalton's law were found to have no significant effect on the overall rate constant $\langle k_2 \rangle$. The slight effect on the liquid-phase rate constant k_2 has been discussed in Section J-4.

L-3. On the Reaction $(C_2H_5)_2NH + HDO \rightleftharpoons (C_2H_5)_2ND + H_2O$

In deriving the rate equation it was assumed that the exchange reaction

$$(C_2H_5)_2NH + HDO \rightleftharpoons (C_2H_5)_2ND + H_2O$$

took place so rapidly than equilibrium was maintained at every instant while HDO and H_2O were being interconverted through the exchange reaction with hydrogen gas. It was also assumed that hydrogen atoms in the alkyl group of the amine did not participate in an exchange reaction. Thirdly, it was assumed that the isotope effect of deuterium on the distribution of hydrogen atoms between water and diethylamine was negligible so that the separation factor was unity.

Justification of these three assumptions directly on diethylamine was not possible since there were no such experimental verifications available. It was, however, found that the three points were generally true for other amines. The results of the literature survey is presented here.

It had been reported, (L-1), (L-2), (L-3), that deuterium, upon contact of partially enriched heavy water with hydrochloride of dimethylamine or ethylamine, rapidly went into amine and the exchange equilibria were reached

almost instantaneously.

In the case of dimethylamine, it has been found (L-2) that the available deuterium distributed itself "evenly" between the two hydrogen atoms of water and the secondary hydrogen attached to nitrogen, but did not exchange at all with the hydrogen atoms of the methyl groups.

To prove the point that the aliphatic hydrogen hardly participated in any exchange reactions, Roberts and his co-workers (L-3) conducted three different experiments in which they exposed various mixtures of amines and deuterium gas to heated nickel catalyst. It was found that

1) an exchange reaction between CH_3NH_2 and D_2 on the nickel catalyst did not go any farther than the point at which all CH_3NH_2 was converted to CH_3ND_2, and

2) an attempted farther exchange reaction between CH_3ND_2 and D_2 on the catalyst only increased the deuterium atom fraction in the amino group from the original 99.5% to 99.9% after two repeated treatments, and

3) there was no exchange observed between $(CH_3)_3N$ and D_2 after treatment on the heated nickel catalyst at 170°C for a period of three days.

The results also indicated that there was no possibility of exchange of the aliphatic hydrogen through a tautomerism such as

$$CH_3 - NH_2 \rightleftharpoons CH_2 = NH_3$$

Distribution of deuterium had been investigated (L-4) on various organic compounds such as succinic acid, glycine,

o-aminobenzoic acid, hydrazine sulfate, acetamide, urea, hydroquinone and acetone. The distribution ratio

$$\frac{\text{D/H in water}}{\text{D/H in functional group of solute}}$$

was found to be approximately unity for each compound except acetone, for which it was 1.21 ± 0.01 at 18° to 20°C. The term functional group above referred to those chemically active groups such as amino group NH_2, alcoholic and phenolic OH, carboxylic group COOH, etc. The deviation from unity with acetone was ascribed to a tautomeric transformation

$$CH_3\text{-}\underset{\underset{O}{\|}}{C}\text{-}CH_3 \rightleftharpoons CH_3\text{-}\underset{\underset{O\text{-}H}{|}}{C} = CH_2$$

which brings aliphatic hydrogen into the exchange reaction.

Because there was no tautomerism known with diethylamine, the distribution ratio for deuterium between water and diethylamine was assumed to be unity.

L-4. On the Effect of Several Percents of D_2O Present in Water

In deriving the rate equation the effects of several percents of D_2O present in the liquid phase in equilibrium with H_2O and HDO were neglected. That is, it was assumed that that portion of total deuterium atoms which were initially bound in molecules of D_2O were considered fixed on them and taken aside from the exchange reactions throughout a run. This assumption is justified here.

To simplify the treatment, the reaction is limited to within the liquid phase only, and the reaction involving

deuterated amine is omitted. The treatment of D_2O in the first steps is similar to that of deuterated diethylamine. Two competitive reactions are considered:

$$\underset{(A-X)}{H_2} + \underset{(B-Y)}{HDO} = \underset{(C+X)}{HD} + \underset{(D+W)}{H_2O} \qquad \text{(L-10)}$$

$$\underset{(A-X)}{H_2} + \underset{(H-Z)}{D_2O} = \underset{(C+X)}{HD} + \underset{(B-Y)}{HDO} \qquad \text{(L-11)}$$

The quantity in parentheses under each chemical symbol indicates the amount of that compound in grammoles present at time t. From the material balance on water molecules,

$$W = Y + Z \qquad \text{(L-12)}$$

From the material balance on hydrogen atoms,

$$Z = \frac{X - Y}{2} \qquad \text{(L-13)}$$

Equations (L-10) and (L-11) can then be written as

$$\underset{(A-X)}{H_2} + \underset{(B-Y)}{HDO} \underset{k_2}{\overset{k_1}{\rightleftharpoons}} \underset{(C+X)}{HD} + \underset{D + \frac{(X+Y)}{2}}{H_2O} \qquad \text{(L-14)}$$

$$\underset{(A-X)}{H_2} + \underset{H - \frac{(X-Y)}{2}}{D_2O} \underset{k_2}{\overset{k_1''}{\rightleftharpoons}} \underset{(C+X)}{HD} + \underset{(B-Y)}{HDO} \qquad \text{(L-15)}$$

At the same time the equilibrium between water molecules has

to be satisfied. This reaction is very rapid.

$$\underset{D + \frac{(X+Y)}{2}}{H_2O} + \underset{H - \frac{(X-Y)}{2}}{D_2O} \rightleftharpoons \underset{(B-Y)}{2HDO} \qquad \text{(L-16)}$$

Therefore, the equilibrium constant of the reaction (L-16), K_W, has to be satisfied at every moment. At time zero,

$$\frac{B^2}{DH} = K_W \qquad \text{(L-17)}$$

and, at time t,

$$\frac{(B - Y)^2}{\left[D + \frac{(X + Y)}{2}\right]\left[H - \frac{(X - Y)}{2}\right]} = K_W \qquad \text{(L-18)}$$

Assuming $K_W \simeq 4$, Eqn. (L-17) yields

$$B = 2n_1 f_W (1 - f_W) \qquad \text{(L-19)}$$

where

$$n_1 \equiv B + D + H \qquad \text{(L-20)}$$

and

$$f_W \equiv \frac{B + 2H}{2n_1} \qquad \text{(L-21)}$$

Also, Eqn. (L-18) yields

$$B - Y = 2n_1 f_W' (1 - f_W') \qquad \text{(L-22)}$$

where

$$f_W' = f_W - \frac{X}{2n_1} \qquad \text{(L-23)}$$

Eliminating B from Eqn's (L-19) and (L-22),

$$Y = 2n_1 \left(f_w - f_w'\right) \left(1 - f_w - f_w'\right) \qquad \text{(L-24)}$$

$$= \frac{X(2D - 2H + X)}{2n_1}$$

or

$$Y \simeq \frac{X(D - H)}{n_1} \qquad \text{(L-25)}$$

then, the rate equation representing the reactions (L-14) and (L-15) becomes

$$\frac{1}{V}\frac{d(A - X)}{dt} = k_1(A - X)\,(B - Y) + k_1''\,(A - X)\left[H - \frac{(X - Y)}{2}\right]$$

$$- k_2(C + X)\left[D + \frac{(X + Y)}{2}\right] - k_2''(C + X)\,(B - Y) \qquad \text{(L-26)}$$

Setting

$$\frac{k_1''}{k_1} \equiv r \qquad \text{(L-27)}$$

and, recalling a relation among the equilibrium constants of the reaction (L-14), K, reaction (L-15), K'', and reaction (L-16), K_w,

$$\frac{K''}{K} = K_w \qquad \text{(L-28)}$$

the rate equation becomes

$$-\frac{1}{V}\frac{dX}{dt} = k_1(A - X)\left[(B - Y) + r\left(H - \frac{X - Y}{2}\right)\right]$$

$$- k_2(C + X)\left[D + \frac{X + Y}{2} + \frac{rK}{K'}(B - Y)\right] \qquad \text{(L-29)}$$

Using Eq. (L-25) to eliminate Y, the rate equation becomes

$$-\frac{1}{V}\frac{dX}{dt} = k_1(A - X)\left[(B + rH) - F_bX\right] - k_2(C + X)\left[(D + \frac{rB}{K_w}) + F_dX\right] \tag{L-30}$$

where

$$F_b \equiv 1 - \frac{(2 - r)(B + 2H)}{2h_1} \tag{L-31}$$

and

$$F_d \equiv 1 + \frac{(D - h)}{n_1}(1 - \frac{2r}{K_w}) \ . \tag{L-32}$$

It is quite possible that the value of r, defined by Eqn. (L-27) was in the vicinity of two. This is because there could be roughly twice as much chance for a D_2O molecule which had made a collision with a H_2 molecule to come out with one of its deuterium atoms exchanged with hydrogen as for a HDO molecule colliding with a H_2 molecule to emerge with its deuterium atom transferred to hydrogen gas. Therefore, very possibly,

$$F_b \simeq F_d \simeq 1. \tag{L-33}$$

If F_b and F_d were slightly different from unity, they could be approximately treated in exactly the same manner as F for the consideration of exchange reaction with deuterated diethylamine. Then, its effect on the value of β would have been negligible because F was used only in two places where its effect on the result was very negligible; that is, first in calculating B_n and B_n from B_{n-1} and D_{n-1} (Eqn's (J-62) to (J-63)) and, then, in calculating δ_1 (Eqn. (J-24)).

It was then proved that the additional constant terms in Eqn. (L-30), rh and $\frac{rB}{K_w}$, did not affect the equilibrium value of X, or β, of the original equation without these additional terms, as follows. Comparison of Eqn. (L-30) with a rate equation representing a system in which only the reaction (L-14) was taking place,

$$\frac{dX}{dt} = k_1(A - X)(B - X) - k_2(C + X)(D + X) \qquad \text{(L-34)}$$

yielded following correspondences;

B versus B + rH

and D versus $D + \frac{rB}{K_w}$.

Then, the quantity (KAB - CD) which would appear in solving Eqn. (L-34), (see Eqn. (J-25)), should be replaced, in solving Eqn. (L-30), by

$$KA(B + rH) - C(D + \frac{rB}{K_w})$$

which could be rewritten as

$$KAB(1 + \frac{rH}{B}) - CD(1 + \frac{rB}{DK_w}) \qquad \text{(L-35)}$$

But, because of Eqn. (L-17),

$$\frac{rB}{DK_w} = \frac{rH}{B} \qquad \text{(L-36)}$$

and the quantity of expression (L-35) became

$$(1 + \frac{rH}{B})(KAB - CD) \ .$$

Also, a quantity δ_1 that would appear in solving Eqn. (L-34), (see Eqn. (J-24)), and was given by

$$\begin{aligned}\delta_1 &= K(A + B) + (C + D) \\ &\simeq KB + D \end{aligned} \qquad \text{(L-37)}$$

should be replaced by a quantity

$$K(B + rH) + (D + \frac{rB}{K_w})$$

which could be rewritten as

$$(KB + D)(1 + \frac{rH}{B}) \ .$$

Thus,

$$\begin{aligned}\beta &\equiv \frac{-\delta_1 + \sqrt{\delta_1^2 - \delta_2}}{2(1 - K)} \\ &\simeq \frac{KAB - CD}{\delta_1} \end{aligned} \qquad \text{(L-38)}$$

should be replaced by a quantity

$$\frac{(1 + \frac{rH}{B})(KAB - CD)}{(KB + D)(1 + \frac{rH}{B})}$$

which could be rewritten as

$$\frac{KAB - CD}{\delta_1} \ .$$

But, the last expression was identical with the approximation formula for the original β, given by Eqn. (L-38). Thus, with a given value of X, the value of L, as defined by Eqn. (J-27), would remain unaltered even if the additional reaction

involving D_2O were taken into account in processing the given experimental data.

L-5. On the Ionization Constant of Diethylamine in Water

Data on the ionization constant of diethylamine were needed for the estimation of the catalytic effect of hydroxyl ion on the exchange reaction under investigation. They were, however, available only for the temperature of 25°C. Typical values are shown in Table L-VI.

Table L-VI

Ionization Constant of Diethylamine at 25°C

Source	Ionization Constant, K_a
Scudder, H., (L-5)	1.26×10^{-3}
International Critical Table, (L-6)	1.01×10^{-3}

The ionization constant here was defined as the equilibrium constant of following ionization reaction.

$$(C_2H_5)_2NH(aq.) + H_2O(l) = (C_2H_5)_2NH_2^+(aq.) + OH^-(aq.) \quad (L\text{-}39)$$

The data needed were for temperatures above 100°C. Because no data were available either on the specific heat or the heat of formation of diethylamine and the ammonium ion, $(C_2H_5)_2NH_2^+$, it was impossible to directly calculate the ionization constant at the higher temperature. Under those circumstances the best estimate which could be made was by analogy with data on other amines.

It was found that ammonia was the only amine for which the ionization constant was known at higher temperatures. The data taken from International Critical Table, (L-6), are presented in the second column of Table L-VII. The ionization constant here was defined as the equilibrium constant of following reaction.

$$NH_3(aq.) + H_2O(l) = NH_4^+(aq.) + OH^-(aq.) \qquad (L\text{-}40)$$

These data were fit to an equation of a form

$$\ln K_a = c_5\tau + c_o \qquad (L\text{-}41)$$

where

$$\tau \equiv \frac{T_m}{T} + \ln T \ . \qquad (L\text{-}42)$$

The theoretical basis for using this form of relation is as follows. In general, the equilibrium constant, K_a, of a reaction

$$A + B \rightleftharpoons C + D \qquad (L\text{-}43)$$

is expressed as

$$\ln K_a = - \frac{\Delta H_o}{RT} + \frac{\Delta c_1}{R} \ln T + \frac{1}{2} \frac{\Delta c_2}{R} T + \frac{1}{6} \frac{\Delta c_3}{R} T^2 + \ldots + c_o \qquad (L\text{-}44)$$

where c_o is a constant of integration, and ΔH_o, Δc_1, Δc_2 and Δc_3 are differences in coefficients, H_o, c_1, c_2, and c_3, respectively, for the expression of the heat of formation of individual reaction participants,

$$H = H_o + c_1 T + \frac{1}{2} c_2 T^2 + \frac{1}{3} c_3 T^3 + \ldots \qquad (L\text{-}45)$$

Table L-VII

Ionization Constant of Ammonia

Temperature (^{o}K)	Ionization Constant, K_a	ln K_a	$c_5 + c_o$
273	1.39×10^{-5}	-11.184	-11.193
283	1.63×10^{-5}	-11.024	-10.971
288	1.70×10^{-5}	-10.982	-10.971
291	1.72×10^{-5}	-10.971	-10.907
298	1.81×10^{-5}	-10.920	-10.876
313	1.98×10^{-5}	-10.830	-10.844
323	1.81×10^{-5}	-10.920	-10.653
348	1.64×10^{-5}	-11.018	-11.035
373	1.35×10^{-5}	-11.213	-11.320
429	6.28×10^{-6}	-11.978	-12.305
491	1.80×10^{-6}	-13.228	-13.640
579	9.30×10^{-8}	-16.191	-15.800

That is,

$$\Delta c_1 = (c_1)_C + (c_1)_D - (c_1)_A - (c_1)_B \qquad \text{(L-46)}$$

and so on. Keeping only the first two terms, Eqn. (L-44) becomes

$$\ln K_a = -\frac{\Delta H_o}{RT} + \frac{\Delta c_1}{R} \ln T + c_o \ . \qquad \text{(L-47)}$$

This function $\ln K_a$ took on a maximum at

$$T_m = -\frac{H_o}{c_1} \qquad \text{(L-48)}$$

if ΔH_o was positive. Then, in terms of T_m, Eq. (L-47) becomes

$$\ln K_a = -\frac{\Delta H_o}{RT_m}\frac{T_m}{T} + \ln T + c_o \ , \qquad \text{(L-49)}$$

thus leading to the form of Eqn. (L-41).

With an estimated optimum temperature of $T_m = 313^oK$, the standard procedure of the method of least-squares led to the following numerical values of c_5 and c_o:

$$c_5 = 31.77 \qquad \text{(L-50)}$$

and $$c_o = 203.49 \text{ for ammonia.} \qquad \text{(L-51)}$$

Numerical values of $\ln K_a$ computed by using these values of c_5 and c_o are compared with values of $\ln K_a$ computed from the data taken from the International Critical Table in the last two columns of Table L-VII. The probable error of $\ln K_a$ thus calculated is estimated as follows:

$$P(\ln K_a) = 0.675 \sqrt{\frac{\sum^{10} (\ln K_a - c_5\tau - c_o)^2}{10}} = 0.154 \qquad \text{(L-52)}$$

and

$$\frac{P(\ln K_a)}{|\ln K_{a,max}|} = \frac{0.154}{10.83} = 0.0142 \ . \qquad \text{(L-53)}$$

Thus, for ammonia,

$$\ln K_a = -31.77\tau + 203.49 \ . \qquad \text{(L-54)}$$

To apply this result to other amines, it was assumed that, to a first approximation,

$$(H_o)_{NH_4^+} - (H_o)_{NH_3} = (H_o)_{RNH_3^+} - (H_o)_{RNH_2} \qquad \text{(L-55)}$$

and

$$(c_1)_{NH_4^+} - (c_1)_{NH_3} = (c_1)_{RNH_3^+} - (c_1)_{RNH_2} \qquad \text{(L-56)}$$

where RNH_2 and RNH_3^+ refer to an amine and its ammonium ion, respectively. Then, the same values of c_5 and T_m would apply for both ammonia and other amines. This was tested by comparing ionization constant data of other amines at various temperatures with a formula obtained by best-fitting the data to Eqn. (L-41) with the assumption of constancy of c_5 and T_m. That is, the values of $c_5 = -31.77$ and $T_m = 313^oK$ were used for amines other than ammonia and a value of c_o was determined so that data available fit the resulting equation best. The data used for this purpose were taken from the International Critical Table, (L-6), and are shown in Table L-VIII. The best fit values of c_o were obtained by

$$c_o = \frac{\sum^n \ln K_a + (31.77)\sum^n \tau}{n} \qquad \text{(L-57)}$$

Table L-VIII

Ionization Constant of Dimethylamine and Triethylamine

Temperature (°K)	Dimethylamine	Triethylamine
273	3.71×10^{-4}	2.2×10^{-4}
278.5	4.18×10^{-4}	---
283	5.01×10^{-4}	---
292	---	3.9×10^{-4}
293	5.10×10^{-4}	---
298	5.35×10^{-4}	4.4×10^{-4}
303	5.36×10^{-4}	4.6×10^{-4}
308	5.45×10^{-4}	4.6×10^{-4}
313	5.67×10^{-4}	5.1×10^{-4}
318	5.67×10^{-4}	---
323	5.63×10^{-4}	5.0×10^{-4}

where n was 10 for dimethylamine and 7 for triethylamine. The results were as follows: for dimethylamine,

$$c_o = 206.80 \tag{L-58}$$

and

$$\frac{P(\ln K_a)}{\left|\ln K_{a,max}\right|} = \frac{0.0377}{7.475} = 0.0050 \ , \tag{L-59}$$

and for triethylamine,

$$c_o = 206.58 \tag{L-60}$$

and

$$\frac{P(\ln K_a)}{\left|\ln K_{a,max}\right|} = \frac{0.1035}{7.581} = 0.0137 \ . \tag{L-61}$$

Comparison of these values of relative probable error with that for ammonia, 0.0142, showed that the assumption of constancy of c_5 and T_m were fairly reliable for these chemically like compounds.

Application of these findings to the estimation of the ionization constant of diethylamine was made through a relation at 25°C.

$$\ln \frac{(K_a)_{\text{diethylamine}}}{(K_a)_{\text{ammonia}}} = (c_o)_{\text{diethylamine}} - (c_o)_{\text{ammonia}} \ . \tag{L-62}$$

Using $(K_a)_{\text{diethylamine}} = 1.26 \times 10^{-3}$ with an estimated error of $\pm 0.2 \times 10^{-3}$, this yielded

$$\begin{aligned}(c_o)_{\text{diethylamine}} &= 203.49 + \ln(1.26 \times 10^{-3} \pm 0.2 \times 10^{-3}) \\ &\quad - \left[(\ln 1.81 \times 10^{-5}) \pm 0.154\right] \\ &= 207.73 \pm 0.22 \ .\end{aligned} \tag{L-63}$$

Thus, for diethylamine

$$\ln K_a = -31.77 \left(\frac{313}{T} + \ln T\right) + (207.73 \pm 0.189) \; . \qquad \text{(L-64)}$$

Numerical values of K_a computed from Eqn. (L-64) are summarized in Table L-IX.

Table L-IX

Ionization Constant of Diethylamine

Temperature (°C)	Ionization Constant, K_a
100	$(8.6 \pm 1.6) \times 10^{-4}$
150	$(3.75 \pm 0.71) \times 10^{-4}$
200	$(1.27 \pm 0.24) \times 10^{-4}$

M. Summary of Data and Calculated Values

Experimental data and the results calculated from them by using the theoretical set of the equilibrium constant, K, are summarized in Table M-I to M-XVII.

Values of the temperature, the stirring rate, the catalyst concentration, the total amount of liquid charged, the time, the residual pressures, and the thermal conductivity cell output are the quantities directly measured, and all the rest of the quantities in the tables are those calculated from the measured quantities.

Basic experimental conditions of a run appear at the upper left-hand corner of each table. Results of the phase-equilibrium calculations are presented in the upper central and right portions of each table. Results of the rate calculations for individual partial runs are tabulated in the middle portion. Results of calculations on the slope and the rate constants are shown in the bottom right portion of the table.

Partial runs for which the T/C-cell output, E_n, are not given but other sampling data are given, are the ones which were disregarded either because the sample was lost due to failures in manipulation of stopcocks and valves or because the sample was contaminated by air. Partial runs for which no figures appear in any column are the ones whose samples were not taken at all. "Amount of Reactants after Sampling" for the last sample of a run were not calculated

because these values were not required for the rate-calculations of the last partial run.

For definitions of various probable errors, equation numbers are cited in the footnotes of each table.

TABLE M-I

Data and Calculated Results of Run 9

Temperature: 150 °C

Stirring Rate: 8 strokes/sec.

Catalyst: Zero Normal diethylamine in charged solution

Hydroxyl-Ion Concentration: h = Zero Normal

Total Amount of Liquid Charged: G = 459 grams

Total Amount of H_2 Charged: $n'_{o,o}$ = A_o = 1.18 gmoles

Total Amount of HDO Charged: B_o = 7.50 gmoles

Total Amount of HD Charged: C_o = 0 gmoles

Total Amount of H_2O Charged: D_o = 16.20 gmoles

F = 1.000

λ_o = 0.0238 λ_1 = 0.9975 λ'_o = 0.9762 λ'_1 = 0.0025

Volume of Vapor Phase: V' = 501 ml.

Amount of Water in Liquid Phase: m_1 = 457.8 grams

Amount of Water in Vapor Phase: m'_1 = 1.16 grams

Amount of Amine in Liquid Phase: m_2 = 0 grams

Amount of Amine in Vapor Phase: m'_2 = 0 grams

$\lambda_o\lambda_1$ = 0.0238

$\lambda'_o\lambda'_1$ = 0.00245

Sample Number n	Time t_n (hr)	Time Δt_n (hr)	Total Pressure after Sampling $p_{(n+1)}$ (at.)	T/C-Cell Output * E_n (mV)	Amount of Hydrogen after Sampling $n'_{o,(n+1)}$ (gmole)	Atom Fraction D in Hydrogen $f'_{d,n}$ (%)	Amounts of Reactants after Sampling: H_2 A_{n+1} (gmole)	HD C_{n+1} (gmole)	HDO B_{n+1} (gmole)	H_2O D_{n+1} (gmole)	β_{n+1} (gmole)	Extent of Reaction: ΔX_n (gmole)	ΔL_n (gmole^{-1}) **	L_n (gmole^{-1}) **	Weight w_n
0	0	0.5	84.0	0	1.14	0	1.14	0	7.50	16.20	0.1847	-	-	-	-
1	0.5	0.5	83.4	-	1.13	-	-	-	-	-	-	-	-	-	-
2	1.0	0.5	82.4	-	1.12	-	-	-	-	-	-	-	-	-	-
3	1.5	1.0	81.3	-	1.10	-	-	-	-	-	-	0.0028	$(4.3\pm3.1)\times10^{-4}$	$(4.3\pm3.1)\times10^{-4}$	1.00
4	2.5	1.0	80.0	0.10	1.09	0.12	1.09	0.0027	7.50	16.20	0.1741	0.0013	$(2.2\pm4.4)\times10^{-4}$	$(6.5\pm5.3)\times10^{-4}$	0.33
5	3.5	3.5	78.6	0.15	1.07	0.18	1.07	0.0039	7.50	16.20	0.1697	0.0026	$(4.4\pm4.4)\times10^{-4}$	$(10.9\pm7.0)\times10^{-4}$	0.20
6	7.0	5.0	78.5	0.25	1.06	0.31	1.05	0.0065	7.49	16.21	0.1656	0.0039	$(6.7\pm4.5)\times10^{-4}$	$(17.6\pm8.3)\times10^{-4}$	0.14
7	12.0	5.0	75.9	0.40	1.03	0.49	1.02	0.0100	7.49	16.21	0.1673	0.0075	$(13.8\pm4.8)\times10^{-4}$	$(31.5\pm9.2)\times10^{-4}$	0.10
8	17.0	-	72.5	0.70	0.977	0.85						-		-	-
9	-	-	-	-	-	-	-	-	-	-	-				

Notes:

* Sensitivity "2"; Calibration (2).

** Probable error, $P(\Delta L_n)$ and $P(L_n)$, defined by Eqns. (J-86) and (J-87), respectively.

*** Probable error, obtained from deviations of experimental points from the best-fit straight line by using Eqn. (J-91).

**** Probable error, obtained as a mean of probable errors of experimental points directly calculated from experimental errors by using Eqn. (J-92).

***** Probable error corresponding to $P(\bar{L})$.

$P(\bar{L})$ = 3.71 x 10^{-5} *** gmole^{-1}

$\overline{P(L)}$ = 2.58 x 10^{-4} **** gmole^{-1}

Slope: $S = (1.68\pm0.021)\times10^{-4}$ ***** gmole^{-1}hr^{-1}

Overall Rate Constant: $\langle k_2 \rangle = 0.303\pm0.004$ ***** g-atom D/ml.hr.(gmole/ml)^2

Rate Constant in Vapor Phase: $k'_2 = 62.0\pm0.8$ ***** g-atom D/ml.hr.(gmole/ml)^2

TABLE M- II

Data and Calculated Results of Run 10

Temperature: 200 °C

Stirring Rate: 6 strokes/sec.

Catalyst: Zero Normal diethylamine in charged solution

Hydroxyl-Ion Concentration: h = Zero Normal

Total Amount of Liquid Charged: G = 460 grams

Total Amount of H_2 Charged: $n'_{o,o}$ = A_o = 0.834 gmoles

Total Amount of HDO Charged: B_o = 7.72 gmoles

Total Amount of HD Charged: C_o = 0 gmoles

Total Amount of H_2O Charged: D_o = 16.14 gmoles

F = 1.000

λ_o = 0.0294 λ_1 = 0.9936 λ'_o = 0.9706 λ'_1 = 0.0064

Volume of Vapor Phase: V' = 472 ml.

Amount of Water in Liquid Phase: m_1 = 457.1 grams

Amount of Water in Vapor Phase: m'_1 = 2.94 grams

Amount of Amine in Liquid Phase: m_2 = 0 grams

Amount of Amine in Vapor Phase: m'_2 = 0 grams

$\lambda_o\lambda_1$ = 0.0293

$\lambda'_o\lambda'_1$ = 0.00623

Sample Number n	Time t_n (hr)	Time Δt_n (hr)	Total Pressure after Sampling $p_{(n+1)}$ (at.)	T/C-Cell Output * E_n (mV)	Amount of Hydrogen after Sampling $n'_{o,(n+1)}$ (gmole)	Atom Fraction D in Hydrogen $f'_{d,n}$ (%)	Amounts of Reactants after Sampling: H_2 A_{n+1} (gmole)	HD C_{n+1} (gmole)	HDO B_{n+1} (gmole)	H_2O D_{n+1} (gmole)	β_{n+1} (gmole)	Extent of Reaction: ΔX_n (gmole)	ΔL_n (gmole^{-1}) **	L_n (gmole^{-1}) **	Weight w_n
0	0	0.5	82.6	0	0.818	0	0.818	0	7.72	16.14	0.1487	--	---	---	-
1	0.5	0.5	79.3	-	0.777	-	--	--	-	-	--	0.0044	$(7.7\pm2.5)\times10^{-4}$	$(7.7\pm2.5)\times10^{-4}$	1.00
2	1.0	0.5	78.5	0.22	0.756	0.27	0.752	0.0041	7.72	16.14	0.1336	--	---	---	-
3	1.5	1.5	78.2	-	0.740	-	--	--	-	-	--	--	---	---	-
4	3.0	2.5	75.9	-	0.736	-	--	--	-	-	--	0.0024	$(4.7\pm3.6)\times10^{-4}$	$(12.4\pm4.4)\times10^{-4}$	0.33
5	5.5	3.0	75.2	0.35	0.727	0.43	0.721	0.0062	7.71	16.15	0.1263	0.0018	$(3.6\pm3.7)\times10^{-4}$	$(16.0\pm5.7)\times10^{-4}$	0.19
6	8.5	3.8	74.1	0.45	0.715	0.55	0.707	0.0078	7.71	16.15	0.1225	0.0086	$(18.8\pm4.0)\times10^{-4}$	$(34.8\pm7.0)\times10^{-4}$	0.13
7	12.3	4.7	71.1	0.95	0.678	1.15	0.663	0.0154	7.70	16.16	0.1083	0.0016	$(3.9\pm4.0)\times10^{-4}$	$(38.8\pm8.0)\times10^{-4}$	0.10
8	17.0	7.0	69.0	1.05	0.656	1.27	0.639	0.0165	7.70	16.16	0.1033		$(24.4\pm4.4)\times10^{-4}$	$(63.2\pm9.1)\times10^{-4}$	0.08
9	24.0		67.6	1.65	0.639	1.98									

Notes:

* Sensitivity "2"; Calibration (2).

** Probable error, $P(\Delta L_n)$ and $P(L_n)$, defined by Eqns. (J-86) and (J-87), respectively.

*** Probable error, obtained from deviations of experimental points from the best-fit straight line by using Eqn. (J-91).

**** Probable error, obtained as a mean of probable errors of experimental points directly calculated from experimental errors by using Eqn. (J-92).

***** Probable error corresponding to $P(\overline{L})$.

$P(\overline{L})$ = 1.37×10^{-4} *** gmole^{-1}

$\overline{P(L)}$ = 2.04×10^{-4} **** gmole^{-1}

Slope: S = $(2.56\pm0.046)\times10^{-4}$ ***** gmole^{-1}hr^{-1}

Overall Rate Constant: $\langle k_2 \rangle$ = 0.513 ± 0.010 ***** g-atom D/ml.hr.(gmole/ml)^2

Rate Constant in Vapor Phase: k'_2 = 38.9 ± 0.7 ***** g-atom D/ml.hr.(gmole/ml)^2

TABLE M-III

Data and Calculated Results of Run 11

Temperature: 200° C
Stirring Rate: 1.5 strokes/sec.
Catalyst: Zero Normal diethylamine in charged solution
Hydroxyl-Ion Concentration: h = Zero Normal

Total Amount of Liquid Charged: G = 460 grams
Total Amount of H_2 Charged: $n'_{o,o}$ = A_o = 0.875 gmoles
Total Amount of HDO Charged: B_o = 7.71 gmoles
Total Amount of HD Charged: C_o = 0 gmoles
Total Amount of H_2O Charged: D_o = 16.14 gmoles
F = 1.000

Volume of Vapor Phase: V' = 472 ml.
Amount of Water in Liquid Phase: m_1 = 457.1 grams
Amount of Water in Vapor Phase: m'_1 = 2.94 grams
Amount of Amine in Liquid Phase: m_2 = 0 grams
Amount of Amine in Vapor Phase: m'_2 = 0 grams
$\lambda_o\lambda_1$ = 0.0293
$\lambda'_o\lambda'_1$ = 0.00622

λ_o = 0.0294 λ_1 = 0.9936 λ'_o = 0.9706 λ'_1 = 0.0064

Sample Number n	Time t_n (hr)	Time Δt_n (hr)	Total Pressure after Sampling $P_{(n+1)}$ (at.)	T/C-Cell Output * E_n (mV)	Amount of Hydrogen after Sampling $n'_{o,(n+1)}$ (gmole)	Atom Fraction D in Hydrogen $f'_{d,n}$ (%)	Amounts of Reactants after Sampling: H_2 A_{n+1} (gmole)	HD C_{n+1} (gmole)	HDO B_{n+1} (gmole)	H_2O D_{n+1} (gmole)	β_{n+1} (gmole)	Extent of Reaction: ΔX_n (gmole)	ΔL_n (gmole^{-1}) **	L_n (gmole^{-1}) **	Weight w_n
0	0	0.5	86.8	0	0.867	0	0.867	0	7.72	16.14	0.1574	-	-	-	-
1	0.5	0.5	85.7	-	0.855	-	-	-	-	-	-	0.0021	$(3.5\pm2.5)\times10^{-4}$	$(3.5\pm2.5)\times10^{-4}$	1.00
2	1.0	0.5	84.6	0.10	0.843	0.12	0.841	0.0021	7.72	16.14	0.1511	-	-	-	-
3	1.5	1.0	84.0	-	0.834	-	-	-	-	-	-	0.0031	$(5.3\pm3.6)\times10^{-4}$	$(8.8\pm4.4)\times10^{-4}$	0.33
4	2.5	2.0	82.6	0.25	0.818	0.31	0.813	0.0050	7.72	16.15	0.1437	0.0024	$(4.3\pm3.6)\times10^{-4}$	$(13.1\pm5.7)\times10^{-4}$	0.19
5	4.5	3.0	82.0	0.37	0.810	0.45	0.803	0.0073	7.71	16.15	0.1400	0.0055	$(10.3\pm3.8)\times10^{-4}$	$(23.4\pm6.8)\times10^{-4}$	0.13
6	7.5	4.5	80.6	0.65	0.792	0.79	0.780	0.0124	7.71	16.15	0.1316	0.0048	$(9.5\pm3.9)\times10^{-4}$	$(32.9\pm7.8)\times10^{-4}$	0.10
7	12.0	-	79.9	0.90	0.785	1.09						-	-	-	-
8	-	-	-	-	-	-	-	-	-	-	-	-	-	-	-
9	-	-	-	-	-	-	-	-	-	-	-	-			

Notes:
* Sensitivity "2"; Calibration (2).
** Probable error, $P(\Delta L_n)$ and $P(L_n)$, defined by Eqns. (J-86) and (J-87), respectively.
*** Probable error, obtained from deviations of experimental points from the best-fit straight line by using Eqn. (J-91).
**** Probable error, obtained as a mean of probable errors of experimental points directly calculated from experimental errors by using Eqn. (J-92).
***** Probable error corresponding to $P(\overline{L})$.

$P(\overline{L})$ = 3.41×10^{-5} *** gmole^{-1}
$\overline{P(L)}$ = 2.09×10^{-4} **** gmole^{-1}

Slope: S = $(2.94\pm0.026)\times10^{-4}$ ***** gmole^{-1}hr^{-1}

Overall Rate Constant: $\langle k_2 \rangle$ = 0.589 ± 0.006 ***** g-atom D/ml.hr.(gmole/ml)^2

Rate Constant in Vapor Phase: k'_2 = 44.7 ± 0.4 ***** g-atom D/ml.hr.(gmole/ml)^2

TABLE M-IV

Data and Calculated Results of Run 12

Temperature: 200 °C

Stirring Rate: 8 strokes/sec.

Catalyst: Zero Normal diethylamine in charged solution

Hydroxyl-Ion Concentration: h = Zero Normal

Total Amount of Liquid Charged: G = 461 grams

Total Amount of H_2 Charged: $n'_{o,o}$ = A_o = 0.791 gmoles

Total Amount of HDO Charged: B_o = 7.73 gmoles

Total Amount of HD Charged: C_o = 0 gmoles

Total Amount of H_2O Charged: D_o = 16.18 gmoles

F = 1.000

Volume of Vapor Phase: V' = 470 ml.

Amount of Water in Liquid Phase: m_1 = 4.581 grams

Amount of Water in Vapor Phase: m'_1 = 2.94 grams

Amount of Amine in Liquid Phase: m_2 = 0 grams

Amount of Amine in Vapor Phase: m'_2 = 0 grams

$\lambda_o\lambda_1$ = 0.0294

$\lambda_o\lambda'_1$ = 0.00619

λ_o = 0.0295 λ_1 = 0.9936 λ'_o = 0.9705 λ'_1 = 0.0064

Sample Number n	Time t_n (hr)	Time Δt_n (hr)	Total Pressure after Sampling $p_{(n+1)}$ (at.)	T/C-Cell Output * E_n (mV)	Amount of Hydrogen after Sampling $n'_{o,(n+1)}$ (gmole)	Atom Fraction D in Hydrogen $f'_{d,n}$ (%)	Amounts of Reactants after Sampling: H_2 A_{n+1} (gmole)	HD C_{n+1} (gmole)	HDO B_{n+1} (gmole)	H_2O D_{n+1} (gmole)	β_{n+1} (gmole)	Extent of Reaction: ΔX_n (gmole)	ΔL_n ** ($gmole^{-1}$)	L_n ** ($gmole^{-1}$)	Weight w_n
0	0	0.5	78.6	0	0.766	0	0.766	0	7.73	16.18	0.1393	0.0019	$(3.5\pm2.5)\times10^{-4}$	$(3.5\pm2.5)\times10^{-4}$	1.00
1	0.5	0.5	77.2	0.10	0.750	0.12	0.748	0.0018	7.73	16.18	0.1346	-	-	-	-
2	1.0	0.5	74.5	-	0.717	-	-	-	-	-	-	-	-	-	-
3	1.5	1.0	73.1	-	0.701	-	-	-	-	-	-	0.0015	$(2.8\pm3.5)\times10^{-4}$	$(6.3\pm4.3)\times10^{-4}$	0.33
4	2.5	2.0	71.8	0.18	0.686	0.22	0.683	0.0030	7.73	16.18	0.1220	0.0020	$(4.3\pm3.6)\times10^{-4}$	$(10.6\pm5.6)\times10^{-4}$	0.20
5	4.5	3.0	67.6	0.30	0.637	0.37	0.632	0.0047	7.73	16.19	0.1116	0.0019	$(4.3\pm3.7)\times10^{-4}$	$(14.9\pm6.7)\times10^{-4}$	0.14
6	7.5	4.5	67.0	0.42	0.629	0.51	0.623	0.0064	7.72	16.19	0.1084	0.0095	$(23.7\pm4.0)\times10^{-4}$	$(38.6\pm7.8)\times10^{-4}$	0.10
7	12.0	6.0	65.6	1.05	0.612	1.27	0.597	0.0154	7.71	16.20	0.0964	0.0015	$(3.9\pm4.0)\times10^{-4}$	$(42.5\pm8.8)\times10^{-4}$	0.08
8	18.0	-	64.9	1.15	0.604	1.39									
9	-	-	-	-	-	-	-	-	-	-	-	-	-	-	-

Notes:

* Sensitivity "2"; Calibration (2).

** Probable error, $P(\Delta L_n)$ and $P(L_n)$, defined by Eqns. (J-86) and (J-87), respectively.

*** Probable error, obtained from deviations of experimental points from the best-fit straight line by using Eqn. (J-91).

**** Probable error, obtained as a mean of probable errors of experimental points directly calculated from experimental errors by using Eqn. (J-92).

***** Probable error corresponding to P(L).

$P(\bar{L}) = 8.55 \times 10^{-5}$ *** $gmole^{-1}$

$\overline{P(L)} = 2.00 \times 10^{-4}$ **** $gmole^{-1}$

Slope: $S = (2.56\pm0.040)\times10^{-4}$ ***** $gmole^{-1}hr^{-1}$

Overall Rate Constant: $\langle k_2 \rangle = 0.513\pm0.008$ ***** g-atom D/ml.hr.$(gmole/ml)^2$

Rate Constant in Vapor Phase: $k'_2 = 39.0\pm0.6$ ***** g-atom D/ml.hr.$(gmole/ml)^2$

TABLE M-V

Data and Calculated Results of Run 13

Temperature: 100 °C
Stirring Rate: 8 strokes/sec.
Catalyst: Zero — Normal diethylamine in charged solution
Hydroxyl-Ion Concentration: h = Zero Normal

Total Amount of Liquid Charged: G = 460 grams
Total Amount of H_2 Charged: $n'_{o,o}$ = A_o = 1.37 gmoles
Total Amount of HDO Charged: B_o = 7.32 gmoles
Total Amount of HD Charged: C_o = 0 gmoles
Total Amount of H_2O Charged: D_o = 16.31 gmoles
F = 1.000

Volume of Vapor Phase: V' = 521 ml.
Amount of Water in Liquid Phase: m_1 = 459.7 grams
Amount of Water in Vapor Phase: m'_1 = 0.26 grams
Amount of Amine in Liquid Phase: m_2 = 0 grams
Amount of Amine in Vapor Phase: m'_2 = 0 grams
$\lambda_o\lambda_1$ = 0.0197
$\lambda'_o\lambda'_1$ = 0.00058

λ_o = 0.0197 λ_1 = 0.9996 λ'_o = 0.9803 λ'_1 = 0.00059

Sample Number n	Time t_n (hr)	Time Δt_n (hr)	Total Pressure after Sampling $p_{(n+1)}$ (at.)	T/C-Cell Output * E_n (mV)	Amount of Hydrogen after Sampling $n'_{o,(n+1)}$ (gmole)	Atom Fraction D in Hydrogen $f'_{d,n}$ (%)	Amounts of Reactants after Sampling: H_2 A_{n+1} (gmole)	HD C_{n+1} (gmole)	HDO B_{n+1} (gmole)	H_2O D_{n+1} (gmole)	β_{n+1} (gmole)	Extent of Reaction: ΔX_n (gmole)	ΔL_n ** ($gmole^{-1}$)	L_n ** ($gmole^{-1}$)	Weight w_n
0	0		80.7	0	1.35	0	1.35	0	7.32	16.31	0.1862				
1	1.0	1.0	78.5	-	1.31	-	-	-	-	-	-	-	-	-	-
2	3.0	2.0	76.2	0.04	1.30	0.05	1.30	0.0013	7.32	16.31	0.1782	0.0013	$(2.3\pm5.0)\times10^{-4}$	$(2.3\pm5.0)\times10^{-4}$	1.00
3	6.0	3.0	74.5	0.10	1.25	0.12	1.25	0.0031	7.32	16.31	0.1698	0.0019	$(3.5\pm6.5)\times10^{-4}$	$(5.8\pm8.2)\times10^{-4}$	0.37
4	10.0	4.0	72.8	0.20	1.22	0.24	1.21	0.0060	7.31	16.32	0.1628	0.0031	$(5.8\pm5.9)\times10^{-4}$	$(11.6\pm10.1)\times10^{-4}$	0.24
5	15.0	5.0	70.4	0.33	1.18	0.40	1.17	0.0095	7.31	16.32	0.1539	0.0039	$(7.7\pm6.0)\times10^{-4}$	$(19.3\pm11.7)\times10^{-4}$	0.18
6	24.5	9.5	56.7	0.45	0.95	0.55	0.94	0.0104	7.31	16.32	0.1218	0.0034	$(7.3\pm6.2)\times10^{-4}$	$(26.6\pm13.2)\times10^{-4}$	0.14
7	31.0	6.5	53.4	0.60	0.89	0.73	0.88	0.0129	7.30	16.33	0.1111	0.0035	$(9.3\pm6.3)\times10^{-4}$	$(35.9\pm14.7)\times10^{-4}$	0.11
8	45.0	6.0	51.3	0.92	0.86	1.11						0.0069	$(20.6\pm6.7)\times10^{-4}$	$(56.5\pm16.1)\times10^{-4}$	0.09
9	-	-	-	-	-	-	-	-	-	-	-	-	-	-	-

Notes:
* Sensitivity "2"; Calibration (2).
** Probable error, $P(\Delta L_n)$ and $P(L_n)$, defined by Eqns. (J-86) and (J-87), respectively.
*** Probable error, obtained from deviations of experimental points from the best-fit straight line by using Eqn. (J-91).
**** Probable error, obtained as a mean of probable errors of experimental points directly calculated from experimental errors by using Eqn. (J-92).
***** Probable error corresponding to $P(\overline{L})$.

$P(\overline{L})$ = 4.03×10^{-5} *** $gmole^{-1}$
$\overline{P(L)}$ = 3.67×10^{-4} **** $gmole^{-1}$

Slope: S = $(1.18\pm0.007)\times10^{-4}$ ***** $gmole^{-1}hr^{-1}$

Overall Rate Constant: $\langle k_2 \rangle = 0.191\pm0.002$ ***** g-atom D/ml.hr.$(gmole/ml)^2$

Rate Constant in Vapor Phase: $k'_2 = 173.2\pm1.1$ ***** g-atom D/ml.hr.$(gmole/ml)^2$

TABLE M- VI

Data and Calculated Results of Run 14

Temperature: 100 °C
Stirring Rate: 8 strokes/sec.
Catalyst: Zero Normal diethylamine in charged solution
Hydroxyl-Ion Concentration: h = Zero Normal

Total Amount of Liquid Charged: G = 460 grams
Total Amount of H_2 Charged: $n'_{o,o}$ = A_o = 1.37 gmoles
Total Amount of HDO Charged: B_o = 7.32 gmoles
Total Amount of HD Charged: C_o = 0 gmoles
Total Amount of H_2O Charged: D_o = 16.31 gmoles
F = 1.000

Volume of Vapor Phase: V' = 521 ml.
Amount of Water in Liquid Phase: m_1 = 459.7 grams
Amount of Water in Vapor Phase: m'_1 = 0.27 grams
Amount of Amine in Liquid Phase: m_2 = 0 grams
Amount of Amine in Vapor Phase: m'_2 = 0 grams
$\lambda_o\lambda_1$ = 0.0197

λ_o =0.0197 λ_1 =0.9996 λ'_o =0.9803 λ'_1 =0.00059
$\lambda'_o\lambda'_1$ = 0.00058

Sample Number n	Time t_n (hr)	Time Δt_n (hr)	Total Pressure after Sampling $P_{(n+1)}$ (at.)	T/C-Cell Output * E_n (mV)	Amount of Hydrogen after Sampling $n'_{o,(n+1)}$ (gmole)	Atom Fraction D in Hydrogen $f'_{d,n}$ (%)	Amounts of Reactants after Sampling: H_2 A_{n+1} (gmole)	HD C_{n+1} (gmole)	HDO B_{n+1} (gmole)	H_2O D_{n+1} (gmole)	β_{n+1} (gmole)	Extent of Reaction: ΔX_n (gmole)	ΔL_n (gmole^{-1}) **	L_n (gmole^{-1}) **	Weight w_n
0	0	3	80.7	0	1.36	0	1.36	0	7.32	16.31	0.1875				
1	3	7	77.9	0.05	1.31	0.06	1.31	0.0016	7.32	16.31	0.1793	0.0017	$(2.9\pm4.1)\times10^{-4}$	$(2.9\pm4.1)\times10^{-4}$	1.00
2	10	10	77.2	0.17	1.30	0.21	1.29	0.0054	7.31	16.32	0.1741	0.0038	$(7.0\pm5.9)\times10^{-4}$	$(9.8\pm7.1)\times10^{-4}$	0.32
3	20	10	74.5	0.35	1.25	0.43	1.24	0.0106	7.31	16.32	0.1622	0.0057	$(10.7\pm6.1)\times10^{-4}$	$(20.5\pm9.4)\times10^{-4}$	0.18
4	30	10	72.0	----	1.21	----	----	----	----	----	----	----	----	----	----
5	40	10	69.7	0.75	1.17	0.91	1.15	0.0211	7.30	16.33	0.1409	0.0121	$(24.9\pm6.6)\times10^{-4}$	$(45.4\pm11.4)\times10^{-4}$	0.13
6	50	10	63.5	----	1.07	----	----	----	----	----	----	----	----	----	----
7	60	10	60.2	----	1.01	----	----	----	----	----	----	----	----	----	----
8	70	--	58.1	1.35	0.97	1.63						0.0168	$(40.8\pm7.4)\times10^{-4}$	$(86.2\pm13.6)\times10^{-4}$	0.09
9	--		----	----	----	----	----	----	----	----	----	----	----	----	----

Notes:
* Sensitivity "2"; Calibration (2).
** Probable error, $P(\Delta L_n)$ and $P(L_n)$, defined by Eqns. (J-86) and (J-87), respectively.
*** Probable error, obtained from deviations of experimental points from the best-fit straight line by using Eqn. (J-91).
**** Probable error, obtained as a mean of probable errors of experimental points directly calculated from experimental errors by using Eqn. (J-92).
***** Probable error corresponding to $P(\bar{L})$.

$P(\bar{L})$ = 5.74×10^{-5} *** gmole^{-1}
$\overline{P(L)}$ = 3.45×10^{-4} **** gmole^{-1}

Slope: S = $(1.17\pm0.008)\times10^{-4}$ ***** gmole^{-1}hr^{-1}

Overall Rate Constant: $\langle k_2 \rangle$ = 0.189 ± 0.002 ***** g-atom D/ml.hr.(gmole/ml)^2

Rate Constant in Vapor Phase: k'_2 = 171.3 ± 1.2 ***** g-atom D/ml.hr.(gmole/ml)^2

TABLE M-VII

Data and Calculated Results of Run 15

Temperature: 200 °C

Stirring Rate: 6 strokes/sec.

Catalyst: 1.78 Normal diethylamine in charged solution

Hydroxyl-Ion Concentration: h = 0.015 Normal

Total Amount of Liquid Charged: G = 431 grams

Total Amount of H_2 Charged: $n'_{o,o}$ = A_o = 0.769 gmoles

Total Amount of HDO Charged: B_o = 7.88 gmoles

Total Amount of HD Charged: C_o = 0 gmoles

Total Amount of H_2O Charged: D_o = 10.91 gmoles

F = 0.979

λ_o = 0.0269 λ_1 = 0.9908 λ'_o = 0.9731 λ'_1 = 0.0092

Volume of Vapor Phase: V' = 433 ml.

Amount of Water in Liquid Phase: m_1 = 368.4 grams

Amount of Water in Vapor Phase: m'_1 = 3.43 grams

Amount of Amine in Liquid Phase: m_2 = 58.46 grams

Amount of Amine in Vapor Phase: m'_2 = 0.72 grams

$\lambda_o\lambda_1$ = 0.0267

$\lambda'_o\lambda'_1$ = 0.00895

Sample Number n	Time t_n (hr)	Time Δt_n (hr)	Total Pressure after Sampling $P_{(n+1)}$ (at.)	T/C-Cell Output * E_n (mV)	Amount of Hydrogen after Sampling $n'_{o,(n+1)}$ (gmole)	Atom Fraction D in Hydrogen $f'_{d,n}$ (%)	Amounts of Reactants after Sampling: H_2 A_{n+1} (gmole)	HD C_{n+1} (gmole)	HDO B_{n+1} (gmole)	H_2O D_{n+1} (gmole)	β_{n+1} (gmole)	Extent of Reaction: ΔX_n (gmole)	ΔL_n ** ($gmole^{-1}$)	L_n ** ($gmole^{-1}$)	Weight w_n
0	0		75.8	0 *	0.672	0	0.672	0	7.88	10.91	0.1679				
1	0.5	0.5	74.5	4.00 *	0.656	4.67	0.596	0.0584	7.82	10.97	0.1051	0.0628	$(1.59\pm0.04)\times10^{-2}$	$(1.59\pm0.04)\times10^{-2}$	1.00
2	1.0	0.5	73.2	6.45 *	0.641	7.32	0.551	0.0870	7.78	11.01	0.0722	0.0348	$(1.36\pm0.08)\times10^{-2}$	$(2.95\pm0.09)\times10^{-2}$	0.22
3	1.5	0.5	72.2	8.18 *	0.630	9.11	0.521	0.1043	7.76	11.03	0.0517	0.0229	$(1.29\pm0.11)\times10^{-2}$	$(4.24\pm0.14)\times10^{-2}$	0.10
4	3.0	1.5	70.4	5.40 †	0.611	10.5	0.489	0.115	7.75	11.05	0.0360	0.0176	$(1.40\pm0.24)\times10^{-2}$	$(5.64\pm0.28)\times10^{-2}$	0.03
5	5.5	2.5	67.4	6.05 †	0.578	11.6	0.452	0.119	7.73	11.06	0.0236	0.0137	$(1.62\pm0.46)\times10^{-2}$	$(7.26\pm0.54)\times10^{-2}$	0.01
6	8.5	3.0	62.6	6.30 †	0.525	12.0	0.406	0.111	7.73	11.06	0.0179	0.0049	$(0.79\pm0.50)\times10^{-2}$	$(8.05\pm0.74)\times10^{-2}$	(0.004)
7	12.33	3.83	59.5	6.35 †	0.491	12.1	0.379	0.105	7.73	11.06	0.0161	0.0009	$(0.17\pm0.49)\times10^{-2}$	$(8.22\pm0.88)\times10^{-2}$	(0.002)
8	17.0	4.67	56.4	----	0.457	---	---	---	--	---	---	----	----	----	----
9	24.0	7.0	55.1	7.20 †	0.441	13.5						0.0138	$(6.56\pm3.86)\times10^{-2}$	$(14.78\pm3.96)\times10^{-2}$	----

Notes:

* Sensitivity "2"; Calibration (2). † Sensitivity "1"; Calibration (1).

** Probable error, $P(\Delta L_n)$ and $P(L_n)$, defined by Eqns. (J-86) and (J-87), respectively.

*** Probable error, obtained from deviations of experimental points from the best-fit straight line by using Eqn. (J-91).

**** Probable error, obtained as a mean of probable errors of experimental points directly calculated from experimental errors by using Eqn. (J-92).

***** Probable error corresponding to $P(\overline{L})$.

$P(\overline{L}) = 1.55 \times 10^{-3}$ *** $gmole^{-1}$

$\overline{P(L)} = 4.33 \times 10^{-4}$ **** $gmole^{-1}$

Slope: $S = (2.72\pm0.097)\times10^{-2}$ **** $gmole^{-1}hr^{-1}$

Overall Rate Constant: $\langle k_2 \rangle = 53.2\pm1.9$ ***** g-atom D/ml.hr.$(gmole/ml)^2$

Rate Constant in Liquid Phase: $k_2 = 1121\pm41$ ***** g-atom D/ml.hr.$(gmole/ml)^2$

TABLE M-VIII

Data and Calculated Results of Run 16

Temperature: 200°C

Stirring Rate: 8 strokes/sec.

Catalyst: 1.60 Normal diethylamine in charged solution

Hydroxyl-Ion Concentration: h = 0.014 Normal

Total Amount of Liquid Charged: G = 4.43 grams

Total Amount of H_2 Charged: $n'_{o,o}$ = A_o = 0.689 gmoles

Total Amount of HDO Charged: B_o = 8.23 gmoles

Total Amount of HD Charged: C_o = 0 gmoles

Total Amount of H_2O Charged: D_o = 11.36 gmoles

F = 0.985

λ_o = 0.0284 λ_1 = 0.9913 λ'_o = 0.9716 λ'_1 = 0.0087

Volume of Vapor Phase: V' = 425 ml.

Amount of Water in Liquid Phase: m_1 = 385.3 grams

Amount of Water in Vapor Phase: m'_1 = 3.48 grams

Amount of Amine in Liquid Phase: m_2 = 53.57 grams

Amount of Amine in Vapor Phase: m'_2 = 0.63 grams

$\lambda_o\lambda_1$ = 0.0281

$\lambda'_o\lambda'_1$ = 0.00847

Sample Number n	Time t_n (hr)	Time Δt_n (hr)	Total Pressure after Sampling $p_{(n+1)}$ (at.)	T/C-Cell Output * E_n (mV)	Amount of Hydrogen after Sampling $n'_{o,(n+1)}$ (gmole)	Atom Fraction D in Hydrogen $f'_{d,n}$ (%)	Amounts of Reactants after Sampling: H_2 A_{n+1} (gmole)	HD C_{n+1} (gmole)	HDO B_{n+1} (gmole)	H_2O D_{n+1} (gmole)	β_{n+1} (gmole)	Extent of Reaction: ΔX_n (gmole)	ΔL_n ** (gmole^{-1})	L_n ** (gmole^{-1})	Weight w_n
0	0		77.9	0	0.681	0	0.681	0	8.23	11.36	0.1706				
		0.5										0.0567	$(1.32\pm0.06)\times10^{-2}$	$(1.32\pm0.06)\times10^{-2}$	1.00
1	0.5		77.2	2.00	0.674	4.17	0.619	0.0538	8.17	11.42	0.1147				
		0.5										0.0442	$(1.59\pm0.14)\times10^{-2}$	$(2.91\pm0.15)\times10^{-2}$	0.16
2	1.0		76.2	3.70	0.663	7.44	0.568	0.0913	8.13	11.46	0.0737				
		0.5										-	-	-	-
3	1.5		75.1	-	0.652	-	-	-	-	-	-				
		1.0										0.0383	$(2.39\pm0.27)\times10^{-2}$	$(5.30\pm0.31)\times10^{-2}$	0.04
4	2.5		73.8	5.30	0.637	10.3	0.512	0.118	8.09	11.50	0.0397				
		2.0										0.0143	$(1.46\pm0.34)\times10^{-2}$	$(6.76\pm0.46)\times10^{-2}$	0.02
5	4.5		71.7	5.95	0.615	11.4	0.482	0.125	8.08	11.51	0.0271				
		3.0										-	-	-	-
6	7.5		69.7	-	0.593	-	-	-	-	-	-				
		4.5										0.0083	$(1.20\pm0.43)\times10^{-2}$	$(7.96\pm0.63)\times10^{-2}$	0.01
7	12.0		65.6	6.35	0.548	12.1	0.423	0.117	8.07	11.52	0.0183				
		6.0										(0)	-	-	-
8	18.0		62.2	6.35	0.510	12.1									
		-										-	-	- -	-
9	-		-	-	-	-	-	-	-	-	-				

Notes:

* Sensitivity "1"; Calibration (1).

** Probable error, $P(\Delta L_n)$ and $P(L_n)$, defined by Eqns. (J-86) and (J-87), respectively.

*** Probable error, obtained from deviations of experimental points from the best-fit straight line by using Eqn. (J-91).

**** Probable error, obtained as a mean of probable errors of experimental points directly calculated from experimental errors by using Eqn. (J-92).

***** Probable error corresponding to $P(\overline{L})$.

$P(\overline{L})$ = 1.96×10^{-3} *** gmole^{-1}

$\overline{P(L)}$ = 6.35×10^{-4} **** gmole^{-1}

Slope: S = $(2.14\pm0.10)\times10^{-2}$ ***** gmole^{-1}hr^{-1}

Overall Rate Constant: $\langle k_2 \rangle = 41.6\pm2.0$ ***** g-atom D/ml.hr.(gmole/ml)^2

Rate Constant in Liquid Phase: k_2 = 834 ± 40 ***** g-atom D/ml.hr.(gmole/ml)^2

TABLE M-IX

Data and Calculated Results of Run 17

Temperature: 200 °C

Stirring Rate: 1.5 strokes/sec.

Catalyst: 1.67 Normal diethylamine in charged solution

Hydroxyl-Ion Concentration: h = 0.015 Normal

Total Amount of Liquid Charged: G = 440 grams

Total Amount of H_2 Charged: $n'_{o,o} = A_o$ = 0.749 gmoles

Total Amount of HDO Charged: B_o = 7.98 gmoles

Total Amount of HD Charged: C_o = 0 gmoles

Total Amount of H_2O Charged: D_o = 11.19 gmoles

F = 0.985

Volume of Vapor Phase: V' = 425 ml.

Amount of Water in Liquid Phase: m_1 = 380.2 grams

Amount of Water in Vapor Phase: m'_1 = 3.37 grams

Amount of Amine in Liquid Phase: m_2 = 55.80 grams

Amount of Amine in Vapor Phase: m'_2 = 0.67 grams

$\lambda_o\lambda_1$ = 0.0279

$\lambda_o = 0.0281$ $\lambda_1 = 0.9912$ $\lambda'_o = 0.9719$ $\lambda'_1 = 0.0088$ $\lambda'_o\lambda'_1 = 0.00852$

Sample Number n	Time t_n (hr)	Time Δt_n (hr)	Total Pressure after Sampling $P_{(n+1)}$ (at.)	T/C-Cell Output * E_n (mV)	Amount of Hydrogen after Sampling $n'_{o,(n+1)}$ (gmole)	Atom Fraction D in Hydrogen $f'_{d,n}$ (%)	Amounts of Reactants after Sampling: H_2 A_{n+1} (gmole)	HD C_{n+1} (gmole)	HDO B_{n+1} (gmole)	H_2O D_{n+1} (gmole)	β_{n+1} (gmole)	Extent of Reaction: ΔX_n (gmole)	ΔL_n ** (gmole^{-1})	L_n ** (gmole^{-1})	Weight w_n
0	0		82.6	0	0.734	0	0.734	0	7.98	11.19	0.1813				
		0.5										0.0403	$(0.84\pm0.05)\times10^{-2}$	$(0.84\pm0.05)\times10^{-2}$	1.00
1	0.5		80.6	1.30	0.712	2.75	0.673	0.0381	7.94	11.23	0.1378				
		0.5										0.0398	$(1.13\pm0.11)\times10^{-2}$	$(1.97\pm0.12)\times10^{-2}$	0.20
2	1.0		77.2	2.70	0.675	5.54	0.602	0.0707	7.90	11.27	0.0957				
		0.5										-	-	-	-
3	1.5		75.1	-	0.652	-	-	-	-	-	-				
		1.0										0.0356	$(1.55\pm0.16)\times10^{-2}$	$(3.52\pm0.20)\times10^{-2}$	0.07
4	2.5		71.1	4.10	0.608	8.18	0.513	0.0913	7.87	11.30	0.0580				
		2.0										0.0154	$(1.03\pm0.20)\times10^{-2}$	$(4.55\pm0.28)\times10^{-2}$	0.04
5	4.5		70.1	4.80	0.596	9.45	0.489	0.102	7.85	11.32	0.0441				
		3.0										-	-	-	-
6	7.5		68.4	-	0.578	-	-	-	-	-	-				
		4.5										0.0299	$(3.79\pm0.62)\times10^{-2}$	$(8.34\pm0.68)\times10^{-2}$	(0.006)
7	12.0		65.6	6.25	0.548	12.0	0.425	0.115	7.82	11.35	0.0181				
		6.0										0.0073	$(1.73\pm0.70)\times10^{-2}$	$(10.07\pm1.80)\times10^{-2}$	(0.003)
8	18.0		61.2	6.65	0.499	12.6									
		-										-	-	-	-
9	-		-	-	-	-	-	-	-	-	-				

Notes:

* Sensitivity "1"; Calibration (1).

** Probable error, $P(\Delta L_n)$ and $P(L_n)$, defined by Eqns. (J-86) and (J-87), respectively.

*** Probable error, obtained from deviations of experimental points from the best-fit straight line by using Eqn. (J-91).

**** Probable error, obtained as a mean of probable errors of experimental points directly calculated from experimental errors by using Eqn. (J-92).

***** Probable error corresponding to $P(\overline{L})$.

$P(\overline{L}) = 1.30 \times 10^{-3}$ *** gmole^{-1}

$\overline{P(L)} = 5.17 \times 10^{-4}$ **** gmole^{-1}

Slope: $S = (1.34\pm0.031)\times10^{-4}$ ***** gmole^{-1}hr^{-1}

Overall Rate Constant: $\langle k_2 \rangle = 26.1\pm0.6$ ***** g-atom D/ml.hr.(gmole/ml)^2

Rate Constant in Liquid Phase: $k_2 = 520\pm13$ ***** g-atom D/ml.hr.(gmole/ml)^2

TABLE M-X

Data and Calculated Results of Run 19

Temperature: 100°C

Stirring Rate: 8 strokes/sec.

Catalyst: 1.83 Normal diethylamine in charged solution

Hydroxyl-Ion Concentration: h = 0.040 Normal

Total Amount of Liquid Charged: G = 441 grams

Total Amount of H_2 Charged: $n'_{o,o}$ = A_o = 1.42 gmoles

Total Amount of HDO Charged: B_o = 7.89 gmoles

Total Amount of HD Charged: C_o = 0 gmoles

Total Amount of H_2O Charged: D_o = 11.17 gmoles

F = 0.978

λ_o = 0.0172 λ_1 = 0.9993 λ'_o = 0.9828 λ'_1 = 0.00069

Volume of Vapor Phase: V' = 508 ml.

Amount of Water in Liquid Phase: m_1 = 378.5 grams

Amount of Water in Vapor Phase: m'_1 = 0.26 grams

Amount of Amine in Liquid Phase: m_2 = 60.27 grams

Amount of Amine in Vapor Phase: m'_2 = 0.16 grams

$\lambda_o\lambda_1$ = 0.0172

$\lambda'_o\lambda'_1$ = 0.00067

Sample Number n	Time t_n (hr)	Time Δt_n (hr)	Total Pressure after Sampling $P_{(n+1)}$ (at.)	T/C-Cell Output * E_n (mV)	Amount of Hydrogen after Sampling $n'_{o,(n+1)}$ (gmole)	Atom Fraction D in Hydrogen $f'_{d,n}$ (%)	Amounts of Reactants after Sampling: H_2 A_{n+1} (gmole)	HD C_{n+1} (gmole)	HDO B_{n+1} (gmole)	H_2O D_{n+1} (gmole)	β_{n+1} (gmole)	Extent of Reaction: ΔX_n (gmole)	ΔL_n (gmole^{-1}) **	L_n (gmole^{-1}) **	Weight w_n
0	0		84.7	0	1.39	0	1.39	0	7.89	11.17	0.2749				
1	1.0	1.0	83.3	0.40	1.36	0.86	1.34	0.0232	7.87	11.19	0.2459	0.0240	$(0.38\pm0.07)\times10^{-2}$	$(0.38\pm0.07)\times10^{-2}$	1.00
2	2.0	1.0	82.0	0.70	1.34	1.50	1.30	0.0396	7.85	11.21	0.2257	0.0173	$(0.31\pm0.11)\times10^{-2}$	$(0.69\pm0.13)\times10^{-2}$	0.31
3	3.0	1.0	80.6	1.00	1.32	2.13	1.26	0.0550	7.83	11.23	0.2064	0.0168	$(0.32\pm0.12)\times10^{-2}$	$(1.01\pm0.17)\times10^{-2}$	0.17
4	6.0	3.0	77.2	-	1.26	-	-	-	-	-	-	-	-	-	-
5	10.0	4.0	72.4	2.30	1.18	4.76	1.07	0.107	7.77	11.30	0.1267	0.0695	$(1.71\pm0.18)\times10^{-2}$	$(2.72\pm0.25)\times10^{-2}$	0.08
6	15.0	5.0	68.4	3.20	1.12	6.50	0.98	0.136	7.73	11.34	0.0852	0.0411	$(1.64\pm0.25)\times10^{-2}$	$(4.36\pm0.35)\times10^{-2}$	0.04
7	24.5	9.5	62.2	3.90	1.01	7.81	0.86	0.145	7.70	11.36	0.0538	0.0294	$(1.77\pm0.36)\times10^{-2}$	$(6.13\pm0.50)\times10^{-2}$	0.02
8	31.0	6.5	58.5	4.30	0.95	8.55							$(1.35\pm0.45)\times10^{-2}$	$(7.48\pm0.67)\times10^{-2}$	0.01
9	-	-	-	-	-	-	-	-	-	-	-	-	-	-	-

Notes:

* Sensitivity "1"; Calibration (1).

** Probable error, $P(\Delta L_n)$ and $P(L_n)$, defined by Eqns. (J-86) and (J-87), respectively.

*** Probable error, obtained from deviations of experimental points from the best-fit straight line by using Eqn. (J-91).

**** Probable error, obtained as a mean of probable errors of experimental points directly calculated from experimental errors by using Eqn. (J-92).

***** Probable error corresponding to $P(\overline{L})$.

$P(\overline{L})$ = 4.43×10^{-4} *** gmole^{-1}

$\overline{P(L)}$ = 6.01×10^{-4} **** gmole^{-1}

Slope: S = $(2.70\pm0.018)\times10^{-3}$ ***** gmole^{-1}hr^{-1}

Overall Rate Constant: $\langle k_2 \rangle = 4.38\pm0.03$ ***** g-atom D/ml.hr.(gmole/ml)^2

Rate Constant in Liquid Phase: $k_2 = 119\pm2$ ***** g-atom D/ml.hr.(gmole/ml)^2

TABLE M-XI

Data and Calculated Results of Run 21

Temperature: 200°C

Stirring Rate: 6 strokes/sec.

Catalyst: 0.84 Normal diethylamine in charged solution

Hydroxyl-Ion Concentration: h = 0.010 Normal

Total Amount of Liquid Charged: G = 433 grams

Total Amount of H_2 Charged: $n'_{o,o}$ = A_o = 0.920 gmoles

Total Amount of HDO Charged: B_o = 9.22 gmoles

Total Amount of HD Charged: C_o = 0 gmoles

Total Amount of H_2O Charged: D_o = 12.80 gmoles

F = 0.992

λ_o = 0.0264 λ_1 = 0.9908 λ'_o = 0.9736 λ'_1 = 0.0092

Volume of Vapor Phase: V' = 470 ml.

Amount of Water in Liquid Phase: m_1 = 402.1 grams

Amount of Water in Vapor Phase: m'_1 = 3.72 grams

Amount of Amine in Liquid Phase: m_2 = 26.86 grams

Amount of Amine in Vapor Phase: m'_2 = 0.34 grams

$\lambda_o\lambda_1$ = 0.0261

$\lambda'_o\lambda'_1$ = 0.00894

Sample Number n	Time t_n (hr)	Time Δt_n (hr)	Total Pressure after Sampling $P_{(n+1)}$ (at.)	T/C-Cell Output * E_n (mV)	Amount of Hydrogen after Sampling $n'_{o,(n+1)}$ (gmole)	Atom Fraction D in Hydrogen $f^i_{d,n}$ (%)	Amounts of Reactants after Sampling: H_2 A_{n+1} (gmole)	HD C_{n+1} (gmole)	HDO B_{n+1} (gmole)	H_2O D_{n+1} (gmole)	β_{n+1} (gmole)	Extent of Reaction: ΔX_n (gmole)	ΔL_n (gmole^{-1}) **	L_n (gmole^{-1}) **	Weight W_n
0	0		89.4	0	0.896	0	0.896	0	9.22	12.80	0.2225	0.0287	$(0.40\pm0.04)\times10^{-2}$	$(0.40\pm0.04)\times10^{-2}$	1.00
1	0.5	0.5	87.4	0.75	0.871	1.60	0.843	0.0275	9.19	12.83	0.1889	0.0270	$(0.45\pm0.07)\times10^{-2}$	$(0.85\pm0.08)\times10^{-2}$	0.27
2	1.0	0.5	86.0	1.50	0.855	3.16	0.802	0.0523	9.17	12.86	0.1600	0.0257	$(0.51\pm0.08)\times10^{-2}$	$(1.37\pm0.11)\times10^{-2}$	0.14
3	1.5	0.5	84.7	2.25	0.838	4.66	0.762	0.0745	9.14	12.88	0.1334	0.0503	$(1.38\pm0.14)\times10^{-2}$	$(2.75\pm0.18)\times10^{-2}$	0.05
4	3.0	1.5	81.3	3.82	0.797	7.67	0.680	0.113	9.09	12.93	0.0841	0.0397	$(1.86\pm0.27)\times10^{-2}$	$(4.61\pm0.33)\times10^{-2}$	0.02
5	5.5	2.5	77.5	5.20	0.776	10.2	0.626	0.142	9.05	12.97	0.0492	0.0162	$(1.16\pm0.34)\times10^{-2}$	$(5.77\pm0.47)\times10^{-2}$	0.01
6	7.5	2.0	75.8	5.80	0.731	11.2	0.577	0.145	9.03	12.99	0.0340	0.0270	$(4.62\pm1.61)\times10^{-2}$	$(10.39\pm1.68)\times10^{-2}$	(0.0006)
7	12.0	4.5	72.4	6.90	0.690	13.04									
8	17.0	5.0	69.4	-	0.653	-	-	-	-	-	-	-	-	-	-
9	24.0	7.0	65.6	-	0.609	-	-	-	-	-	-	-	-	-	-

Notes:

* Sensitivity "1"; Calibration (1).

** Probable error, $P(\Delta L_n)$ and $P(L_n)$, defined by Eqns. (J-86) and (J-87), respectively.

*** Probable error, obtained from deviations of experimental points from the best-fit straight line by using Eqn. (J-91).

**** Probable error, obtained as a mean of probable errors of experimental points directly calculated from experimental errors by using Eqn. (J-92).

***** Probable error corresponding to $P(\overline{L})$.

$P(\overline{L})$ = 2.82×10^{-4} *** gmole^{-1}

$\overline{P(L)}$ = 3.65×10^{-4} **** gmole^{-1}

Slope: S = $(8.67\pm0.10)\times10^{-3}$ ***** gmole^{-1}hr^{-1}

Overall Rate Constant: $\langle k_2 \rangle = 16.8\pm0.2$ ***** g-atom D/ml.hr.(gmole/ml)^2

Rate Constant in Liquid Phase: $k_2 = 324\pm6$ ***** g-atom D/ml.hr.(gmole/ml)^2

TABLE M- XII

Data and Calculated Results of Run 24

Temperature: 150 °C
Stirring Rate: 8 strokes/sec.
Catalyst: 0.78 Normal diethylamine in charged solution
Hydroxyl-Ion Concentration: h = 0.017 Normal

Total Amount of Liquid Charged: G = 452 grams
Total Amount of H_2 Charged: $n'_{o,o} = A_o$ = 1.22 gmoles
Total Amount of HDO Charged: B_o = 8.20 gmoles
Total Amount of HD Charged: C_o = 0 gmoles
Total Amount of H_2O Charged: D_o = 13.74 gmoles
F = 0.993

Volume of Vapor Phase: V' = 487 ml.
Amount of Water in Liquid Phase: m_1 = 424.3 grams
Amount of Water in Vapor Phase: m'_1 = 1.20 grams
Amount of Amine in Liquid Phase: m_2 = 26.32 grams
Amount of Amine in Vapor Phase: m'_2 = 0.16 grams
$\lambda_o\lambda_1$ = 0.0230

λ_o =0.0231 λ_1 = 0.9972 λ_o' =0.9769 λ_1' =0.0028 $\lambda_o'\lambda_1'$ = 0.00281

Sample Number n	Time t_n (hr)	Time Δt_n (hr)	Total Pressure after Sampling $P_{(n+1)}$ (at.)	T/C-Cell Output * E_n (mV)	Amount of Hydrogen after Sampling $n'_{o,(n+1)}$ (gmole)	Atom Fraction D in Hydrogen $f'_{d,n}$ (%)	Amounts of Reactants after Sampling: H_2 A_{n+1} (gmole)	HD C_{n+1} (gmole)	HDO B_{n+1} (gmole)	H_2O D_{n+1} (gmole)	β_{n+1} (gmole)	Extent of Reaction: ΔX_n (gmole)	ΔL_n (gmole^{-1})**	L_n (gmole^{-1})**	Weight w_n
0	0	0.5	88.4	0	1.17	0	1.17	0	8.20	13.74	0.2318				
1	0.5	0.5	86.9	0.25	1.15	0.54	1.14	0.0124	8.19	13.75	0.2156	0.0126	$(1.76\pm0.51)\times10^{-3}$	$(1.76\pm0.51)\times10^{-3}$	1.00
2	1.0	0.5	84.7	0.52	1.12	1.12	1.10	0.0248	8.17	13.77	0.1974	0.0133	$(2.00\pm0.77)\times10^{-3}$	$(3.76\pm0.93)\times10^{-3}$	0.31
3	1.5	1.0	83.7	0.78	1.11	1.67	1.07	0.0364	8.16	13.78	0.1838	0.0123	$(2.02\pm0.82)\times10^{-3}$	$(5.78\pm1.24)\times10^{-3}$	0.17
4	2.5	1.0	82.5	1.20	1.09	2.54	1.04	0.0540	8.14	13.80	0.1622	0.0194	$(3.51\pm1.01)\times10^{-3}$	$(9.29\pm1.60)\times10^{-3}$	0.10
5	3.5	3.5	81.3	1.55	1.07	3.26	1.00	0.0675	8.13	13.81	0.1447	0.0156	$(3.18\pm1.21)\times10^{-3}$	$(12.47\pm2.00)\times10^{-3}$	0.07
6	7.0	5.0	80.3	---	1.06	---	---	---	---	---	---	---	---	---	---
7	12.0	5.0	78.6	3.62	1.03	7.29	0.89	0.139	8.04	13.90	0.0639	0.0863	$(28.5\pm3.2)\times10^{-3}$	$(40.91\pm3.80)\times10^{-3}$	0.02
8	17.0	7.0	75.2	---	0.99	---	---	---	---	---	---	---	---	---	---
9	24.0		68.4	3.65	0.89	7.35						0.0012	$(5.7\pm3.8)\times10^{-3}$	$(46.61\pm5.31)\times10^{-3}$	(0.009)

Notes:
* Sensitivity "1"; Calibration (1).
** Probable error, $P(\Delta L_n)$ and $P(L_n)$, defined by Eqns. (J-86) and (J-87), respectively.
*** Probable error, obtained from deviations of experimental points from the best-fit straight line by using Eqn. (J-91).
**** Probable error, obtained as a mean of probable errors of experimental points directly calculated from experimental errors by using Eqn. (J-92).
***** Probable error corresponding to $P(\overline{L})$.

$P(\overline{L})$ = 8.25×10^{-5} *** gmole^{-1}
$\overline{P(L)}$ = 4.20×10^{-4} **** gmole^{-1}

Slope: S = $(3.54\pm0.012)\times10^{-3}$ ***** gmole^{-1}hr^{-1}

Overall Rate Constant: $\langle k_2 \rangle = 6.29\pm0.02$ ***** g-atom D/ml.hr.(gmole/ml)^2

Rate Constant in Liquid Phase: $k_2 = 132 \pm 2$ ***** g-atom D/ml.hr.(gmole/ml)^2

TABLE M-XIII

Data and Calculated Results of Run 25

Temperature: 100 °C
Stirring Rate: 8 strokes/sec.
Catalyst: 0.76 Normal diethylamine in charged solution
Hydroxyl-Ion Concentration: h = 0.026 Normal

Total Amount of Liquid Charged: G = 452 grams
Total Amount of H_2 Charged: $n'_{o,o}$ = A_o = 1.46 gmoles
Total Amount of HDO Charged: B_o = 8.32 gmoles
Total Amount of HD Charged: C_o = 0 gmoles
Total Amount of H_2O Charged: D_o = 13.70 gmoles
F = 0.993
λ_o =0.0187 λ_1=0.9988 λ_o'=0.9813 λ_1'=0.0012

Volume of Vapor Phase: V' = 515 ml.
Amount of Water in Liquid Phase: m_1 = 425.5 grams
Amount of Water in Vapor Phase: m_1' = 0.50 grams
Amount of Amine in Liquid Phase: m_2 = 25.95 grams
Amount of Amine in Vapor Phase: m_2' = 0.05 grams
$\lambda_o\lambda_1$ = 0.0186
$\lambda_o'\lambda_1'$ = 0.00116

Sample Number n	Time t_n (hr)	Time Δt_n (hr)	Total Pressure after Sampling $P_{(n+1)}$ (at.)	T/C-Cell Output * E_n (mV)	Amount of Hydrogen after Sampling $n'_{o,(n+1)}$ (gmole)	Atom Fraction D in Hydrogen $f'_{d,n}$ (%)	Amounts of Reactants after Sampling: H_2 A_{n+1} (gmole)	HD C_{n+1} (gmole)	HDO B_{n+1} (gmole)	H_2O D_{n+1} (gmole)	β_{n+1} (gmole)	Extent of Reaction: ΔX_n (gmole)	ΔL_n ($gmole^{-1}$)**	L_n ($gmole^{-1}$)**	Weight w_n
0	0	1.5	85.1	0	1.42	0	1.42	0	8.32	13.70	0.2504				
1	1.5	1.0	79.0	0.15	1.31	0.33	1.30	0.0085	8.31	13.71	0.2232	0.0092	$(1.35\pm0.65)\times10^{-3}$	$(1.35\pm0.65)\times10^{-3}$	1.00
2	2.5	1.0	78.3	0.20	1.30	0.43	1.29	0.0112	8.31	13.71	0.2188	0.0028	$(0.46\pm0.93)\times10^{-3}$	$(1.81\pm1.13)\times10^{-3}$	0.33
3	3.5	2.5	76.9	0.42	1.28	0.90	1.26	0.0229	8.30	13.72	0.2036	0.0123	$(2.07\pm0.98)\times10^{-3}$	$(3.88\pm1.49)\times10^{-3}$	0.19
4	6.0	4.0	73.7	0.80	1.22	1.71	1.18	0.0410	8.28	13.75	0.1751	0.0206	$(3.83\pm1.09)\times10^{-3}$	$(7.71\pm1.85)\times10^{-3}$	0.11
5	10.0	5.0	72.1	1.30	1.16	2.75	1.10	0.0620	8.25	13.77	0.1436	0.0253	$(5.62\pm1.26)\times10^{-3}$	$(13.33\pm2.24)\times10^{-3}$	0.08
6	15.0	9.5	63.9	---	1.06	---	---	---	---	---	---	---	----	----	---
7	24.5	2.5	53.4	---	0.88	---	---	---	---	---	---	---	----	----	---
8	27.0	9.0	48.6	3.30	0.80	6.69	0.70	0.0998	8.16	13.86	0.0416	0.0915	$(36.4\pm3.8)\times10^{-3}$	$(49.7\pm4.4)\times10^{-3}$	0.02
9	36.0		44.5	4.30	0.73	8.55						0.0296	$(45.2\pm11.2)\times10^{-3}$	$(94.9\pm12.0)\times10^{-3}$	(0.004)

Notes:
* Sensitivity "1"; Calibration (1).
** Probable error, $P(\Delta L_n)$ and $P(L_n)$, defined by Eqns. (J-86) and (J-87), respectively.
*** Probable error, obtained from deviations of experimental points from the best-fit straight line by using Eqn. (J-91).
**** Probable error, obtained as a mean of probable errors of experimental points directly calculated from experimental errors by using Eqn. (J-92).
***** Probable error corresponding to $P(\overline{L})$.

$P(\overline{L})$ = 4.85×10^{-4} *** $gmole^{-1}$
$\overline{P(L)}$ = 5.35×10^{-4} **** $gmole^{-1}$

Slope: S = $(1.47\pm0.031)\times10^{-3}$ ***** $gmole^{-1}hr^{-1}$

Overall Rate Constant: $\langle k_2 \rangle = 2.35\pm0.05$ ***** g-atom D/ml.hr.$(gmole/ml)^2$

Rate Constant in Liquid Phase: $k_2 = 51.0\pm1.2$ ***** g-atom D/ml.hr.$(gmole/ml)^2$

TABLE M-XIV

Data and Calculated Results of Run 26

Temperature: 200 °C

Stirring Rate: 8 strokes/sec.

Catalyst: 1.55 Normal diethylamine in charged solution

Hydroxyl-Ion Concentration: h = 0.014 Normal

Total Amount of Liquid Charged: G = 427 grams

Total Amount of H_2 Charged: $n'_{o,o} = A_o$ = 0.456 gmoles

Total Amount of HDO Charged: B_o = 7.87 gmoles

Total Amount of HD Charged: C_o = 0 gmoles

Total Amount of H_2O Charged: D_o = 11.05 gmoles

F = 0.983

λ_o =0.0261 λ_1=0.9912 λ_o'=0.9739 λ_1'=0.0088

Volume of Vapor Phase: V' = 449 ml.

Amount of Water in Liquid Phase: m_1 = 373.2 grams

Amount of Water in Vapor Phase: m_1' = 3.30 grams

Amount of Amine in Liquid Phase: m_2 = 49.95 grams

Amount of Amine in Vapor Phase: m_2' = 0.55 grams

$\lambda_o\lambda_1$ = 0.0259

$\lambda_o'\lambda_1'$ = 0.00853

Sample Number n	Time t_n (hr)	Time Δt_n (hr)	Total Pressure after Sampling $p_{(n+1)}$ (at.)	T/C-Cell Output * E_n (mV)	Amount of Hydrogen after Sampling $n'_{o,(n+1)}$ (gmole)	Atom Fraction D in Hydrogen $f'_{d,n}$ (%)	Amounts of Reactants after Sampling: H_2 A_{n+1} (gmole)	HD C_{n+1} (gmole)	HDO B_{n+1} (gmole)	H_2O D_{n+1} (gmole)	β_{n+1} (gmole)	Extent of Reaction: ΔX_n (gmole)	ΔL_n ($gmole^{-1}$)**	L_n ($gmole^{-1}$)**	Weight w_n
0	0	0.5	53.7	0	0.440	0	0.440	0	7.87	11.05	0.1098				
1	0.5	0.5	52.7	1.80	0.429	3.76	0.397	0.0311	7.84	11.08	0.0758	0.0331	$(1.22\pm0.06)\times10^{-2}$	$(1.22\pm0.06)\times10^{-2}$	1.00
2	1.0	0.5	51.7	3.35	0.416	6.79	0.362	0.0526	7.81	11.11	0.0507	0.0259	$(1.42\pm0.13)\times10^{-2}$	$(2.64\pm0.15)\times10^{-2}$	0.19
3	1.5	1.0	50.3	4.13	0.401	8.24	0.338	0.0606	7.80	11.12	0.0388	0.0121	$(0.92\pm0.16)\times10^{-2}$	$(3.56\pm0.21)\times10^{-2}$	0.09
4	2.5	2.0	49.3	4.85	0.389	9.53	0.318	0.0671	7.79	11.13	0.0291	0.0104	$(1.06\pm0.20)\times10^{-2}$	$(4.62\pm0.30)\times10^{-2}$	0.05
5	4.5	2.0	48.6	5.60	0.381	10.8	0.303	0.0737	7.78	11.14	0.0202	0.0102	$(1.47\pm0.33)\times10^{-2}$	$(6.09\pm0.44)\times10^{-2}$	0.02
6	6.5	3.5	46.9	6.40	0.362	12.2	0.279	0.0776	7.77	11.15	0.0113	0.0104	$(2.44\pm0.70)\times10^{-2}$	$(8.53\pm0.83)\times10^{-2}$	(0.004)
7	10.0	5.0	45.3	6.45	0.343	12.3						0.0006	$(0.19\pm0.54)\times10^{-2}$	$(8.72\pm0.99)\times10^{-2}$	(0.002)
8	15.0	--	44.6	--	0.335	--	---	---	--	---	---	---	----	----	---
9	--		--	--	---	--	---	---	--	---	---	---	----	----	---

Notes:

* Sensitivity "1"; Calibration (1).

** Probable error, $P(\Delta L_n)$ and $P(L_n)$, defined by Eqns. (J-86) and (J-87), respectively.

*** Probable error, obtained from deviations of experimental points from the best-fit straight line by using Eqn. (J-91).

**** Probable error, obtained as a mean of probable errors of experimental points directly calculated from experimental errors by using Eqn. (J-92).

***** Probable error corresponding to $P(\bar{L})$.

$P(\bar{L}) = 9.85 \times 10^{-4}$ *** $gmole^{-1}$

$\overline{P(L)} = 6.36 \times 10^{-4}$ **** $gmole^{-1}$

Slope: $S = (2.28\pm0.059)\times10^{-2}$ ***** $gmole^{-1}hr^{-1}$

Overall Rate Constant: $\langle k_2 \rangle = 44.4\pm1.2$ ***** g-atom D/ml.hr.$(gmole/ml)^2$

Rate Constant in Liquid Phase: $k_2 = 928\pm26$ ***** g-atom D/ml.hr.$(gmole/ml)^2$

TABLE M-XV

Data and Calculated Results of Run 27

Temperature: 200 °C
Stirring Rate: 6 strokes/sec.
Catalyst: 1.50 Normal diethylamine in charged solution
Hydroxyl-Ion Concentration: h = 0.014 Normal

Total Amount of Liquid Charged: G = 435 grams
Total Amount of H_2 Charged: $n'_{o,o}$ = A_o = 0.710 gmoles
Total Amount of HDO Charged: B_o = 8.62 gmoles
Total Amount of HD Charged: C_o = 0 gmoles
Total Amount of H_2O Charged: D_o = 12.09 gmoles
F =

Volume of Vapor Phase: V' = 442 ml.
Amount of Water in Liquid Phase: m_1 = 383.2 grams
Amount of Water in Vapor Phase: m'_1 = 3.33 grams
Amount of Amine in Liquid Phase: m_2 = 47.90 grams
Amount of Amine in Vapor Phase: m'_2 = 0.60 grams
$\lambda_o\lambda_1$ = 0.0271
$\lambda'_o\lambda'_1$ = 0.00786

λ_o = 0.0272 λ_1 = 0.9919 λ'_o = 0.9728 λ'_1 = 0.0081

Sample Number n	Time t_n (hr)	Time Δt_n (hr)	Total Pressure after Sampling $p_{(n+1)}$ (at.)	T/C-Cell Output * E_n (mV)	Amount of Hydrogen after Sampling $n'_{o,(n+1)}$ (gmole)	Atom Fraction D in Hydrogen $f'_{d,n}$ (%)	Amounts of Reactants after Sampling: H_2 A_{n+1} (gmole)	HD C_{n+1} (gmole)	HDO B_{n+1} (gmole)	H_2O D_{n+1} (gmole)	β_{n+1} (gmole)	Extent of Reaction: ΔX_n (gmole)	ΔL_n ** ($gmole^{-1}$)	L_n ** ($gmole^{-1}$)	Weight W_n
0	0	0.5	82.9	0	0.691	0	0.691	0	8.62	12.09	0.1713				
1	0.5	0.5	80.3	1.55	0.663	3.26	0.621	0.0418	8.58	12.13	0.1225	0.0450	$(0.94\pm0.05)\times10^{-2}$	$(0.94\pm0.05)\times10^{-2}$	1.00
2	1.0	0.5	79.3	3.25	0.653	6.60	0.570	0.0805	8.53	12.18	0.0807	0.0443	$(1.38\pm0.13)\times10^{-2}$	$(2.32\pm0.14)\times10^{-2}$	0.14
3	1.5	0.5	77.9	4.30	0.640	8.55	0.535	0.100	8.51	12.20	0.0574	0.0255	$(1.17\pm0.19)\times10^{-2}$	$(3.49\pm0.23)\times10^{-2}$	0.05
4	2.0	0.5	75.8	5.05	0.618	9.89	0.502	0.110	8.49	12.22	0.0415	0.0172	$(1.10\pm0.25)\times10^{-2}$	$(4.59\pm0.34)\times10^{-2}$	0.02
5	2.5	0.5	74.5	-	0.604	-	-	-	-	-	-	-	-	-	-
6	3.0	0.5	72.5	6.75	0.584	12.8	0.444	0.130	8.46	12.26	0.0119	0.0359	$(6.16\pm1.83)\times10^{-2}$	$(10.8\pm1.6)\times10^{-2}$	0.01
7	3.5	0.5	71.4	6.80	0.573	12.9	0.435	0.129	8.45	12.26	0.0110	0.0010	$(0.26\pm0.77)\times10^{-2}$	$(11.0\pm2.0)\times10^{-2}$	(0.005)
8	4.0	0.5	70.4	9.00	0.562	16.4						0.0399	-	-	-
9	4.5		69.0	-	-	-	-	-	-	-	-	-	-	-	-

Notes:
* Sensitivity "1"; Calibration (1).
** Probable error, $P(\Delta L_n)$ and $P(L_n)$, defined by Eqns. (J-86) and (J-87), respectively.
*** Probable error, obtained from deviations of experimental points from the best-fit straight line by using Eqn. (J-91).
**** Probable error, obtained as a mean of probable errors of experimental points directly calculated from experimental errors by using Eqn. (J-92).
***** Probable error corresponding to $P(\overline{L})$.

$P(\overline{L})$ = 5.80×10^{-4} *** $gmole^{-1}$
$\overline{P(L)}$ = 5.43×10^{-4} **** $gmole^{-1}$

Slope: S = $(2.14\pm0.049)\times10^{-2}$ ***** $gmole^{-1}hr^{-1}$

Overall Rate Constant: $\langle k_2 \rangle$ = 41.7 ± 1.0 ***** g-atom D/ml.hr.$(gmole/ml)^2$

Rate Constant in Liquid Phase: k_2 = 843 ± 21 ***** g-atom D/ml.hr.$(gmole/ml)^2$

TABLE M-XVI

Data and Calculated Results of Run 28

Temperature: 150°C

Stirring Rate: 8 strokes/sec.

Catalyst: 0.84 Normal diethylamine in charged solution

Hydroxyl-Ion Concentration: h = 0.018 Normal

Total Amount of Liquid Charged: G = 452 grams

Total Amount of H_2 Charged: $n'_{o,o}$ = A_o = 0.936 gmoles

Total Amount of HDO Charged: B_o = 8.11 gmoles

Total Amount of HD Charged: C_o = 0 gmoles

Total Amount of H_2O Charged: D_o = 13.72 gmoles

F = 0.991

λ_o = 0.0231 λ_1 = 0.9969 λ'_o = 0.9769 λ'_1 = 0.0031

Volume of Vapor Phase: V' = 485 ml.

Amount of Water in Liquid Phase: m_1 = 421.7 grams

Amount of Water in Vapor Phase: m'_1 = 1.31 grams

Amount of Amine in Liquid Phase: m_2 = 28.73 grams

Amount of Amine in Vapor Phase: m'_2 = 0.27 grams

$\lambda_o\lambda_1$ = 0.0230

$\lambda'_o\lambda'_1$ = 0.00300

Sample Number n	Time t_n (hr)	Time Δt_n (hr)	Total Pressure after Sampling $P_{(n+1)}$ (at.)	T/C-Cell Output * E_n (mV)	Amount of Hydrogen after Sampling $n'_{o,(n+1)}$ (gmole)	Atom Fraction D in Hydrogen $f'_{d,n}$ (%)	Amounts of Reactants after Sampling: H_2 A_{n+1} (gmole)	HD C_{n+1} (gmole)	HDO B_{n+1} (gmole)	H_2O D_{n+1} (gmole)	β_{n+1} (gmole)	Extent of Reaction: ΔX_n (gmole)	ΔL_n (gmole^{-1}) **	L_n (gmole^{-1}) **	Weight w_n
0	0		70.1	0	0.912	0	0.912	0	8.11	13.72	0.1807	-	-	-	-
1	0.5	0.5	69.1	-	0.898	-	-	-	-	-	-	0.0215	$(4.02\pm0.55)\times10^{-3}$	$(4.02\pm0.55)\times10^{-3}$	1.00
2	1.0	0.5	67.6	0.55	0.877	1.18	0.856	0.0205	8.09	13.74	0.1534	0.0093	$(1.97\pm0.83)\times10^{-3}$	$(5.99\pm1.00)\times10^{-3}$	0.31
3	1.5	0.5	67.0	0.80	0.869	1.71	0.840	0.0292	8.08	13.75	0.1431	0.0073	$(1.65\pm0.87)\times10^{-3}$	$(7.64\pm1.32)\times10^{-3}$	0.18
4	2.0	0.5	65.6	1.00	0.849	2.13	0.813	0.0353	8.07	13.76	0.1330	0.0105	$(2.62\pm1.05)\times10^{-3}$	$(10.26\pm1.69)\times10^{-3}$	0.11
5	2.5	0.5	64.2	1.30	0.830	2.75	0.785	0.0444	8.06	13.77	0.1203	0.0017	$(0.45\pm1.15)\times10^{-3}$	$(10.71\pm2.04)\times10^{-3}$	0.07
6	3.0	0.5	62.9	1.35	0.811	2.85	0.765	0.0449	8.06	13.77	0.1160	0.0099	$(2.84\pm1.26)\times10^{-3}$	$(13.55\pm2.40)\times10^{-3}$	0.05
7	3.5	0.5	60.5	1.65	0.778	3.46						-	-	-	-
8	4.0	0.5	58.1	-	-	-	-	-	-	-	-	-	-	-	-
9	4.5		55.4	-	-	-	-	-	-	-	-				

Notes:

* Sensitivity "1"; Calibration (1).

** Probable error, $P(\Delta L_n)$ and $P(L_n)$, defined by Eqns. (J-86) and (J-87), respectively.

*** Probable error, obtained from deviations of experimental points from the best-fit straight line by using Eqn. (J-91).

**** Probable error, obtained as a mean of probable errors of experimental points directly calculated from experimental errors by using Eqn. (J-92).

***** Probable error corresponding to $P(\overline{L})$.

$P(\overline{L})$ = 8.14×10^{-5} *** gmole^{-1}

$\overline{P(L)}$ = 4.63×10^{-4} **** gmole^{-1}

Slope: $S = (3.91\pm0.023)\times10^{-3}$ ***** gmole^{-1}hr^{-1}

Overall Rate Constant: $\langle k_2 \rangle = 6.96\pm0.04$ ***** g-atom D/ml.hr.(gmole/ml)^2

Rate Constant in Liquid Phase: $k_2 = 147\pm2$ ***** g-atom D/ml.hr.(gmole/ml)^2

TABLE M-XVII

Data and Calculated Results of Run 29

Temperature: 150 °C
Stirring Rate: 8 strokes/sec.
Catalyst: 1.80 Normal diethylamine in charged solution
Hydroxyl-Ion Concentration: h = 0.036 Normal

Total Amount of Liquid Charged: G = 438 grams
Total Amount of H_2 Charged: $n'_{o,o}$ = A_o = 0.930 gmoles
Total Amount of HDO Charged: B_o = 7.84 gmoles
Total Amount of HD Charged: C_o = 0 gmoles
Total Amount of H_2O Charged: D_o = 11.08 gmoles
F = 0.978
λ_o = 0.0215 λ_1 = 0.9969 λ_o' = 0.9785 λ_1' = 0.0031

Volume of Vapor Phase: V' = 473 ml.
Amount of Water in Liquid Phase: m_1 = 375.5 grams
Amount of Water in Vapor Phase: m_1' = 1.16 grams
Amount of Amine in Liquid Phase: m_2 = 60.92 grams
Amount of Amine in Vapor Phase: m_2' = 0.40 grams
$\lambda_o\lambda_1$ = 0.0235
$\lambda_o'\lambda_1'$ = 0.00301

Sample Number n	Time t_n (hr)	Time Δt_n (hr)	Total Pressure after Sampling $P_{(n+1)}$ (at.)	T/C-Cell Output * E_n (mV)	Amount of Hydrogen after Sampling $n'_{o,(n+1)}$ (gmole)	Atom Fraction D in Hydrogen $f'_{d,n}$ (%)	Amounts of Reactants after Sampling: H_2 A_{n+1} (gmole)	HD C_{n+1} (gmole)	HDO B_{n+1} (gmole)	H_2O D_{n+1} (gmole)	β_{n+1} (gmole)	Extent of Reaction: ΔX_n (gmole)	ΔL_n (gmole^{-1})**	L_n (gmole^{-1})**	Weight w_n
0	0	0.5	71.8	0	0.911	0	0.911	0	7.84	11.08	0.2065	0.0281	$(5.41\pm0.58)\times10^{-3}$	$(5.41\pm0.58)\times10^{-3}$	1.00
1	0.5	0.5	71.1	0.72	0.902	1.54	0.874	0.0274	7.81	11.11	0.1771	0.0255	$(5.74\pm0.95)\times10^{-3}$	$(11.2\pm1.1)\times10^{-3}$	0.27
2	1.0	0.5	70.1	1.40	0.888	2.95	0.836	0.0509	7.79	11.13	0.1503	0.0251	$(6.75\pm1.12)\times10^{-3}$	$(17.9\pm1.6)\times10^{-3}$	0.13
3	1.5	0.5	69.4	2.10	0.879	4.36	0.804	0.0734	7.76	11.16	0.1256	0.0180	$(5.71\pm1.26)\times10^{-3}$	$(23.6\pm2.0)\times10^{-3}$	0.08
4	2.0	0.5	68.0	2.62	0.860	5.39	0.770	0.0877	7.75	11.17	0.1068	0.0159	$(5.96\pm1.45)\times10^{-3}$	$(29.6\pm2.5)\times10^{-3}$	0.05
5	2.5	0.5	67.4	3.10	0.851	6.31	0.747	0.1006	7.73	11.19	0.0916	0.0129	$(5.60\pm1.64)\times10^{-3}$	$(35.2\pm3.0)\times10^{-3}$	0.04
6	3.0	--	66.0	3.50	0.833	7.07						---	-----	----	--
7	--	--	--	--	---	--	---	---	--	---	---	---	-----	----	--
8	--	--	--	--	---	--	---	---	--	---	---	---	-----	----	--
9	--	--	--	--	---	--	---	---	--	---	---	---	-----	----	--

Notes:
* Sensitivity "1"; Calibration (;).
** Probable error, $P(\Delta L_n)$ and $P(L_n)$, defined by Eqns. (J-86) and (J-87), respectively.
*** Probable error, obtained from deviations of experimental points from the best-fit straight line by using Eqn. (J-91).
**** Probable error, obtained as a mean of probable errors of experimental points directly calculated from experimental errors by using Eqn. (J-92).
***** Probable error corresponding to $P(\overline{L})$.

$P(\overline{L})$ = 1.26×10^{-4} *** gmole^{-1}
$\overline{P(L)}$ = 5.03×10^{-4} **** gmole^{-1}

Slope: S = $(1.16\pm0.004)\times10^{-2}$ ***** gmole^{-1}hr^{-1}

Overall Rate Constant: $\langle k_2 \rangle$ = 20.9 ± 0.1 ***** g-atom D/ml.hr.(gmole/ml)^2

Rate Constant in Liquid Phase: k_2 = 460 ± 6 ***** g-atom D/ml.hr.(gmole/ml)^2

N. NOMENCLATURE

A

a Area of internal wall surface of the autoclave which is exposed to the vapor, cm^2.

A Initial total amount of hydrogen gas, H_2, in both phases, gmoles.

B

B Initial total amount of water, HDO, in both phases, gmoles.

C

c Henry's law constant, mmHg/mole fraction of gas in liquid.

c_o An integration constant in an expression for the ionization constant.

c_1, c_2 and c_3 Constant coefficients of terms in a polynominal expression of the heat of formation.

c_5 A constant coefficient of a temperature-dependent term in an expression for the ionization constant.

D

D Initial total amount of water, H_2O, in both phases, gmoles.

E

E Initial total amount of diethylamine, $(C_2H_5)_2NH$, in both phases, gmoles.

E Output of the thermal conductivity cell, millivolts.

ΔE_1 Average activation energy of the liquid-phase reaction, $H_2 + HDO \rightarrow HD + H_2O$, calories/gram mole.

ΔE_2 Average activation energy of the liquid-phase reaction, $HD + H_2O \rightarrow H_2 + HDO$, calories/gram mole.

$\Delta E_{2,OH^-}$ Activation energy of the liquid-phase reaction, $OH^- + HD \rightarrow (H\text{—}O\cdots D\text{—}H)^{\ominus}$.

$\Delta E_{2,R_2NH}$ Activation energy of the liquid-phase reaction, $R_2NH + HD \rightarrow (R_2N\cdots D\text{—}H)$.

F

F Fraction of total exhangeable hydrogen isotopes in water and diethylamine that is in the molecules of water.

F_b A factor with which X is to be multiplied to take into account an effect on the reacting amount of HDO of an additional reaction due to D_2O. (Used in Section L-4 of the APPENDIX.)

F_d A factor with which X is to be multiplied to take into account an effect on the reacting amount of H_2O of an additional reaction due to D_2O. (Used in Section L-4 of the APPENDIX.)

f_d Atom fraction of deuterium in the total exchangeable atoms of hydrogen isotopes in the liquid before exchange is started.

f_d' Atom fraction of deuterium in hydrogen gas at a given time.

f_w Atom fraction of deuterium in water molecules at time zero. (Used in Section L-4 of the APPENDIX.)

f_w' Atom fraction of deuterium in water molecules at time t. (Used in Section L-4 of the APPENDIX.)

G

G Initial total amount of diethylamine, $(C_2H_5)_2ND$, in both phases, gmoles. G was also used for total amount of liquid charged, grams.

H

h Concentration of hydroxyl ion in ghe liquid phase, grammoles per milliliter of liquid solution.

H Initial amount of heavy water molecule, D_2O, in grammoles. (Used in Section L-4 of the APPENDIX.)

I

i Dummy parameter used to represent a partial run. In DISCUSSION OF RESULTS, i is used to represent a mechanism number.

J

j Atom fraction of deuterium in water used for preparing charging solution. Equals to 0.2285 for "blank" and "1N" runs, and 0.2667 for "2N" runs.

K

k_1 Specific rate constant for the reaction, $H_2 + HDO \rightarrow HD + H_2O$, in the liquid phase which, when multiplied with the concentrations of H_2 and HDO in the liquid phase and the volume of the liquid phase, gives the rate of transfer of deuterium atoms to HD; g-atoms/ml·hour·$(gmole/ml)^2$.

k_2 Specific rate constant for the reaction, $HD + H_2O \rightarrow H_2 + HDO$, in the liquid phase which, when multiplied with the concentrations of HD and H_2O in the liquid phase and the volume of the liquid phase, gives the rate of transfer of deuterium atoms to H_2; g-atoms/ml·hour·$(gmole/ml)^2$.

$k_{2,i}$ Rate constant for the reaction $HD + H_2O \rightarrow H_2 + HDO$, in the liquid phase, due to a meghanism characterized by i; g-atoms/ml·hour·$(gmole/ml)^2$.

k_1' Specific rate constant for the reaction, $H_2 + HDO \rightarrow HD + H_2O$, in the vapor phase which, when multiplied with the concentrations of H_2 and HDO in the vapor phase and the volume of the vapor phase, gives the rate of transfer of deuterium atoms to HD; g-atoms/ml·hour·$(gmole/ml)^2$.

k_2^s Specific rate constant for the reaction $HD + H_2O \rightarrow H_2 + HDO$, on the internal walls of the autoclave, expressed as g-atom D transferred per cm^2 per hour per partial hydrogem pressure (atm.).

k_2' Specific rate constant for the reaction, $HD + H_2O \rightarrow H_2 + HDO$, in the vapor phase which, when multiplied with the concentrations of HD and H_2O in the vapor phase and the volume of the vapor phase, gives the rate of transfer of deuterium atoms to H_2; g-atoms/ml·hour·(gmole/ml)^2.

k_1'' Specific rate constant for the reaction, $H_2 + D_2O \rightarrow HD + HDO$, in the liquid phase which, when multiplied with the concentrations of H_2 and HDO in the liquid phase and the volume of the liquid phase, gives the rate of transfer of deuterium atoms to HD; g-atoms/ml·hour·(gmoles/ml)^2.

k_2'' Specific rate constant for the reaction, $HD + HDO \rightarrow H_2 + D_2O$, in the liquid phase which, when multiplied with the concentrations of HD and H_2O in the liquid phase and the volume of the liquid phase, gives the rate of transfer of deuterium atoms to H_2; g-atoms/ml·hour·(gmoles/ml)^2.

$\langle k_2 \rangle$ Overall rate constant for the reaction, $HD + H_2O \rightarrow H_2 + HDO$, including the reaction in both phases, defined by Eqn. (J-19); g-atoms/ml·hour·(gmoles/ml)^2.

K Equilibrium constant for the reaction, $H_2 + HDO \rightleftharpoons HD + H_2O$ in the liquid phase.

K' Equilibrium constant for the reaction, $H_2 + HDO \rightleftharpoons HD + H_2O$ in the gas phase.

K'' Equilibrium constant for the reaction, $H_2 + D_2O \rightleftharpoons HD + HDO$ in the liquid phase.

K_a Ionization constant of amine, gram moles per liter.

K_w Equilibrium constant for the reaction, $H_2O + D_2O \rightleftharpoons 2HDO$ in the liquid phase.

$K^{(s)}$ Equilibrium constant for the reaction, $H_2S + HDO \rightleftharpoons HDS + H_2O$.

$\underline{L}$

L equals $\frac{1}{\beta - \alpha} \ln \frac{\beta(X-\alpha)}{\alpha(X-\beta)}$, defined by Eqn. (J-27); gmole^{-1}.

L_n equals $\sum_{i=1}^{n} \Delta L_n$, defined by Eqn. (J-52); gmole^{-1}.

ΔL_n equals $\frac{1}{\beta_n - \alpha_n} \ln \frac{\beta_n(\Delta X_n - \alpha_n)}{\alpha_n(\Delta X_n - \beta_n)}$, defined by Eqn. (J-48); gmole^{-1}.

M

m_1 Total weight of water, including all isotopic species, in the liquid phase, grams.

m_2 Total weight of amine, including all isotopic species, in the liquid phase, grams.

m_1' Total weight of water, including all isotopic species, in the vapor phase, grams.

m_2' Total weight of amine, including all isotopic species, in the vapor phase, grams.

M Sample number of the last sample of a complete run.

M_1 Average molecular weight of water.

M_2 Average molecular weight of diethylamine.

N

n_o Total number of grammoles of hydrogen gas, including all isotopic species, in the liquid phase.

n_1 Total number of grammoles of water, including all isotopic species, in the liquid phase.

n_2 Total number of grammoles of diethylamine, including all isotopic species, in the liquid phase.

n_o' Total number of grammoles of hydrogen gas, including all isotopic species, in the vapor phase.

n_1' Total number of grammoles of water, including all isotopic species, in the vapor phase.

n_2' Total number of grammoles of diethylamine, including all isotopic species, in the vapor phase.

n_d Total number of gramatoms of deuterium in the liquid phase.

N Normality of amine in an aqueous solution.

P

p Total pressure of the system, atmospheres.

p_o Partial pressure of hydrogen gas, of all isotopic species, atmospheres. (In millimeters in Section D-1 of the APPENDIX.)

p_o' Partial pressure of HD in the sample gas being analyzed, (used in Section D-1 of the APPENDIX), millimeters Hg.

p_1 Partial pressure of steam, of all isotopic species, atmospheres.

p_2 Partial pressure of the vapor of diethylamine, of all isotopic species, atmospheres.

p_a Partial pressure of impurity air in the sample gas being analyzed, (used in Section D-1 of the APPENDIX), millimeters Hg.

$P(q)$ Probable error of a quantity q.

$P(E^o)$ Probable error of a single measurement of the thermal conductivity bridge, millivolts.

$P_o(q)$ Limit of uncertainty of a quantity q.

R

r Ratio of rate constants k_1'' to k_1.

r' Isotopic ratio of deuterium to hydrogen atoms in hydrogen gas.

r_a Isotopic ratio of deuterium to hydrogen atoms of those that are bound to nitrogen of diethylamine.

r_w Isotopic ratio of deuterium to hydrogen atoms bound in water molecules.

R Gas constant per grammole, 82.06 ml·atm·/gmole·^oK.

R_{th} Gas constant per grammole in the thermal unit, 1.987 cal./gmole·^oK.

S

S Slope of a best-fit straight line of plot of a quantity L vs. time.

T

t Time elapsed from the time zero of a complete run, hours.

Δt_n Period of time of a partial run n, hours.

T Absolute temperature, ^{o}K.

T_m Absolute temperature at which a plot of the ionization constant K_a takes on a maxium, ^{o}K.

V

v_{f1} Specific volume of saturated water of natural composition, ml./gram.

v_{f2} Specific volume of saturated liquid of diethylamine, of natural composition, ml./gram.

v_{g1} Specific volume of steam of natural composition under its partial pressure at a given temperature, ml./gram.

v^{s}_{g1} Specific volume of saturated steam at a given temperature, ml./gram.

v_{g2} Specific volume of diethylamine of natural composition under its partial pressure at a given temperature, ml./gram.

v_{fg1} Change in the specific volume of water associated with vaporization of liquid to the saturated steam at a given temperature, ml./gram.

v_{fg2} Change in the specific volume of diethylamine associated with vaporization of liquid to vapor of a pressure p_2 at a given temperature, ml./gram.

V Volume of liquid phase in equilibrium with a vapor phase in the autoclave, milliliters.

V' Volume of vapor phase in equilbrium with a liquid phase in the autoclave, milliliters.

V^{o} Total volume of the system. Equals to $V + V'$; milliliters.

W

w Weight of a quantity L.

W Amount of water molecule, H_2O, which reacted in liquid phase in the time period t hours, gmoles. (Used in Section L-4 of the APPENDIX.)

W_1 Total weight of water, of all isotopic species, in both liquid and vapor phases, grams.

W_2 Total weight of amine of all isotopic species, in both liquid and vapor phases, grams.

X

x_o Mole fraction of hydrogen gas dissolved in the liquid phase.

x_1 Mole fraction of water in the liquid phase.

x_2 Mole fraction of diethylamine in the liquid phase.

X Amount of hydrogen molecules reacted in both phases in the time period t hours, gmoles.

ΔX_n Amount of hydrogen molecules reacted in both phases in the n-th partial run, gmoles.

Y

$\bar{y}$ Average order of the liquid-phase reaction $HD + H_2O \rightarrow H_2 + HDO$ with respect to the amine concentration at a given temperature.

y_i Order of the liquid-phase reaction $HD + H_2O \rightarrow H_2 + HDO$ through a mechanism i with respect to the amine concentration.

Z

z_{f2} Compressibility factor for the saturated liquid of diethylamine, dimensionless.

Z Amount of diethylamine which exchanged deuterium with water in the time period of t hours, gmoles.

Greek Letters

α A root of a quadratic equation derived from the rate equation of the exchange reaction, gmoles. Defined by Eqn. (J-2

α^* Relative volatility of H_2O to HDO.

β A root of a quadratic equation derived from the rate equation of the exchange reaction, which represents an amount of reaction that will take place before an equilibrium is reached, gmoles. Defined by Eqn. (J-22)

β_1 A correction term for an expression of the specific volume of a superheated steam, ml./gram.

β_2 A correction term for an expression of the specific volume of a superheated diethylamine, ml./gram.

γ Slope of calibration line of the thermal conductivity analysis, being equal to the ratio of the atom ratio of deuterium in hydrogen gas to the output of the thermal conductivity cell; numerically equal to 0.02175 mv^{-1} for the calibration curve No. 1 and to 0.01225 mv^{-1} for the calibration curve No. 2.

δ_1 Defined by (J-19).

δ_2 Defined by (J-20).

ζ_o Mole fraction of $(C_2H_5)_2NH$ in the total diethylamine.

ζ_1 Mole fraction of $(C_2H_5)_2ND$ in the total diethylamine.

η Sum of mole fraction of HDO and D_2O in the total water.

κ_o Thermal conductivity of H_2 at a mean temperature of gas in the thermal conductivity cell, cal./cm^2sec.^oC/cm.

κ_o' Thermal conductivity of HD at a mean temperature of gas in the thermal conductivity cell, cal./cm^2sec.^oC/cm.

κ_a Thermal conductivity of air at a mean temperature of gas in the thermal conductivity cell, cal./cm^2sec.^oC/cm.

λ_o Fraction of hydrogen, of all isotopic species, that is dissolved in the liquid phase.

λ_1 Fraction of water, of all isotopic species, that is in the liquid phase.

λ_{11} Fraction of HDO that is in the liquid phase.

λ_o' Fraction of hydrogen, of all isotopic species, that is in the vapor phase.

λ_1' Fraction of water, of all isotopic species, that is in the vapor phase.

λ_{11}' Fraction of HDO that is in the vapor phase.

ξ_o Mole fraction of H_2O in the total water.

ξ_1 Mole fraction of HDO in the total water.

ξ_2 Mole fraction of D_2O in the total water.

π_1 Vapor pressure of water of the natural composition, atmospheres.

π_2 Vapor pressure of diethylamine of the natural composition, atmospheres.

ρ Density of an amine solution at room temperature, gram/milliliter.

ρ_2 Density of pure diethylamine of the natural composition, grams per milliliter.

ρ_g Density of saturated vapor of diethylamine, gram/ml.

$\bar{\rho}$ Density of an amine solution at room temperature as calculated from the ideal law of solution, grams per milliliter.

$\bar{\rho}_1$ Average density of partially enriched heavy water, grams per milliliter.

τ A function of temperature used for correlating data of the ionization constant, K_a.

Subscripts

o, 1 or 2	In most cases, refers to hydrogen gas, water and diethylamine, respectively. When there are two subscripts on one symbol, the first subscript always represents a compound in this manner.
n	Refers to the sample No. n or the n-th partial run of a run. When there are two subscripts on one symbol, the second subscript always refers to a number of sample.
(n)	Used to refer to the total pressure of the reaction system during the n-th partial run.

Superscripts

' (prime)	Refers to value of the quantity in the vapor phase.
o	When used on A, B, C, D, X and ΔX, this is a reminder that a reaction system is ideal in the sense that no material is withdrawn from the system.

O. REFERENCES

(1) Benedict, M., PICG(I), P/819 (1955).

(2) Murphy, G. M., editor, "Production of Heavy Water", Natl. Nucl. Energy Ser., McGraw-Hill Book Co., N.Y. (1955).

(3) Roth, E. et al, PICG(II), P/1261 (1958).

(4) Bar-Eli, K. and Klein, F.S., J. Chem. Soc., 1962, 1378.

(5) Dirian, G., Botter, F., Ravoire, J. and Grandcollot, P., J. Chim. Phys., 60, 139 (1963).

(6) Bar-Eli, K. and Klein, F.S., J. Chem. Soc., 1962, 3083.

(A-1) Becker, E.W., Angew. Chem., 68, 6 (1956), AERE-Lib/Trans-734.

(A-2) Becker, E.W., Bier, K., Hubener, R.P. and Kessler, R. W., PICG (II), P/1000 (1958).

(A-3) Becker, E.W., Hubener, R.P. and Kessler, R. W., Chem. Ing. Tech., 30, 288 (1958); AERE-Lib/Trans-799.

(A-4) Roth, E., Private Communication (1960).

(A-5) Bigelow, J.E., ScD Thesis, Chemical Engineering Department, Massachusetts Institute of Technology (1956).

(A-6) Allen, A. O., Radiation Research, 1, 85 (1954).

(A-7) Allen, A. O., PICG (I), P/738 (1955).

(A-8) Dewhurst, H.A., Samuel, A. H., and Magee, J. L., Rad. Res., 1, 62 (1954).

(A-9) Hart, E. J., Rad. Res., 1, 53 (1954).

(A-10) Hart, E. J., Ann. Rev. Phys. Chem., 5, 139 (1954).

(A-11) Hart, E. J., PICG (II), P/951 (1958).

(A-12) Toulis, W. J., UCRL-583 (1950).

(A-13) Boyle, J. W., Hochanadel, C. J., Sworski, T. J., Ghormley, J. A. and Kieffer, W. F., PICG (I), P/741 (1955).

(A-14) Hart, E. J., Rad. Res., 2, 33 (1955).

(A-15) Gordon, S. and Hart, E. J., PICG (II), P/952 (1958).

(A-16) Gordon, S., Hart, E. J., and Walsh, P., ANL-4526, p77 (1951).

(A-17) Friedman, H. L., and Zeltmann, A. H., J. Chem. Phys., 28, 878 (1958).

(A-18) Gordon, S. and Hart, E. J., J. Am. Chem. Soc., 77, 3981 (1955).

(A-19) Selwood, P. W., "Magnetochemistry", Interscience Publishers, N. Y. (1956).

(A-20) Korman, S. and LaMer, V. K., J. Am. Chem. Soc., 58, 1396 (1936).

(A-21) Gray, D. E., Editor, "American Institute of Physics Handbook", McGraw-Hill Book Co., N.Y. (1957).

(A-22) Wilmarth, W. K., Dayton, J. C. and Flournoy, J. M., J. Am. Chem. Soc., 75, 4549 (1953).

(A-23) Miller, S. L. and Rittenberg, D., J. Am. Chem. Soc., 80, 64 (1958).

(A-24) Latimer, W. M., "Oxidation Potentials", Prentice-Hall, N.Y. (1952).

(A-25) Wilmarth, W. K., and Dayton, J. C., J. Am. Chem. Soc., 75, 4553 (1953).

(A-26) Flournoy, J. M. and Wilmarth, W. K., J. Am. Chem. Soc., 83, 2257 (1961).

(A-27) Seidell, A., "Solubilities of Organic Compounds", D. Van Nostrand Co., N.Y. (1941).

(A-28) Copp, J. L. and Everett, J. L., Discuss. Farad. Soc., 15, 174 (1953); Ishiguro, T., Yagyu, M. and Takagi, K., Yakugaku-Zasshi, 79, 1138 (1959); (C. A., 54, 2857 i).

(B-1) Collins, S. C., Rev. Sci. Instr., 7, No. 12, 502 (1936).

(B-2) Corruccini, R. J. and Shenker, H., J. Research Natl. Bur. Standards, 50, 229 (1953).

(B-3) Shenker, H., Lauritzen, J. L. Jr., and Corruccini, R. J., Natl. Bur. Standards, (U.S.) Circ., 508 (May 7, 1951).

(D-1) Farkas, A., "Orthohydrogen, Parahydrogen and Heavy Hydrogen", Cambridge Univ. Press (1935).

(D-2) Farkas, A. and Melville, H. W., "Experimental Methods in Gas Reactions", MacMillan and Co., London (1939).

(E-1) Worthing, A. G. and Geffner, J., "Treatment of Experimental Data", John Wiley and Sons, N.Y. (1959).

(H-1) Keenan, J. H. and Keyes, F. G., "Thermodynamic Properties of Steam", John Wiley and Sons, N.Y. (1959).

(H-2) "Advances in Chemistry Series, No. 29; Physical Properties of Chemical Compounds III", Am. Chem. Soc., Wash., D.C., (1961).

(H-3) Circular of the Bureau of Standards, No. 142, "Tables of Thermodynamic Properties of Ammonia", Department of Commerce, Wash., D.C. (1923).

(H-4) Scatchard G., Epstein, L. R., Warburton, J. and Cody, P. J., Refrigerating Engineering, May (1947).

(H-5) Meissner, H. P. and Paddison, O. H., Int. Eng. Chem. 33, 1189 (1941).

(H-6) "International Critical Table", Vol. III, p. 256.

(H-7) "International Critical Table", Vol. III, p. 271.

(H-8) Kirschenbaum, I., "Physical Properties and Analysis of Heavy Water", Nat'l Nuclear Energy Series, III-4A, McGraw-Hill Book Co., N.Y. (1951).

(H-9) Kimball, G. E., and Stockmayer, W. H., SAM Report A-144 (April, 1942).

(H-10) Libby, W. F., J. Chem. Phys., 11, 101 (1943).

(H-11) Cerrai, E., Marchetti, C., Renzoni, R., Roseo, L., Silvestri, M., and Villani, S., Chem. Eng. Progr. Symposium Ser., 50 (11), 271 (1954).

(J-1) Armstrong, G. T., "A Compilation of Vapor Pressure Data of Deuterium Compounds", NBS Report No. 2306 (Feb., 1953).

(L-1) Goldfinder, P. and Lazareff, W., Compt. rend., 200, 1671 (1935).

(L-2) Emeléus, H. J. and Briscoe, H. V. A., Chem. Soc. London J., 127 (1937).

(L-3) Roberts, E. R., Emeléus, H. J., and Briscoe, H. V. A., Chem. Soc. London J., 41 (1939).

(L-4) Brodskiĭ, A. I., Trans. Farad. Soc., 33, 1180 (1937).

(L-5) Scudder, H., "Electrical Conductivity and Ionization Constants of Organic Compound", D. van Nostrand Co., N.Y. (1914).

(L-6) "International Critical Table", Vol. VI, p. 260.